TECHNOLOGY TO IMPROVE COMPETITIVENESS IN WARM AND HOT FORGING

-INCREASING DIE LIFE AND MATERIAL UTILIZATION-

DISSERTATION

Presented in Partial Fulfillment of the Requirements for

the Degree Doctor of Philosophy in the Graduate

School of The Ohio State University

By

Manas Shirgaokar, M.S.

* * * * *

The Ohio State University
2008

Dissertation Committee: Approved by:

Professor Taylan Altan, Adviser

_____

Professor Jerald Brevick   Adviser

Professor Allen Yi   Industrial and Systems Engineering

Graduate Program

ProQuest Number: 10631261

ProQuest 10631261

www.manaraa.com

ABSTRACT

The main thrust of this research was on improvement of profitability in industrial warm and hot forging processes by increasing die life and material yield. In order to achieve these goals and remain competitive, forging companies in industrialized countries need to apply advanced computational tools such as FE simulation, besides practicing efficient shop-floor management. Some of the needs of the forging industry deemed relevant to the theme of this dissertation were a) determination of die-workpiece interface conditions under steady-state production, b) selection and comparison of optimum die materials (prediction of die life), c) design of shrink-fit dies with ceramic and/or carbide inserts for warm and hot forging, and d) optimization of preform and blocker die design for improved die life and material yield. The desired solutions and computational techniques were developed using actual production examples through active cooperation with the forging industry and affiliated companies.

To achieve the outlined goals it was first necessary to identify the root causes of die failure and material loss. This was done by developing "fishbone" (Ishikawa) diagrams identifying the main causes as well as interactions between them. This background work was supplemented with an in-depth technical literature review on die life research conducted by industry and academia. Using a hot forging process as an example, FE simulation techniques were developed for determination of die-workpiece interface conditions at start-up and under steady-state production. The current industry and academic practice in forging simulations is to consider only the deformation part of the forging cycle. The simulation methods developed during this research used detailed production cycle-time data to simulate the forging cycle from the time the billet is placed on the die to the time the forged part is removed. Additionally, the lubrication spray process was also analyzed using FEA. Repetitive simulations of these discrete process steps facilitated the prediction of steady-state interface conditions. This simulation approach added a significant amount of accuracy to the analysis of cyclic thermo-mechanical loading of the die surface and, subsequently, the prediction of die life. Alternative die materials were selected based upon a virtual FEA comparison of their thermal fatigue performance under the predicted interface conditions. Also crucial to this analysis process was the optimization of the preform shape to reduce contact times and relative sliding. Production trials with the new preform design and an

alternative die material showed 50% reduction in scrap rates with significantly reduced thermal fatigue on the critical regions of the die.

Current shrink-fit die design methods used by the forging industry make use of room temperature dimensions for the analysis of compressive pre-stress under warm forging conditions. The thermal expansion and subsequent loss of pre-stress during pre-heating and forging is not accounted for, which is critical when considering ceramic or carbide inserts. A simulation technique was developed for analysis of die assembly and pre-heating as well as the effect of different pre-heat methods. This, in combination with the multiple-cycle simulation technique developed earlier, helped to determine the loss of shrink-fit in the die inserts. Thus, the corrections and process changes necessary to maintain the inserts under compression were determined. The effect of dimensional tolerances of the die components on the compressive pre-stress was also analyzed. Carbides and matrix steels were recommended for improved thermal fatigue performance on the basis of FEA predictions.

The research goals of material yield improvement were accomplished using the forging process of an aluminum upper control arm as an example. Based on the metal flow and volume distribution analysis of the existing process, two optimized preform geometries were developed, while maintaining the die design. A material yield improvement of 10-15% was predicted and subsequently, validated on the shop floor ($\approx$ 10% improvement). The blocker die design was then optimized by varying selected geometrical parameters to achieve a total predicted yield improvement of $\approx$ 19%. The reduced lead time from quotation to production, upon application of the developed FEA methods, was expected to further maximize the total potential cost savings.

The goals outlined at the outset were, thus, achieved by forming mutually beneficial alliances with the forging industry in order to develop the necessary computational design and analysis techniques, and to validate them under actual production settings. The application of these methods in an efficiently managed production environment will enable forging companies to achieve and maintain a competitive edge in the global marketplace.

ACKNOWLEDGMENTS

VITA

May 2, 1979…………………………………… Born – Pune, India

July 1996 – June 2000………………………... B.E – Mechanical Engineering, Vishwakarma Institute of Technology, University of Pune, Pune – India.

September 2000 - August 2002………………… M.S. – Mechanical Engineering, The Ohio State University, Columbus, OH.

June 2003 - September 2003…………………… Development Engineer Intern, Johnson Controls, Holland, MI.

October 2005 – April 2006……………………… Engineering Intern, Kaiser Aluminum and Chemical Corp., Heath, OH.

March 21-24, 2006……………………………. Awarded travel grant to Nara, Japan for the 4th International Seminar on Precision Forging (ISPF) organized by the Japan Society for Technology of Plasticity (JSTP).

September 2000- February 2008 Graduate Research Associate, Engineering Research Center for Net Shape Manufacturing (ERC/NSM), The Ohio State University, Columbus, OH.

February 2008 - present Engineer - Breakthrough Technologies, Advanced Materials Machining, Kennametal, Latrobe, PA.

PUBLICATIONS

Handbooks and Textbooks:

1. Shirgaokar, M. and Altan, T., "Hammers and Presses for Forging", ASM Handbook Volume 14A: Metalworking: Bulk Forming, Edited by S.L. Semiatin, American Society for Metals (ASM), October 2005.

2. Shirgaokar, M. and Altan, T., "Selection of Forging Equipment", ASM Handbook Volume 14A: Metalworking: Bulk Forming, Edited by S.L. Semiatin, American Society for Metals (ASM), October 2005.

3. Shirgaokar, M., "Metal Forming Processes in Manufacturing", Cold and Hot Forging: Fundamentals and Applications, Edited by T. Altan, G. Ngaile and G. Shen, American Society for Metals (ASM), March 2005.

4. Shirgaokar, M., "Forging Process-Variables and Descriptions", Cold and Hot Forging: Fundamentals and Applications, Edited by T. Altan, G. Ngaile and G. Shen, American Society for Metals (ASM), March 2005.

5. Shirgaokar, M. and Ngaile, G., "Plastic Deformation - Strain and Strain Rate", Cold and Hot Forging: Fundamentals and Applications, Edited by T. Altan, G. Ngaile and G. Shen, American Society for Metals (ASM), March 2005.

6. Shirgaokar, M., "Flow Stress and Forgeability", Cold and Hot Forging: Fundamentals and Applications, Edited by T. Altan, G. Ngaile and G. Shen, American Society for Metals (ASM), March 2005.

7. Shirgaokar, M., "Methods of Analysis for Forging Operations", Cold and Hot Forging: Fundamentals and Applications, Edited by T. Altan, G. Ngaile and G. Shen, American Society for Metals (ASM), March 2005.

8. Shirgaokar, M., "Principles of Forging Machines", Cold and Hot Forging: Fundamentals and Applications, Edited by T. Altan, G. Ngaile and G. Shen, American Society for Metals (ASM), March 2005.

9. Shirgaokar, M., "Presses and Hammers for Forging", Cold and Hot Forging: Fundamentals and Applications, Edited by T. Altan, G. Ngaile and G. Shen, American Society for Metals (ASM), March 2005.

10. Shirgaokar, M., "Process Design in Impression Die Forging", Cold and Hot Forging: Fundamentals and Applications, Edited by T. Altan, G. Ngaile and G. Shen, American Society for Metals (ASM), March 2005.

11. M Shirgaokar, M. and Ngaile, G., "Process Modeling in Impression Die Forging using Finite Element Analysis", Cold and Hot Forging: Fundamentals and Applications, Edited by T. Altan, G. Ngaile and G. Shen, American Society for Metals (ASM), March 2005.

12. Shirgaokar, M. and Ngaile, G., "Isothermal and Hot Die Forging", Cold and Hot Forging: Fundamentals and Applications, Edited by T. Altan, G. Ngaile and G. Shen, American Society for Metals (ASM), March 2005.

13. Shirgaokar, M. and Ngaile, G., "Near Net Shape Forging and New Developments", Cold and Hot Forging: Fundamentals and Applications, Edited by T. Altan, G. Ngaile and G. Shen, American Society for Metals (ASM), March 2005.

14. Shirgaokar, M. and Altan, T., "Process Design for Impression-die Forging", Handbook of Workability and Process Design, Edited by G. E. Dieter, H.A. Kuhn, and S.L. Semiatin, American Society for Metals (ASM), August 2003.

Journal Publications:

1. Schrader, T., Shirgaokar, M. and Altan, T., "A Critical Evaluation of the Double Cup Extrusion Test for Selection of Cold Forging Lubricants", Journal of Materials Processing Technology, Volume: 189, Issue: 1, July 6, 2007, pp. 36-44.

2. Shirgaokar, M., Ngaile, G., Cho, H. and Altan, T., "Optimization of Mechanical Crimping to Assemble Tubular Components", Journal of Materials Processing Technology, Volume: 146, Issue: 1, February 15, 2004, pp. 35-43.

3. Shirgaokar, M., Ngaile, G., and Altan, T., "Hydraulic Crimping: Application to Assembly of Tubular Components", Journal of Materials Processing Technology, Volume: 146, Issue: 1, February 15, 2004, pp. 44-51.

Selected Conference Publications:

1. Shirgaokar, M. and Altan, T., "Advanced Die Materials and Lubrication Systems to Reduce Die Wear in Warm and Hot Forging", 27th Forging Industry Technical Conference and Energy Summit, March 27-29, 2007, Fort Worth, Texas, U.S.A.

2. Schrader, T., Shirgaokar, M. and Altan, T., "Analysis of the Double Cup Extrusion Test for Evaluation of Lubricants", 4th International Seminar on Precision Forging, organized by the Japan Society for Technology of Plasticity, March 21-24, 2006, Nara, Japan.

3. Shirgaokar, M., Cho, H. and Altan, T., "New Developments in FEM Based Process Simulation to Predict & Eliminate Material Failure in Cold Extrusion", International Conference on "New Developments in Forging Technology", Institute for Metal Forming Technology (IFU), Stuttgart, May 30- June 1, 2005.

FIELDS OF STUDY

Major Field: Industrial and Systems Engineering.

Studies in: Metal-forming Processes and Equipment (Forging and Stamping), Process Simulation for Design and Optimization, Lubrication and Die Failure.

TABLE OF CONTENTS

ix

LIST OF FIGURES

xiii

xiv

xvi

xvii

xviii

xix

xxii

xxiii

LIST OF TABLES

xxiv

CHAPTER 1

FORGING INDUSTRY IN THE GLOBAL ECONOMY

1.1.   Global Competition in the Forging Industry

Competition has intensified globally in the manufacturing world, and specifically in the forging industry. Forging firms from developing countries, especially China and India, have established a significant presence in the global market by improving their technology and innovation, and delivering cost-effective solutions. They also have the added advantage of an inexpensive and highly motivated labor force. Some of these countries also receive support from their government in the form of tax breaks, free training, and a favorable foreign exchange rate. Thus, the forging industry of industrialized high labor-rate countries can only survive in this global market by a) reducing labor costs (which often requires extensive capital investment for automation), b) increasing die service life and equipment utilization, c) increasing material utilization by reducing flash and scrap losses, d) reducing lead times for new products and above all e) by maintaining a technological advantage over their competition.

Global competition in the forging industry has, thus, brought to the forefront the issues of managing innovation and technological development while demanding continuous improvement of products and processes. Strategies for development and application of new technology are extremely important for maintaining a competitive position and protecting sales. As a result of inexpensive labor, it is expected that forging buyers will gradually shift to developing nations for acquisition of components with high labor content. In order to succeed in the global marketplace, forging suppliers from developed nations must focus on production of high value-added forgings, finished parts and sub-assemblies with the aid of new developments such as a) advances in the use of computer modeling in forging process development, b) advances in equipment design, c) use of innovative die design techniques for complex forging operations, d) appropriate training in advanced forging technologies, and e) information management and automation in forge shops.

1.2. Improvement of Profitability in Warm and Hot Forging

The profitability of a forging process depends upon various factors such as a) material utilization, b) defects and scrap rate, c) die wear and tool service life, d) utilization of forging equipment, e) selection of (optimum) process parameters by use of engineering tools such as Finite Element (FE) simulation, f) automation and labor content, and g) information management to name a few. To survive and make reasonable profit in today's highly competitive environment, forging companies must:

a. Increase material utilization by 1) maintaining consistent part quality and reducing scrap rates, and 2) reducing material lost in the form of flash.

b. Increase die life by reducing die wear and thermal fatigue.

c. Introduce advanced die design and manufacturing methods to reduce lead time from quotation to production, thus reducing die costs.

d. Implement process modeling techniques using three-dimensional (3-D) FE simulation-based simulation software instead of using trial-and-error methods that require long lead times.

e. Work with their customer in developing "forging-friendly" assemblies and components for future applications.

The implementation of these action items, seemingly logical and straight forward, is not easy, especially for companies of medium to small size, that represent the majority of the forging industry. In order to achieve their goal of being competitive in a global marketplace, these companies need to make a conscious effort towards improving their technical expertise by making appropriate investments in hardware, software and human resources.

1.3. Computer Aided Engineering (CAE) in Warm and Hot Forging: Significance and Requirements

Global competition requires that the forging industry utilize practical and proven computer aided design (CAD), computer aided manufacturing (CAM) and computer aided engineering (CAE) technologies for rapid and cost-effective process design and die manufacturing. Recently, finite element (FE) simulation software has become an integral part of forging process design to analyze and optimize the metal flow, and to conduct die stress analysis before conducting forging trials.

2

The main goal of simulation in manufacturing process design is to reduce part development time and cost, while increasing quality and productivity. For instance, process simulation can be used to develop the die design and establish process parameters by a) predicting metal flow and final dimensions of the part, b) preventing flow-induced defects such as laps, and c) predicting temperatures so that part properties, friction conditions, and die life can be controlled. Furthermore, process simulation can be very beneficial in predicting and improving grain flow and microstructure, reducing scrap, optimizing product design and increasing die life.
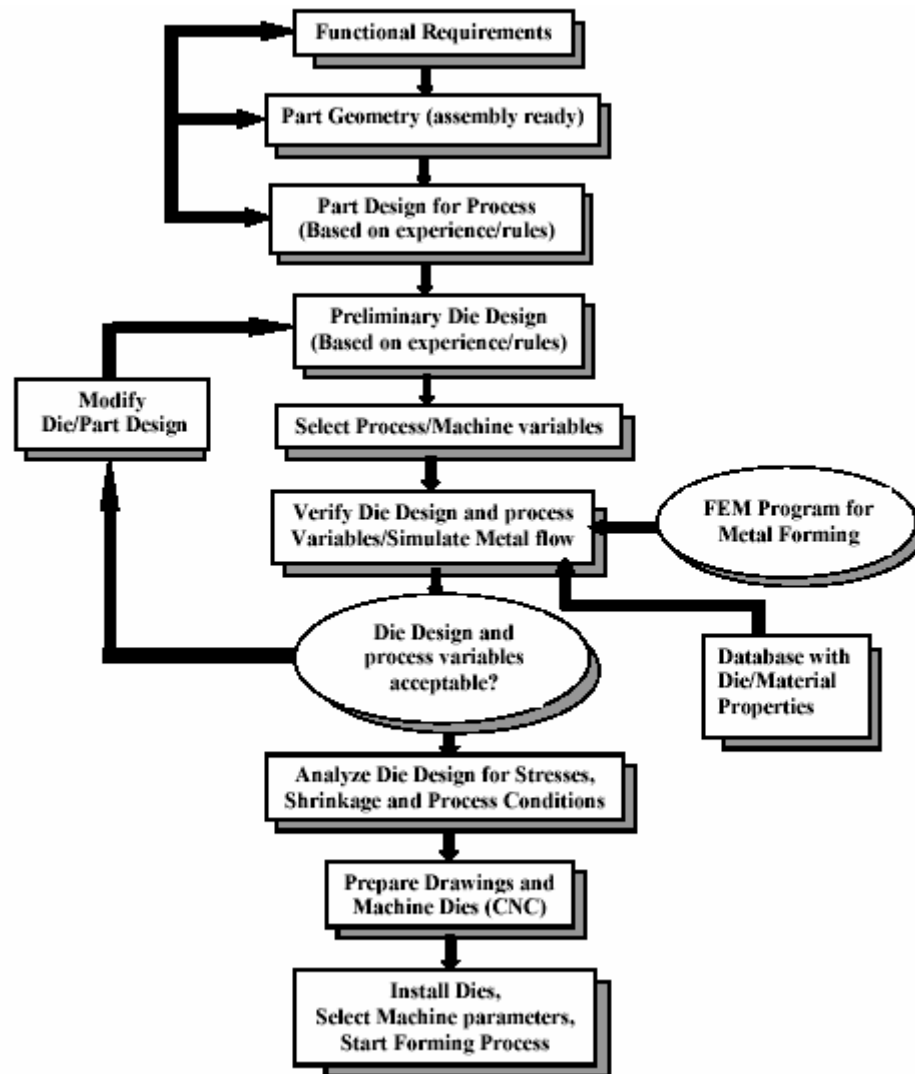
Figure 1.1: Flow chart illustrating the role of FEM in forging process design [Vasquez et al, 2000].

3

Two-dimensional (2-D) FE simulation has been state-of-the-art in forging process design for more than a decade. However, when dealing with asymmetrical complicated parts, the use of 3-D FE simulations is a must. During recent years, 3-D simulation has also gained widespread acceptance in the industry. Improvements in computer algorithm efficiency and user interface development have resulted in 3-D FE simulation becoming both robust and practical in a wide range of applications [Walters et al, 2000]. Figure 1.1 illustrates the role of FEM in forging process design by means of a flow chart [Vasquez et al, 2000].

1.3.1. Determination of Reliable Input Parameters

The accuracy of FE process simulation depends on reliable input data such as tool-workpiece geometries, material properties, thermal data, equipment characteristics, interface friction conditions, etc. Material properties of the deforming workpiece need to be estimated friction conditions, along with interface friction conditions, through tests that emulate production conditions.

1.3.1.1. Determination of Workpiece Material Properties

The cylinder compression test is a widely accepted method of determining the flow stress data (true stress/true strain relationships) for metals at various temperatures and strain rates. The basic fundamentals of the test are explained here in the context of warm and hot forging processes, but apply to room temperature testing as well.
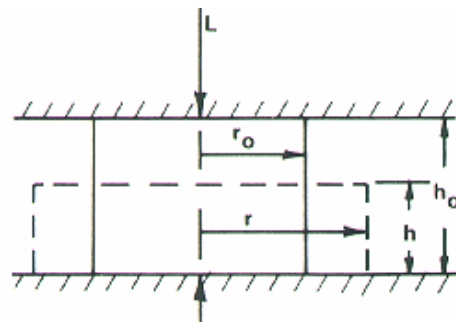
a) Test schematic.

b) Specimen showing barreling.

Figure 1.2: Cylinder compression test for determination of flow stress [Altan et al, 2005].

In this test the flat platens and the cylindrical sample are maintained at the same temperature so that die chilling, with its influence on metal flow, is prevented. To be applicable without corrections

4

or errors, the cylindrical sample must be upset without any barreling (Figure 1.2b), i.e. the state of uniform stress in the sample must be maintained as shown in Figure 1.2a. Barreling is prevented by using adequate lubrication, e.g. Teflon or machine oil at room temperature and at hot working temperatures, graphite in oil for aluminum alloys and glass for steel, titanium and high temperature alloys. The load and displacement, or sample height, are measured during the test. From this information the flow stress is calculated at each stage of deformation, or for increasing strain [Altan et al, 2005].
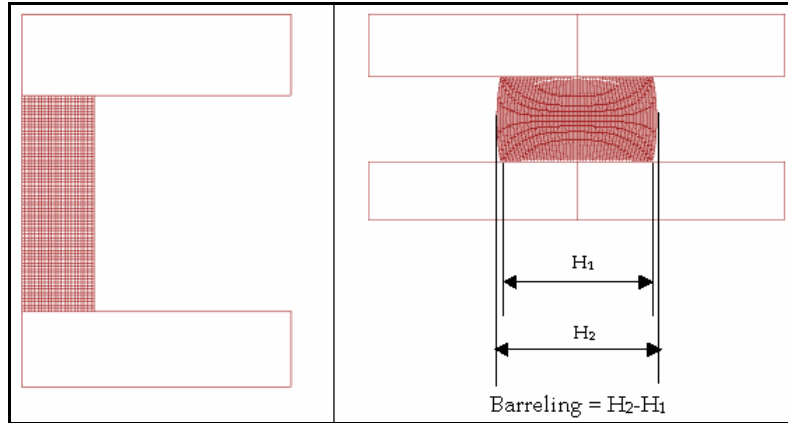
a)   Barreling due to friction.
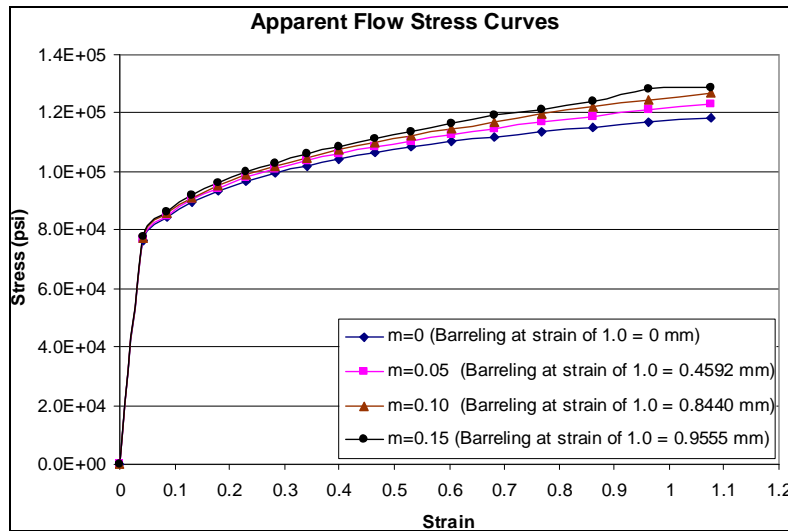
b)   Error introduced in the flow stress due to barreling.

Figure 1.3: Correction for barreling in compression test on the basis of FE simulations [Altan et al, 2005].

5

One way of correcting the flow stress, or determining approximately the error magnitude at high strain levels caused by inadequate lubrication (barreling), is to simulate the compression process in FEM using various friction factors (Figure 1.3) [Altan et al, 2005]. By measuring the amount of barreling (Figure 1.3a) and comparing the experimental data with FEM predictions (Figure 1.3b), it is possible to obtain more reliable flow stress data at higher strain levels. This method, called inverse analysis technique, has also been used to simultaneously determine friction and flow stress data using the ring compression test discussed in the next section [Cho et al, 2003 and 2005].

1.3.1.2. Determination of Die-Workpiece Interface Conditions

In forging, the ring compression and double cup extrusion tests are commonly used to evaluate and estimate the friction factor (m) of lubricants and coatings. The choice of the test depends on the contact pressure and surface expansion in the process that is being studied.

a) **Ring compression test (RCT).**   b) **Double cup extrusion test (DCET).**
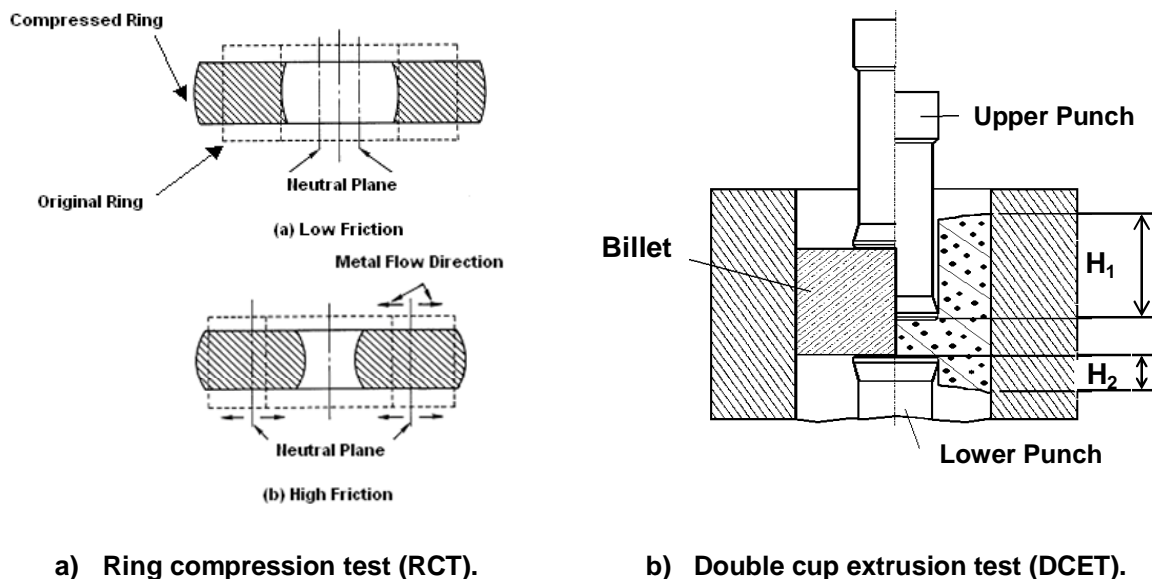
Figure 1.4: Fundamentals of the ring compression test (RCT) and the double cup extrusion test (DCET) [Altan et al, 2005].

In the ring test, a flat ring-shaped specimen is compressed to a known reduction (Figure 1.4a). The change in internal and external diameters of the forged ring is very sensitive to the friction at the die-ring interface. If friction were equal to zero, the ring would deform in the same way as a solid disk, with each element flowing radially outward at a rate proportional to its distance from the center. With increasing deformation, the internal/inner diameter (I.D.) of the ring is reduced if friction is high, and is increased if friction is low. Thus, the change in the internal diameter

6

represents a simple method for evaluating interface friction. The actual friction value is determined by running FE simulations with different friction factors to generate a set of calibration curves (Figure 1.5a). Experimental results (change in ring I.D with reduction in height) are superimposed on the calibration curves to determine the interface friction.

The double cup extrusion test (DCET) is the combination of a forward-cup and backward-cup extrusion processes. The ratio of the cup heights after deformation, H_1/H_2, is an indication of lubricity. This ratio increases as the friction factor increases. Thus, if there is no friction, the cup heights are the same and the ratio, H_1/H_2, is equal to one. In the DCET, the upper punch moves down with the ram while the lower punch and container are stationary. Thus, the container has relative velocity with respect to the upper punch, but not to the lower punch. Therefore, the material flow towards the lower punch is more restricted. In the presence of friction, the height of the upper cup is larger than the height of the lower cup. As in the RCT, the friction value is determined from FEA-generated calibration curves of cup height ratio vs., stroke (Figure 1.5b).

a) RCT.   b) DCET.
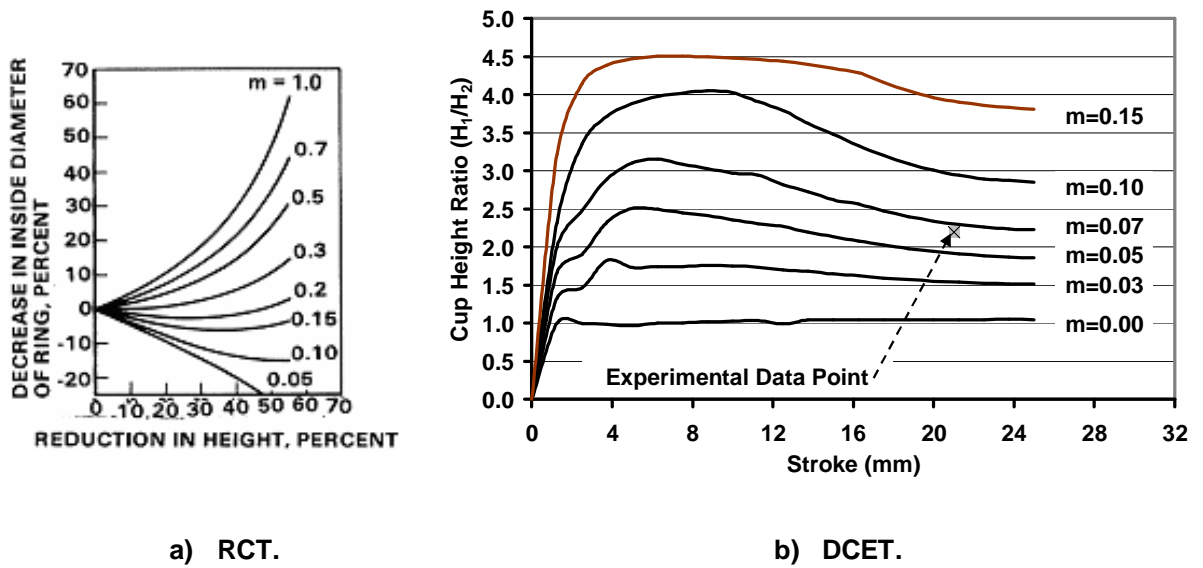
Figure 1.5: Calibration curves for determination of friction factor in the RCT and DCET [Altan et al, 2005].

The RCT has been the preferred method of lubricant evaluation for cold, warm and hot forging primarily due to its simplicity. The DCET has been commonly used for evaluation of cold and warm forging lubricants due to higher contact pressures ($\approx$ 2500 MPa/360 ksi) and surface generation characteristic of these processes. A critical evaluation of the DCET for selection of cold forging lubricants can be found in [Schrader et al, 2007].

7

1.3.2. Application of Technology to Maintain Competitiveness: Selected Examples

1.3.2.1. Process Design for Multistage Forging of Aircraft Components

One of the primary applications of FE simulation is for validation of die and process sequence design prior to production tryouts. Multistage forging simulations of two aircraft components (a titanium landing gear component and an aluminum wheel) were conducted for an aerospace supplier in order to evaluate die designs and part quality [Shirgaokar et al, 2002]. The commercial FEM code DEFORM-3D™ (Scientific Forming Technologies Corporation, Columbus, Ohio) was used for these simulations. The two components considered for this study were produced by closed-die forging with flash generation to achieve die filling. Because the parts were forged at elevated temperatures, it was necessary to run non-isothermal simulations i.e. heat-transfer between the dies and the workpiece, as well as heat-generation during deformation, was considered. Each of the components was forged in three stages, namely, two blocker stages followed by a finisher stage. Figures 1.6 and 1.7 show the simulated forging sequence of the titanium component and the aluminum wheel, respectively. The results obtained at the end of the simulations were the part quality and metal flow during forging (die filling, defects, if any, etc.), temperature distribution, and strain distribution. Flash removal between the forging stages was included in the simulation process since this influences the volume of material available for the subsequent forging stage, thus affecting die filling and die stresses. The simulation strategy adopted for the two components was to remove the flash in between stages by using the Boolean operation capability of DEFORM™ i.e. workpiece volume manipulation by element deletion. Die filling and part quality were checked by examining various cross sections along the length of the forging (Figures 1.8 and 1.9).
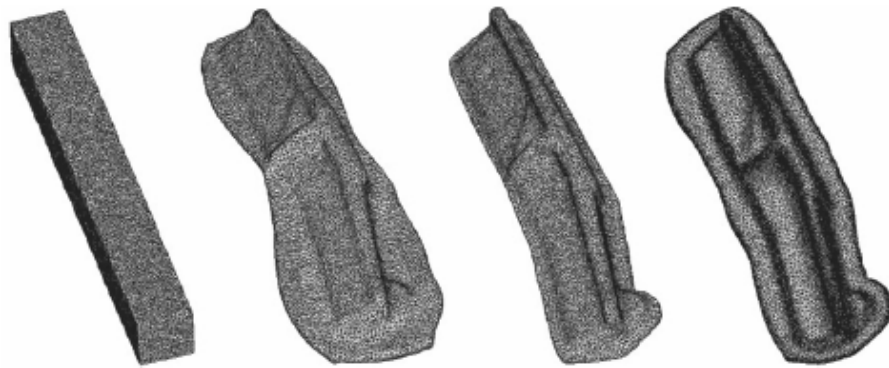
Figure 1.6: Forging process sequence for a titanium landing gear component [Shirgaokar et al, 2002].

8
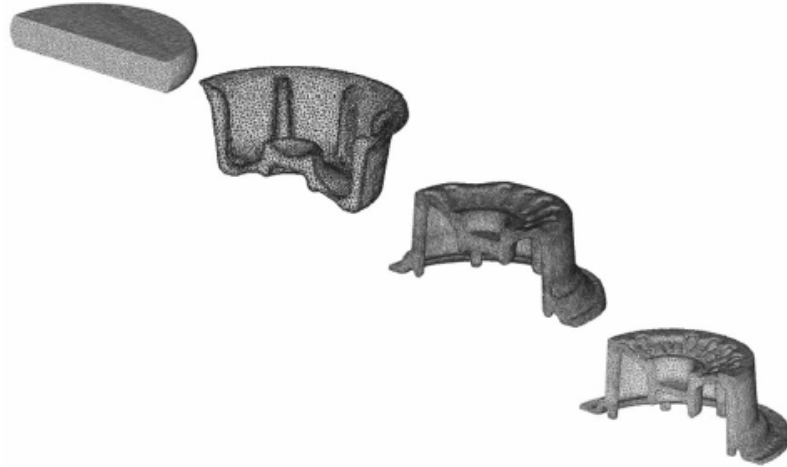
Figure 1.7: Forging process sequence for an aluminum aircraft wheel [Shirgaokar et al, 2002].

The selected parts are forged in a hydraulic press with kissing die faces i.e. the top and bottom die faces touch at the end of the stroke to achieve precise flash and part thickness. This stage of the simulations was used to determine the stresses in the dies. In order to reduce computational time, the dies were kept rigid throughout the deformation simulation. For die stress analysis the die models were changed to elastic in the last step, and the forces from the workpiece were interpolated onto the dies. The stress magnitudes predicted by these simulations were compared to the elevated temperature limits of the die materials. Die designs for the entire process sequence were verified using this process.
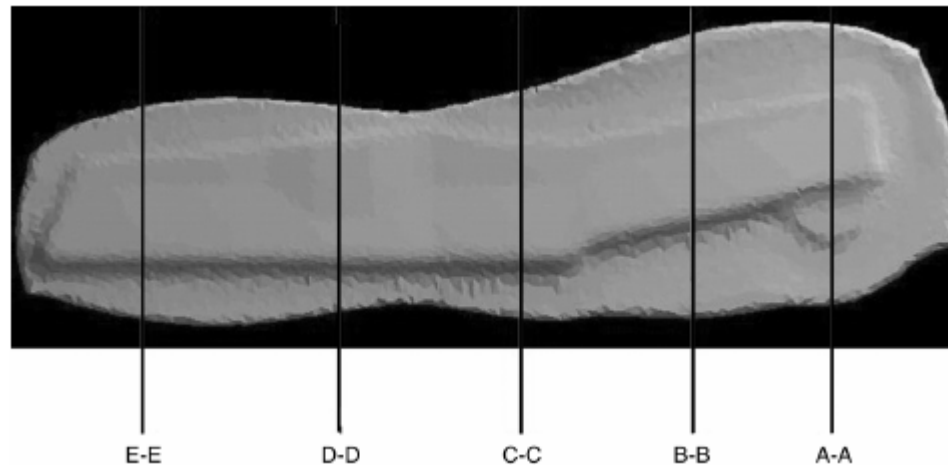
Figure 1.8: 2-D cross-sections selected for evaluation of part quality (filling, defects, etc. for the landing gear component) [Shirgaokar et al, 2002].

9
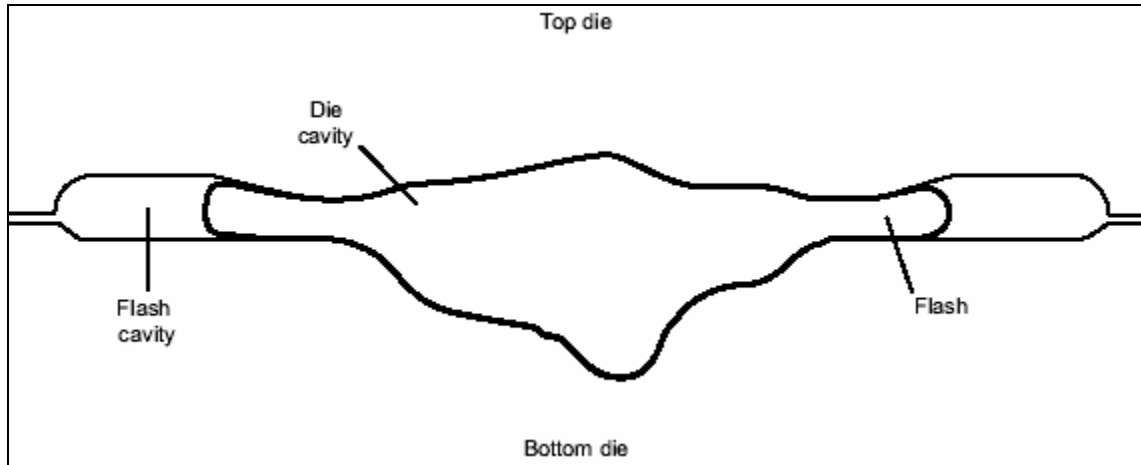
Figure 1.9: Section A-A (Figure 1.8), with relevant nomenclature, after the first blocker forging operation for the landing gear component [Shirgaokar et al, 2002].

1.3.2.2.   Process Design for Forging High Performance Aluminum Pistons

Internal combustion engine (ICE) pistons for high-performance racing engines are commonly made from aluminum alloy 2618 by conventional forging, powder forging or machining. This study was sponsored by the performance division of a major automotive company with the objective of optimizing the preform geometry and location during forging in order to obtain the desired grain flow (Figure 1.10a) and mechanical properties. To save computational time the actual piston was approximated by a geometrically similar axisymmetric part for the initial stages of the study. The effect of different preform shapes and billet orientations on the metal flow and mechanical properties of the finished part were studied (Figure 1.10b). The results obtained for this simplified part were then used for design and optimization of the forging process for the actual piston.

10

No	Type	Simulation Sequence
1	2 D	
2	3 D	
3	3 D	
4	3 D	Circular preform cut from bread-basket extrusion
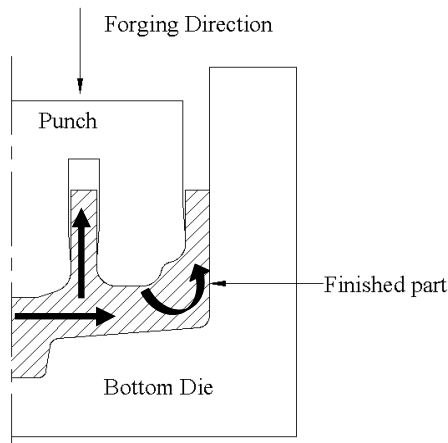
a) Schematic of the forging process showing desired grain directionality.

b) Preform geometries and locations evaluated.

Figure 1.10: Forging of the axisymmetric part, which approximates the actual geometry [Shirgaokar et al, 2003].

Pistons are generally forged from extruded billets. The grain flow during extrusion affects the quality of the piston and, hence, it was necessary to simulate the extrusion operation prior to piston forging. The objective was, therefore, to include the extrusion strain history and grain directionality into the billet prior to the forging sequence. The extrusion simulation was carried out until a steady state of strain was achieved (Figure 1.11a). A billet of predetermined length was then "cut" from this region of constant strain and upset between flat platens (Figure 1.11b) to fit it horizontally inside the die. Thus, the grain flow and strains induced during extrusion were included into the FE analysis of the forging process.

11
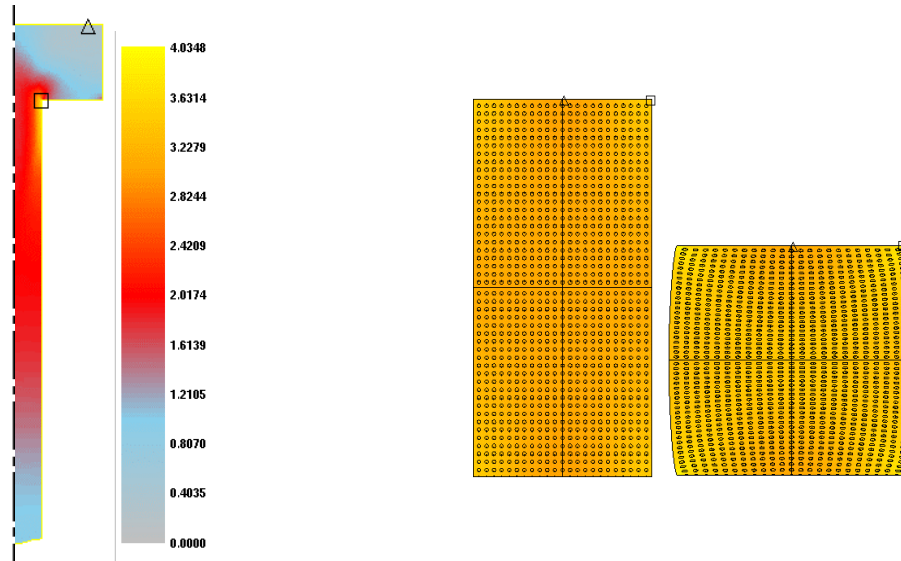
a) Simulation of extrusion showing a region of constant strain.

b) Axial upsetting of the billet obtained from extrusion.

Figure 1.11: Determination of strain gradient and grain directionality from the extrusion process [Shirgaokar et al, 2003].
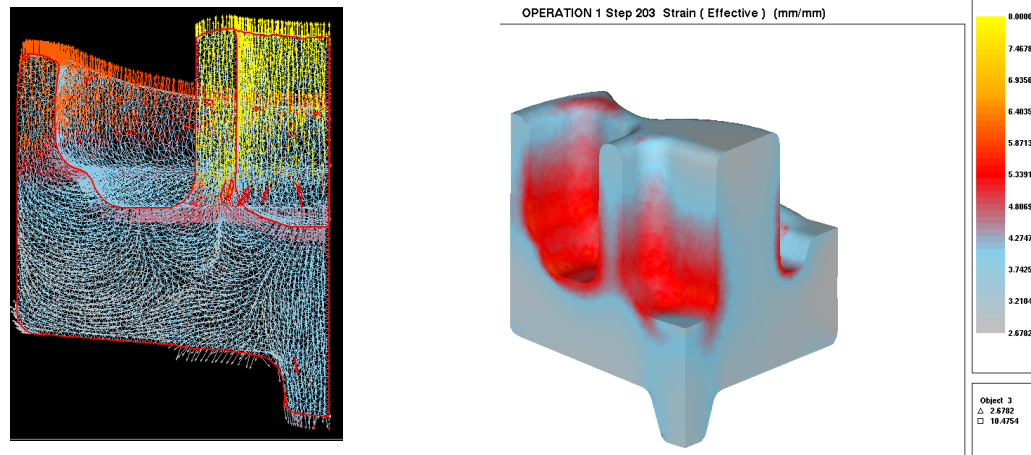
a) Grain directionality predicted by FEA for selected preform design and location.

b) Strain distribution predicted by FEA (1/4th model used due to symmetry).

Figure 1.12: Determination of optimum preform alignment in order to achieve desired grain directionality [Shirgaokar et al, 2003].

12

It was concluded from these results that forging the piston perpendicular to the extrusion direction would result in higher strains and a desirable grain flow (Figure 1.12). The actual piston geometry was simulated with the inclusion of extrusion strain history in a horizontally placed billet. The flow-net and velocity vectors were used to analyze the grain flow during deformation. The grain flow at the end of forging was similar to what was desired in the actual piston (Figure 1.10a). The flow in the webs was vertical whereas that in the bottom of the piston was in the horizontal direction. FE simulation was, thus, used successfully to determine the ideal billet orientation and preform shape for the piston to yield the desired metal flow and mechanical properties.

1.3.3. *Information Management and Training of Personnel*

Management of complex engineering information in the forging environment plays a big role in ensuring that the desired production outputs are met. A forging company should have the ability to organize engineering knowledge and properly disseminate useful information to the respective departments for implementation. A number of forging companies have gone global with branches in various locations. Thus, information flow becomes complex and difficult to manage efficiently.

To date, companies such as Plexus Systems™ have developed computerized systems that can assist the management of information flow at various departmental levels e.g. inventory tracking, shipping, receiving, engineering, purchasing etc. [Beatty, 1997]. At the engineering departmental level, information management systems can be helpful for storing and retrieving data pertaining to: a) tool designs, b) changing tool materials, c) product specification, d) process instructions, e) just-in-time jobs/rush jobs, f) process control plan, g) tool life tracking, h) machine specifications and drawings, i) press stress analysis, j) engineering drawing management, and k) dimensional control plans.

Due to global competition, the training of metal forming engineers, who are expected to plan and supervise the design and production of parts and dies, becomes increasingly important. Continuous improvements in forging technology and application of recently generated R&D results require that engineers be continuously updated in new methods, machines and process technology. Universities may be required to restructure their design courses or develop new ones that address real design issues pertaining to forging. More importantly, for the course to be successful and cost effective there is a need to link universities to the forging industry in areas such as a) process sequence development, b) die/tool designs, c) press automation and design and d) computational tools such as CAE software, CAD and CAM systems.

13

1.4. Focus Areas Identified for Research and Development

Competition to the forging industry presently comes from two primary areas: competing processes and materials, and the highly competitive global market. For the forging industry to remain viable and successful, there is a need for a comprehensive approach, through alliances with academia, to support and address research and development programs for reducing costs and lead times [Beatty, 2001]. Global off-shore forging competitors are further strengthened by trade-offset programs, direct and aggressive foreign government support, lower labor costs, and relatively cheap cost of capital.

On the basis of the background presented in this chapter, the following two focus areas were selected for this research initiative in cooperation with the forging industry and affiliated companies:

1. Improvement of die life in warm and hot forging processes through application of advanced die materials and lubrication systems.

2. Improvement of material utilization through optimization of preform and blocker die designs.

The results of this study were obtained through a combination of computational analysis and shop-floor validation for a selected set of forgings, which were representative of part families with persistent die life and material yield problems.

14

CHAPTER 2

RESEARCH FOCUS AND OBJECTIVES

2.1.   Problem Statement

Die costs can constitute up to 30% of the production cost of a part and also affect its profitability directly (die manufacturing cost) and indirectly (repair, press downtime, scrap, rework etc). Hot and warm forging processes subject the dies to severe thermal and mechanical fatigue due to high pressure and heat transfer between the dies and the workpiece. High cyclic surface temperatures result in thermal softening of the surface layers of the dies, subsequently increasing die wear as well as the susceptibility to heat checking (thermal fatigue). Most current methods developed for prediction and reduction of die wear or thermal fatigue are laboratory-based and have not gained widespread acceptance due to the lack of correlation with production observations. These methods rely on experimentation using techniques such as scratch tests, pin-on-disc tests, thermal cycling tests, etc., which do not emulate realistic die-workpiece interface conditions. Forging tests such as ring compression and spike forging, though reliable for lubricant evaluation, also do not lend themselves to reliable die life prediction due to the complexity involved in emulating shop floor conditions in the laboratory.

Conventional surface treatment methods, such as nitriding or boriding, result in a significant increase in surface hardness but have not resulted in substantial improvements in die service life. A number of advanced grades of proprietary hot-work tool steels have recently been introduced specifically for warm and hot forging applications. However, there is currently no reliable method for selecting and comparing die materials using FE simulation. The potential use of ceramic and carbide-based materials in appropriate applications is also of interest. The generally accepted method of forging process simulation only involves analysis of the deformation stage. The effect of dwell times or lubrication spray is not included in the process analysis. This, in addition to the prediction of start-up and steady-state interface conditions, is extremely crucial for a) virtual selection and comparison of tool steels using FEA, and b) successful implementation of ceramic and carbide materials with shrink-fit die assemblies. The design of shrink-fit dies for warm and hot forging requires the determination of the loss of pre-stress due to thermal expansion after

15

preheating, and under steady-state production. Current forging industry design practices lack this approach.

The other main thrust of this study was on improvement of material yield. Material costs in hot forging account for 40-60 % of the part cost, depending upon geometrical complexity, material type and the production volume. Current product development techniques in the forging industry involve trial-and-error approaches with experience-based design of preform (reducer or cross-rolled) and blocker geometries. FE simulation-based design of reduce rolling and cross/wedge rolling is a critical requirement for material yield optimization. Thus, the use of 2-D and 3-D FEA has the potential to drastically cut down development lead times, while also optimizing the preform design to improve material utilization.

The research undertaken in the current study addresses each of these requirements of the forging industry by considering individual case-studies involving mass-produced automotive components. The desired solutions and recommendations were developed through computational analyses followed by validation under production conditions in cooperation with forging companies.

2.2. Objectives

The overall objective of this study is the improvement of productivity and profitability in warm and hot forging processes by predicting and improving die life and material utilization.

- Identification of the die-workpiece interface conditions (temperatures, stress-strain reversals, sliding velocity, etc.) a) at start-up, and b) during steady-state production.

- Selection of die materials on the basis of their material properties and prediction of performance under selected process conditions.

- Design of shrink-fit die assemblies with ceramic or carbide inserts by accounting for thermal expansion during pre-heating and forging.

- Development of die and preform design methodologies for improvement of die life and material utilization.

- Application of developed information in forging practice through collaborative efforts with the industry.

These goals were achieved through detailed computational analysis and optimization of selected production processes, followed by shop-floor validation during normal production runs. This

16

research was funded by the Forging Industry Educational and Research Foundation (FIERF), the Forging Industry Association (FIA) and additional individual industrial sponsors. The die materials considered in this study were categorized as follows:

- Hot-work tool steels: Proprietary grades developed specifically for warm and hot forging processes e.g. W360™ from Böhler-Uddeholm (www.bucorp.com), Thyrotherm™ 2999 EFS-SUPRA™ from Schmolz-Bickenbach (www.schmolz-bickenbach.com).

- Matrix high-speed steels (MHSS): MDS™ series from Nachi-Fujikoshi/Walter Metals (www.waltermetals.com), DRM™ series from Daido Steel (www.daidosteel.com).

- Coated/uncoated carbides and ceramics: Silicon Aluminum Oxynitride (Sialon), silicon nitride, tungsten carbide, etc.

- Welded overlays: Heat and wear resistant steels and super-alloys welded on top of hot-work tool steel substrates e.g. Hastelloy™ (www.haynesinternational.com).

Table 2.1 shows the example parts, which were selected in cooperation with the forge shops participating in this research study. The selected parts span different types of forging equipment and process conditions leading to varying die failure mechanisms.

Name	Description	Research Focus
Reverse piston (Case Study 1)	Axisymmetric disc shaped part with upsetting and extrusion on a mechanical press.	Thermal fatigue.
Turbine shaft (Case Studies 2 and 3)	Axisymmetric shaft with upsetting operation on a hydraulic press.	Thermal fatigue.
Automotive pinion (Case Study 4)	Axisymmetric part with warm extrusion on a mechanical press.	Wear
Control arm (Case Study 5)	Asymmetric part forged on a mechanical press.	Wear and excessive flash losses.

Table 2.1: Example production parts with die life problems (submitted by participating FIA member companies).

17

CHAPTER 3

TECHNICAL BACKGROUND

3.1. Introduction

As discussed in previous chapters, die costs make a significant contribution to the final part cost and profitability through direct and direct effects. Conventional methodologies employed by the forging industry to improve die life generally involve diffusion-based surface hardening treatments like nitriding, boriding, thermo-reactive diffusion, etc. on the selected tool steel. Additionally, the use of chemically and physically deposited coatings as well as welded overlays of super-alloys has also been explored. These techniques, though beneficial in reducing tool wear with conventional die materials, still do not provide satisfactory die life in today's competitive economy. Thus, tooling companies are continuously developing newer steel grades to target die life issues in specific forging processes. These materials include proprietary hot-work tool steels as well as matrix high-speed steels (MHSS). Ceramic and carbide materials (with or without coatings), which are an established technology in the machining industry, are also being considered for use in certain forging applications. Since tool-workpiece interface conditions in machining (high localized pressures and temperatures) far exceed those in forging in terms of severity, it is proposed that similar coating and insert technology could be transferred to the forging or extrusion industry to successfully improve die life.

In light of this background, this chapter summarizes some of the industrial and academic developments and on-going research in a) analysis of tool-workpiece interface conditions and their effect on die life, b) advanced tool material (steels, carbides, ceramics, etc.) and coating technologies for warm and hot forging, c) computational methods for prediction of die wear and die life, and d) characterization of tool and workpiece surfaces to analyze failure mechanisms.

3.2. Factors Influencing Die Life

In warm and hot forging processes, the process parameters (equipment characteristics, workpiece materials, lubrication), and the die material and surface treatments together determine the tool-workpiece interface conditions, which control the die failure mechanisms. Die failure can

18

be broadly classified as catastrophic failure, wear (abrasive and adhesive), thermo-mechanical fatigue (heat checking) and plastic deformation (thermal softening) [Knoerr et al, 1989; Dahl et al, 1998; Lange et al, 1992]. While it is common to have more than one type of failure mechanism occurring in a single die, wear has been found to be the dominant reason for failure in forging, accounting for up to 70% of tool failures in production [Cser et al, 1993].

Process parameters affecting wear in metal forming can be categorized as those related to a) the workpiece (material, geometry, preparation and heating), b) equipment (contact time and loading conditions), c) dies (material, manufacturing method, heat treatment, surface finish and coatings), d) lubrication and cooling, and e) process conditions (die temperature, transfer time, etc.) [Dahl et al, 1998]. During the preliminary stages of this research project, the effects of various factors, as well as the interactions between them, were identified using Ishikawa diagrams. These results are discussed in detail in Chapter 4.

3.3.   Characterization of Tool and Workpiece Surfaces

Analytical and computational methods have been developed using indentation tests (macro-, micro- and nano-scale) to determine the material properties and residual stress states in surfaces that have been modified by prior work-hardening or coating [Herbert et al, 2001; Haggag et al, 1993; Dao et al, 2001 and Chollacoop et al, 2003]. Techniques have been suggested to determine hardness from the maximum load, and Young's modulus from the initial unloading slope [Oliver et al, 1992]. An inverse analysis methodology has been developed to determine the material properties of surfaces modified by prior work-hardening, using micro-indentation tests [Morris et al, 2005a and b]. Both conical and spherical indentation tests were investigated as part of their study.

Several researchers have applied FE simulation to model the surface roughness of the die and workpiece in order to investigate their influence on the contact pressure and friction (Figure 3.1) [Saiki et al, 1997 and 2003; Klocke et al, 2002; Zhang et al, 2003; Mahrenholtz et al, 2005]. The solid lubricant in cold forging was also modeled in order to investigate the effect of the flow stress of the lubricant layer on tribological conditions at the die-workpiece interface [Saiki et al, 2003].

19
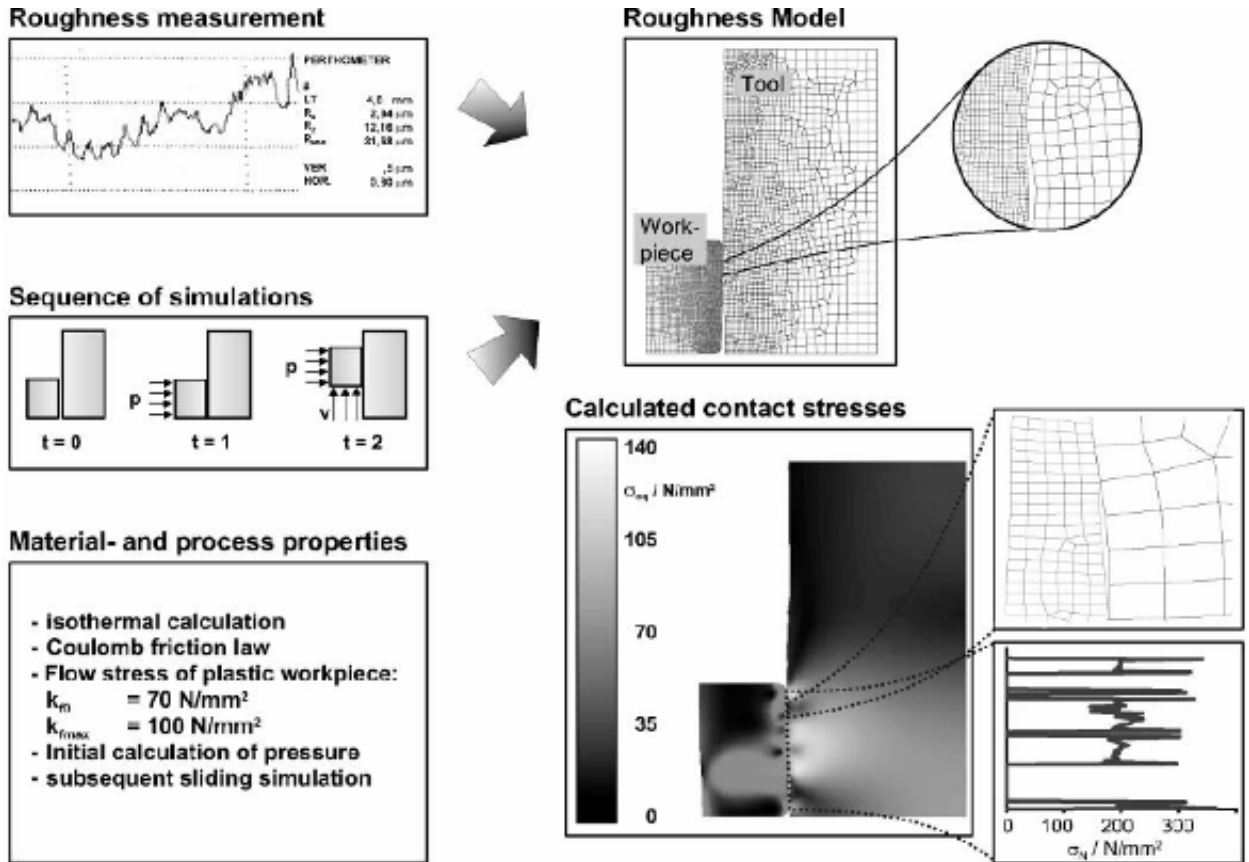
Figure 3.1: Simulation of die-workpiece contact, including the surface roughness [Klocke et al, 2002].

3.4. Tribological Evaluation of Tool Materials

Most of the laboratory-based testing done for evaluation of the tribological performance (friction and wear) of die-workpiece materials and coatings is restricted to scratch, ring/pin-on-disc and block-on-ring testing techniques [Salas et al, 2003; Lee et al, 2003; Bjork et al, 2001]. These tests are commonly used to determine the wear coefficients for use in wear prediction models. Besides friction and wear, these "tribotests" can also simultaneously evaluate coating adhesion in terms of the critical normal load required to strip-off the coating from the substrate. The Twist Compression Test (TCT), which is similar to the ring-on-disc test, has been commonly used in the stamping industry as a tribotest (Figure 3.2) [Dohda et al, 1989; Dalton et al, 1999; Gariety et al, 2003a and b; Schneider et al, 2006].

The wear profile generated is usually analyzed with optical micrographs, atomic force microscope (AFM), scanning electron microscope (SEM) or X-ray diffraction to a) quantify wear volume, and

b) analyze the wear pattern (cracks, delamination, etc.), especially with coatings [Müller, 2002; Mitterer et al, 2000 and 2001; Bjork et al, 2001; Navinsek et al, 2001; Salas et al, 2003; Dobrzanski et al, 2005]. SEM results were used to compare the adhesion properties of TiBN coating on substrates with and without a compound layer (Fe_4N) formed as a consequence of nitriding time and N_2 concentration [Müller, 2002]. Adhesion was found to be superior with a compound layer.

Alternative tests, specifically targeted towards forging, have also been developed to more realistically duplicate deformation conditions. The Ring Compression Test (RCT) and the Double Cup Extrusion Test (DCET) are routinely used for lubricant evaluation in forging. Spike forging tests, similar in geometry to exhaust valves, have been used for a more accurate evaluation of lubricants and ceramic-based coatings in cold, warm and hot forging [Nishimura et al, 1995 and 1996; Sheljaskow, 2001]. Other tests used for evaluation of die life and design of lubrication systems in hot forging include hot-ironing and spray lubrication, respectively [Sawamura et al, 2005; Tanaka et al, 2005].

a) Principle of the TCT   b) FE simulation of the TCT.
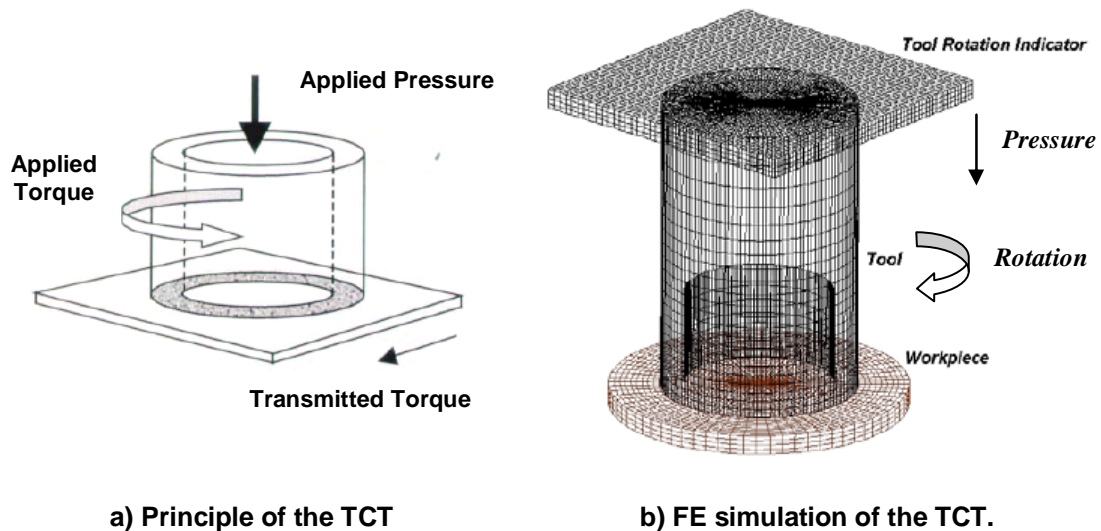
Figure 3.2: Principle of the Twist Compression Test (TCT) [Gariety et al, 2003a and b].

3.5.   Warm and Hot Forging Lubrication Systems

Oil-graphite emulsions or water-graphite suspensions are commonly used as lubricants in warm forging. However, increasing environmental concern has prompted the development of new lubricants to ensure better working conditions, reduced pollution and higher efficiency in the forging process.

21

A schematic of a warm forging set-up is shown in Figure 3.3. The billets/slugs are heated to a temperature between 90-160°C (195-320°F), which allows for the use of water-based coatings (graphite) [Sheljaskow, 2001]. The water evaporates leaving behind an adhesive coating. The billets are then heated to the forging temperature. Forging is carried out with the use of die lubricants. The main function of the slug coating is to prevent oxide/scale formation and decarburization besides serving as an additional lubricant during forging.
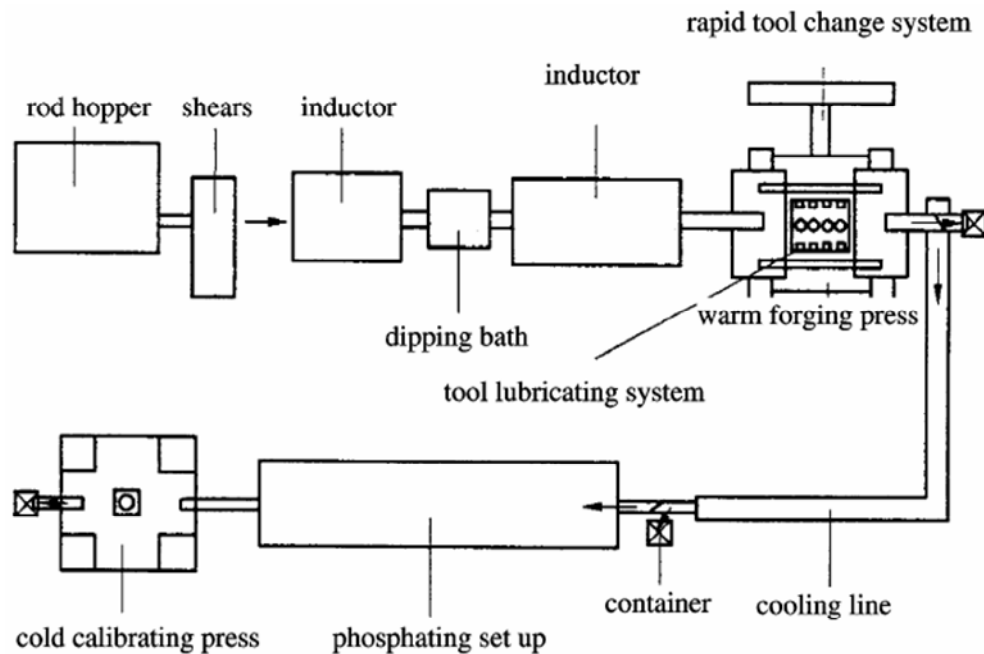
Figure 3.3: Typical warm forging line set-up [Sheljaskow, 2001].

A study was conducted for the development of new lubricants in cooperation with two lubricant suppliers (Acheson Colloiden B.V and Carl Bechem GmbH), a press manufacturer (Schuler GmbH), an environmental company (Fisia S.p.A, Italy) and three forging companies (Teksid S.p.A, Hirschvogel Unformtechnik GmbH and SNR Roulements, France) [Sheljaskow, 2001].

A spike forging test (Figure 3.4a) was used to evaluate the lubricant performance. Figure 3.4b shows the effect of having a slug coating in addition to the die lubricant. The lubricants developed as part of this project are shown in Table 3.1. An increase in mean tool life from 12,000 parts to 37,000 and 42,000 for the die and punch respectively, was observed in warm forging of continuous velocity joint (C.V.J) outer races. Recommendations were made on the applicability of the developed lubricants to different forging processes.

22
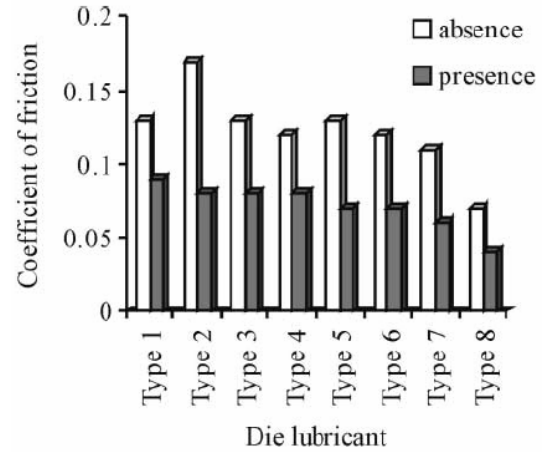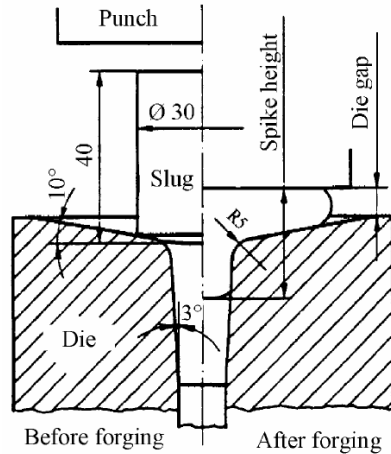
a) Die, slug and workpiece geometry for spike forging test.

b) Friction values in the presence and absence of a slug coating.

Figure 3.4: Lubricants developed for warm forging [Sheljaskow, 2001].

Acheson Colloiden B.V.	
Slug coating	
Deltaforge™ FB-400	A graphite/water-based slug coating for warm forging operations with excellent coating and lubricating properties and temperature stability up to the highest temperatures of warm forging
Die lubricants	
Deltaforge™ F-400	A graphite/water-based die lubricant. It is a further improvement of Deltaforge 31, the most widely sold hot forging die lubricant with lower ammonia content. It has also better redissolving characteristics of dried out material (easy wash-off)
Deltaforge™ F-410	A graphite/water-based die lubricant with similar characteristics as Deltaforge™ F-400 however, a lower film forming temperature capability and better performance for difficult forward extrusion operations
Deltaforge™ F-405	A synthetic graphite-free oil-based die lubricant to be used in combination with the slug coating Deltaforge™ FB-400
Deltaforge™ F-401	A graphite-free water-based lubricant and further improvement of Acheson's well known lubricant in hot forging Deltaforge™ 1105M
Carl Bechem GmbH	
Slug coatings	
Berulit™ 935	A graphite/water-based slug coating for warm forging operations with excellent lubricating properties and good film and anti-oxidation characteristics up to the highest temperatures in warm forging
Berulit™ 932	A stable graphite/water-based slug coating for warm forging operations. It shows a uniform wetting of slugs also at lower temperatures using in dipping baths
Die lubricants	
Berulit™ 625/1	An ester-based, graphite-free emulsion for warm forging operations. It is especially developed for lateral extrusion and production of bevel gears
Berulit™ 630	An ester-based emulsion with a high emulsion stability, also in combination with selected slug coatings
Berulit™ 392	A white dry film forming, graphite and oil-free solution, to be used for moderately severe forging operations up to die temperatures of 280°C
Berulit™ 396EP	A synthetic water soluble and graphite-free die lubricant with good release properties, to be used for severe operations up to die temperatures of 360°C
Beruforge™ 393	A synthetic, graphite-free water soluble die lubricant, to be used in warm forging operations in a die temperature range between 130 and 280°C

Table 3.1: Lubricants developed for warm forging [Sheljaskow, 2001].

23

3.6. Prediction of Die Wear

The majority of predictive models are based on Archard's equation, which defines wear volume (W_V) as a function of normal pressure (P_N), sliding distance (D_S) and local hardness (H) [Archard, 1953; Holm, 1946; Dahl et al, 1999].

$$W_V = K * \frac{P_N * D_S}{H}$$

Equation 3.1

where, K = experimentally determined wear coefficient.

FE simulations have been used for predicting wear in forging using Archard's equation as the starting point. The basic concept is to determine the process conditions from a single simulation and then use these as an input to the wear prediction equations [Vardan et al, 1987; Painter et al, 1995]. The commercial code DEFORM™ uses a wear prediction technique based on research conducted at OSU on the application of Archard's equation [Painter et al, 1996]. The model can be stated as follows:

$$Z = K \frac{p^a * V^b * \Delta t}{H_d^c}$$

Equation 3.2

where

Z = wear depth (in)

K = wear coefficient (a dimensionless parameter)

a, b = experimentally determined coefficients (assigned a value of unity for steel based on empirical data)

c = hardness coefficient (recommended value of 2 based on empirical data)

p = local normal pressure (ksi)

V = local sliding velocity (in/sec)

H_d = die material hardness as a function of die temperature (ksi)

Δt = time interval (sec)

In its discretized form, the model can be stated as follows:

24

$$Z_i = \sum_{j=1}^{M} \Delta Z_{ij} = K \sum_{j=1}^{M} \frac{p_{ij}.V_{ij}.\Delta t}{H_{ij}} \quad \text{with i = 0 to N.}$$ Equation 3.3

where

Δt = the user defined time step (seconds) which will be used for the wear calculation during the simulation. This is usually selected based upon smallest element edge length in order to avoid excessive remeshing.

M = the total number of user-defined calculation steps. This is usually selected based upon the process duration or punch stroke and the smallest element edge length.

N = the total number of boundary nodes on the die surface in contact with the workpiece.

i = the ith node on the die surface.

j = the jth time step.

p_{ij}, V_{ij}, H_{ij} = nodal pressure (ksi), velocity (in/sec) and hardness (function of nodal temperature) at jth time step.

ΔZ_{ij} = the incremental wear depth (inches) calculated for the ith node at the jth time step during the simulation.

Z_i = accumulated wear depth (inches) calculated as a summation of the incremental wear depths.

The goal behind including a wear model and prediction method in a commercial FE code is to enable the engineer to forecast die life in the design stage and select the appropriate die design and forging process parameters. With regard to this objective, the current prediction technique in DEFORM™ has the following limitations:

- Wear coefficient K requires calibration: In its current format, the wear coefficient K has to be estimated based on process data (wear profile) available for the geometry being forged. The wear coefficient is then calibrated until an acceptable match is obtained with experimental data for the current process. This is done by measuring the die wear profile using a CMM and comparing it to that predicted by DEFORM™ using some initial guess for the wear coefficient. This validated FE model can then be used to modify the die design and predict die wear (die life) for different design modifications.

25

- Wear coefficient K is a constant: The wear coefficient is currently taken to be constant for all the boundary nodes irrespective of the interface conditions at the die-workpiece contact region. A common wear coefficient is used for all boundary nodes without taking into account a) the change in friction with deformation and surface expansion, b) the local temperature of the node, and c) the surface modification (material property gradient) of the die.

- Uniform starting temperature for the die: The issue of local nodal temperatures brings to the forefront the practice of using a uniform pre-heat die temperature for the forging simulation. This may be acceptable for analysis of overall metal flow but introduces an error into wear calculations. As part of the current research study, FE simulations of an entire forging cycle (i.e. one revolution of the ram, plus cooling) were conducted in order to obtain the die temperature distribution at start-up and steady-state production. The die surface temperatures were found to vary between 60-80% of the initial pre-heat temperature prior to the start of the next forging stroke. Thus, the assumption of a uniform die temperature is not valid, especially for the surface layers of the die.

- Interface conditions: In general the die-workpiece contact conditions are influenced by the friction, normal pressure, sliding velocity, interface heat transfer coefficient and the temperatures of the contacting pair. The current approach of using constant friction and heat transfer thus, affects the accuracy of the wear prediction technique.

- Tool life prediction: The accumulated wear depth at each location is scaled up linearly by the number of forging cycles to compare wear profiles with the corresponding production data available. On the other hand, to predict tool life, a pre-determined critical wear depth can be specified to DEFORM™ based upon production part tolerances. Given the wear amount at each discrete die location (node) , it is possible to predict the die life for the given location in terms of number of parts forged until the specified critical wear depth is reached.

- Hardness data for the die: Currently, the hardness of the die material is expressed as a function of temperature alone. The holding time at elevated temperature does not get considered in the analysis i.e. the tempering effect (thermal softening) is ignored. In order to accurately forecast die life, the tempering curves for the die material need to be included in the analysis.

- Uniform die material properties: Surface modification of the die material results in a material property gradient and also a change in the tribological performance of the die

26

surface. At present the die material is assumed to have uniform hardness in the surface layers; this value is assumed to be the same as the bulk heat-treated hardness of the die. Research has been done to determine the wear coefficients for a die material with different surface treatments using pin-on-disc tests [Kang et al, 1999a and b].

- Die geometry updating: Updating the tool geometry is not a critical issue for the current format of the wear prediction technique since only one simulation is conducted and wear values are scaled linearly to predict die wear and die life after multiple forging cycles. Unlike the simulation of machining processes, it is not practical or feasible to update the die geometry during the simulation of a single forging step. However, if for instance, an iterative simulation approach is adopted to predict die life, geometry updating will be essential for each subsequent simulation step. In such a case, forging simulation would be repeated with updated die geometries until the calculated wear depth matches the specified critical wear depth at any given node. Thus, the final output would be a) the worn tool geometry and b) number of forging cycles till die failure. Also the earlier mentioned issue of die material properties becomes crucial as the geometry is updated. If the die material properties and wear coefficients are specified as a function of depth, appropriate values for each of these would be used for the die surface as the geometry is updated.

Some of the recent studies into die life prediction in warm and hot forging have taken into account the reduction in the surface hardness of the die due to thermal softening over subsequent forging cycles. Wear depth was predicted using a modified form of Archard's equation with hardness represented as a function of temperature and time [Kim et al, 2005a and b; Kang et al, 1999a and b]. A modified version of Archard's equation was also used for predicting die wear in warm forging [Lee et al, 2003]. The wear coefficient and the hardness were expressed as functions of temperature, and were estimated using ring-on-disc and hot hardness tests, respectively. While the results from these studies match production data qualitatively, a consistent quantitative match was not obtained. Consequently, alternative approaches have also been explored. Archard's model was compared to an alternative model based on the energy dissipated on the tool-workpiece interface [Stahlberg et al, 1999]. A wear model based on the relationship between calculated die loads and degree of wear observed in actual manufacturing has been suggested by [Tanaka et al, 2005]. Application of neural network with FEM has also been explored [Tercelj et al, 2003]. [Doege et al, 2004] used a design of experiments (DOE) technique with FE simulation of backward can extrusion, in order to model the friction and heat transfer as functions of normal pressure and sliding velocity instead of assuming them as constant.

27

Tool wear in machining has also been investigated intensively. A continuous cutting simulation technique was used with Usui's adhesive wear equation and geometry updating to predict tool wear in machining [Usui, 1982; Yen et al, 2004a]. Accurate prediction of tool wear also requires that the thermal effect of tool coatings be considered in the forming simulation [Yen et al, 2004b]. In machining, this was done by a) modeling the coating/coatings as individual layers on the tool substrate or b) by providing a gradient in thermal and mechanical properties of the tool substrate corresponding to the approximate thickness of the coatings.

3.7. Advanced Die Materials and Surface Treatments

A wide variety of surface treatments and coatings are employed to increase wear resistance and die life in warm and hot forging. These methods include diffusive processes (nitriding, boriding, thermo-reactive diffusion, etc.), weld overlays, physical and chemical vapor deposition, as well as a combination of these processes, known as duplex treatments [Babu et al, 1999 and 2004; Salas et al, 2003]. One of the recent developments in surface modification has been molybdenum disulphide (MoS_2) and graphite powder coating for cold and warm forging, respectively [Hanada et al, 2004 and 2005]. The modified and hardened surface layer of approximately 1.5µm was found to enhance lubrication in ring compression and extrusion tests in the warm forging temperature range.

Advanced hot-work tool steels manufactured using vacuum arc re-melting (VAR) and special heat treatments guarantee a high level of micro-cleanliness, which can delay the onset of thermal fatigue. Matrix-type high speed tool steels have also been developed for warm and hot forging applications, with and without additional surface treatments. These steels have high initial hardness values ranging from 58-66 HRC and are produced by electro-slag re-melting (ESR) [Nakahama et al, 2005; Tamura, 2006]. They are characterized by their more finely dispersed carbides, and higher toughness and fatigue strength than conventional steels.

A number of researchers have studied the application of ceramic die materials and PVD/CVD coatings in forging and extrusion [Doege et al, 1994, 2001a, b and c; Salas et al, 2003; Bjork et al, 2001; Klimek et al, 2003; Müller, 2002; Navinsek et al, 2001; Behrens et al, 2005b and c]. Ceramic die materials include alumina (Al_2O_3), silicon nitride (Si_3N_4), silicon aluminum oxynitride (SiAlON), stabilized zirconias (ZrO_2), etc. Commonly used coatings are TiN, [(Ti, Al) N], CrN, TiB_2, etc. either as monolayer, multilayer or duplex coatings (i.e. with a prior gas or plasma nitriding surface treatment). The effect of a duplex treatment on coating wear performance has been investigated in numerous studies [Cooke et al, 2004; Salas et al, 2003; Klimek et al, 2003]. Nitriding was found to enhance the performance of the coating by providing a gradual transition

28

from the mechanical and thermal properties of the substrate to that of the hard coating. Another advantage of the duplex process was found to be improved adhesion of the coating.

3.7.1. Case Study 1: Application of Multi-Layer Coatings in Hot Forging

Preliminary studies conducted at the Institute of Metal Forming and Metal Forming Machine Tools (IFUM), University of Hannover compared the performance of multi-layer hard coatings to ceramic die inserts in hot forging processes such as the one shown in Figure 3.5.
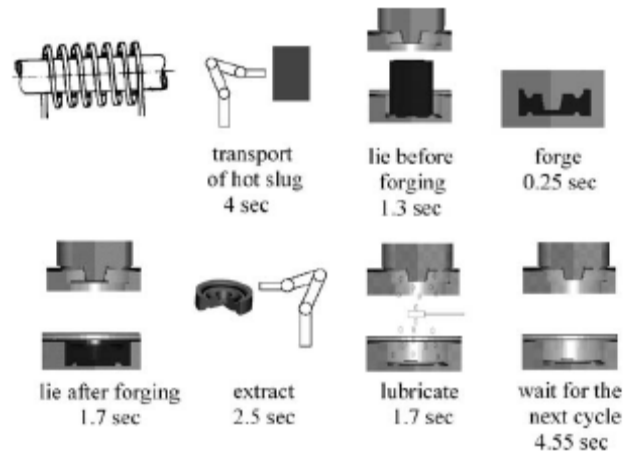
Figure 3.5: Example hot forging process cycle [Behrens et al, 2005a].
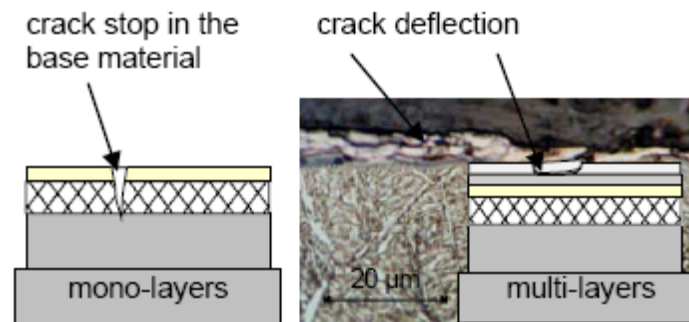
Figure 3.6: Comparison of performance characteristics of mono (single) and multi-layer coatings [Doege et al, 2001].

Single-layer ceramic coatings were investigated extensively and were found to be susceptible to cracking and delamination due to thermal fatigue [Doege et al, 2001a and b]. Multi-layer coatings are expected to deliver better performance by a) providing a gradual transition in thermal and

29

mechanical properties, and b) by deflecting the crack propagation at the inter-layer transitions (Figure 3.6).

All of the coatings were used with a nitrided substrate material, and can therefore be considered as duplex coating systems. The nitriding and coating was done in a continuous plasma-assisted chemical vapor deposition (PACVD) process at 500℃ (930℉). The factors which affect coating performance are a) the type of layers selected, b) the number of coating layers, and c) the thickness of each layer. Coating systems comprising of 3, 9, 18 and 27 layers (1.7µm, 2.4µm, 3.4µm, 5.4µm, respectively) were investigated on hot-work tool steels (H10/DIN 1.2365 or H11/DIN 1.2367) with nitriding depth of approximately 150µm (Figure 3.7).
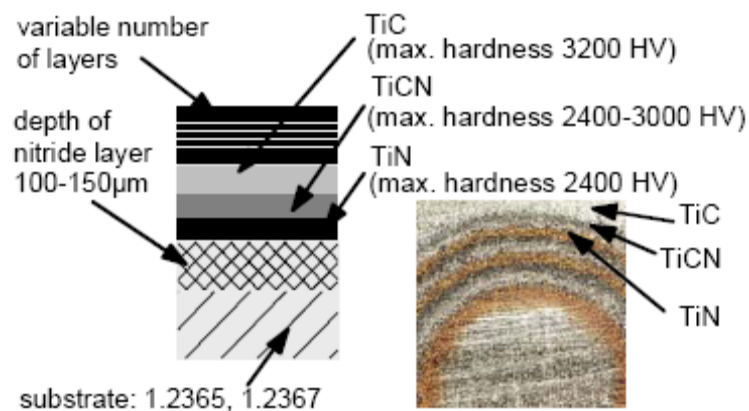
Figure 3.7: Multi-layer duplex coating systems used for hot forging trials [Doege et al, 2001].

Preliminary hot forging tests were conducted with simple cylindrical upsetting using flat dies (pancake shape), followed by axisymmetric dies with flash (Figure 3.8). The forging process set-up was similar to that shown in Figure 3.5 with an overall cycle time of 13 seconds from billet heating to end of forging. Dies were heated to a temperature of 200℃ (390 °F) with an integrated heating system, whereas billets were induction heated to 1150℃ (2100 °F). Multi-layer duplex coatings showed a reduction in die wear of approximately 70% compared to simple nitrided dies (Figure 3.9; number of cycles not specified). The same die geometry was also used for trials with ceramic dies using a cone-shaped insert-based design as shown in Figure 3.8 (discussed in next section).

30
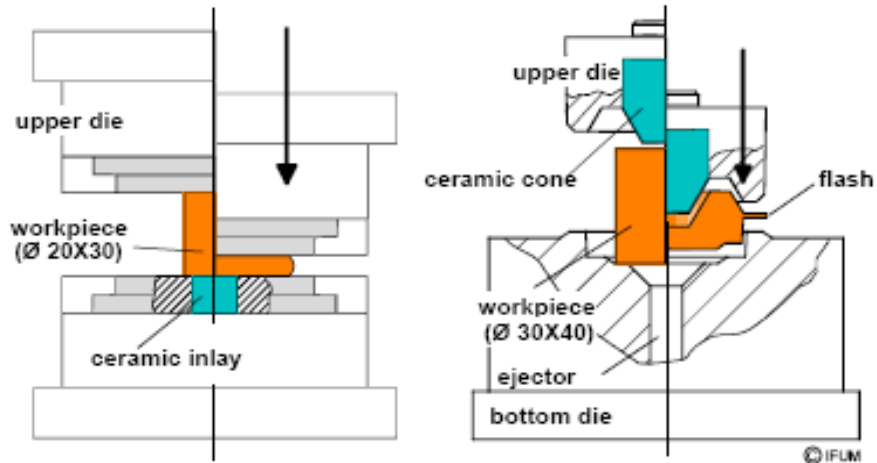
Figure 3.8: Test geometry: left upsetting, right cone die [Doege et al, 2001b].
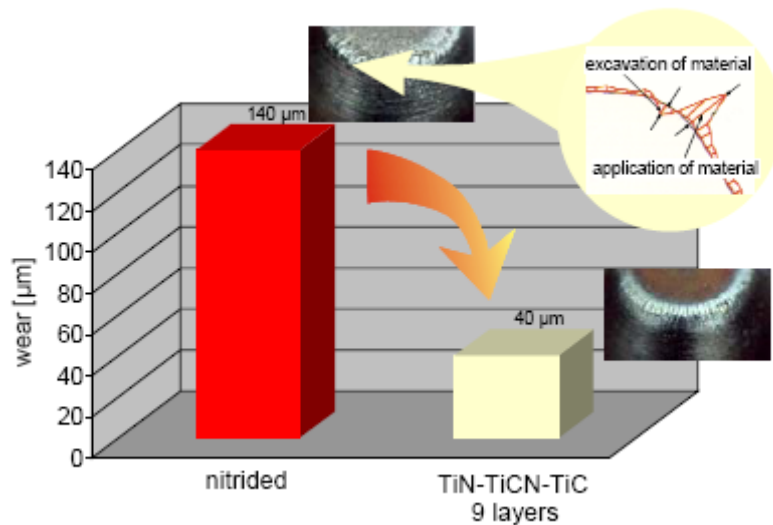
Figure 3.9: Wear reduction on dies with flash [Doege et al, 2001b].

3.7.2.   Case Study 2: Application of Ceramic Inserts in Hot Forging

For investigations with ceramic inserts, two assembly techniques were explored as shown in Figure 3.10a. Of these two techniques, brazing is more flexible since it allows the application of inserts in complex tool geometries in wear critical areas. One of the drawbacks of this method, however, is the residual stresses generated from brazing. Thermal shrinking on the other hand is better suited for axisymmetric geometries. The different insert geometries investigated are shown

31

in Figure 3.10b. The effect of different interference fits and preheat temperatures was not investigated in these studies.

Figure 3.11 shows the wear performance for the ceramic dies compared to nitrided hot-work tool steel for two different forging (workpiece) temperatures after 500 forging cycles. Silicon nitride showed superior wear resistance (3 to 6 times less wear) among the die materials selected.
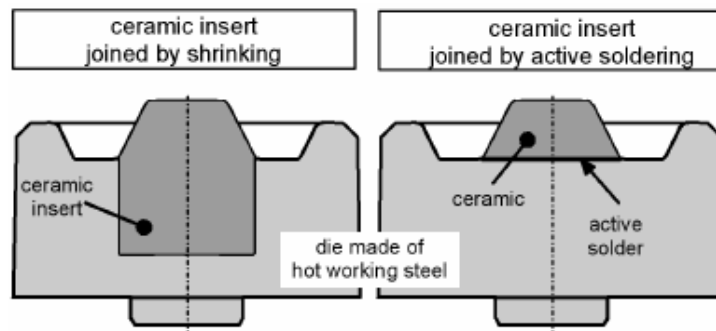
a) Two types of insert design investigated viz. shrink-fit and brazed.
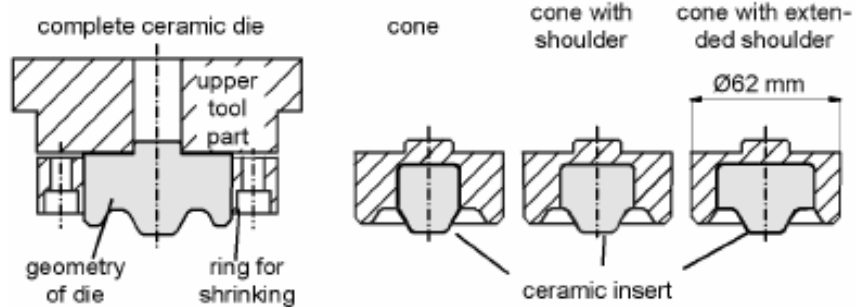
b) Different types of shrink-fit designs investigated in forging trials.

Figure 3.10: Die designs investigated in forging trials with ceramic inserts [Behrens et al, 2005b].

32
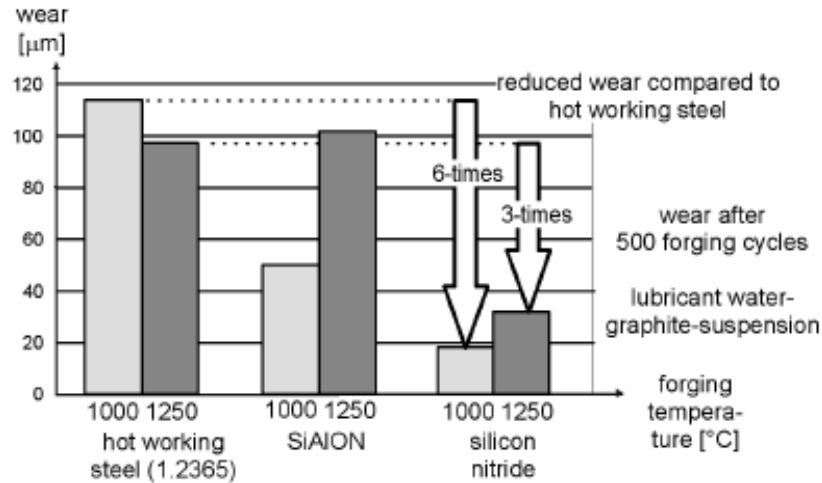
Figure 3.11: Performance of ceramic die materials in forging trials [Behrens et al, 2005b].

It was observed during the trials with active brazed inserts that solder quality has to be controlled consistently in order to prevent premature failure of the die in service. A hot forging die with 16 inserts was being considered for precision forging of spur gears (Figure 3.12). Results from these trials are not currently available.
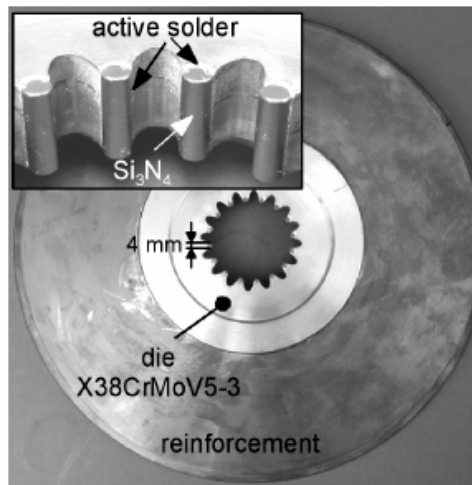
Figure 3.12: Die with ceramic inserts for precision hot forging of spur gears [Behrens et al, 2005b].

3.7.3. Case Study 3: Successful Application of Ceramic Dies in Mass Production

There have been cases of successful production application of cermet/ceramic dies in Japan. These publications were in Japanese and only provided limited information.

33

Nissan Motor Co. is using cermet dies made of MoB (ceramic). The material is powder formed and sintered. In production tests, two die materials were tested on forward extrusion of outer race part under warm forging conditions (Figure 3.13), namely, a) nickel-based superalloy, and b) MoB cermet.
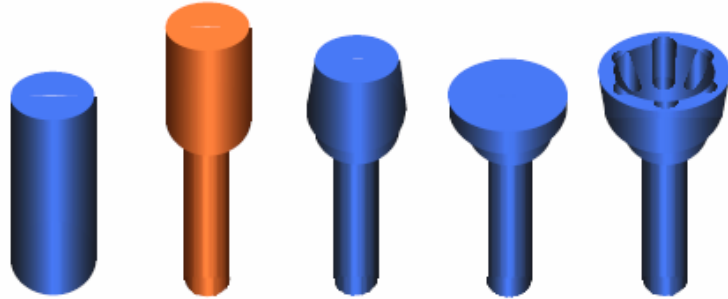
Figure 3.13: Forward extrusion of outer race part [Mitamura et al, 1999].

Figure 3.14a shows the high temperature strength of the two die materials. Though the axes are not labeled, it can clearly be seen that MoB cermet die can withstand higher temperature (800°C/1470°F) than the superalloy. Figure 3.14b sh ows die seizure observed with the superalloy material.
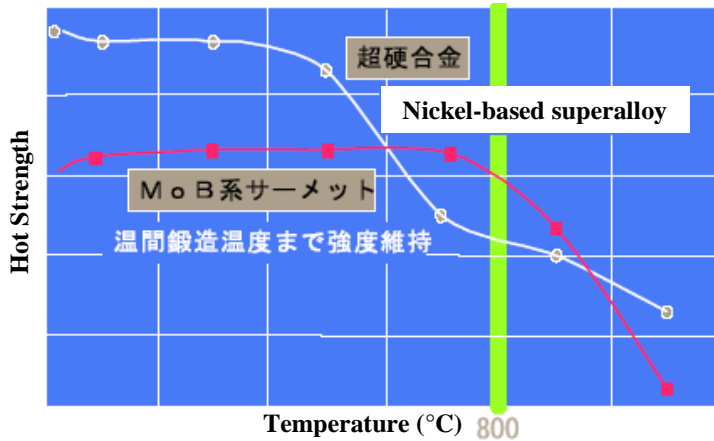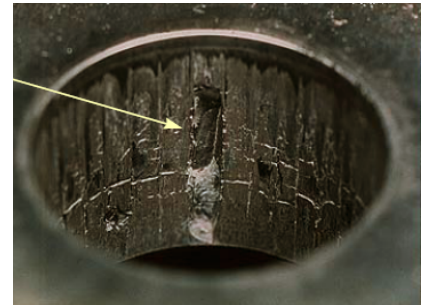
(a)   (b)

Figure 3.14: Forging tests with superalloy and cermet materials. a) Influence of warm forging temperature on the strength of die material, b) Dies seizure when super alloy dies were used [Mitamura et al, 1999].

34

In their study, Nissan also tried to quantify crack formation as seen in Figure 3.15. The values however are not given. As can be seen in the figure superalloy dies lead to high formation of cracks. However, with MoB cermet dies the formation of cracks is minimal. The authors also state that by using MoB cermet the tooling price per part was reduced by 40%. Die life improvements of 2:1 were observed in production.
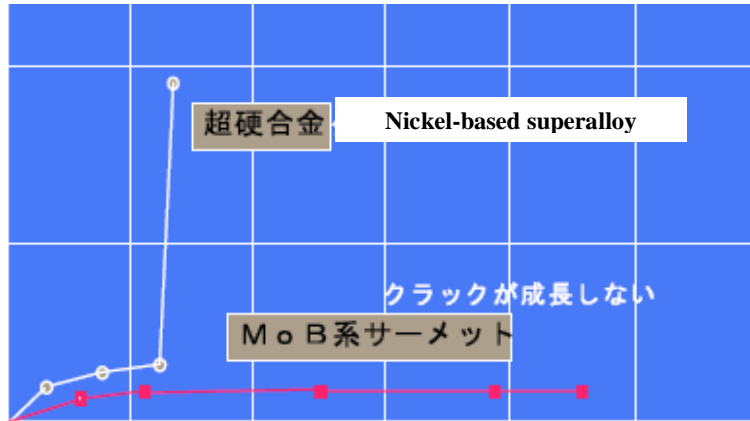
Figure 3.15: Crack formation characteristics between the two die materials [Mitamura et al, 1999].

Figure 3.16 shows the application of ceramic dies in hot forging of exhaust valves using two different insert-based die designs. The insert were made of alumina.
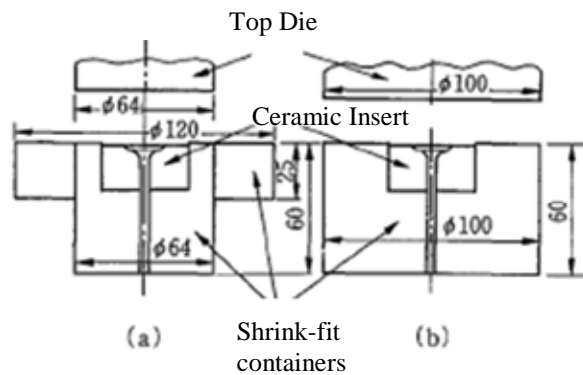
Figure 3.16: Die designs used for application of ceramic inserts [Koitabashi, 1995].

Figure 3.17 shows two shrink-fitted hot forging die design examples using ceramic and cermet die inserts with shrink-rings made of hot-work tool steel. Both die designs were implemented in production and involved in-depth experimental analyses of the effect of preheat and forging

35

temperatures on the interference fits at the shrink ring interfaces. It was found that the thermal expansion from preheating and forging had a significant measurable effect on the pre-stress from shrink-fitting. For the Ti alloy preforms, an 82% reduction in shrink-fit was observed after preheating to a temperature of 540°C (1000°F) with just the inner shrink ring (5 in Figure 3.17a). With the outer shrink ring installed a 47% reduction was observed [Iwase et al, 1999]. These examples demonstrate that the use of room temperature dimensions and shrink-fit values for analysis of hot and warm forging tooling can lead to incorrect judgments.

a) Ti alloy valve preforms [Iwase et al, 1999].   **b) Hot forging [Horie et al, 1995].**
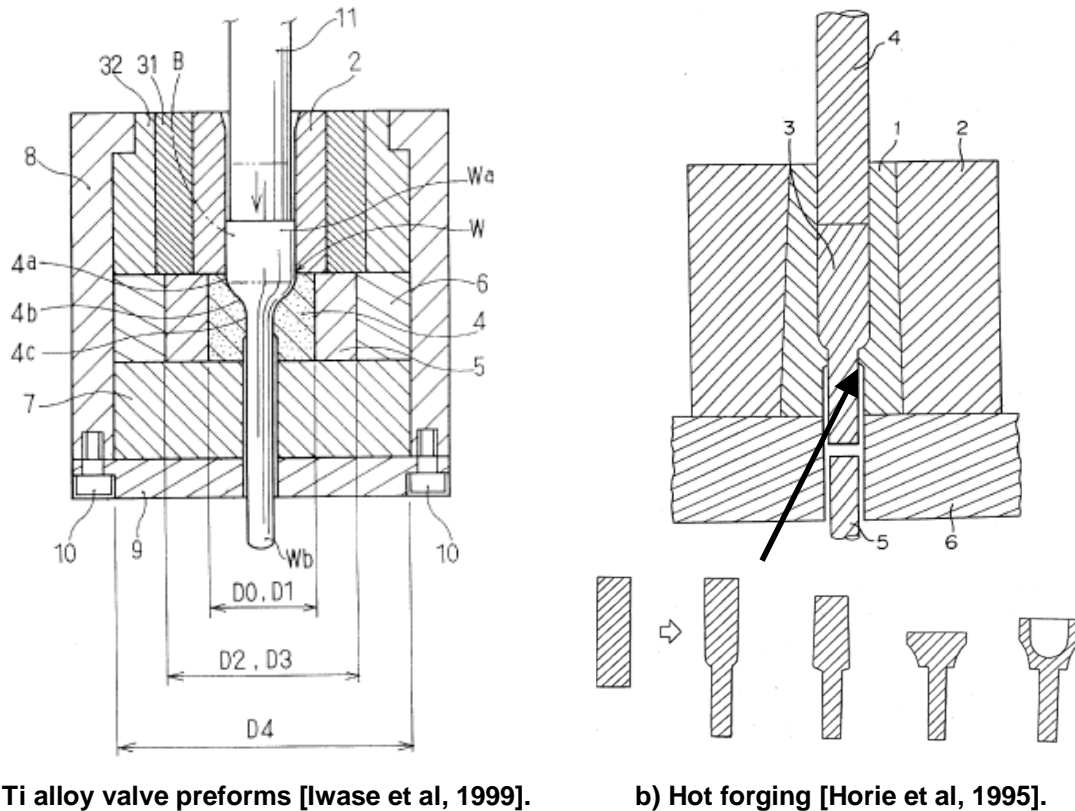
Figure 3.17: Shrink-fit die designs for hot forging with ceramic and cermet inserts.

3.7.4. Case Study 4: Development and Application of Proprietary Hot-work Tool Steels for Warm and Hot Forging

Hot forging dies are subjected to a repeated thermal cycle as shown in Figure 3.18. These repetitive cycles result in softening of the surface layers of the die material, thus accelerating the onset of wear and thermal fatigue. Figure 3.19 shows the microstructure of a hot forging die after a single forging stroke. A white layer of fine-grained martensite is observed at the radius with a thickness of approximately 100 μm. This zone increased to about 200 μm in the subsequent 100 forging cycles.

36
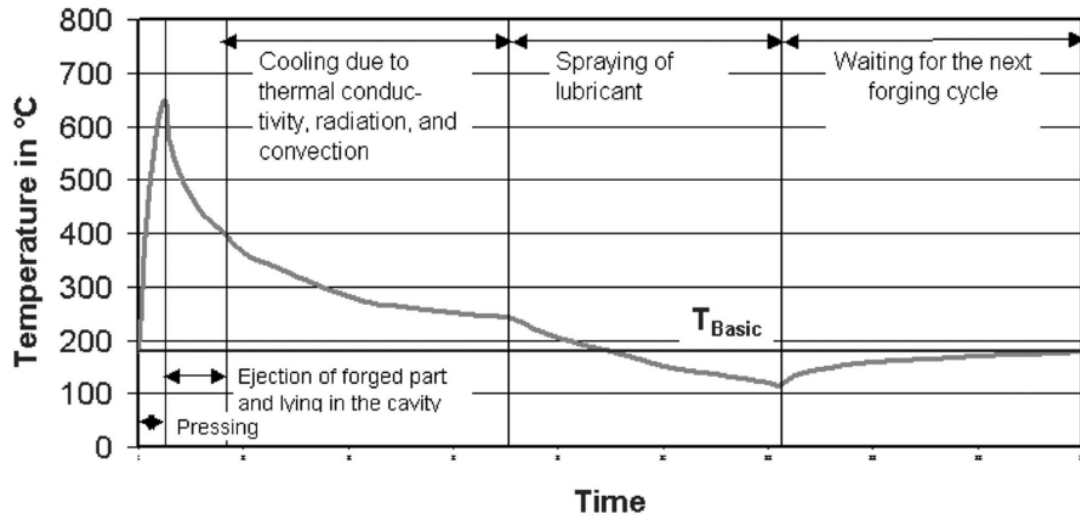
Figure 3.18: Thermal cycle experienced by hot forging dies [Brockhaus et al, 2002].
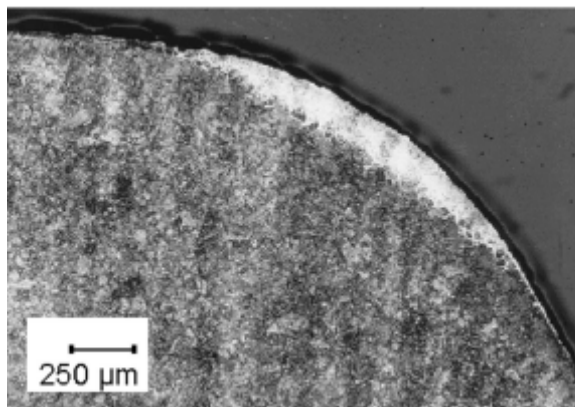
**Figure 3.19: Formation of white layer in the forging die surface after one stroke
[Brockhaus et al, 2002].**

Figure 3.20 shows the hardness of the die as a function of depth at different stages of production. It was observed that the first forging cycle resulted in an increase in hardness due to formation of untempered martensite. The subsequent forging operations result in thermal softening of the die surface layers as seen by the minimum hardness at approximately 80 μm from the die surface.

37
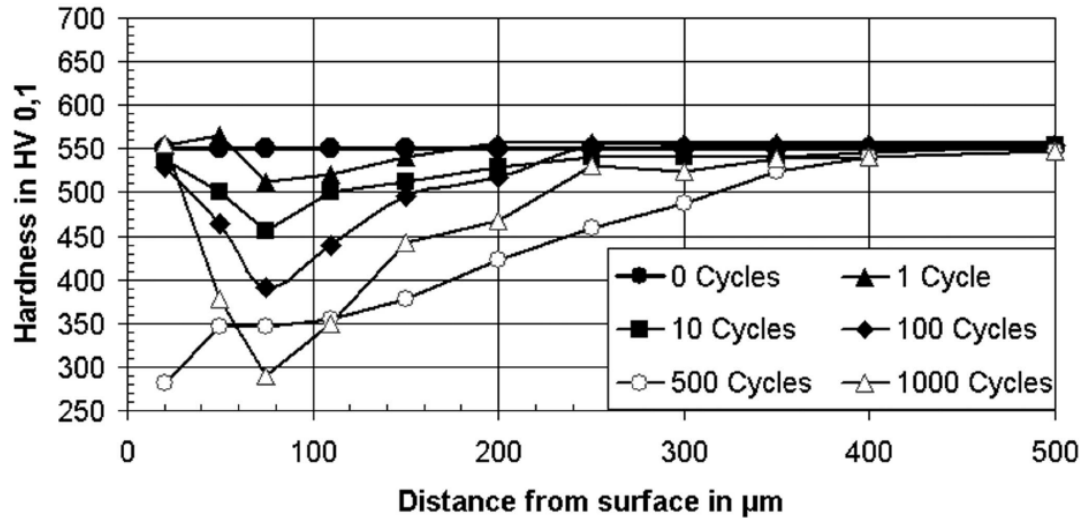
Figure 3.20: Hardness gradient in the die surface layers at different stages of production [Brockhaus et al, 2002].

The hot-work steel Thyrotherm™ 2999 EFS SUPRA (Schmolz-Bickenbach) was developed to deliver improved die life in forging processes that required high hot hardness and thermal conductivity. This steel grade was subjected to extensive independent trials at the University of Hannover and other forge shops with a wide range of equipment and process parameters. The results from these studies are summarized in this section. Figure 3.21 shows a comparison of the tempering response of the Thyrotherm™ steel grade against some commonly used hot-work tool steels. Similarly, this grade also has higher hot hardness and thermal conductivity compared to the other hot-work tool steels. Following initial trials at University of Hannover, production trials of this steel were conducted under various process conditions.

Trial 1: Hammer and Press Forging Processes

These tests included applications with low alloy steels, austenitic stainless steels and through-hardening bearing steels. An average improvement of 50 to 60 % was obtained with the new steel grade in most processes where a standard H-11 or H-13 die was being used in the nitrided condition. In some cases, the Thyrotherm™ grade, in a standard hardened and tempered condition, delivered comparable performance to a hot-work tool steel being used with an expensive nitriding and cladding technique.

38
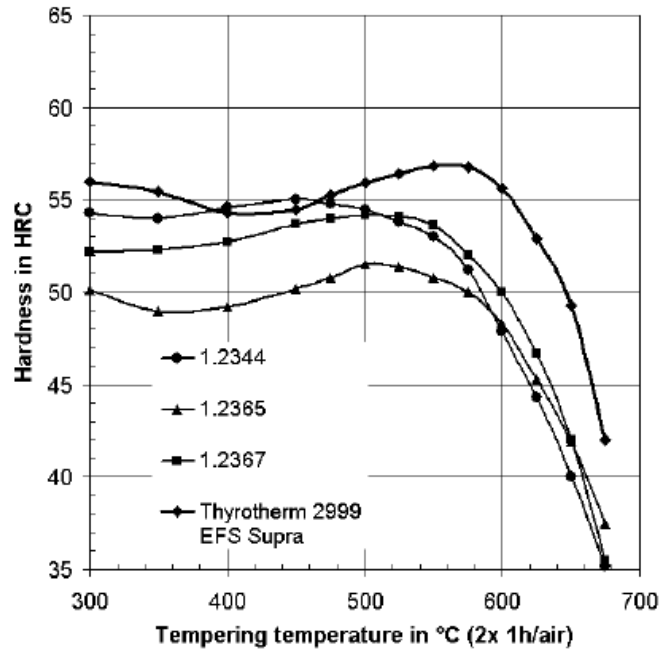
Figure 3.21: Temper resistance of Thyrotherm™ 2999 compared to commonly used hot-work steel grades [Brockhaus et al, 2002].

Trial 2: High Speed Forging Processes

High speed forging refers to hot forging processes carried out on horizontal forging machines (Hatebur™, Sakamura™, National™, etc.) with high production rates of 100-200 parts/min with intensive water cooling. The Thyrotherm grade was used as a replacement for the commonly-used H-10 hot-work tool steel. The results from these trials are summarized in Table 3.2.

Hot-work tool steels intended for hot forging applications are often used in warm forging processes. However, these steels lack the hardness and wear resistance necessary to withstand the high forming pressures encountered in warm forging. Cold work tool steels and cemented carbides similarly find limited application due to lack of toughness and hot hardness.

Most of the proprietary tool steels developed for warm forging have at least one of two disadvantages: either austenitizing must be carried out at a high temperature to achieve the high hardness, or the high hardness has been achieved at the expense of toughness, meaning that thermal shock can cause the material to crack.

The W360 grade was thus developed with the goal of achieving a high hardness (58 HRC) with a hardening temperature of 1050-1070°C (1920-1960°F). Table 3.3 gives the composition of this

39

steel compared to other Böhler-Uddeholm hot-work tool steels and a cold forging high speed steel.

Case	Hot-work Tool Steel / Condition	Previous Tool System	
		Hardness in HRC	No of Forged Parts
1	1.2365 nitrided	47	13,000
2	1.2365 ESR nitrided	53	17,000
3	1.2365 nitrided	52	20,000
4	1.2365 nitrided	50 - 52	4,000
5	1.2365 case-hardened + nitrocar-burized	54 - 57	7.600 Failure: spallings

Case	Thyrotherm 2999 EFS SUPRA			Improvement of Performance	
	Condition	Hardness in HRC	No of Forged Parts	No of Forged Parts	%
1	nitrided	47	17,500	4,500	35
2	nitrided	53	23000	6,000	35
3	hardened+ tempered	52	33,000	13,000	65
4	nitrided	54	10000	6,000	150
5	plasma nitrided	53	11000	3,400	45

Table 3.2: Summary of high speed forging trials with Thyrotherm 2999™ [Brockhaus et al, 2002].

Steel	Grade	C	Mn	S	Cr	Mo	V	W	Co
W303 ISOBLOC	1.2367	0.38	0.40	0.40	5.0	2.8	0.65	—	—
W321 ISOBLOC	~1.2885	0.39	0.30	0.35	2.9	2.8	0.65	—	2.9
S600	1.3343	0.90			4.1	5.0	1.8	6.4	—
W360	—	0.50	0.20	0.20	4.5	3.0	0.55	—	—

Table 3.3: Tool steels selected for benchmarking studies [Fisher et al, 2002].

The following criteria were selected for benchmarking the new tool steel:

- Hardening and tempering behavior (Figure 3.22).
- Toughness at room temperature and above (Figure 3.23).
- Hot hardness and retention of hardness (Figure 3.24).

40

The laboratory testing shows the superiority of W360™ compared to the conventional tool steels. However, data on the performance of this steel in production trials was not provided. This steel was used in forging trials as part of the research presented in this study.
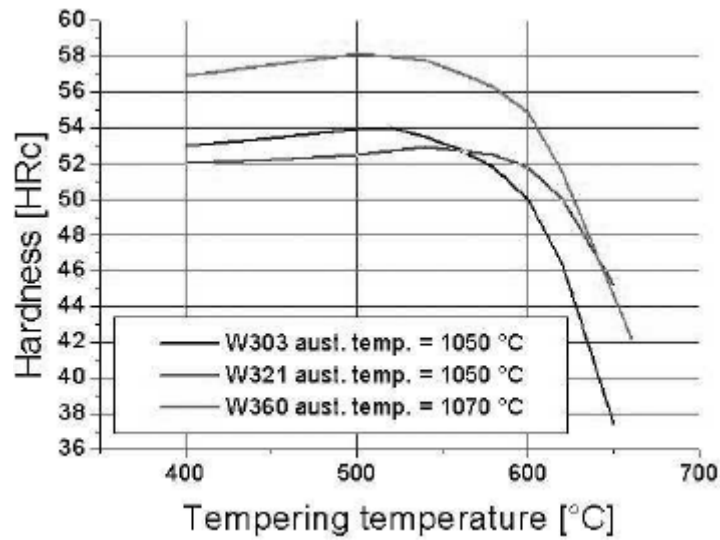
Figure 3.22: Tempering curves of W360™ compared to conventional hot-work tool steels [Fisher et al, 2002].
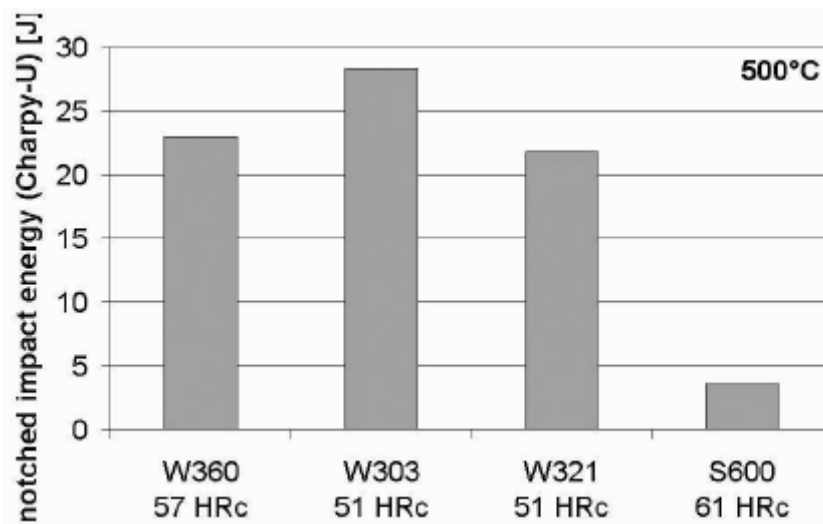
Figure 3.23: Toughness of W360™ at elevated temperature [Fisher et al, 2002].

41
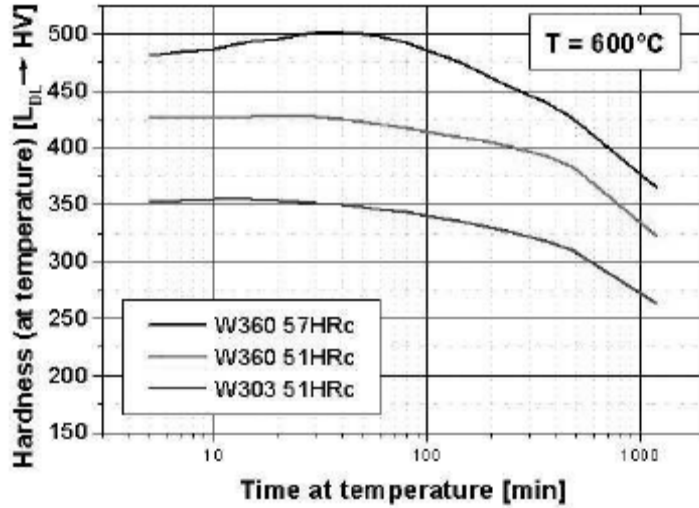
Figure 3.24: Hot hardness of W360™ measured at 600°C as a function of time spent at temperature [Fisher et al, 2002].

3.7.5. *Case Study 5: Impact of Heat-treatment on Thermal Fatigue Resistance of Tool Steels*

In order to withstand thermal fatigue a material should have low coefficient of thermal expansion, high thermal conductivity, high hot yield strength, good temper resistance, high creep strength, adequate ductility and toughness. Significant research on thermal fatigue properties of die materials has been conducted using laboratory-based testing [Persson et al, 2004 and 2005; Sjoestroem et al, 2004 and 2005; Starling et al, 1997]. Thermal fatigue properties of a hot-work tool steel (Uddeholm Dievar™) with different austenitizing treatments were evaluated using the test set-up shown in Figure 3.25 [Sjoestroem et al, 2004]. Four austenitizing temperatures were used (Table 3.4) with subsequent tempering treatments that resulted in the same final hardness for the test specimens. The thermal fatigue test conditions used are typical for die-casting processes (Table 3.5), however, the qualitative effect of heat treatment parameters on thermal fatigue behavior is applicable to hot forging processes as well.

42
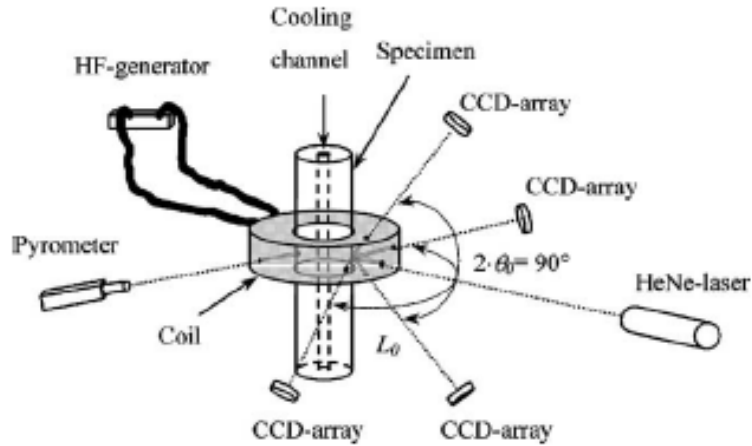
Figure 3.25: Thermal fatigue test rig [Sjoestroem et al, 2004].

Heat treatment and hardness (all hardness measurements are within $\pm 10\,HV_{30}$)

Austenitizing DIEVAR	Tempering 1	Hardness 1 (HV_{30})	Tempering 2	Hardness 2 (HV_{30})
1020 °C/30 min	550 °C/2 × 2 h	590	600 °C/4 × 2 h	470
1060 °C/30 min	550 °C/2 × 2 h	600	610 °C/3 × 2 h	470
1100 °C/30 min	550 °C/2 × 2 h	610	610 °C/3 × 2 h	470
1150 °C/30 min	550 °C/2 × 2 h	630	625 °C/3 × 2 h	470

Table 3.4: Four austenitizing treatments used to study thermal fatigue resistance of hot-work tool steels [Sjoestroem et al, 2004].

Thermal fatigue test conditions

Cycle designation	Maximum temperature (°C)	Minimum temperature (°C)	Time to maximum temperature (s)	Total cycle time (s)
$T_{max} = 600$	600	200	0.2	11.2
$T_{max} = 700$	700	200	0.3	14.3
$T_{max} = 850$	850	200	2.2	26.2

Table 3.5: Testing conditions used for thermal fatigue testing [Sjoestroem et al, 2004].

Figure 3.26a shows the effect of the austenitizing temperature on the mean austenitic grain size. Higher heat treatment temperatures resulted in larger grains sizes due to higher grain growth. Charpy impact tests were conducted at elevated temperatures to evaluate the effect of heat treatment conditions on the toughness of the steel samples (Figure 3.26b). The lowest austenitizing temperature was found to result in significantly higher toughness. This was attributed to the finer grain size resulting from the selected heat treatment. However, the lower austenitizing heat treatments resulted in lower tempering resistance (Figure 3.27). Subsequently, the maximum drop in hardness was observed for the specimen with the lowest austenitizing

43

temperature. Based upon the results in Figures 3.26 and 3.27 it was suggested that, a) in cases where the die surface does not exceed the tempering temperature, higher ductility and toughness could be given priority by using a lower austenitizing temperature, and b) in cases where die temperature exceeds the tempering temperature, a higher austenitizing temperature could possibly improve die life by improving resistance to thermal softening [Sjoestroem et al, 2004]. Thus, an optimum heat treatment selection is required, based upon the interface conditions during the forging process, to obtain maximum die life from the tool steel.
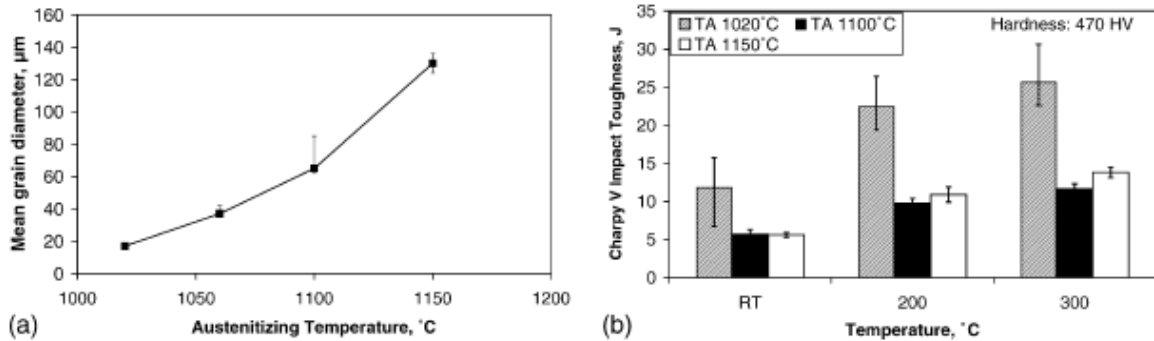
Figure 3.26: Effect of austenitizing treatment (temperature) on grain size and toughness of hot-work tool steel [Sjoestroem et al, 2004].

Hardness decrease measured 0.05 μm from the surface of DIEVAR specimen austenitized at 1020, 1060, 1100 and 1150°C, at $T_{max} = 700$ tested after 5000 and 10 000 thermal cycles

Cycle number	$T_A = 1020$	$T_A = 1060$	$T_A = 1100$	$T_A = 1150$
5000	80 HV	70 HV	50 HV	60 HV
10000	110 HV	90 HV	60 HV	80 HV
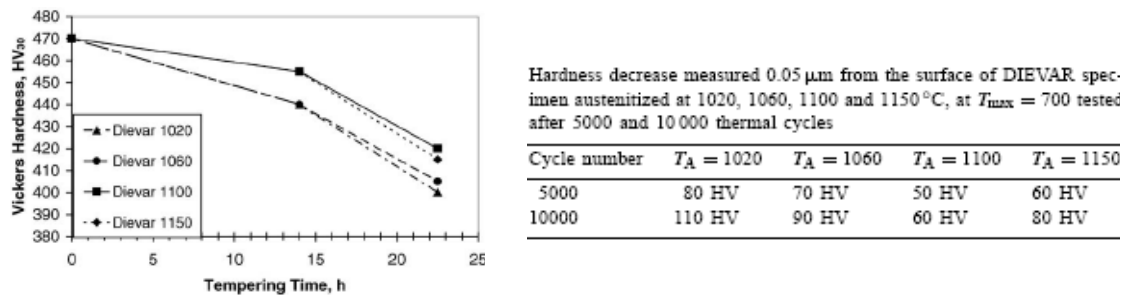
Figure 3.27: Temper resistance of hot-work steel specimens subjected to different austenitizing temperatures [Sjoestroem et al, 2004].

[Sjoestroem et al, 2005] studied thermal fatigue in two production processes viz. die casting and hot forging (Figure 3.28), using a combination of thermal fatigue testing and metallographic analysis of production dies (H-13 hot-work tool steel at ≈45 HRC). Dies used in hot forging (mechanical press) of heavy duty crankshafts were investigated in this study. The workpiece was heated to 1250°C (2280°F), whereas the dies were pr e-heated to 200°C (400°F). The average contact time was estimated to be 0.15 seconds, excluding the pre-forge and post-forge dwell

44

times. Temperatures during production were measured by an infra-red (IR) thermal camera and were found to vary (in hot spots with high contact times) from a maximum of 600°C (1110°F), one second after forging, to 200°C (400°F) after coolin g.

Surface strain measurements during thermal fatigue testing were performed on the tool material to evaluate the surface mechanical strain levels during typical thermal cycling. Isothermal fatigue testing was also performed to determine the stress–strain response in the temperature interval 200–600°C (400-1100°F). Figure 3.28 shows the types of failures observed in the hot-forging die viz. thermal fatigue, wear and plastic deformation. The production results in terms of die surface temperatures and location of heat checking failure agreed well with FE predictions. The FE models were used to determine the effective stress distribution and elastic strains at the locations of die failure.
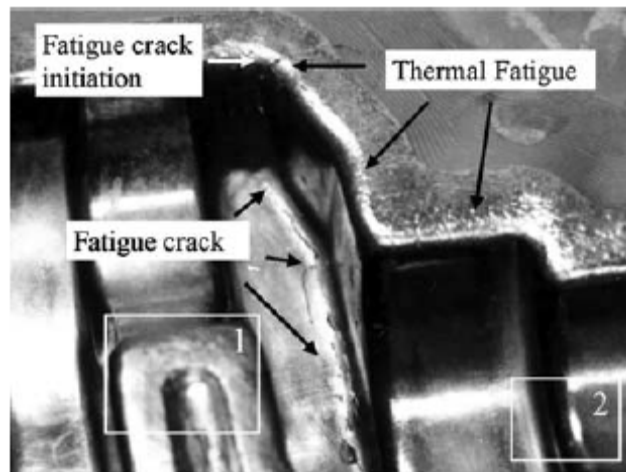
Figure 3.28: Die failure mechanisms observed in the selected hot-forging die [Sjoestroem et al, 2005].

Thermal fatigue cracks were observed on the die surface after only 100 forging strokes (≈1% of the die life). Crack initiation occurred in regions with longer contact times with the workpiece and at geometrical stress-risers in the die. Thus, any die design or process change that can reduce the contact time with the workpiece will improve the die service life.

45

CHAPTER 4

ROOT CAUSE ANALYSIS OF DIE FAILURE MODES IN WARM

AND HOT FORGING

4.1.   Factors Influencing Die Failure and Part Rejection

Multiple failure mechanisms frequently occur in the same die at different locations. Thus, it is crucial to identify the factors related to different failure modes so that the process can be modified and controlled in order to improve productivity. This can be achieved using quality control tools such as cause-and-effect analysis and interaction diagrams on the selected process. An Ishikawa diagram is a graphic total quality management (TQM) tool that helps to identify, sort and display all the possible causes or factors related to a production problem or quality characteristic. This diagram is also called a fishbone diagram due to its appearance. A set of Ishikawa diagrams were prepared in order to a) identify the different die failure mechanisms that are commonly found in warm and hot forging environments, and b) identify the different factors that specifically affect die wear.

4.1.1.   Generating the Ishikawa Diagram

The Ishikawa diagram for poor part quality and die failure in warm and hot forging processes is shown in Figure 4.1. The following is a brief summary of the sequence used in generating this diagram.

Step 1: Identify and define the effect to be analyzed.

For the purpose of this exercise, any forged component is defined to be of poor quality if a) it is out-of-tolerance, and/or b) it has deteriorating accuracy over a production run, and/or c) it has inferior appearance. Such a part is deemed incapable of meeting its functional requirements in the end application and is rejected. Thus, a forging process is considered to have failed when the die (or set of forging dies) delivers a part of poor quality, not necessarily when the die exhibits some form of failure. This generalized view of the forging process failure not only accounts for die

46

failure, but also takes into account a) part defects, and b) the effect of the personnel and infrastructure involved in the forging process.

Step 2: Identify the main/root causes of poor quality or die failure

The root causes form the major labels in the diagram and are used to categorize the many factors that can lead to a part of poor quality. The root causes/categories in this case were identified as those that lead to part rejection (in no particular order):

- Die Wear

- Thermal Fatigue

- Plastic Deformation

- Die Breakage

- Defects

Step 3: Identify the factors related to each branch that affect part quality or die failure

Within each branch the different factors related to that specific root cause are listed. These may again be categorized into different segments. The advantage of doing this is to enable the engineer to focus on specific areas in each branch. New factors in each branch are identified by asking "why/what"-type questions. The different categories are discussed in detail later.

47
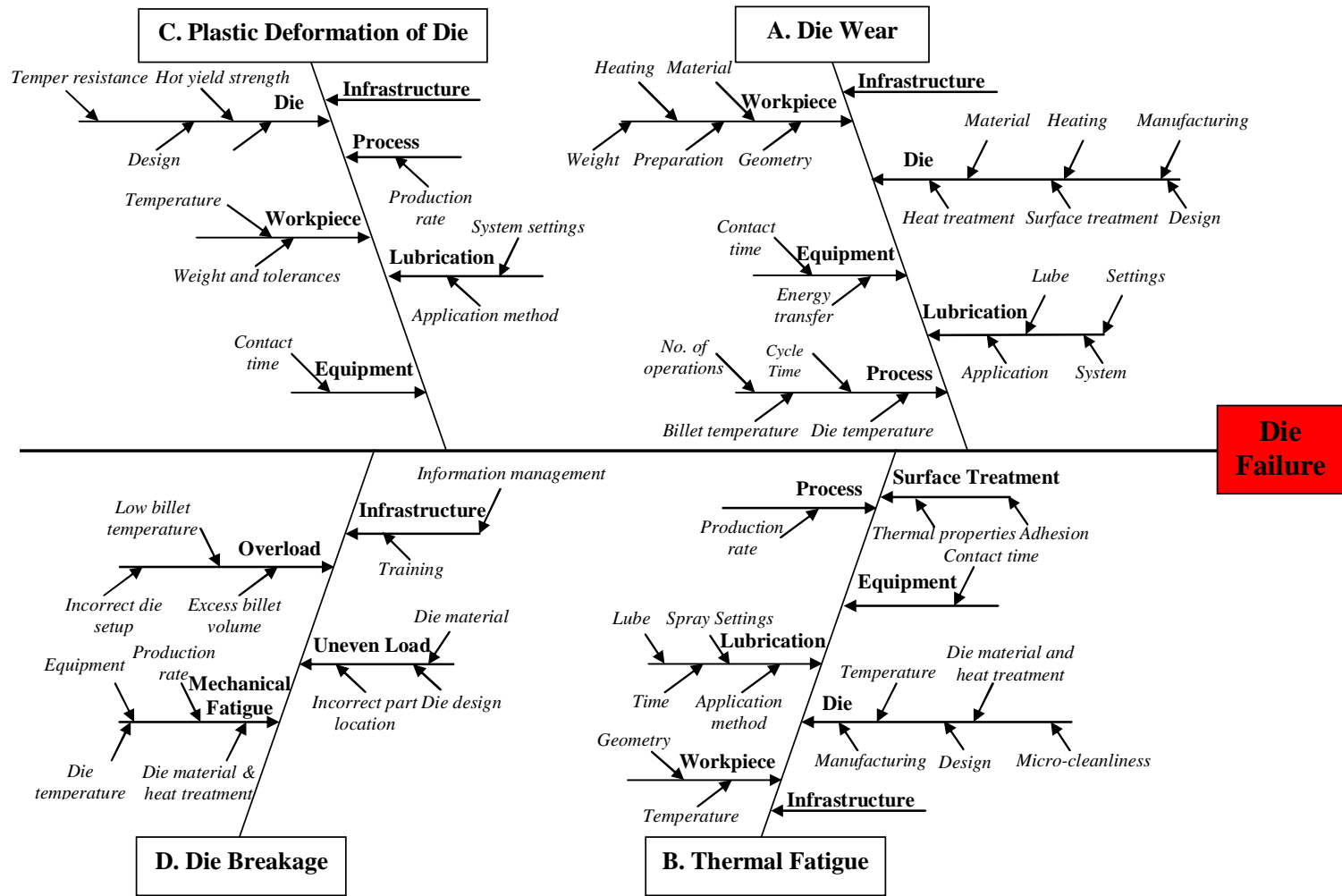
Figure 4.1: Ishikawa diagram for identifying factors leading to die failure and poor part quality in hot and warm forging (in no specific rank or order).

48

The main causes leading to poor part quality or die failure were briefly mentioned in section 4.1.1 and form the main categories of the Ishikawa diagram (Figure 4.1). These factors have been documented and researched in previous studies [Knoerr et al, 1989; Dahl et al, 1999]. Table 4.1 outlines the main effect of each of the factors on part quality. The different factors related to die failure or poor part quality could be ranked based either on frequency (Table 4.2) or on severity (Table 4.3). These rankings are based upon input received from US forging companies through the course of this research.

Main Cause/Factor	Effect on Part
Die Wear	Out-of-tolerance, inferior appearance.
Thermal Fatigue	Surface roughening, inferior appearance.
Plastic Deformation	Out-of-tolerance.
Die Breakage	Production stoppage.
Part Defects	Inferior appearance, out-of-tolerance.

Table 4.1: Effect of main causes on part quality.

Rank	Factor
1	Die Wear
2	Die Breakage (Mechanical Fatigue)
3	Plastic Deformation
4	Thermal Fatigue
5	Part Defects
6	Die Breakage (Catastrophic Failure)

Table 4.2: Factors ranked according to frequency.

Rank	Factor
1	Die Breakage (Catastrophic Failure)
2	Part Defects
3	Die Breakage (Mechanical Fatigue)
4	Plastic Deformation
4	Thermal Fatigue
4	Die Wear

Table 4.3: Factors ranked according to severity.

49

4.1.3. Impact of Factors Affecting Part Quality and Die Failure

The different root causes and sub-branches shown in the Ishikawa diagram in Figure 4.1 are discussed in this section. The impact of each factor in terms of die life and part quality is discussed along with recommendations where applicable.

4.1.3.1. Die Wear

Die wear results in a part that does not meet dimensional tolerances and has inferior surface appearance. The die wear related factors are categorized as shown in Table 4.4 and Figure 4.1. Each category has separate factors within it that affect die life and part quality. These factors are discussed separately in section 4.2 with an Ishikawa diagram targeted specifically at the issue of die wear in warm and hot forging.

4.1.3.2. Die Breakage

Die breakage results in instant production stoppage. This section on die breakage includes both mechanical fatigue and catastrophic failure. Additionally, chipping and flaking, normally associated with coated tools is also included in mechanical fatigue.

4.1.3.3. Mechanical Fatigue

Mechanical fatigue in forging processes occurs due to large magnitudes of cyclic stress at elevated temperatures and is of the low-cycle type i.e. failure occurs in less than 1,000 cycles. Fatigue cracks initiate at locations of stress concentration on the die surface. Thus, the die design and surface condition (surface finish/roughness) have a significant influence on fatigue.

    a. Die:

- The tempering treatment given to the die directly affects its toughness and resistance to mechanical fatigue. Alloy content is also important especially for screw press and hammer dies, which are subjected to impact loads. Low alloy steels are preferred for these applications.

- The die pre-heat and bulk temperature determines the toughness and cracking resistance of the die. The die should always be used above its ductile-to-brittle transition temperature.

50

o   The die design features in the form of fillet radii, draft angles and flash geometry affect stress concentration. Draft angles also add to stress concentration along radii due to a wedge effect.

o   The surface finish of the die is equally important to prevent crack initiation especially in fillet radii. If the die has been manufactured using electro-discharge machining (EDM) the die surface should be polished and re-tempered. Electro-discharge machining (EDM) results in a hard and brittle white layer on the die surface with a large number of micro-cracks, due to melting and re-solidification of the surface layers. Polishing removes the white layer and micro-cracks, and tempering restores the surface heat treatment characteristics that existed prior to machining.

Categories	Factors affecting wear
Workpiece (Billet/preform)	1. Material. 2. Geometry. 3. Preparation. 4. Heating method. 5. Weight and sorting method.
Equipment	1. Characteristics (Contact time, stiffness, etc.). 2. Mode of operation. 3. Knockout system.
Die	1. Die material, heat treatment and surface treatment. 2. Die design and manufacturing. 3. Die heating. 4. Die repair and cleaning.
Lubrication/Cooling	1. Lubricant. 2. Application method. 3. Equipment settings. 4. Die lubricants and billet coatings.
Process conditions	1. Die temperatures and preheating method. 2. Billet temperature. 3. Number of forging operations/stations. 4. Transfer time (cycle time).
Infrastructure	Personnel, training, information management, etc.

Table 4.4: Wear-related factors affecting die life and part quality in warm and hot forging.

51

b. Billet: Temperature directly affects the flow stress of the billet and thus the forming loads during forging. Billet temperature has to be measured and controlled within the specified tolerance to ensure consistent loading of the dies. The same applies to billet weight. Billet temperature and weight tolerances also affect the loading on the press frame.

c. Equipment: The forging equipment influences the type of mechanical loading on the dies and the rate of loading. Hammers and screw presses, which are energy-restricted, result in impact loading of the dies, especially since they employ "kissing" die surfaces i.e. die faces touch at bottom dead center (BDC). Thus, any excess energy goes into elastic deflection of the tooling and press frame.

d. Production Rate: The production rate controls the number of loading cycles on the dies. It also affects the temperature change of the workpiece and dies between successive forging strokes.

4.1.3.4.   Overload (Catastrophic Failure)

Overloading usually results in catastrophic failure or cracking, which is a special case of mechanical fatigue with a life cycle of typically one to a few blows. Overloading can occur because of the following reasons:

a. Excess billet volume: The weight tolerance is a critical factor to prevent overloading of the press and dies. This requires precise control at the billet shearing or sawing station. Sawing is preferred since it has minimal effect on the billet cross-sectional geometry and angularity. Billets are usually sorted according to weight with the smaller billets being forged first. As the dies wear out, the cavity volume increases and can accommodate excess material.

b. Incorrect die setup: In mechanical presses, incorrect die assembly can result in overloading the press and tooling at bottom dead center. This will result in die breakage and locking of the press.

c. Low billet temperature: Excessive drop in billet temperature will result in a significant increase in forming loads. This is especially important when forging high strength materials such as titanium, which have high sensitivity of the flow stress to temperature.

d. Incorrect equipment selection: Overloading can occur if the parts require forming loads that are close to or slightly above the capacity of the press. This has been known to occur in cases where there is no load monitoring and/or overload protection on the equipment.

52

4.1.3.5.   Uneven Loading (Catastrophic Failure)

Uneven loading is a critical issue with die materials that are carbide or ceramic-based as it can result in catastrophic failure or chipping. The reasons for uneven loading are:

a. Incorrect/inconsistent billet placement: This depends upon operator skill in the case of manual feeding. Depending upon the die geometry, the billet can get placed off-center or inclined to the axis of the die set.

b. Die design: The die should have locating features to aid in part placement in the case of manual feeding.

c. Insufficient die material toughness: Die materials such as ceramics have very low fracture toughness and are susceptible to catastrophic failure if a) the billet/workpiece placement results in uneven loading, and/or b) the die material has imperfections or impurities from processing (compaction and sintering).

d. Die positioning in the press: In multi-stage forging operations, die positioning on the press bed affects the eccentric loading of the press. Incorrect die placement, especially of the finisher dies, can cause uneven loading of the blocker or buster operations. Due to larger bearing surfaces, mechanical presses, especially scotch-yoke type, are more tolerant to eccentric loading than screw presses and hammers.

4.1.3.6.   Plastic Deformation

Plastic deformation results in the part being out-of-tolerance. It occurs primarily because of high forming pressures/loads and insufficient hot strength/surface hardness of the die material. The common factors affecting plastic deformation are categorized as shown below:

a. Die-related factors:

o Material and heat treatment: Materials with high hot hardness, temper resistance and thermal conductivity will have higher resistance to thermal softening and plastic deformation. These factors can be controlled by selecting the appropriate alloy content and heat treatment parameters.

o Die design: Plastic deformation occurs frequently at concave radii since they tend to locally retain heat and are more prone to thermal softening.

53

o   Die temperature: The die pre-heat and bulk temperature affects heat transfer from the workpiece and also the hot yield strength of the material.

b.   Workpiece-related factors: As mentioned before, temperature and weight control of the billet/workpiece material influences the forming loads in the die cavity.

c.   Equipment-related: Shorter contact times will result in less heat transfer to the dies and less thermal softening over the production run.

d.   Lubrication/Cooling-related factors:

o   The Leidenfrost effect results in instant evaporation of the cooling spray resulting in a vapor film formation, which prevents further cooling and adhesion of the lubricant. This effect depends mainly upon the die surface temperature after the forging stroke.

o   The lubrication settings in terms of atomization, spray time, pressure, nozzle type, etc. have to be controlled in order to overcome this effect and cool the die efficiently. Modern lubrication systems can be optimized to first cool and clean the die surface with high-pressure air, followed by high-pressure water spray and lube. This method proves to be more efficient in cooling the die and preventing any thermal softening.

e.   Process-related factors:

o   The transfer time or cycle time is related to the production rate for the process. This influences the amount of time available for cooling the die. An efficient spray system will, thus, allow high production rates without sacrificing die life.

4.1.3.7.   Thermal Fatigue

Thermal fatigue results in the part having the heat-checking pattern imprinted on its surface. Though the part may meet dimensional tolerances, the surface roughening is not acceptable for fatigue resistance in the end application. Thermal fatigue is another low-cycle fatigue failure that occurs due to alternate heating and cooling of the die surface layers. When the die contacts the heated workpiece, the expansion of the die surface layers is resisted by the cooler material in the core resulting in high compressive stresses. When the part is removed and the die is sprayed with the lubricant, the sudden cooling of the surface reverses the stress state. The contraction of the die surface is now resisted by the heated material beneath resulting in high tensile stresses.

54

This cyclic process results in heat checking on the die surface and is affected by the following parameters.

a. Die-related factors:

  o Material and heat treatment: The alloy content and heat treatment affect the thermal conductivity and temper resistance of the die material. Thermal fatigue resistance is improved with higher thermal conductivity and lower thermal expansion, since heat is conducted away more rapidly from the die surface without drastic dimensional changes. However, higher temper resistance is a simultaneous requirement in order to prevent thermal softening.

  o Die temperature: The pre-heat and steady-state (production) die surface temperatures directly influence the heat transfer with the workpiece. Higher die temperatures will result in lower heat transfer and thus, lower thermal gradients.

  o Micro-cleanliness and microstructural uniformity: The micro-cleanliness of the die material is primarily dependent upon the secondary refining processes used during steel manufacturing. Processes such as vacuum arc re-melting (VAR) and electro-slag re-melting (ESR) result in removal of non-metallic inclusions, which can act as stress risers and fatigue crack initiation sites. Currently, die materials targeted towards superior thermal fatigue resistance are manufactured using such refining processes.

  o Die manufacturing: A smoother die surface will have fewer stress concentration sites. As mentioned before, removal of the white layer and micro-cracks from EDM is critical in order to prevent crack initiation due to fatigue.

  o Design: The die design factors in terms of concave and convex radii mentioned in the section on plastic deformation also affect thermal fatigue. Concave radii will have lower thermal stresses since they will conduct heat away faster. Convex radii are more prone to thermal fatigue since they experience drastic chilling during lubrication.

b. Surface treatment: The surface treatment given to the die material in the form of reactive or deposited coatings, or a combination of the two (duplex), alters the mechanical and thermal properties of the die surface. The following factors are important:

55

- o Thermal properties: The thermal conductivity and thermal expansion of the coatings is significantly less than that of the die substrate. They are meant to act as thermal barriers resulting in less heat transfer to the die substrate.

- o Adhesion: Coatings are susceptible to cracking and delamination due to the above-mentioned thermal mismatch with the die material. Coating adhesion is improved by a) the use of a reactive treatment such as nitriding prior to the coating process, and b) the use of multi-layer coatings. This gives a smoother transition from the thermal properties of the die material to those of the coatings. However, the use of coatings in hot forging has been largely unsuccessful.

c. Workpiece-related factors:

- o Temperature: A lower temperature differential between die and workpiece results in lower heat transfer. Thus, lower billet temperatures should be used where possible.

- o Geometry: The billet or preform geometry affects thermal fatigue by influencing the area in contact with the die. A geometry that accommodates design features, which hold the billet above the die surface before forging, will result in less thermal fatigue.

d. Equipment-related:

- o The main effect of the equipment used is on the contact time. Mechanical presses slow down towards bottom dead center (BDC) due to the nature of the linkage mechanism and also due to loading. Servo presses allow for an optimization of the press velocity profile in order to reduce contact times.

- o The press stiffness also influences contact time. Elastic deflection of the press under load will increase the contact time with the heated workpiece and result in higher thermal fatigue.

- o The type of knockout mechanism on the press can also have a positive or negative effect on heat transfer to the dies. A programmable knockout mechanism can be used to hold the part above the die surface before and after the forging stroke to reduce contact times.

56

e. Lubrication/Cooling-related factors: The main lubrication factor affecting thermal cycling is the method in which the die is cooled. The lubricant spray results in sudden die chilling and stress reversal. A lubrication system that directly sprays water on the die surface will result in higher thermal fatigue compared to one that follows the sequence of air-water-lube mentioned earlier. Some lubrication systems have a continuous airflow impinging on the dies during forging. This further helps to keep the die temperature under control and also keeps the die surface clean of any build-up prior to the spray.

f. Process-related factors: Production rate and cycle time affect the thermal cycles that the die experiences. Following lube spray, the die surface temperature starts to increase again as heat is conducted from the die interior to the surface. Thus, if permissible an increase in transfer time will result in higher die surface temperatures and lower workpiece temperatures effectively reducing thermal cycling. Such process optimization is possible on servo presses with automated part feeding.

4.1.3.8.   Defects

Part defects include those related to metal flow (underfill, laps/folds, etc.) and those related to surface appearance (pits, surface roughening, etc.). The following factors can affect part quality:

a. Die-related factors:

   o Die temperature: Excessive die chilling can result in non-uniform deformation due to dead metal zones at the die-workpiece interface resulting in the formation of laps or folds.

   o Die design: The design of the die cavity or the preforming operation can result in lap formation. The main factors affecting defective metal flow are fillet radii and draft angles.

   o Die manufacturing: An excessively rough die surface will result in part rejection since the die surface profile will get imprinted on the part. This is critical for precision near-net shape forging operations.

b. Billet-related factors:

   o Edge quality: Burr or crack formation from the billet separation process can result in surface defects after forging.

57

o Billet location: Consistent location of the billet in the die is required to prevent part defects among other failure modes. Automatic feeding systems or operator skill are necessary for tight process control.

c. Lubrication/Cooling-related factors: A breakdown of the lubrication system or insufficient lubrication can result in sticking friction and underfill in hard to fill regions. Excessive lubrication will also result in underfill due to lubricant buildup.

d. Process-related factors: Die positioning in the press affects eccentric loading and part tolerances (parallelism) in the thickness direction.

4.1.3.9.   Infrastructure

The company infrastructure consisting of the equipment, operators, engineers, management and the communication system between them has a significant impact on the successful execution and productivity of the forging process. Following are some of the main factors that affect part quality and die life:

a. Die: The design engineers should have the required training with regard to die design and die material and heat treatment selection. Selection of the appropriate manufacturing and finishing process and specifications for the same are also crucial to prevent premature die failure and/or part defects.

b. Engineering tools: Tools such as process simulation enable the die designer to implement process modifications at the design stage in order to ensure part quality and prolonged die life.

c. Training: Design engineers should have the required training with regard to die design, die material and heat treatment selection, die manufacturing practices, die positioning, etc. Operators need training with regard to billet placement and workplace practices to ensure consistent process control.

d. Quality and process control: The use of standard operating procedures, data logs and control charts help to maintain the process within the specified tolerances. Data logs and operating procedures should be developed by the design engineers in cooperation with the operators.

e. Maintenance: Equipment maintenance helps to prevent breakdowns and unplanned production stoppages. Consistent equipment operation will ensure consistent part quality.

58

f. Information management: The importance of information management for production scheduling and monitoring, among other applications, was discussed in Chapter 1.

g. Worker safety: Attention to worker safety is critical in ensuring a positively motivated workforce that works towards improving product quality and providing useful feedback.

h. Management: The mentality and approach of the company management affects all of the above factors, especially in terms of implementing the quality policy and maintaining a motivated workforce.

4.1.4. Interaction Modes

The different factors affecting part quality and die life are not necessarily independent. Quite often more than one form of die failure is observed in the same forging die as seen in Figure 3.27. The failure mode that requires the die change first is regarded as the dominant failure mechanism. In such cases, the remedial steps taken to alleviate one failure mode will affect the other failure modes. This interaction may be positive or negative and needs to be considered during the die or process design change. This section addresses some of the critical interaction modes between the different failure modes shown in Figure 4.1. Special emphasis is given to interaction between die wear and other failure mechanisms.

4.1.4.1. Interaction between Die Wear and Die Breakage

Some of the die material and forging process requirements targeted towards reducing die wear can have a negative impact on the mechanical fatigue life of the tooling. One of the prime examples is the application of harder die materials such as ceramics and carbides with superior wear resistance. These materials have very low fracture toughness and need to be protected against fatigue and catastrophic failure. This can be done by using pre-stressed tooling with split die inserts.

Table 4.5 outlines the interaction between die wear and die breakage in terms of the factors that affect each of these failure modes and the requirements for reducing them. Thus, the process changes and requirements for reducing one failure mode are compared against those required for the other e.g. wear resistance necessitates the use of harder materials, whereas fatigue resistance is improved by imparting greater toughness to the tool steel. In general, factors that reduce die wear are found to increase the probability of tool failure by mechanical fatigue or gross cracking unless steps are taken to account for them in the tool and process design stage.

59

4.1.4.2. Interaction between Die Wear and Thermal Fatigue

Table 4.6 shows the factors related to die wear compared to those related to thermal fatigue. Similar to the comparison with mechanical fatigue, steps taken to reduce die wear can result in an increase in the susceptibility of the die material to thermal cracking e.g. wear resistance of the die material is very often increased by the use of surface treatment with single or multi-layer coatings. Due to their mismatch with the die material in terms of thermal properties, coatings are prone to cracking and delamination during service.

4.1.4.3. Interaction between Die Wear and Plastic Deformation

Most of the requirements for reducing die wear will also reduce plastic deformation. This can be seen through the comparison provided in Table 4.7. The requirements in terms of die material, heat treatment, equipment characteristics and lubrication are very similar.

4.1.4.4. Interaction between Plastic Deformation and Thermal Fatigue

Table 4.8 summarizes the possible impact of changes made to reduce plastic deformation on the thermal fatigue properties of the die assembly. Since the remedial measures to reduce plastic deformation are similar to those for reduction of die wear, most of these factors have a negative impact on thermal fatigue behavior. Die cooling between forging cycles is critical for preventing thermal softening but results in stress reversals on the surface, which affect the thermal cycling.

4.1.4.5. Interaction between Plastic Deformation and Die Breakage

The requirements for resistance to plastic deformation are similar to those for die wear resistance in terms of the die material properties and heat treatment selection. Thus, changes made to the die material to improve plastic deformation could result in an increase in the probability of mechanical fatigue. However, the commonalities between the two failure modes lie in the requirement for tight control on billet temperature and weight along with optimum die design and cooling.

60

	Wear	**Die Breakage**
Die	• High hot hardness and temper resistance. • High alloying content for the tool steel being used. Possible use of carbide or ceramic based materials due to high hardness and high temperature stability. • Very high or very low thermal conductivity. • Heat treatment to achieve high hardness. • Surface treatments and coatings improve wear resistance. • Optimum surface finish required to retain lubricant without increasing friction and wear.	• High toughness in order to have high fatigue and fracture resistance. • Low alloy content in tool steel in cases where dies are subjected to impact loads. • Heat treatment to achieve higher toughness. Secondary refining processes may be required for the same die material. • Surface treatments and coatings are susceptible to cracking and delamination due to low fracture toughness. • Lower surface roughness is required to reduce stress concentration, especially in fillet radii.
Billet	• Lower billet temperature will increase interface pressure but reduce scale formation. An optimum is required to reduce die wear. • Billet edge quality and weight tolerance control is critical to minimize die wear.	• Higher billet temperature will result in lower forming loads. • Billet edge quality and weight tolerance control is critical to minimize overloading and fatigue.
Equipment	• Short contact times lead to higher rate of loading on the dies.	• Low rate of loading is required to reduce mechanical fatigue.
Lubrication	• Excellent lubricant adhesion and efficient cooling during selected spray time.	• Excessive cooling can lower die surface temperature below ductile to brittle transition.
Process	• Die wear can be reduced by increasing the number of forging operations.	• High production rate will increase fatigue loading of the dies.

Table 4.5: Interaction between die wear and die breakage.

61

	Wear	Thermal Fatigue
Die	• Very high or very low thermal conductivity to reduce heat transfer and possibility of thermal softening. • High hot hardness and temper resistance. • Surface treatments and coatings improve wear resistance. • Optimum surface finish required to retain lubricant without increasing friction and wear. • Die design changes to reduce contact time reduce wear.	• High thermal conductivity to carry heat away from surface resulting in lower gradients and stresses. • High toughness and ductility to resist crack initiation (secondary refining processes may be required). • Coatings are susceptible to cracking due to thermal property mismatch with die substrate. • Lower surface roughness is required to reduce stress concentration, especially in fillet radii. • Similar die design changes will also reduce thermal fatigue.
Billet	• Lower billet temperature will increase interface pressure but reduce scale formation. • Preforming reduces sliding and wear but increases contact area.	• Lower billet temperature will reduce thermal fatigue. • Increase in contact area from preforming could increase thermal fatigue.
Equipment	• Shorter contact times reduce wear.	• Shorter contact times reduce thermal fatigue.
Lubrication	• Cooling prevents thermal softening and promotes lube adhesion, thus reducing wear. • Excessive cooling will increase heat transfer to dies during forging, increasing wear in the long run.	• Cooling spray increases thermal fatigue. Air-water-lube sequence recommended to gradually reduce die temperature. • Excessive cooling will increase thermal stress magnitudes.
Process	• High production rates will reduce cooling time and increase wear.	• High production rate will increase thermal fatigue loading of the dies. • Higher die preheat temperatures will reduce heat transfer.

Table 4.6: Interaction between die wear and thermal fatigue.

62

	Wear	**Plastic Deformation**
Die	• Die material and heat treatment to achieve high hot hardness, yield strength and temper resistance. • Surface treatments and coatings improve wear resistance.	• High hot hardness and yield strength will reduce the possibility of plastic deformation. • Surface treatments and coatings will improve resistance to plastic deformation as well.
Billet	• An optimum billet temperature is required to reduce scale formation and wear.	• Lower billet temperatures will reduce heat transfer to the die and reduce possibility of plastic deformation.
Equipment	• Shorter contact times reduce wear.	• Shorter contact times reduce plastic deformation as well.
Lubrication	• Efficient die cooling will reduce thermal softening and wear.	• Efficient die cooling will reduce chances of plastic deformation.
Process	• High production rates will reduce cooling time and increase wear.	• High production rates will increase chances of thermal softening.

Table 4.7: Interaction between die wear and plastic deformation.

	Plastic Deformation	**Thermal Fatigue**
Die	• High hot hardness and yield strength will reduce the possibility of plastic deformation. • High thermal conductivity will reduce chances of local plastic deformation. • Surface treatments and coatings improve resistance to plastic deformation.	• High toughness is required to improve thermal fatigue resistance. • High thermal conductivity will reduce the magnitude of thermal cycling. • Coatings are susceptible to cracking.
Billet	• Lower billet temperatures will reduce heat transfer to the die and reduce possibility of plastic deformation.	• Lower billet temperature will reduce thermal fatigue.
Equipment	• Shorter contact times reduce plastic deformation as well.	• Shorter contact times reduce thermal fatigue as well.
Lubrication	• Efficient die cooling is required to prevent thermal softening.	• Cooling spray, in general, increases thermal fatigue.
Process	• High production rates will increase chances of thermal softening.	• High production rate will increase thermal fatigue loading of the dies.

Table 4.8: Interaction between plastic deformation and thermal fatigue.

63

4.1.5. Summary of Ishikawa Diagram for Die Failure and Part Rejection

- Die life and poor part quality in warm and hot forging processes are influenced by a number of process, equipment and material related factors. These factors were identified and categorized using an Ishikawa diagram. This method enables identification of the main causes and sub-factors within each main cause. Thus, an Ishikawa diagram is one of the first steps towards improving product and process quality.

- The different die failure modes were identified as die wear, thermal fatigue, mechanical fatigue (including catastrophic failure) and plastic deformation. Additionally, forging defects were also included in order to consider generalized forging process failure rather than just die failure. The effects of the infrastructure in the forging company also influence each of the failure modes.

- The different factors were ranked according to frequency and severity. These rankings are by no means absolute and were based primarily on literature review and feedback obtained from the forging industry during this research study.

- The remedial measures taken to prevent or minimize one form of failure can affect the other failure mechanisms. Thus, the possible interaction modes between die wear and other failure modes were discussed.

4.2. Factors Influencing Die Wear in Warm and Hot Forging

This section concentrates specifically on those factors that affect die wear in warm and hot forging. A second Ishikawa diagram was created using the same procedure as that described in section 4.1 to identify the main factors that affect die wear and categorize other sub-factors within them. These factors are shown in Figure 4.2 and are discussed in the following sections.

4.2.1. Relative Importance of the Main Causes

Die wear is influenced by a number of factors, which are ranked in Table 4.9 on the basis of relative importance. The company infrastructure is given prime importance since it directly affects process design and quality control, and the tools available to achieve it. The die material and lubrication system are considered equally important in order to ensure a quality product. These can be controlled by the engineers and operators and are thus ranked above the billet material, which is customer specified. The choice of equipment is usually restricted in a forge shop and the process conditions are usually dependent upon the billet material and equipment.

64

Rank	Factor
1	Infrastructure
2	Die Material
2	Lubrication system
3	Billet material
3	Equipment
4	Process

Table 4.9: Factors ranked according to relative importance.

4.2.2. Factors Related to the Workpiece

4.2.2.1. Workpiece Material

a. Interface pressure and forming loads: Wear (adhesive and abrasive) is proportional to the pressure at the die-workpiece interface under which relative sliding will occur. This pressure depends upon the flow stress of the billet material in the forging temperature range. Lower flow stress will result in lower forming loads and pressures.

b. Scale formation: Billet materials that experience higher scale formation during heating and forging will cause higher die wear. Thus, most hot forging operations require a busting (open die upsetting) operation prior to the forging process in order to remove the scale. The forging temperature also has an effect on the flow stress of the scale and its adhesion to the billet. One of the positive effects of scale formation is that it acts as an insulating layer, thus reducing further heat loss from the billet.

c. Hardness: Since wear is inversely proportional to the hardness of the workpiece, adhesive wear will increase with softer billet materials (e.g. aluminum).

65
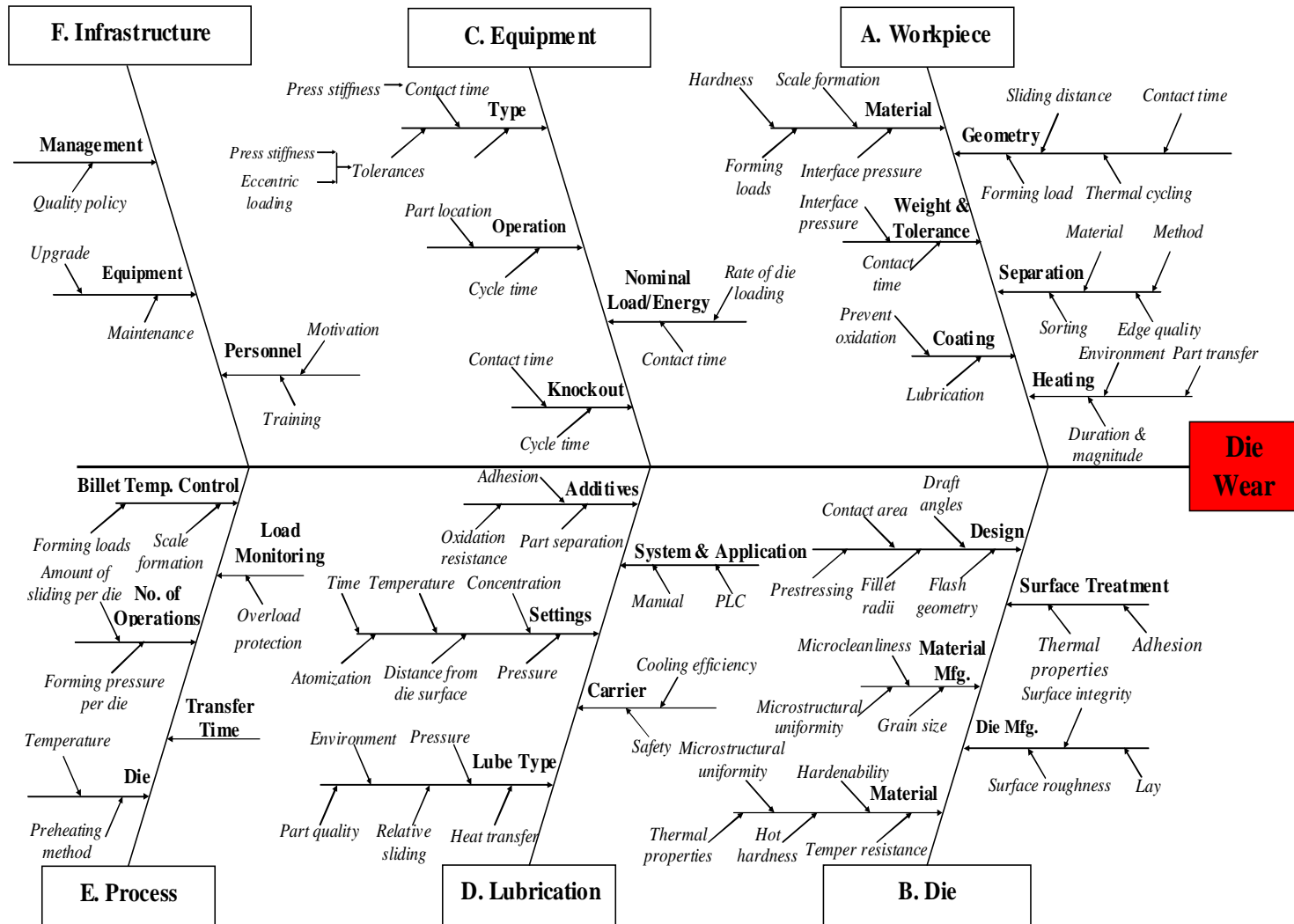
Figure 4.2: Ishikawa diagram for die wear in warm and hot forging (in no specific rank or order).

a. Amount of sliding/Sliding distance: The starting billet geometry (cross-section and general dimensions) affects the amount of deformation required to attain the form of the forged component. Thus, a starting geometry that resembles the final shape will result in less sliding and subsequently less wear. This is because wear is directly proportional to the sliding distance and thus, to sliding velocity during the fixed contact time. This effect also shows the importance of optimum preform design to distribute metal flow in different forging stages to reduce die wear.

b. Contact time and forming load: By the same reasoning given above, a billet/workpiece that closely resembles the final shape will require a smaller amount of deformation and therefore, a shorter contact time and lower forming load. This will directly affect die wear by influencing the interface pressure under which relative sliding occurs.

c. Thermal cycling: Smaller amounts of deformation imply less heat generation during forging and shorter contact times imply that less heat will be transferred to the die during deformation, resulting in less thermal softening. This effect also has an influence on thermal fatigue.

4.2.2.3. Workpiece Weight and Tolerance

Larger forgings will require higher forming loads and longer contact times. Thus, die wear will increase with the size of the forging.

4.2.2.4. Workpiece Separation

This refers to the process used to deliver the volume of the raw material to be used in the forging process. The separation process has a huge impact on the control of die loading and part defects.

a. Workpiece material: The yield strength of the billet material dictates the separation method required. Softer materials have to be sawed in order to prevent any angularity.

b. Separation method: The separation method affects a) the billet cross-section geometry, b) the tolerances (dimensional and weight), c) surface and edge defects (burrs, cracks, etc.) and d) process control in the forging operation. Accurate billet volume and consistent geometry ensure uniform loading of the dies and a defect-free part. Many

67

forge shops have currently transitioned to precision sawing in order to ensure tight process control in terms of billet weight and geometry.

c. Sorting: Sorting on the basis of length or weight is standard practice in most forge shops. Billets with lower weight are forged first. As the dies wear out, the larger billets are used. This helps to prevent overloading the dies and also ensures that dimensional tolerances are met for a longer duration of the production run.

d. Edge quality: Any edge defects from the separation process can result in a defect on the part besides affecting die life. Angular billets will cause repeated uneven loading of the dies in local regions resulting in wear. The same is true for billets that have burr formation.

4.2.2.5. *Workpiece Coating*

Billet coatings are used mostly in warm forging processes and generally consist of a graphite or molybdenum disulphide coating. The purpose of the billet coating is to prevent oxidation and de-carburization of the billet during heating, and to act as a lubricant in addition to the die lubricant.

4.2.2.6. *Workpiece Heating*

The heating method and process parameters affect the temperature uniformity and scale formation and thus, significantly influence die wear.

a. Duration and magnitude: The billet should be heated long enough to ensure uniformity of temperature across the cross-section. This is of greater importance as the billet diameter increases, since most heating systems use non-contact means to measure only surface temperatures for process control. Excessive heating on the other hand will promote scale formation. Since scale is an insulator, this will cause non-uniform temperature gradients in the billet.

b. Heating environment: A controlled heating environment with an inert gas atmosphere will ensure minimal scale formation on the billet. It should be noted that the efficiency of such a heating environment depends on the next stage in the process chain viz. part transfer.

c. Part transfer to press: Consistent part transfer from the heater to the press ensures precise control over the temperature and oxidation of the billet going into the forging process. Transfer time is more critical for smaller billets, which have lower heat capacity and lose heat quickly.

68

4.2.3. *Factors Related to the Die*

The material, in this case, refers to the chemical composition of the die, which affects the following properties that can be achieved from it via further processing and heat treatment:

4.2.3.1. *Die Material and Heat Treatment*

a. Hardenability: This is the ability of the die material to a) attain a particular hardness and b) attain uniform hardness across the cross-section. This is important because dies are hardened prior to machining (HSC/EDM) of the cavity. Thus, uniform hardness is important, not just surface hardness.

b. Hot hardness and temper resistance: These properties are influenced mainly by the alloying elements and their proportion. The appropriate heat treatment provides the final properties desired for the given forging operation. A die with higher hot hardness will have higher wear and abrasion resistance in the forging temperature range. High temper resistance ensures that this hardness is maintained through repeated exposure to the heated workpiece.

c. Thermal properties: A die material with higher thermal conductivity will result in lower localized temperatures and less thermal softening of the die material, and subsequently, less die wear.

d. Microstructural uniformity: A uniform microstructure ensures that the die material properties will be consistent through the cross-section. This is again important for machining and re-sinking purposes.

4.2.3.2. *Die Material Manufacturing*

The original manufacturing process for the die steel affects the microstructure and properties of the die material that comes to the forge shop. The casting, refining (VAR/ESR) and subsequent bulk deformation processes affect the grain size and microstructural uniformity of the die block. These properties are important to wear resistance in terms of response to heat treatment, which determines the final properties of the die.

4.2.3.3. *Die Manufacturing*

a. Surface integrity: The manufacturing process used for making the die cavity affects the surface characteristics of the die material. As mentioned earlier, electro-discharge

69

machining (EDM) requires polishing and re-tempering of the die in order to regain the surface hardness necessary to prevent die wear.

b. Surface roughness and lay: The finishing process imparts the final finish/roughness and lay directionality to the die surface. These parameters have been found to affect lubricant adhesion and wear. A highly polished die surface will not retain the lubricant and will result in adhesion with the workpiece. A rough die surface on the other hand will increase friction and promote wear through direct contact with the workpiece at surface asperities. An optimum surface roughness and lay directionality is required.

4.2.3.4. *Die Design*

a. Interface pressure and sliding: Design features such as flash geometry, fillet radii and draft angles affect the forming loads and pressure under which sliding occurs. Die wear is also influenced by the preform design i.e. the shape of the workpiece coming into the forging die. Optimum preforming sequences can be designed to distribute the metal flow and reduce the contact time and forming load in each station. It should be noted that the finisher operation should preferably be a calibration process with the least amount of sliding since it is used to impart the final dimensions and surface finish to the part.

b. Contact area: The die design also affects the area in contact with the workpiece and affects the heat transfer prior to the start of the forging process. Design features can be implemented to reduce the area in contact and the overall contact time.

4.2.3.5. *Surface Treatment*

a. Coating method:

o Reactive coatings: The depth of hardening obtained from the coating directly affects the wear resistance of the working surface layers of the die material i.e. those subjected to mechanical and thermal loading. Some coatings result in the formation of a brittle white layer on the die surface, which may need removal in order to prevent flaking and chipping during service. This can be avoided by close control of the treatment process.

o Deposited and duplex coatings: Coatings can effectively increase wear resistance and act as a thermal barrier only if proper adhesion to the substrate is ensured. Duplex coatings have enhanced adhesion because the reactive treatment provides a smoother transition from the mechanical and thermal

70

properties of the substrate (die material) to those of the coatings. Thus, wear resistance of a coated die depends upon the thermal fatigue resistance and adhesion of the coating.

b. Surface finish: The surface roughness from the coating process impacts lubricant adhesion and wear. Studies have indicated that as the coating roughness is increased, the amount of lubricant deposited on the die surface increases [Inoue, 2004]. However, data on die life was not provided. As roughness increases, friction and die wear would also be expected to increase. Thus, an optimum value of surface roughness is needed to reduce die wear through improved lubricant retention.

4.2.4. Factors Related to the Equipment

4.2.4.1. Equipment Type

The main influence of the equipment type is on the contact time between the die and workpiece. The longer the die is in contact, the more the thermal softening of the die surface layers. As the hardness of the die surface drops, the wear rate will increase. Additionally, heat transfer to the die will result in a drop in workpiece temperature, thus increasing the interface pressure along with scale formation.

The press stiffness also impacts the thickness tolerances and the contact time under load, due to elastic deflection. This is applicable mainly to mechanical presses while forging thin parts with tight dimensional requirements in the thickness direction. The eccentric loading capability of the forging equipment is also important in order to maintain parallelism of the die faces and ensure uniform loading of the dies.

4.2.4.2. Operation

Presses with automated part feeding and removal guarantee process control by ensuring that the billet is always located consistently. Thus, dies are always loaded evenly, avoiding any localized wear zones. The mode of operation also affects the cycle time and production rate.

4.2.4.3. Nominal Load/Energy

As the load available from the press increases, the contact time reduces for the same amount of deformation. This is because the elastic deflection and deceleration of the press are reduced. Thus, thermal softening and die wear are reduced for the given forging process.

71

4.2.4.4. Knockout System

In most forging processes a die change is dictated by the life of the bottom die, since it has longer contact times with the heated workpiece. An automatic knockout system can be used to support the workpiece above the die surface until the start of the forging stroke. This will reduce the contact time for the bottom die, thus ensuring even wear on both dies.

4.2.5. Factors Related to Lubrication

In most hot and warm forging processes the die is sprayed with the lubricant after the forging operation in order to cool the dies and deliver the lubricant. The following lubricant related factors affect die wear.

4.2.5.1. Lubricant Type

The type of lubricant used for a given combination of die and workpiece temperatures, affects the amount of relative sliding, the interface pressures and the interface heat transfer coefficient. Lubricants should be used within their specified operating temperatures. Any oxidation and breakdown of the lubricant film will result is direct metal-to-metal contact and sticking friction. In hot forging, the most commonly used lubricant is water-based graphite, though synthetic lubricants are also being introduced for environmental reasons. The additives used in the lubricant to enhance its performance affect the following:

a. Adhesion to die.

b. Workpiece separation from die.

c. Oxidation resistance.

4.2.5.2. Lubricant Carrier

The lubricant carrier mainly affects cooling efficiency and lubricant adhesion. The main purpose of the carrier is to cool the die after the forging operation. The most efficient cooling medium is water. However, with high die temperatures the Leidenfrost effect can result in the water vaporizing on contact with the die surface and forming a vapor film which prevents any cooling of the die surface or adhesion of the lubricant. This will accelerate the thermal softening of the die and result in an increase in die wear and plastic deformation.

72

4.2.5.3.   Lubrication System

There are currently two types of lubrication systems being used in forging companies, viz. a) automatic systems that require the operator to select lubricant concentration and other settings manually for each run with automatic spraying during production, and b) those that are fully PLC-controlled and automatically mix the lubricant. The latter are a recent introduction and allow for complete optimization for any job with the settings being stored in the memory. Thus, it is possible to recall lubrication settings for different jobs and ensure the optimum lubricant application and cooling.

4.2.5.4.   Application Method

Inadequate lubrication causes an increase in friction and die wear. Excessive cooling on the other hand will cause increased die chill and might cool the die below the ductile-to-brittle transition temperature. Automatic lubrication systems provide consistent lubricant application based upon the selected settings.

4.2.5.5.   System Settings

The system settings affect the lubricant adhesion, die cooling and the heat transfer characteristics of the die during the forging process. The system settings can be summarized as follows:

    a.   Concentration.

    b.   Temperature.

    c.   Time of application.

    d.   Pressure (lubricant and air).

    e.   Atomization.

    f.   Distance from die surface.

Current state-of-the-art lubrication systems allow the user to optimize the settings for a given forging process and store them in the system memory. The operator, based upon the information contained in the job sheet, can then call up these settings.

73

4.2.6. Factors Related to the Process

4.2.6.1. Die Temperature and Pre-heating

The die pre-heat temperature and its accurate measurement and control are crucial in influencing the heat transfer characteristics of the die during the steady-state production run. A cold die will chill the workpiece more and result in thermal softening of the surface layers. Depending upon the die material and heat treatment, an optimum temperature should be selected to ensure the toughness necessary to resist cracking without sacrificing high surface hardness necessary for wear resistance.

4.2.6.2. Billet Temperature Control

Process control on the billet temperature significantly influences the forming loads and the lubrication conditions. The forging temperature selected for the billet affects the forming pressures and scale formation as discussed previously. For any process with a controlled heating environment, there will be an optimum forging temperature that minimizes both scale formation and forming loads.

4.2.6.3. Number of Forging Operations

As the number of preforming operations increases, the amount of sliding in each die is reduced along with the forming loads. This will result in a reduction of die wear especially in the finisher.

4.2.6.4. Transfer Time

The transfer time between operations affect die and workpiece cooling between successive forging operations. This directly affects the thermal softening of the die while simultaneously affecting forming loads through the cooling of the workpiece.

4.2.7. Interaction Modes

A number of interaction modes can exist between the different factors affecting die wear (Figure 4.3). Each of these factors in turn depends upon the infrastructure available in the forge shop. This was covered in the discussion on die failure modes (section 4.2). Following are some of the important interaction modes that could affect die wear.

74

Die material selection sometimes affects and limits the choice and operating method of the lubrication system and vice-versa.

- Die temperature and adhesion: The interaction between die surface temperature and lubrication has to be investigated under shop-floor conditions in order to optimize the spray settings to ensure adequate cooling and adhesion.

- Surface roughness: The optimum surface roughness to aid lubricant retention and adhesion needs to be determined. Surface roughness also interacts with the die temperature to influence the Leidenfrost temperature. The effect of surface roughness and temperature on film formation and stability in combination with different lubricant spray settings can probably be investigated only with a spray-testing rig.

- Thermal shock: The use of ceramic or carbide dies/inserts requires a change in the cooling method since these materials can crack due to thermal shock. Due to their high temperature strength and stability these die materials can withstand higher surface temperatures with less cooling requirements. A similar situation exists with the use of tungsten-based hot-work tool steels. These die materials require the use of a synthetic or oil-based lubrication system.

- Adhesion with ceramics: Ceramics also have bad wetting and adhesion characteristics with commercial hot forging lubricants, which rely on mechanical adhesion to the die surface.

4.2.7.2. Interaction between Die Material and Equipment

The interaction between die material and equipment has to be considered at the initial stage of die material selection.

- The rate of die loading dictates the die material that can safely be used in the press and also the die design approach.

- The contact time for the given forging process will vary with equipment, thus affecting the heat transfer across the die-workpiece interface and ultimately die temperature during steady-state production. The contact time itself is affected by the knockout and part transfer mechanism on the press.

75

4.2.7.3. Interaction between Billet Material and Equipment

Die wear and the application of die life improvement measures is also affected by the interaction between the workpiece material and the equipment used to forge it.

- The strain-rate and temperature sensitivity of the billet material will affect forming loads and interface pressures differently depending upon the equipment. Materials such as titanium and superalloys are very temperature sensitive and preferably require high strain-rate equipment such as hammer and screw presses.

- Billet geometry and weight also affect the equipment contact time characteristics e.g. thin parts of high strength materials can result in elastic deflection at BDC in mechanical presses, effectively increasing contact times, die temperatures and die wear.

4.2.7.4. Interaction between Billet Material and Die Material

Based upon section 4.2.2 and 4.2.4, one can conclude that the billet material and equipment type dictate die material and heat treatment selection. Die material is selected directly based upon the billet material and geometry as well as the temperature at which it is to be forged. The appropriate equipment can then be selected for the process. In some cases, however, the die material and heat treatment might be selected based upon the equipment available to forge the given part.

4.2.7.5. Interaction between Billet Material and Lubrication

One of the requirements of the lubricant in hot and warm forging is to prevent oxidation of the billet. The billet temperature should be taken into account during lubricant selection and system setup. Excessive billet temperature will result in breakdown of the lubricant film subsequently increasing friction and heat transfer at the die-workpiece interface. [Note: Though glass is used as a lubricant in high temperature applications it is not considered here.]

4.2.7.6. Interaction between Equipment and Lubrication

The mode of operation used for the forging equipment influences the contact time available for lubrication and cooling. The press type and size also affect the lubrication system selection.

76

Figure 4.3: Possible interaction modes between the factors related to die wear in warm and hot forging.

77

The production rate affects the die steady-state temperature and heat transfer characteristics during forging by influencing the time available for lubrication. The lubrication system usually is required to accommodate the production rate by improving the spray efficiency. The number of forging operations and transfer time affect the billet temperature and oxidation and subsequently the interface conditions which affect wear.

Because of the different interaction modes discussed above, a certain amount of calibration will be required in any wear model depending upon drastic changes in the model input, such as a change in billet and die temperatures or a change in the type of equipment being used. For a given forging process the FE simulation-based models takes into account the following factors:

- Die and billet geometries and material properties.

- Equipment characteristics in terms of velocity vs. stroke profile.

- Accurate process duration based on cycle time data.

- The interface heat transfer coefficient (different for forming and free-resting) and friction are currently assumed to be constant throughout the process.

Thus, wear modeling takes into account the effect of the billet and die material on the interface conditions for different forming equipment characteristics using certain assumptions for the interface friction and heat transfer conditions. These interactions will need to be investigated experimentally for different combinations of process conditions in a production setting in order to improve the accuracy of the predictions.

4.3.   Summary of Ishikawa Diagram for Die Wear

- This chapter focused on the factors affecting die wear by developing an Ishikawa diagram. The different factors were categorized as those related to a) the billet/workpiece, b) the die, c) the forging equipment, d) the lubrication system, e) the process and f) the infrastructure.

- The factors affecting wear were ranked according to relative importance with the forging company infrastructure being considered as most critical. The different factors within each category were discussed in detail with current practices and possible recommendations where applicable.

- A number of interaction modes exist between the different factors, making wear prediction a fairly complicated endeavor. The interaction modes between the different

78

factors were discussed along with the capabilities of the wear model in terms of accounting for some of these.

The Ishikawa diagrams developed in this chapter were used for a) development of a questionnaire for collection of production data (Appendix-A), and b) for analysis of the observed die failure mechanisms to identify material properties required of alternative die materials, in addition to process design changes.

79

CHAPTER 5

CASE STUDY 1: IMPROVEMENT OF THERMAL FATIGUE LIFE IN

HOT FORGING ON A MECHANICAL PRESS

5.1. Problem Statement

Most automotive parts have stringent requirements on surface finish in order to minimize the probability of in-service failure due to stress risers on the working surface (e.g. micro-cracks, notches, pits, etc.). After the onset of thermal fatigue on the die surface, the heat checking pattern gets imprinted onto the part surface and can act as regions of stress concentration. Thus, the forged part meets dimensional requirements but not those on the surface condition.

In the forging industry, the current method of comparing die materials in terms of wear or thermal fatigue resistance involves conducting trial-and-error based production tryouts. This approach has proven to be expensive and time consuming due to a) die manufacturing and heat-treatment costs, and b) production downtime and scrap produced if the selected die material proves to be inferior to the existing one. Virtual analysis of die designs with FEA is currently widely used in order to screen design modifications prior to production tryouts. However, there is currently no methodology in place for selection of die materials on the basis of their mechanical and thermal properties, or prediction of either their wear or thermal fatigue resistance. An example automotive component was selected in cooperation with Impact Forge (Columbus, IN) in order to develop the analysis techniques required to achieve improved die life.

5.2. Process Description

Figure 5.1 shows the hot forging sequence for the selected part, a reverse piston. The dominant failure mechanism in the current forging process was identified as thermal fatigue. The general process description is provided below with details sanitized in order to maintain confidentiality:

- A steel billet is induction heated to the hot forging temperature of 2100°F (≈1150°C) and forged to the final shape in three sequential steps in a mechanical press. The initial buster operation generates a pancake shape. Part transfer is done manually.

80

- The dies (buster, blocker and finisher) are pre-heated to 300-325°F (≈150-160°C) in an oven (in-press heating is also used) and cooled during forging using an automatic lubrication system (water-based graphite). The current die material is a precipitation-hardening tool steel (PressDie™), which is hardened to ≈39 HRC prior to forging.
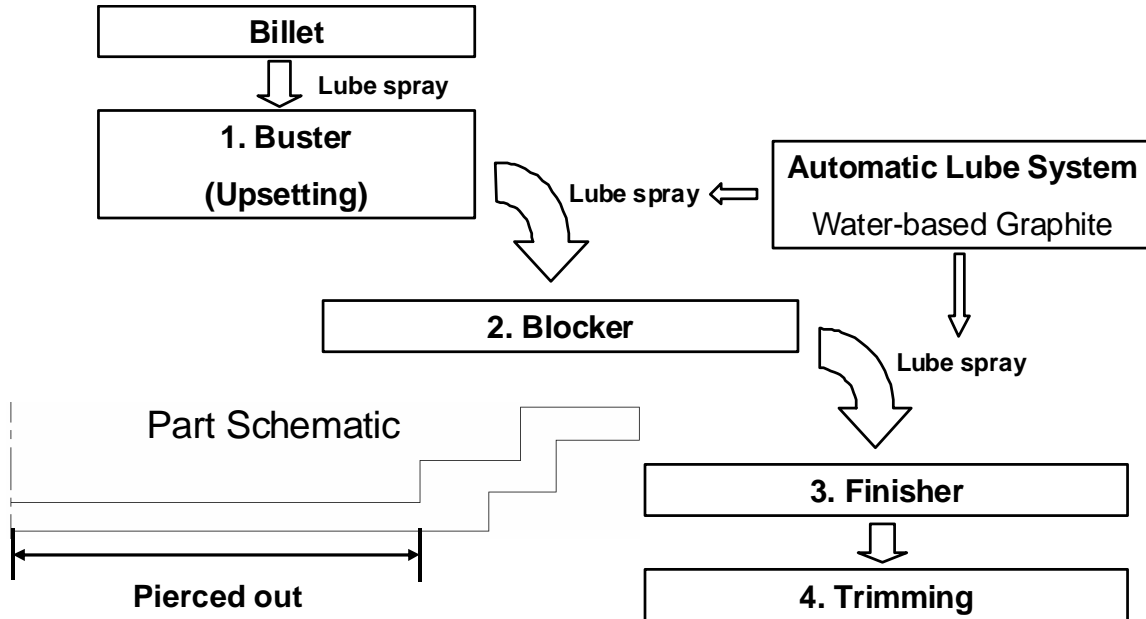
Figure 5.1: Schematic of the hot forging process sequence for the example part.

Since the bottom die is in contact with the workpiece longer than the top die, it is subjected to greater thermal loads and has a shorter lifespan. Thus, the production stoppage and die change is dictated by the life of the bottom blocker die, making it the focus of the analysis conducted in this study. All FEA results presented are, therefore, for the bottom blocker die. It was desired to analyze the existing process so as to select the appropriate die design, tool materials and process conditions for improved service life.

5.3. Objectives

The overall objective of this study was to improve thermal fatigue life of hot forging dies through selection, as well as comparison, of alternative die materials and die designs. This goal was achieved using FE simulations in conjunction with production trials. The following specific research objectives (mentioned in Chapter 2) were addressed through this study:

- Die material selection on the basis of observed failure mechanism and desired material properties (failure modes and effects analysis).

81

- Design of preforming and finisher dies for improvement of die life through reduction of contact time and relative sliding at the die-workpiece interface.

- Development of an FEA methodology for determination of start-up and steady-state conditions (temperatures and temperature gradients, surface stress-strain reversals, etc).

- Comparison of die materials and prediction of thermal fatigue performance using FEA.

- Investigation of the effect of thermo-mechanical loading of the die surface during the forging process.

5.4.   Determination of Interface Conditions in the Existing Process

Information from process and die material questionnaires (Appendix-A) was used as input to the commercial FEM code DEFORM™ in order to determine the die-workpiece interface conditions for the current process set-up. For preliminary simulations the initial die temperature (T_o) was assumed as uniform, based upon the specified pre-heat temperature. Also, the die material was assumed as homogeneous i.e. the effect of surface treatment was neglected.
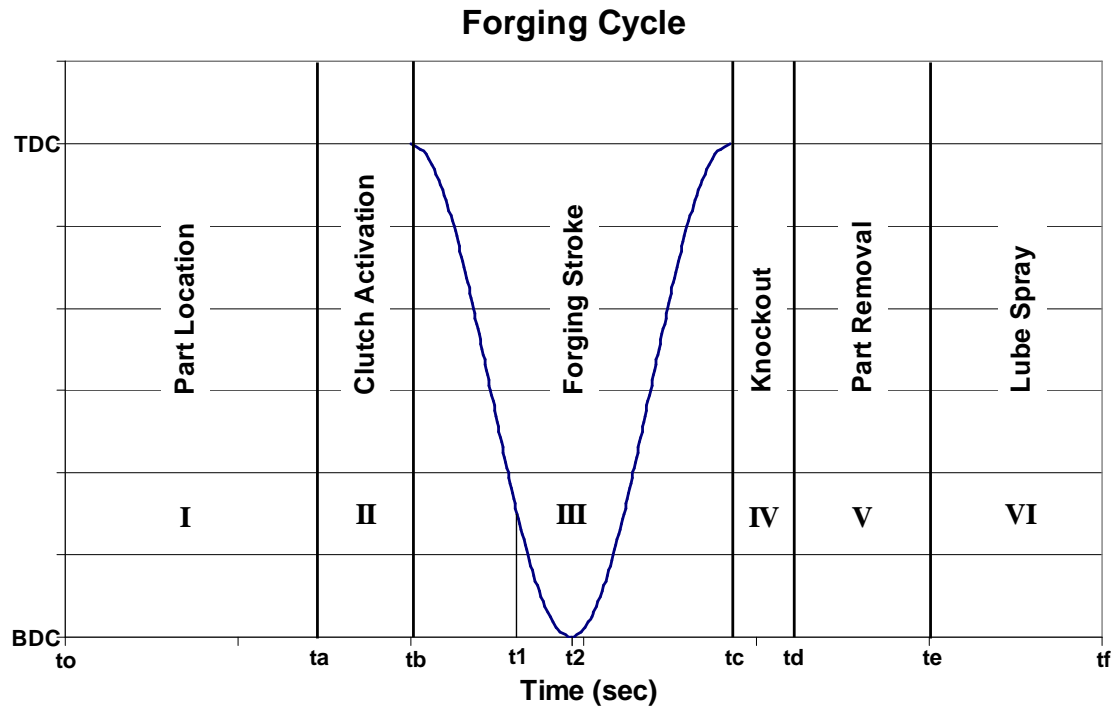
Forging Cycle

Figure 5.2: Description of a single forging cycle on a mechanical press.

The FE simulation strategy to determine the interface conditions for the blocker stage is explained by discretizing a single forging cycle ($t_f - t_o$) in a mechanical press (Figure 5.2):

82

1. Die chill time ($t_0 - t_1$): Part location to start of deformation ≈ 1.23 seconds.

2. Deformation time ($t_1 - t_c$): Determined from press kinematics to be 0.072 seconds for deformation, followed by 0.46 seconds for ram travel from bottom dead center (BDC) to top dead center (TDC).

3. Knockout and part removal time ($t_c - t_e$): Neglected.

4. Lube spray time ($t_e - t_f$): Assumed as 0.42 seconds for spray followed by 0.42 seconds of dwell till the start of the next cycle; based upon a) total cycle times measured during production, b) preliminary input from Impact Forge based upon lubrication system set-up.

5. Total blocker forging cycle time for one part ($t_0 - t_f$): ≈ 2.6 seconds.

All of the stages mentioned above were considered in the simulation of the forging process in DEFORM™. Data pertaining to cycle times and press specifications was obtained from the questionnaires sent out to the forging company and later validated during production trials. The above-mentioned operations comprise a single forging cycle e.g. start-up cycle. In order to estimate interface conditions during steady-state production it is necessary to simulate multiple forging strokes. This strategy is discussed in further detail in later sections and case studies.

5.4.1. Die Temperatures during the First Forging Cycle (Start-up)

Figure 5-3 shows an example hot forging temperature cycle for the dies on a mechanical press. The complete forging cycle was simulated starting with the ram at top dead center (TDC) and with the die at a uniform pre-heat temperature (T_o) (Figure 5.3). Thus, die chilling as well as dwell time before knockout were taken into consideration. During "die chill", the heated billet or preform was on the bottom die. After "forging", the forged part remains on the bottom die during the "dwell" period. After the forging is removed, both, top and bottom dies are sprayed with the lubricant during the "cooling" period. The temperature drop during cooling is shown approximated as linear. This stage was simulated by exposing the die surface to an assumed lubricant temperature (ambient) for a specific time with a convective heat transfer coefficient (HTC) obtained from literature on spray tests [Sawamura et al, 2005 and Tanaka et al, 2005]. The die surface temperature drops rapidly during lubricant spray but increases again in the dwell time during part transfer from the previous forging station (part of the cooling phase in Figure 5.3). This process was simulated by using a lower value of the heat transfer coefficient (corresponding to air; natural convection) to emulate heat transfer with ambient temperature in the forging environment.

83
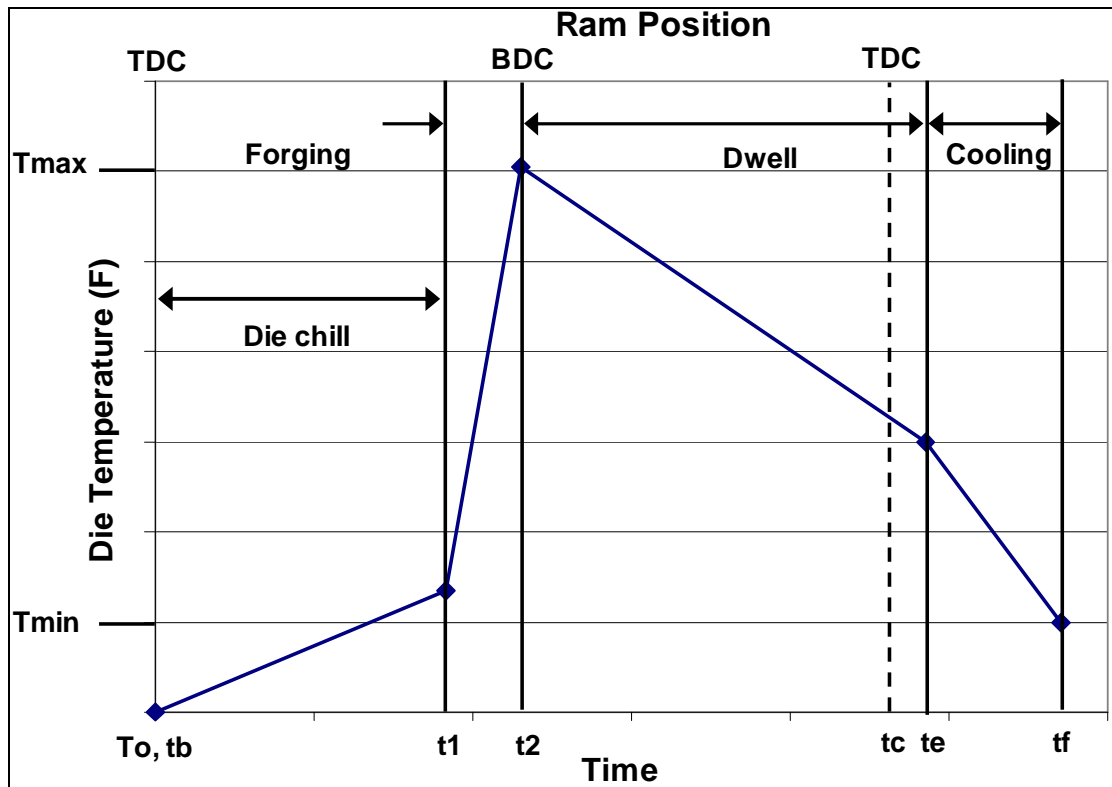
Figure 5.3: Die surface temperature for one forging cycle in a mechanical press.

For the FE analysis of the first cycle, the dies were assumed to be at a uniform pre-heat temperature of 325ºF (≈160ºC). This assumption was based upon production die temperature measurements prior to the first forging stroke. In production, the dies are heated in an oven prior to being brought to the press. They are then heated in the press with gas flames until the set-point of ≈ 300-325ºF (≈ 150-160ºC) before the start of production. Thus, in reality, a temperature gradient is expected in the die surface prior to the first stroke. This gradient was neglected for the first stroke, but is considered in analysis of multiple forging cycles as discussed in later sections. Additionally, Chapters 6 and 7 address the issue of die pre-heating in order to include a temperature gradient in a shrink-fitted die assembly for the first stroke. Inclusion of a temperature gradient is critical in order to consider the loss of compressive pre-stress due from thermal expansion. The die assembly for the hot forging process at hand uses a slip-fit die assembly with no interference between the die components. Figure 5.4 shows the variation of the die surface temperature predicted for the existing process design in the critical die region (surface B; point 3). The die temperature at point 2 is found to increase during die chill (stage 1) by 44% from the pre-heat temperature of 325ºF (≈160ºC). The maximum temperature occurs at the end of deformation when the ram is at BDC (end of stage 2; an increase of 150% over pre-heat). During ram

84

retraction (stage 3) the part in still in contact with the die, but under free-resting conditions, resulting in a 25% drop in the surface temperature compared to BDC. Lubricant spray (stage 4) reduces the die temperature drastically by ≈75% compared to that after ram retraction and part removal. Prior to the next forging stroke (end of stage 5), the die temperature at point 2 increases by ≈100% due to heat transfer from the heated die substrate.
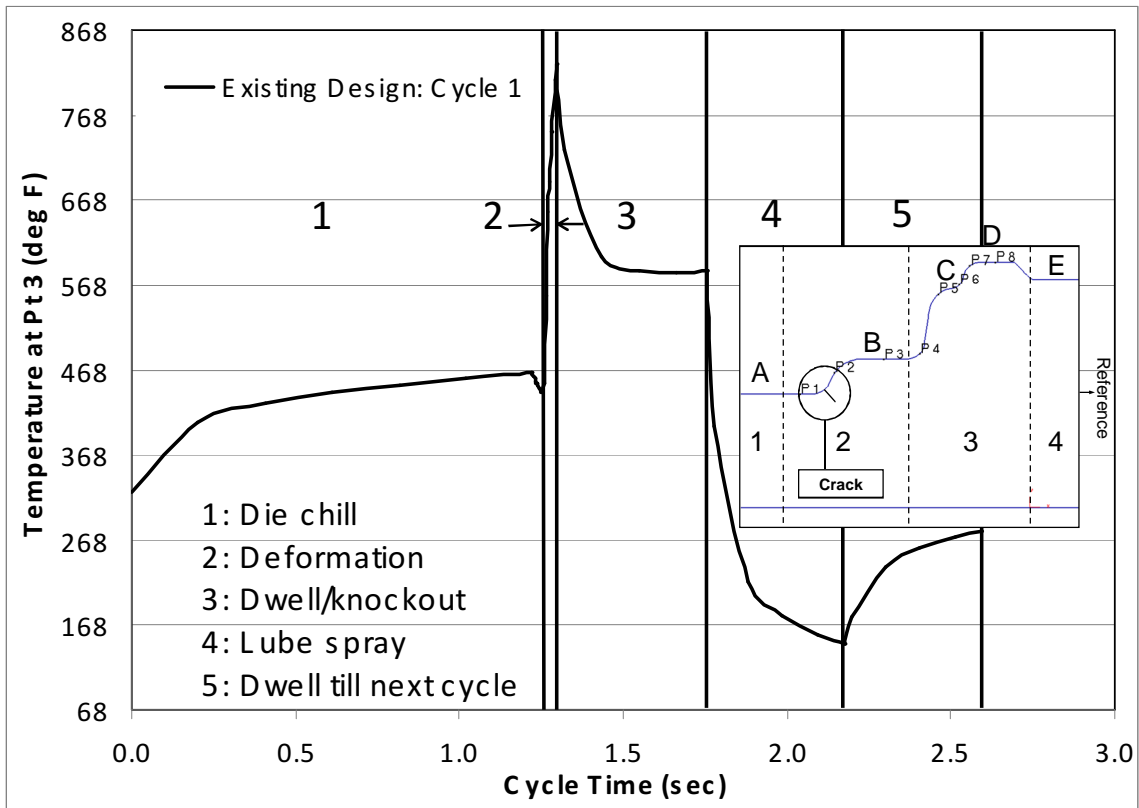
Figure 5.4: Die surface temperature predicted by FEA for the first cycle of the existing blocker die design.

Lubrication boundary conditions were selected and calibrated based on production die temperature and transfer time measurements. For the piston forging process, manual part transfer can introduce a significant amount of noise or variation into the gathered data. Thus, a detailed lubrication calibration process is explained for an automated warm extrusion process in Chapter 8. In the current case, the following boundary conditions, obtained from lubrication spray-tests, were applied to consider die cooling [Sawamura et al, 2005 and Tanaka et al, 2005]:

o   Lube spray: A uniform constant heat transfer coefficient of 35 kW/m^2-^{o}K (6164 Btu/hr-ft^2-^{o}F) was applied (assuming lube temperature of 20°C/68°F).

85

o Dwell time: Assuming ambient temperature of 20°C (68°F), a heat transfer coefficient of 0.02 kW/m²-°K (7.7x10⁻⁰⁶ Btu/hr-ft²-°F) was applied on the die surface.

5.4.2. *Die Temperatures during Steady-State Production*

Accurate die design (stress analysis) and prediction of die life also requires investigation of the production process under steady-state conditions. All forming processes, especially warm and hot forging, have a transient period before the dies reach their steady operating temperature distribution. Most FE simulation-based analyses ignore this transient stage by assuming a uniform pre-heat temperature for the dies, which, in general, is acceptable for metal flow analysis i.e. prediction of defects such as laps, underfill, etc. However, for comparison of die materials in terms of die wear or thermal fatigue resistance it is necessary to predict the temperature distribution under steady-state production.

Figure 5.5 shows a schematic representation of the warm–up phase of hot forging dies with an initial pre-heat temperature of T_o. The average die temperature before the start of the forging stroke (T_i) increases until a steady-state cycle is reached (T_{min}). As shown in Figure 5.5, the starting die temperature at a selected point (T_i) for an arbitrary forging cycle prior to reaching steady-state can be expressed as the summation of the starting temperature (T_o; ambient or pre-heat) and the temperature increase from each of the previous forging cycles (δT):

$$T_i = \delta T_{i-1} + \delta T_{i-2} + \delta T_{i-3} + \ldots\ldots + T_o = T_o + \Delta T \qquad \text{Equation} - 5.1$$

This change in die temperature was considered by simulating multiple forging cycles, each consisting of the distinct stages shown in Figures 5.3 and 5.4. Thus, the temperature history from each forging cycle is carried forward into the next stage. For each cycle, the forging process is simulated with a new preform that has the temperature distribution and strain history from the buster/preforming stage. These forging cycles were simulated only for the blocker stage, a total of 30 times i.e. 30 forging strokes. The resulting temperature cycle at one selected point on the die surface is shown in Figure 5.6. Die materials were compared on the basis of a) maximum surface temperature (at BDC), b) minimum surface temperature (after lube spray), c) temperature at the start of each cycle, and d) the temperature gradients and corresponding stress-strain magnitudes, which affect the thermal fatigue performance.
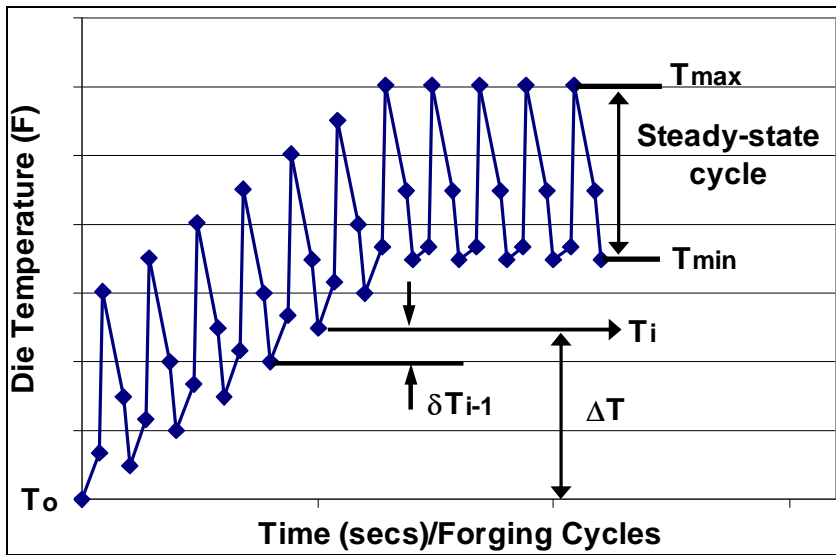
Figure 5.5: Schematic representation of warm-up in forging dies.
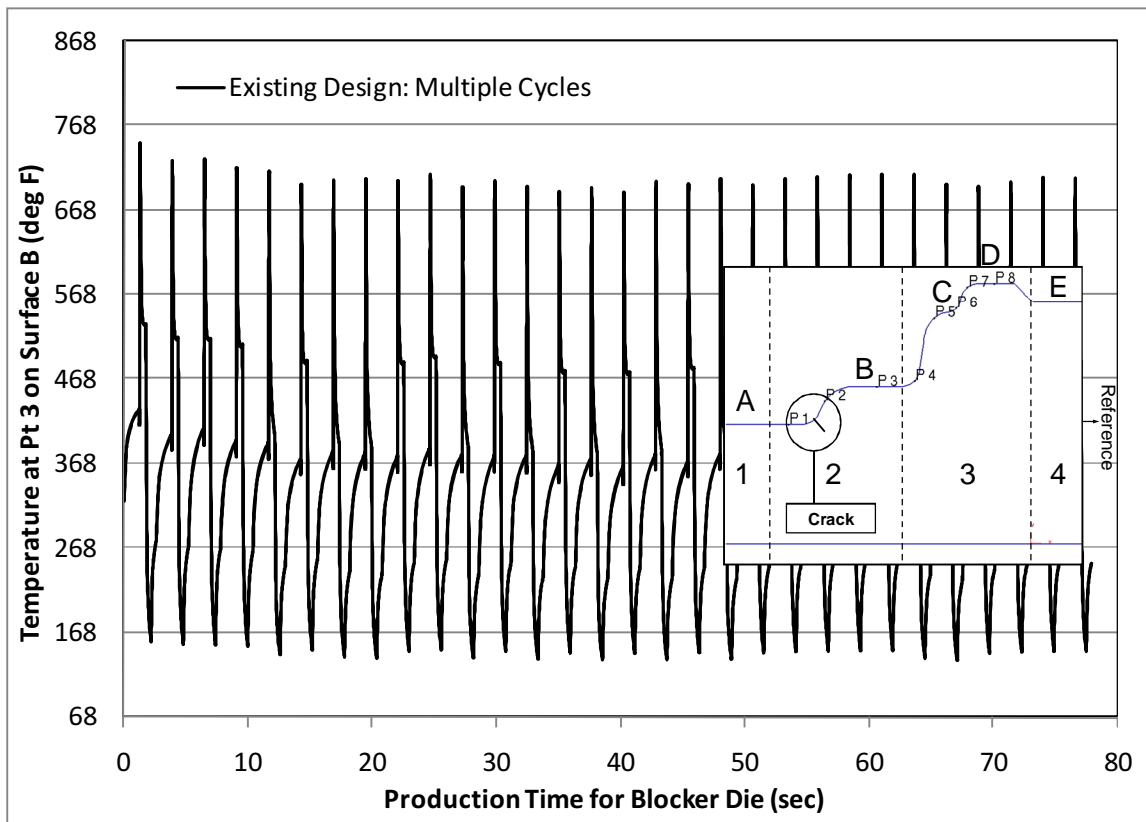
Figure 5.6: Temperature variation on surface B (bottom blocker) from start-up until steady-state.

87

5.5. Selection of Candidate Die Materials on the Basis of Failure Modes Analysis and Material Properties

During deformation, the die surface temperature rises drastically from contact with the heated workpiece (Figure 5.4). The surface layers tend to expand as a result of this temperature increase. The resulting thermal strains (thermal expansion; $\varepsilon_{th.}$) on the surface are resisted by the cooler die material below the surface i.e. die substrate. Thus, a theoretical compressive mechanical strain acts on the die surface ($\varepsilon_{mech.}$) during deformation. The summation of these two strain components can be defined as the total strain ($\varepsilon_{tot} = \varepsilon_{th} + \varepsilon_{mech}$). It should be noted that thermal strain (tension) is positive in magnitude, whereas the mechanical strain is negative (compression). The situation reverses during lubricant spray when the die surface is subjected to a sudden cooling effect resulting in a tensile mechanical strain. The total strain can be obtained readily from FE analysis of the forging cycle. The thermal strain, also, can be obtained from FE analysis or from the coefficient of thermal expansion of the die material (in the die temperature range) and the temperature increase ($\varepsilon_{th} = \alpha * \Delta T$).The opposing strain components induce corresponding stress amplitudes in the surface layers. Thus, the compressive surface stress increases rapidly during deformation and then goes into tension when the die is sprayed with lubricant. Depending upon the process conditions and die material properties, the surface stress during deformation can exceed the hot yield strength of the die material resulting in plastic straining of the die surface i.e. low-cycle fatigue. Depending upon the critical temperature (T_c) at which yielding is initiated, a plastic strain ($\varepsilon_{pl.}$) can be calculated for a selected forging cycle as $\varepsilon_{pl} = \varepsilon_{mech/Tmax} - \varepsilon_{mech/Tc}$. This cyclic phenomenon has been studied experimentally by applying thermal cycles on test coupons and measuring the total strain cycle (amplitude) on the die surface in order to study thermal fatigue performance [Persson et al., 2004; Sjoestroem et al, 2004].

Since the thermal shock is maximum in the first forging cycle, this start-up phase is critical for thermal fatigue performance. This is the reason for selecting the appropriate pre-heating temperature for the die prior to the forging process. The cyclic amplitude/reversal of ε_{mech} influences the crack nucleation and growth leading to the thermal fatigue cracks i.e. heat checking. In order to determine the relative effect/importance of selected die material properties on thermal fatigue resistance, a design of experiments (DOE) approach was used. The results of this approach are outlined in Chapter 6. For a fixed set of process conditions the following properties of the die material affect its thermal fatigue performance:

- Thermal conductivity (K): Influences the temperature gradients and thermal amplitude in the die surface during the forging cycle.

88

- Coefficient of thermal expansion (α): Influences the strain amplitude as a result of the temperature gradients.

- Young's modulus (E): Influences the stresses in the die surface during forging and lubrication.

- Hot hardness/hot yield strength: Determines whether die surface undergoes plastic straining (low-cycle fatigue) during thermal cycling.

- Tool steel manufacturing process: Secondary refining processes, such as electro-slag re-melting, help to eliminate inclusions that can act as stress risers for crack nucleation.

For the selected application, any alternative die materials are required to have higher thermal conductivity, lower thermal expansion, lower elastic modulus and higher yield strength than the current die material (PressDie™), in the temperature range observed during forging. Candidate die materials were selected based upon a) mechanical and thermal properties in the temperature range predicted by FEA, and b) discussions with the forging and tooling companies involved in this study.
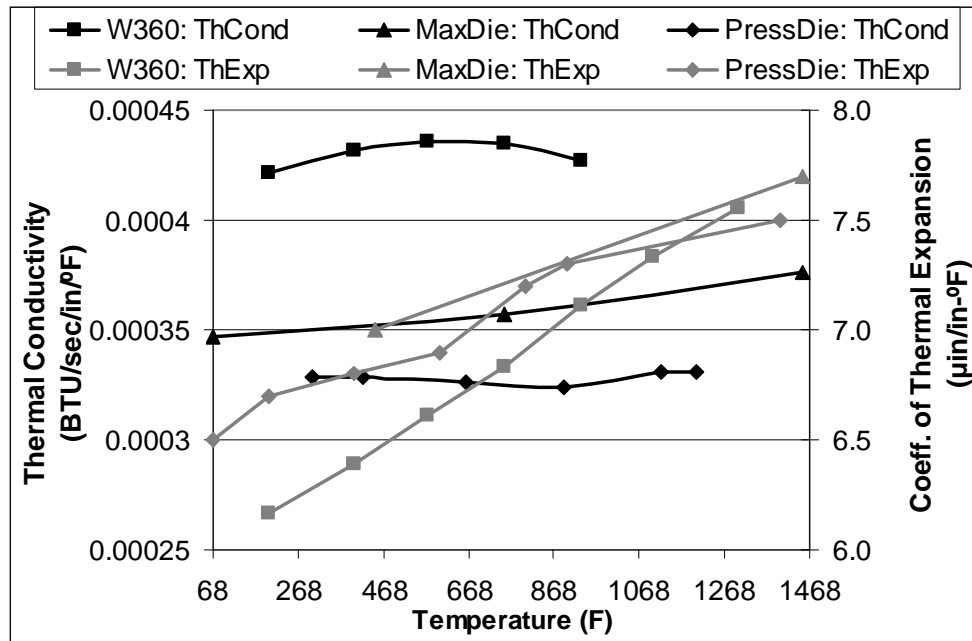
Figure 5.7: Comparison of thermal properties of the selected die materials (ThCond: Thermal Conductivity; ThExp: Coefficient of Thermal Expansion) (Courtesy: Böhler-Uddeholm, Walter Metals and A. Finkl & Sons).

89
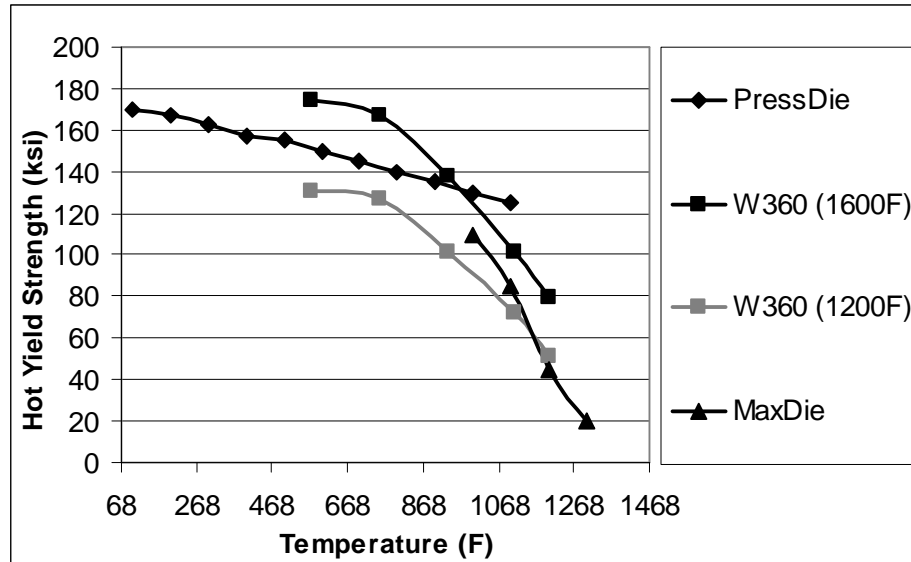
Figure 5.8: Comparison of hot yield strength of selected die materials; numbers in parentheses indicate tempering temperatures (Courtesy: Böhler-Uddeholm, Walter Metals and A. Finkl & Sons).

Two die materials were selected viz. W360™ from Böhler-Uddeholm and MaxDie™ from Walter Metals. Figures 5.7 and 5.8 compare the selected die materials in terms of their thermal properties and yield strength, respectively. It should be noted that the yield strength values are only representative of the selected materials and were not obtained from the same lots as the actual tools used in the production trials. The thermal and elastic mechanical properties were used as input to the FE analysis of the forging process to compare die material performance.

5.6. Virtual Comparison of Die Materials using FE Analysis

The thermal properties of the die material affect the absolute surface temperatures and thermal gradients in the die surface. These in turn affect the resulting stress and strain magnitudes and reversals of these state variables from deformation (heating) to lube spray (cooling). Thus, FE analysis can compare die materials using these state variables as response variables.

5.6.1.   *Modified Preform and Buster Die Design for Improved Service Life*

Based upon the initial analysis of the die-workpiece interface conditions a two-pronged approach was adopted to improve die life for the selected process. Along with the application of an advanced die material, the forging process design was modified in order to reduce the contact time in critical regions of the bottom dies in the blocker and finisher stage. The buster operation

90

was modified such that the preform does not contact the functional surfaces (surface B) of the bottom blocker when placed on it (Figure 5.9). Additionally, the height of the flash land in the finisher was increased in order to hold the blocker forging above the die surface until the top die contacts it.

a) Old pancake-shaped preform design (contact in Zone B).

b) New preform with a protrusion (no contact in Zone B).
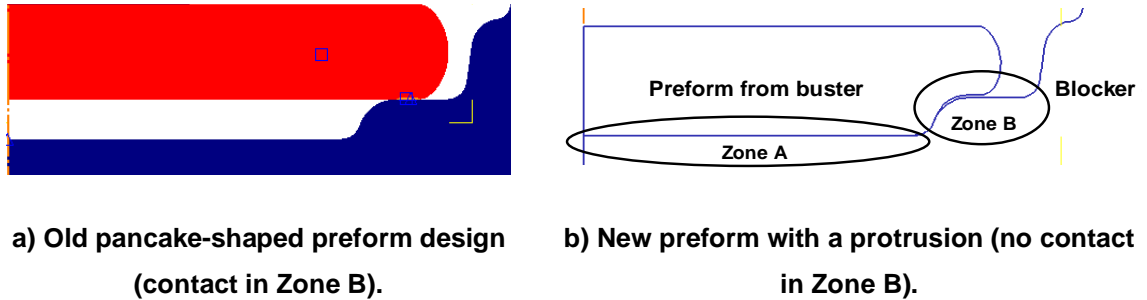
Figure 5.9: Preform design modification to reduce contact time between the die and workpiece.
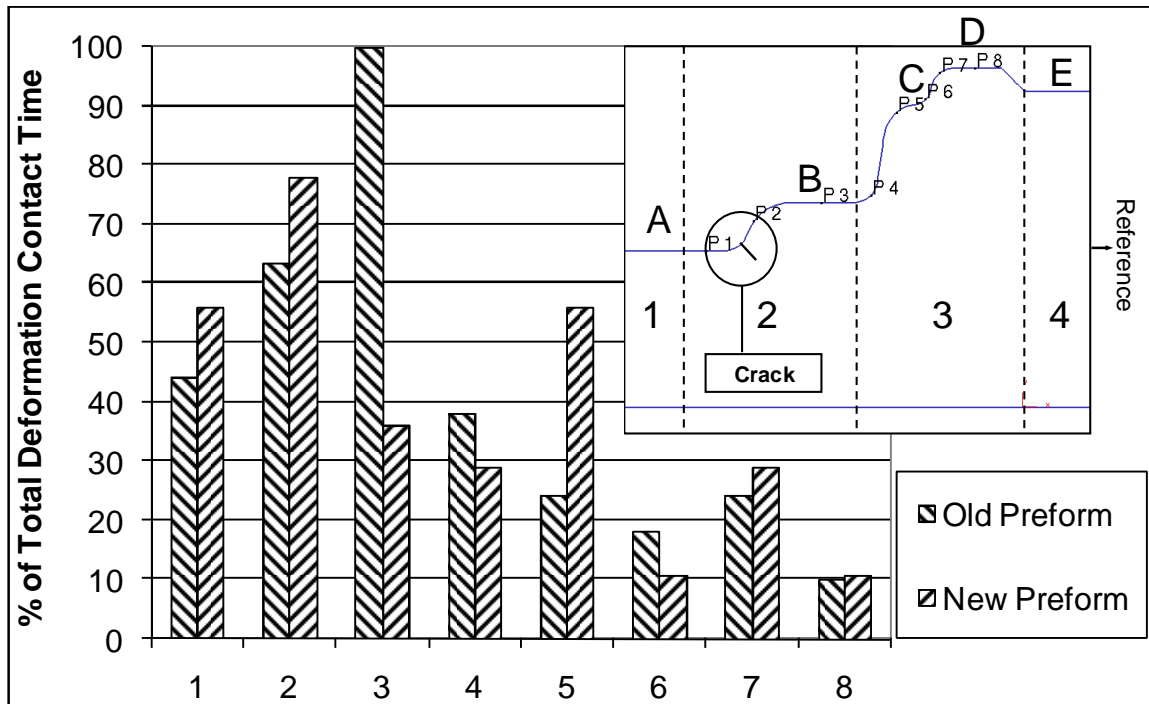
Figure 5.10: Comparison of preform designs on the basis of contact time between die and workpiece from the start of deformation to BDC.

The design modification suggested results in ≈ 65% reduction in the contact time at the critical surface B during deformation (Figure 5.10). This is expected to not only reduce surface temperatures, but also the corresponding gradients (temperature, strain and stress), resulting in higher thermal fatigue life. The new preform design requires a minor modification of the buster stage and results in a 10% increase in contact time on the non-critical surface A. This region of the workpiece is trimmed at the final station.

5.6.2. Interface Conditions and Thermal Fatigue Resistance of Selected Die Materials

The next few sections summarize the results of the FE simulations conducted to investigate the effect of the die material properties and preform designs on the interface conditions and corresponding thermal fatigue resistance. The results of this analysis formed the basis for die material as well as preform design selection for the production trials.

5.6.2.1. Die Surface Temperatures during Forging

The thermal conductivity of the die material influences the maximum surface temperature observed during the forging stroke. The ≈ 30% higher thermal conductivity of W360™ reduced the maximum surface temperature by ≈ 10 % compared to that with PressDie™ for the existing pancake preform. For the new preform design, the maximum surface temperature was reduced by ≈ 24% for W360™ compared to the old design with the PressDie™ material. Table 5.1 summarizes the results for the first forging stroke. The new preform design was found to reduce the maximum surface temperature by ≈ 16% compared to the old design. Thus, a redesign of the preform/buster operation alone was expected to show significant improvements in die life.

92
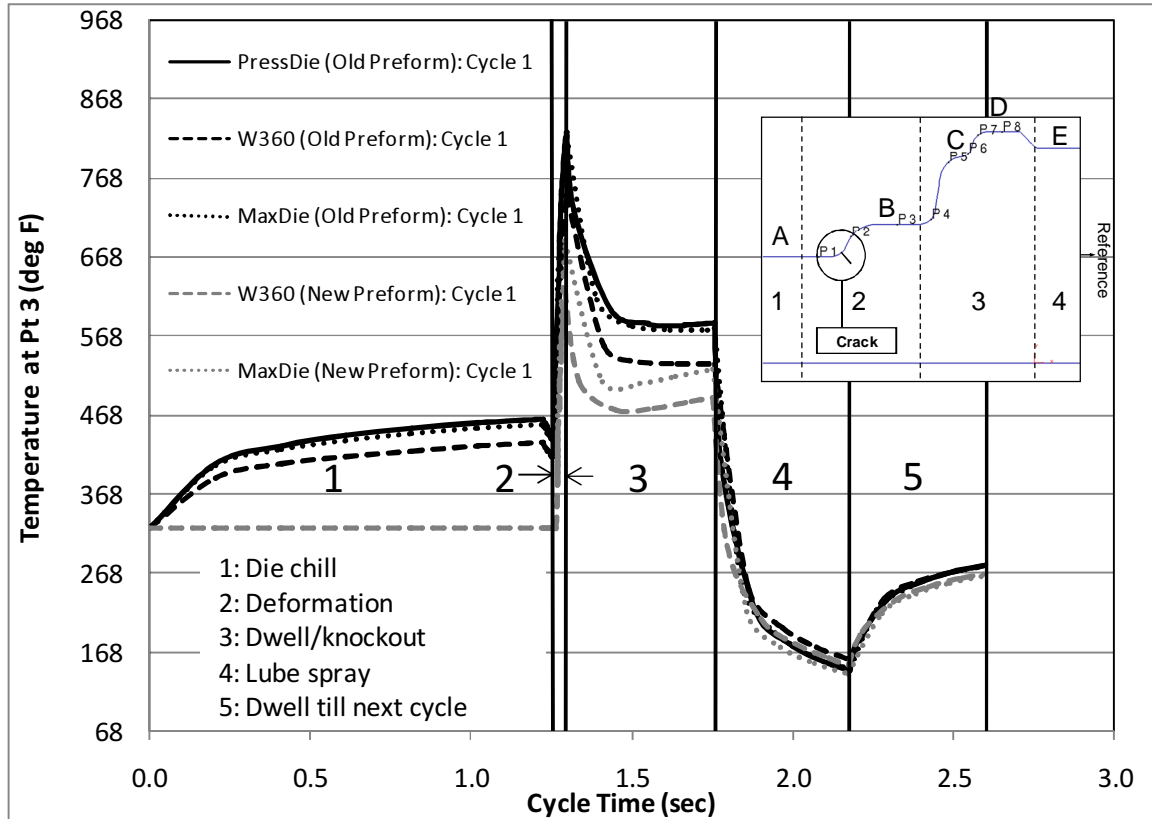
Figure 5.11: Temperature profile on surface B for the selected die materials and preform designs.

The impact of the new preform design was most obvious in the die chill stage of the forging cycle (Figure 5.11) due to the elimination of contact with the heated workpiece on surface B. Thermal conductivity dominates the temperature during deformation (stage 2) and prior to knockout (stage 3) as seen in Figure 5.11. The die surface temperature at the start of each forging stroke was predicted to reach a steady-state value of ≈ 265ºF (130ºC) for the existing process with PressDie™ (Figure 5.12). The corresponding values for the new preform design with W360™ and MaxDie™ were estimated to be ≈ 230ºF (110ºC).

93

Compared to →	PressDie™ (Old Preform)	Old Preform
W360™: Old Preform	≈ 10-15%	N/A
MaxDie™: Old Preform	≈ 2-6%	N/A
W360™: New Preform	≈ 25-30%	≈ 16%
MaxDie™: New Preform	≈ 17-22%	≈ 16%

Table 5.1: Effect of preform design and thermal properties on the maximum surface temperature (occurring at BDC).
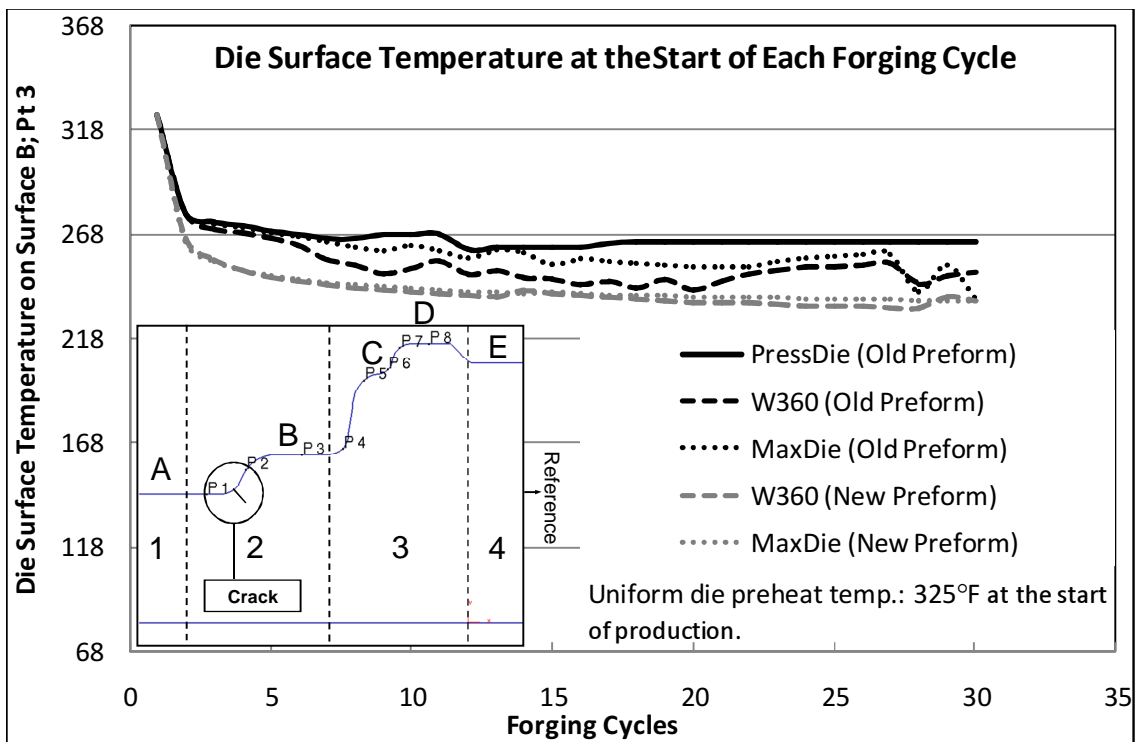
Figure 5.12: Die surface temperature on surface B at the start of each forging cycle.

94
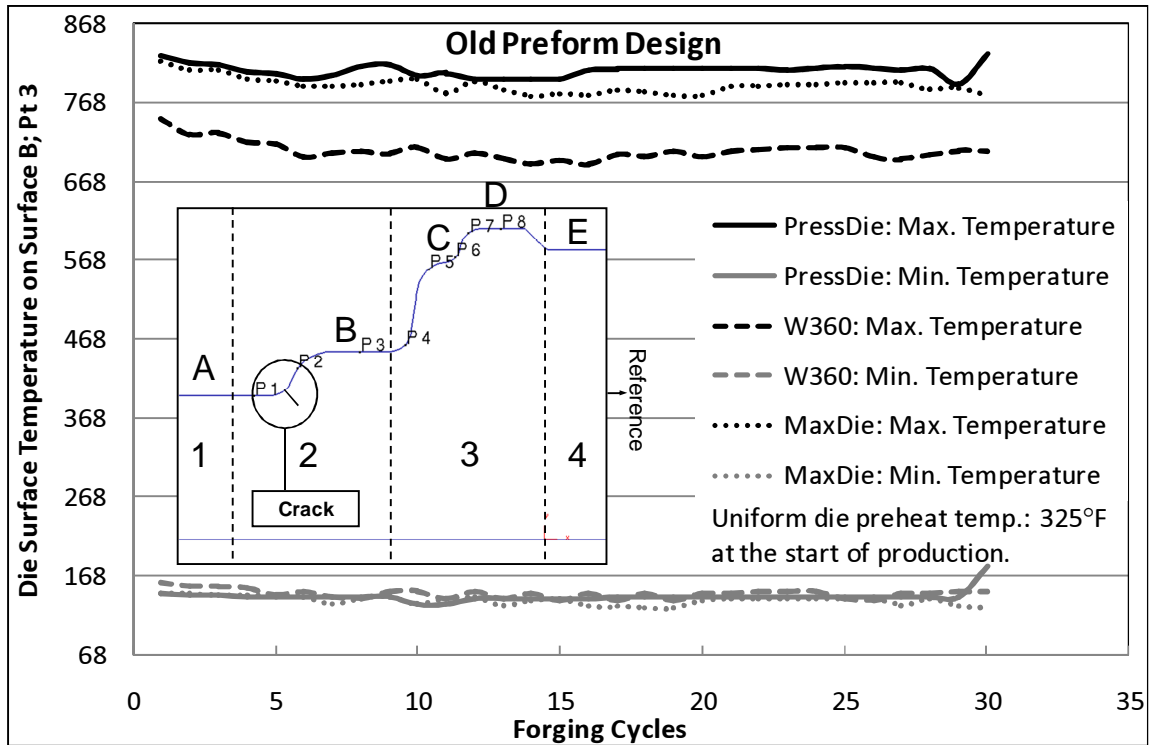
Figure 5.13: Temperature range on surface B with pancake (old) preform; different die materials over multiple forging cycles.

Figure 5.6 showed the temperature cycles on the die surface for the 30 strokes simulated in DEFORM™. The maximum and minimum temperature range on the die surface was obtained from this data for different die materials and preform designs (Figure 5.13). In the existing process design (PressDie™; pancake preform) the maximum die surface temperature (occurring at BDC) was predicted to be in the range of 800-820°F (425-440°C) (Figure 5.13).

The effect of thermal conductivity and preform design, on the maximum die surface temperature, is summarized in Figure 5.14. As indicated in Table 5.1, a combination of W360™ (or equivalent die material with high thermal conductivity) along with the modified preform design resulted in 25-30% lower die surface temperatures at BDC compared to the existing process design. It was expected that the W360™ and MaxDie™ materials, along with the new preform design, would result in lower temperature gradients and higher thermal fatigue life compared to the PressDie™ tools. Additionally, lower die surface temperatures would also result in lower thermal softening of the die surface over the production cycle. Thus, the die surface would retain its hot yield strength and wear resistance. These effects are quantified in the next few sections in order to predict thermal fatigue performance of the selected die materials.

95
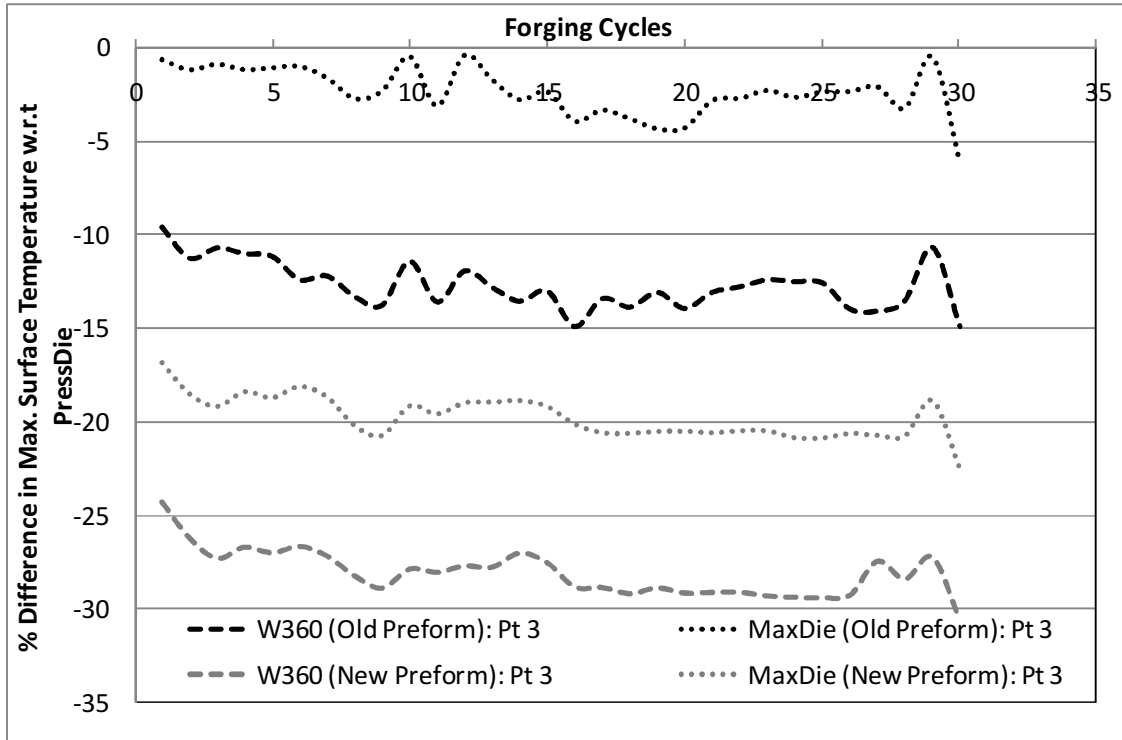
Figure 5.14: Difference in the maximum surface temperature; different preform designs and die materials over multiple forging cycles.

5.6.2.2.   Temperature Gradient during Forging

The thermal conductivity of the die material determines the temperature gradient through the surface layers for a given pre-heat temperature (or pre-heat temperature distribution). During deformation, the die surface temperature increases drastically until BDC (Figure 5.11), resulting in a negative gradient through the surface layers i.e. the temperature drops off into the depth since the core of the die is cooler. The reverse situation occurs during lube spray when the die surface is suddenly exposed to the room temperature lubricant. Thus, the extreme values of temperature and temperature gradient are generally observed at BDC (end of deformation) and end of lube spray (Figure 5.11; Figure 5.15).

96
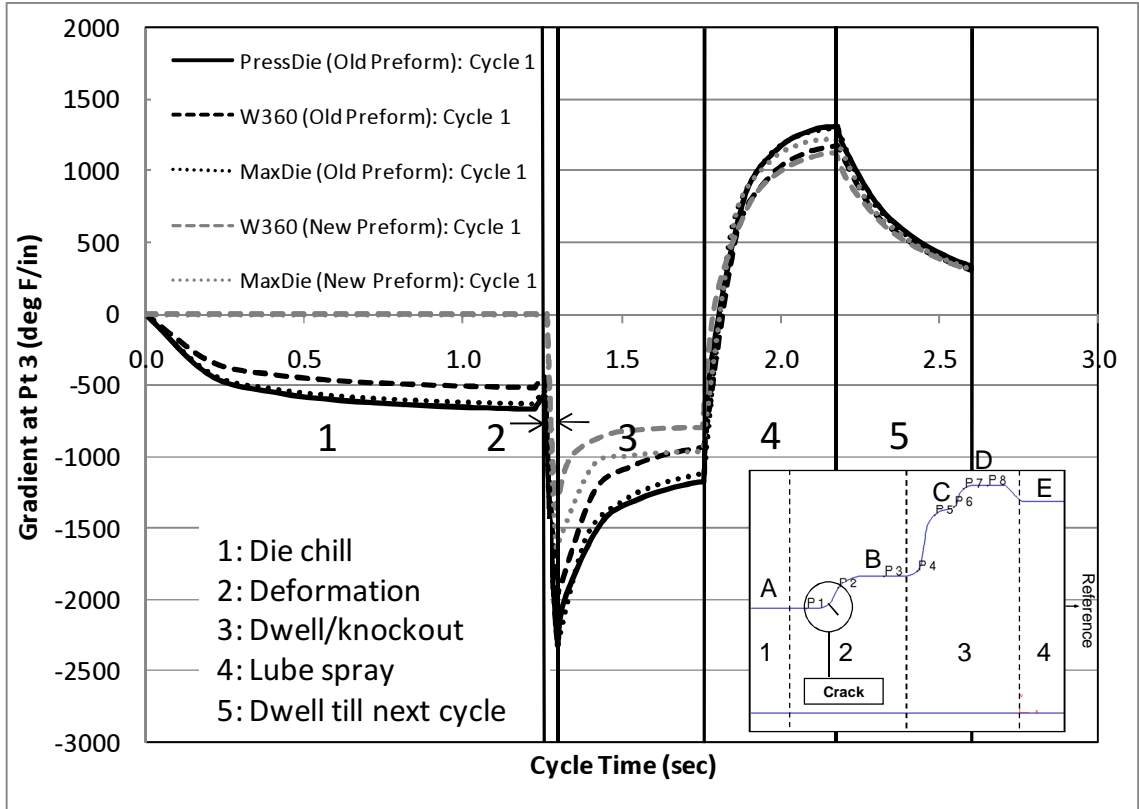
Figure 5.15: Temperature gradient and its amplitude at start-up.

As will be discussed later, the temperature gradient has a direct influence on the stress and strain amplitudes experienced by the surface layers. Thus, a die material resulting in lower temperature gradients (i.e. one with higher thermal conductivity) is preferred when the dominant failure mechanism is thermal fatigue. Die materials were compared on the basis of the difference between the extreme values of temperature gradient over the simulated production cycle of 30 strokes (Figure 5.16). W360™ was found to have the least difference between the temperature gradient at BDC and end of lube spray with both preform designs. The temperature analysis from Figures 5.14 (maximum surface temperature) and 5.16 (temperature gradient) provides a preliminary basis for selection of die materials on the basis of thermal conductivity. However, thermal fatigue performance can only be predicted by analyzing the effect of these interface conditions on the corresponding surface stresses and strains. Thus, the thermal conditions need to be correlated to the elastic properties of the selected die materials.

97
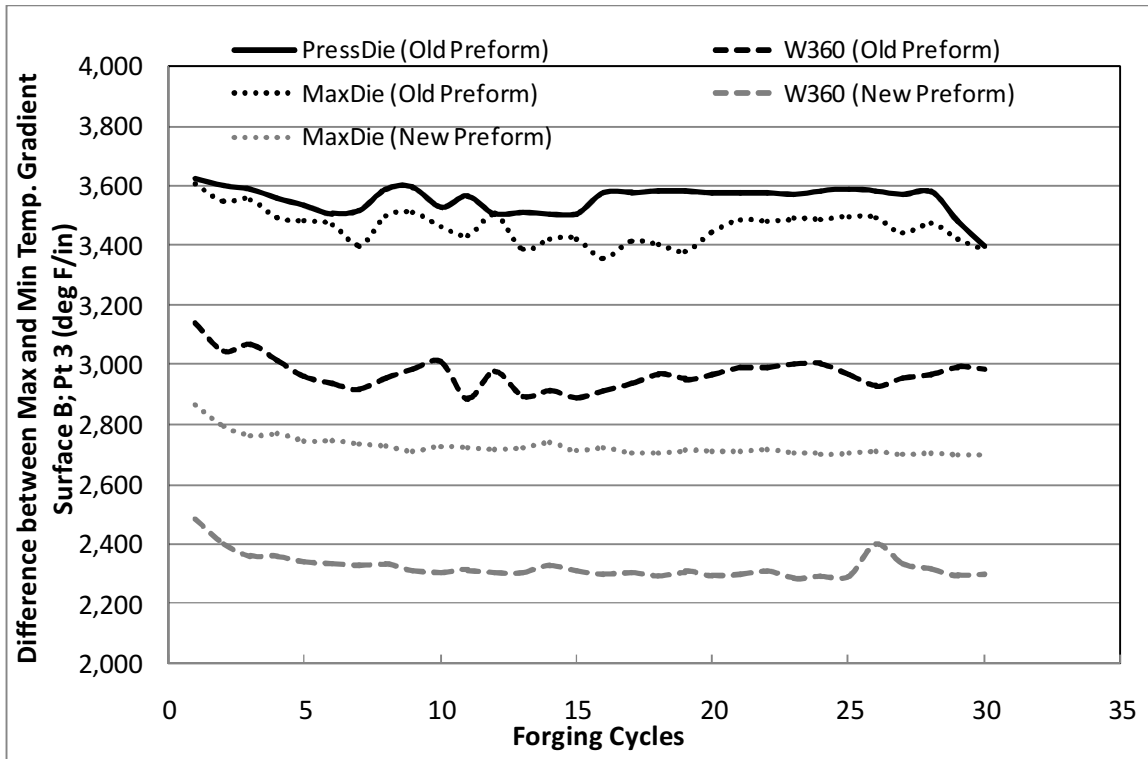
Figure 5.16: Amplitude of the temperature gradient over 30 forging cycles.

5.6.2.3.   Surface Strain Amplitude at Start-up

As explained earlier, the thermal expansion of the die surface during deformation (contact with heated workpiece) is resisted by the cooler die substrate resulting in a theoretical compressive mechanical strain (Figure 5.17). The opposite situation occurs during lubricant spray. The strain amplitude at these extreme points depends upon the temperature, temperature gradient and coefficient of thermal expansion of the die material. Since the heat transfer and thermal shock are greatest at start-up, the first forging cycle can be considered as the worst-case scenario for thermal fatigue. Thus, die materials were compared in terms of thermal fatigue performance using the thermal conditions from the first cycle as input data.

Figure 5.18 compares die materials and preform designs on the basis of the theoretical mechanical strain experienced by the surface layers at BDC (compressive) and lube spray (tensile) during start-up. For a given temperature range, a die material with lower thermal expansion results in lower strain amplitudes e.g. W360™ with new preform design has ≈ 23% lower strain amplitude compared to MaxDie™. The modified preform design also reduces the strain amplitude (≈ 25%) by reducing the contact time and the resulting temperature gradient. A

98

higher die pre-heat temperature, additionally, helps to reduce the strain amplitude by reducing thermal expansion during forging, and can prolong the thermal fatigue resistance of the dies. Additionally, the compressive strains during deformation were larger in magnitude than the tensile strains during lubricant spray.
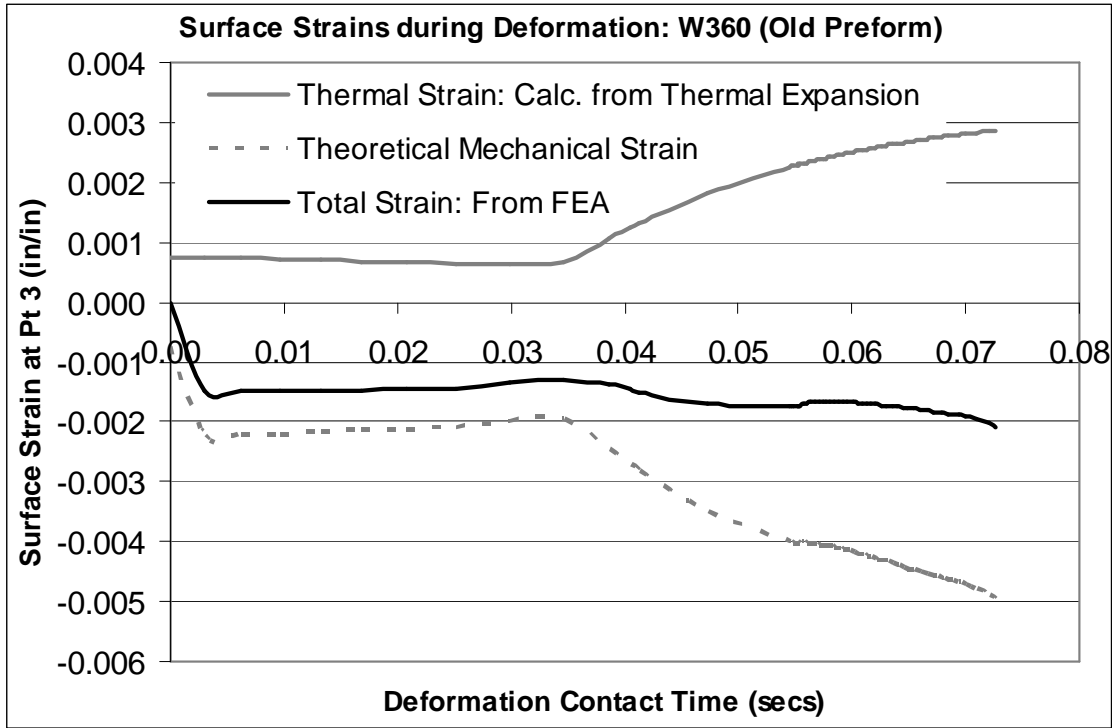
Figure 5.17: Surface strains at Point 3 during deformation (until BDC).
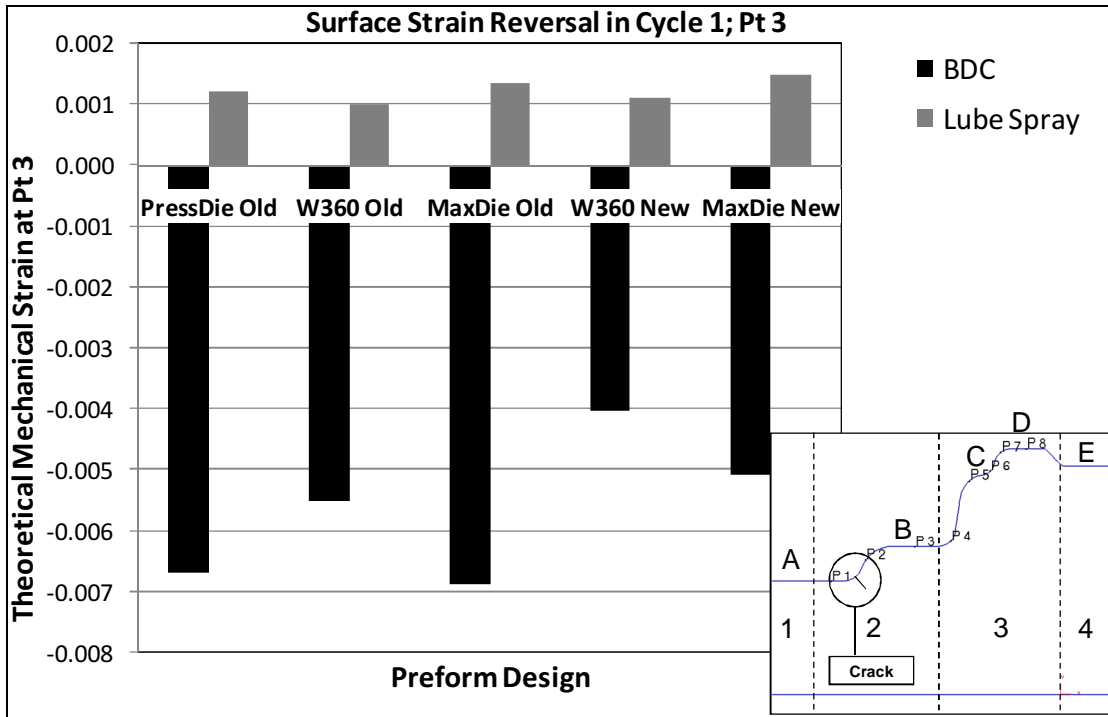
Figure 5.18: Surface strain amplitude at Point 3 for the selected die materials and preform designs (start-up).

5.6.2.4. Surface Stress Amplitude at Start-up

The surface strains from thermal expansion result in surface stresses, which follow the same cyclic pattern over the selected forging cycles, with the first forging stroke being the worst case for thermal fatigue. Figure 5.19 compares the stress amplitude of the selected die materials and preform designs. As observed in Figure 5.18 (strain amplitude), the W360™ die material with the new preform design was predicted to have the least stress amplitude (≈20% less than that with MaxDie™).

100
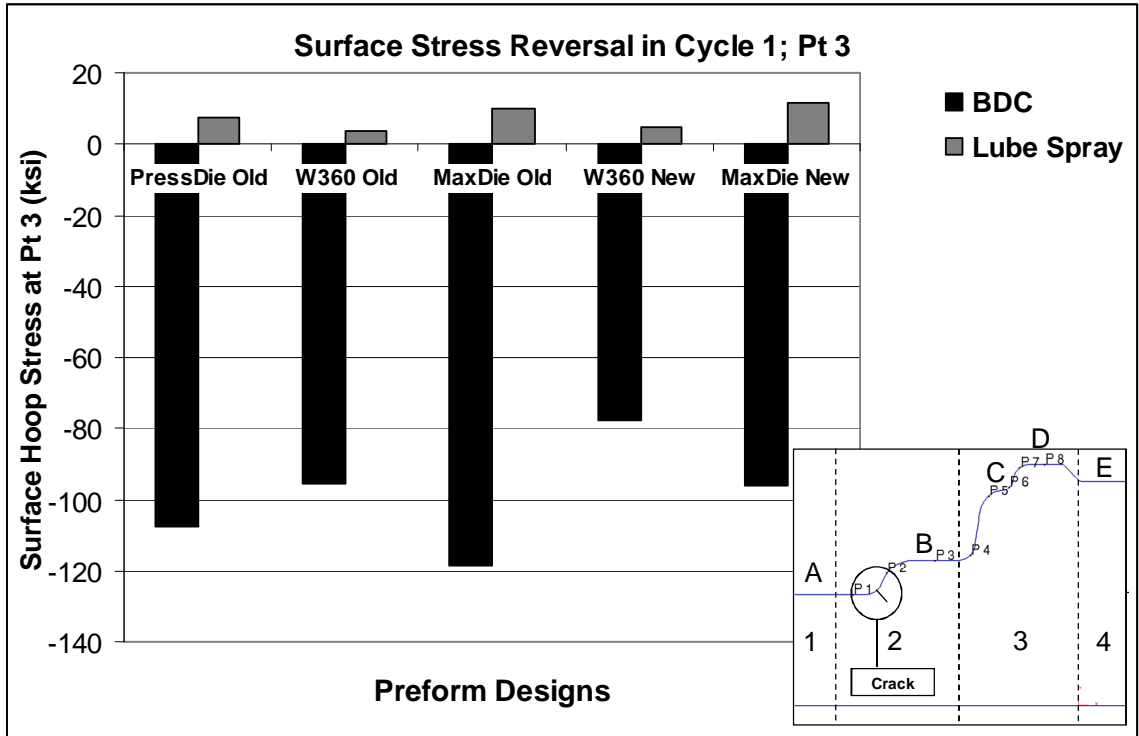
Figure 5.19: Surface stress reversal at Point 3 for the selected die materials and preform designs.

5.6.2.5. Thermal Fatigue Resistance of Selected Die Materials

As the die surface heats up from contact with the workpiece, the mechanical compressive stress on the surface increases until the maximum temperature is reached at BDC. If the elastic stress corresponding to the mechanical strain exceeds the hot yield strength of the material, plastic straining of the die surface occurs (i.e. low-cycle fatigue). During lubrication, the surface goes into tension, however, the tensile strains and stresses are significantly lower in magnitude (Figures 5.18 and 5.19) and do not exceed the yield strength. Thus, die materials were compared on the basis of stress magnitudes observed on surface B (Point 3) during the deformation stage viz. a) ratio of compressive hoop stress (minimum principal stress) to hot yield strength (Figure 5.20), b) ratio of effective (von Mises) stress to hot yield strength (Figure 5.21). Comparisons were made for the existing preform design in order to isolate the effect of thermal properties.

101
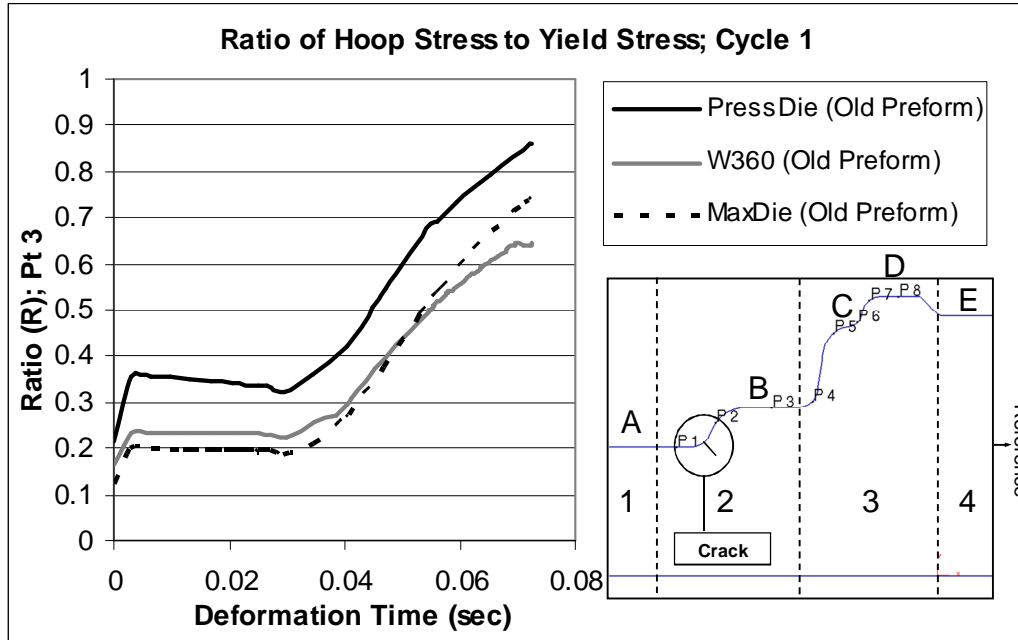
Figure 5.20: Compressive hoop stress as a percentage of the hot yield strength for the selected die materials.
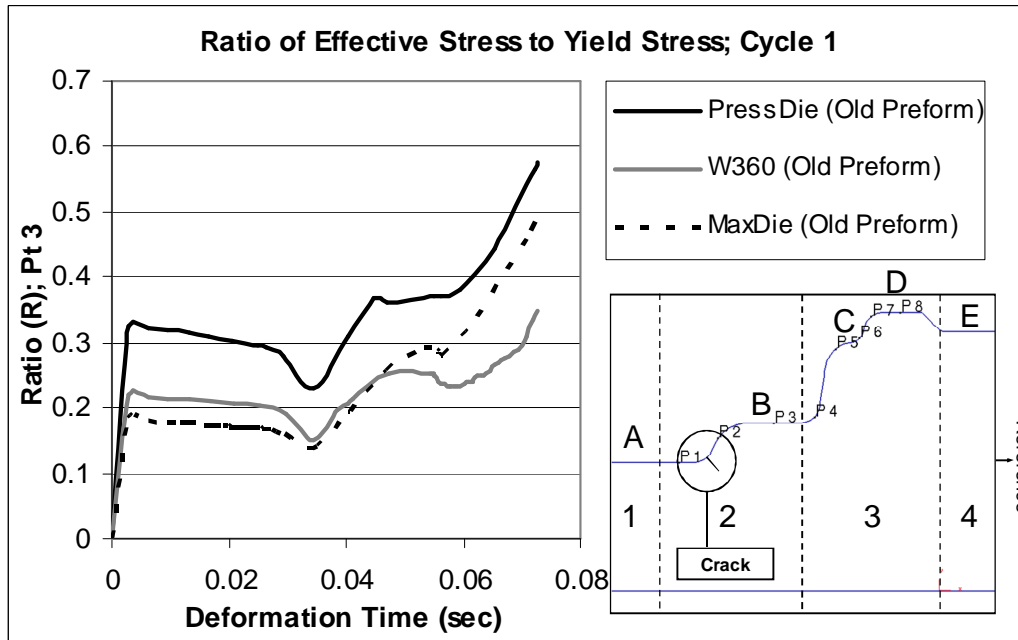
Figure 5.21: Effective stress as a percentage of the hot yield strength for the selected die materials.

102

Highest thermal fatigue resistance was predicted for W360™, with MaxDie™ being intermediate (Figures 5.20 and 5.21).The surface stresses reached a maximum of 65%-85% in hoop (principal stress) and 35-55% for effective, and, thus, did not exceed the yield strength. However, this is based on the assumption of a) a uniform pre-heat temperature of 300⁰F (150⁰C) at start-up, and b) generic material properties for the selected tool steels (from brochures). Thus, the analysis in Figures 5.20 and 5.21 is only applicable for selection and comparison of die materials using FEA, and not for prediction of the precise production quantity for a die prior to failure. The new preform design was expected to show further improvement in die life.

It should be noted that analysis of stresses throughout deformation requires that the FE model be run with the dies modeled as elastic. This significantly influences the computational time and effort. Thus, an efficient alternative would be to consider the stresses and strains at BDC only (along with selected intermediate points), using a single step die-stress analysis method.

5.7.   Production Trials with Selected Die Materials and Surface Conditions

Based on the FE analysis of start-up and steady-state production with the selected die materials, production trials were planned in consultation with the forging company (Impact Forge, IN). Trials were conducted under standard production conditions with a required lot size of 14,000 parts. Die materials were provided by the tooling companies along with recommended heat-treatment conditions. Die manufacturing was done in-house by Impact Forge, whereas the heat-treatment and surface-treatment was done at a vendors location.

5.7.1.   Die Materials and Surface Treatments Selected

Trials were conducted using the W360™ die material and the original PressDie™ material for a planned lot size of 14,000 parts (≈ 6 shifts at a rate of 300-320 parts/hour). The buster die was modified to accommodate the changes recommended for the preform design (Figure 5.9). Blocker and finisher dies (top and bottom) were made with the selected die materials and surface treatments as shown in Table 5.2. Two bottom blocker dies were made with W360™ using a proprietary nitriding treatment on one. This was done solely to determine the effect of nitriding and to investigate the effect of the forging process (cyclic mechanical and thermal loading) on the condition of the nitrided surface layers. In the existing process all dies are used with nitriding. The W360™ dies were heat-treated to 50-52 HRC, whereas the PressDie™ blocker was heat-treated to ≈ 39 HRC. The effect of the nitriding treatment on change in the surface hardness is discussed in later sections on die coupon analysis.

103

	Blocker		Finisher	
Material	Top	Bottom	Top	Bottom
W360™	HT	1. HT/ST 2. HT	HT	HT
PressDie™	N/A	HT/ST	N/A	N/A
HT: Heat-treated.			HT/ST: Heat-treated and surface-treated (nitriding).	

Table 5.2: Die materials and surface treatments selected for trials.

5.7.2. *Production Trials: Comparison with FE Predictions*

Trials were conducted under normal production conditions in ten-hour shifts with a 4-hour break in between to allow for maintenance or set-up changes viz. 6.00 am- 4.00 pm (first shift) and 8.00 pm to 6.00 am (third shift). A 1600-ton mechanical press was used with manual part-transfer between stations and automatic lubrication, as outlined in the process description given earlier. The FE analysis was conducted using specifications of this equipment in order to calculate the exact deformation contact times.
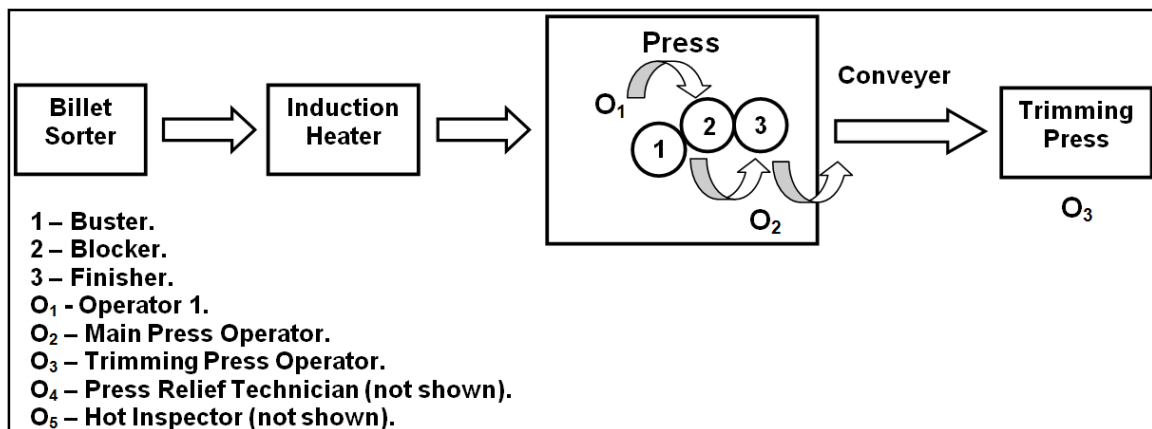
Figure 5.22: Production set-up for the selected forging cell.

The forging cell consisted of a billet sorter, induction heater, forging press and trimming press as shown in Figure 5.22. The cell is manned by five operators viz. one, to locate the billet on the buster and to transfer the preform to the blocker (Operator 1), one main press operator to transfer the blocker to the finisher and then onto the conveyor (Operator 2), one trimming press operator

(Operator 3), one press-relief technician to sequentially replace the three operators for breaks (Operator 4), and one hot-inspector responsible for quality checks at pre-determined intervals.

As shown, in Figure 5.22, the dies were arranged in a buster-blocker-finisher sequence and pre-assembled in the tool shop on a die cassette. Dies were pre-heated at the press prior to the start of production. The set-point for the dies was around 300-325℉ (≈ 160℃). An infrared thermometer was used at the press to monitor the die surface temperature a) before the start of the forging run, and b) during the forging run (at the end of lube spray just before the next workpiece was placed on the die). The parts were forged with the buster and finisher dies loaded at the same time. The following data was collected during the forging runs:

- Billet temperature at exit from the induction heater (from induction heater display).

- Die temperatures before and during production (at the start of the forging stroke).

- Press tonnage for the blocker and "buster + finisher" operations along with corresponding average billet temperature range (Note: Buster and finisher dies were loaded at the same time).

- Cycle times during production for different operators in different shifts.

- Lubricant concentration (provided by the shift supervisor) obtained through a laboratory sample burn-off procedure.

- Miscellaneous observations on production stoppages, operator part transfer/loading techniques, etc.

Figure 5.23 shows the production cycle-time measurements obtained during the trials. Data was collected over two shifts, for the main operator and the press-relief technician, who took over during breaks (refer Figure 5.22). The data indicates total cycle times for the buster, blocker and finisher operations i.e. starting from the time the workpiece is placed on the die until the start of the next cycle.

Trials were initiated with the W360™ HT bottom blocker die along with a W360™ finisher die set, using the set-up process described earlier. The production data was gathered over the entire first shift and over half of the second shift. The W360™ HT die showed significantly improved thermal fatigue performance based upon the quality checks performed at the press and through visual observation during equipment-related production stoppages. However, die failure occurred through mechanical fatigue cracking late into the second shift. A total of 4,431 parts were forged

105

on this die before failure. Subsequently, the W360™ HT/ST die (bottom blocker) was put into production with the same pre-heating procedures prior to the first stroke. Process data was again gathered starting from the third shift. The production yield from this die was 2,769 parts before mechanical fatigue failure was observed identical to that for the HT condition. The remaining 6,905 parts were then forged with the original PressDie™ blocker with the HT/ST condition for a total lot size of 14,105 parts.
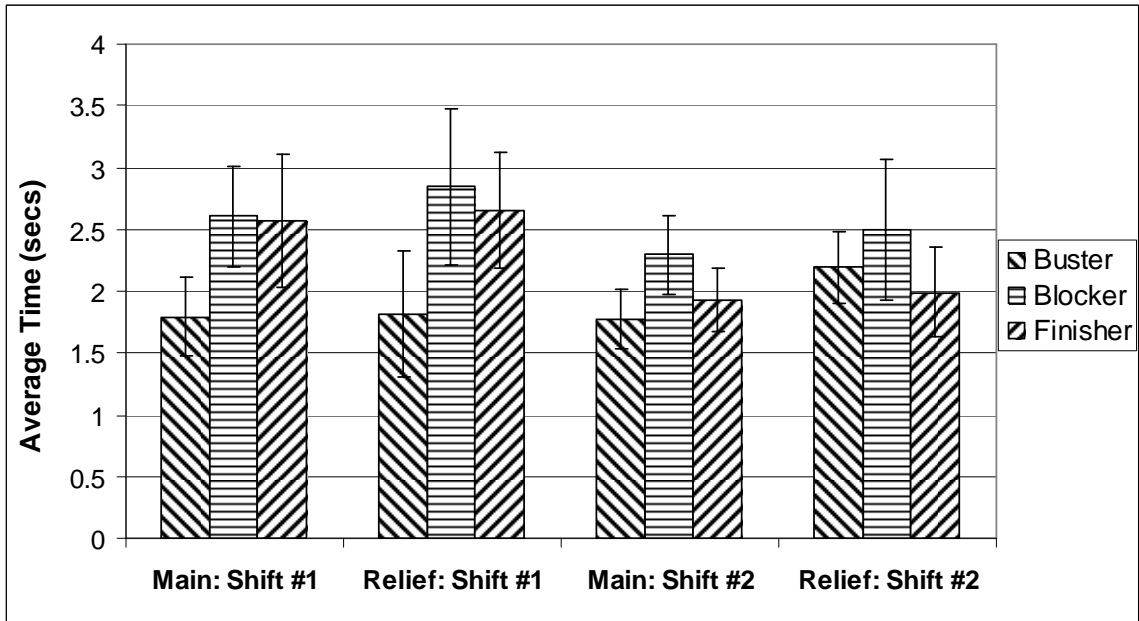
Figure 5.23: Production cycle times measured for the main operators and press-relief technicians, who take over for them during breaks (data over two shifts).

In the current production run, a ≈ 50% reduction in scrap rate was obtained through an improved preform design and a change in the blocker die material. The alternative die material was used for 51% of the required production lot size and failure through mechanical fatigue. No visual signs of thermal fatigue were observed on the critical region of the die surface (surface B) and part rejection due to pits and heat-checking was significantly reduced. Detailed analysis of the die surface was conducted through analysis of coupons taken from the used production dies.

5.8. Analysis of Die Coupons from Production

Sample coupon plates of the W360™ die material were heat-treated and surface-treated with the production dies in order to form a benchmark for comparison before and after forging. Coupons were also obtained from the production dies (blocker and finisher dies; top and bottom). Four coupons were made from each production die as shown in Figures 5.24 and 5.25 for the bottom

106

blocker. Coupons were prepared using electro-discharge machining (EDM) followed by polishing to 0.05 μm surface finish using standard specimen preparation guidelines for metallurgical analysis. Figure 5.25 also shows the points selected on the die surface for tracking state variables in FEA. The location and directionality of the crack observed in production is also shown. The crack occurrence was found to be radially symmetric about the centerline of the die (Figure 5.24). In the case of the W360™ dies (HT: heat-treated as well as HT/ST: heat-treated and surface-treated) the crack initiated circumferentially and then transversely through the die, splitting it lengthwise into two pieces (Figure 5.25 plan view). The crack location and pattern for both W360™ dies was found to be identical with respect to the die orientation in the press.
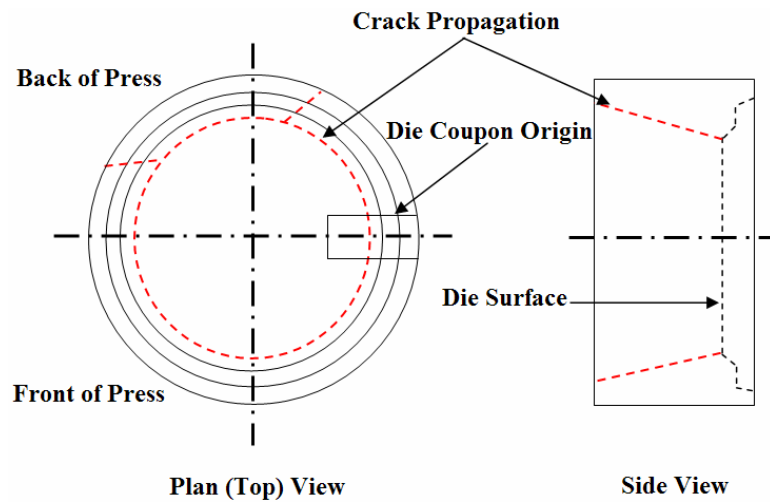
Figure 5.24: Crack location and directionality shown on a schematic diagram of the blocker die.
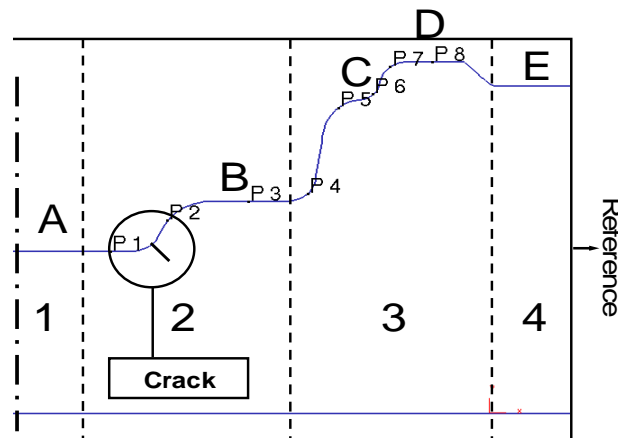
Figure 5.25: Die coupons selected for analysis from the used production dies.

107

Of the four coupons obtained from each used die, the one located outside the flash region (i.e. coupon 4 with surface E) was considered as the reference since it is not a functional forging surface, and does not interact with the workpiece. Thus, it is expected to show minimal thermal softening and change in the die surface, including the nitrided layer. Any changes observed on this surface are expected to be solely due to exposure to the gas flame (die pre-heating) and lubricant spray. The polished coupons were subjected to hardness and metallographic testing in order to investigate the effect of the forging process on the characteristics of the die surface.

5.8.1. *Characterization of Surface Layers using Hardness Profiling*

Die coupons were initially subjected to macro-hardness testing on the forging surface to get a preliminary trend in thermal softening. The sample coupon plates (sample plates heat-treated and surface-treated with production dies) were found to have a hardness of ≈ 50 HRC. Figure 5.26 shows the hardness variation (Rockwell C-scale) across the die surface starting from the inner region (surface A) to the outermost reference region (surface E). For the W360™ dies, maximum thermal softening (≈36% assuming initial hardness of 50 HRC) was observed in the region of surface A due to higher contact times with the new preform design (Figures 5.9 and 5.10). PressDie™ starting at a hardness of ≈39 HRC does not show significant thermal softening due to the precipitation phenomenon over the production run, which initially results in an increase in hardness (maximum of ≈ 48 HRC; Figure 5.27). The hardness drops off drastically after an aging (tempering) temperature of 1100ºF (590ºC), which is ≈ 35% greater than the maximum surface temperature in the existing process design. The aging time for this aging data was not specified; however, it should be noted that the same hardness change can be obtained by different time-temperature combinations i.e. higher temperature for shorter time or vice-versa. Thus, based on Figure 5.27, the alternative die materials were expected to retain their hot hardness and hot yield strength for a longer period compared to PressDie™. For W360™ and MaxDie™, the hardness-temperature relationship in Figure 5.27 only applies for a coupon heat-treated to maximum hardness and tempered for a minimum of 2 hours at each temperature. Data for different temperatures and different time periods is required in order to make an accurate comparison. Also, the hardness specified in Figure 5.27 is at room temperature and should not be confused with the hot-hardness, which is measured at an elevated temperature.

108
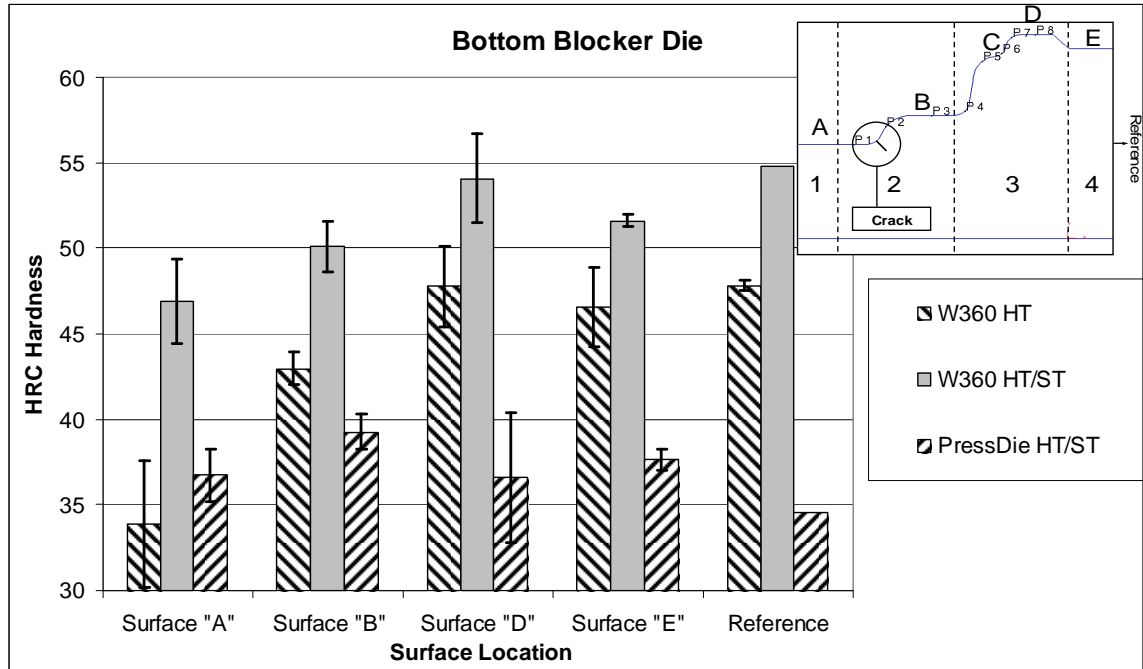
Figure 5.26: Macro-hardness measurements on the forging surface of the bottom blocker dies.

The macro-hardness measurements did not reflect the effect of surface hardening from nitriding. Nitriding processes, in general, result in local hardening of the surface layers to a depth of 150-200μm (0.006-0.008 in.) depending upon the process type and duration. Thus, macro-measurements are not suited for characterization of surface engineered components. Additionally, the surface of the sample coupon plates was rough machined, resulting in significant variation in the recorded measurements. Thus, reliable data was gathered using micro-hardness testing across the polished coupon cross-sections (Figures 5.28 and 5.29).

109
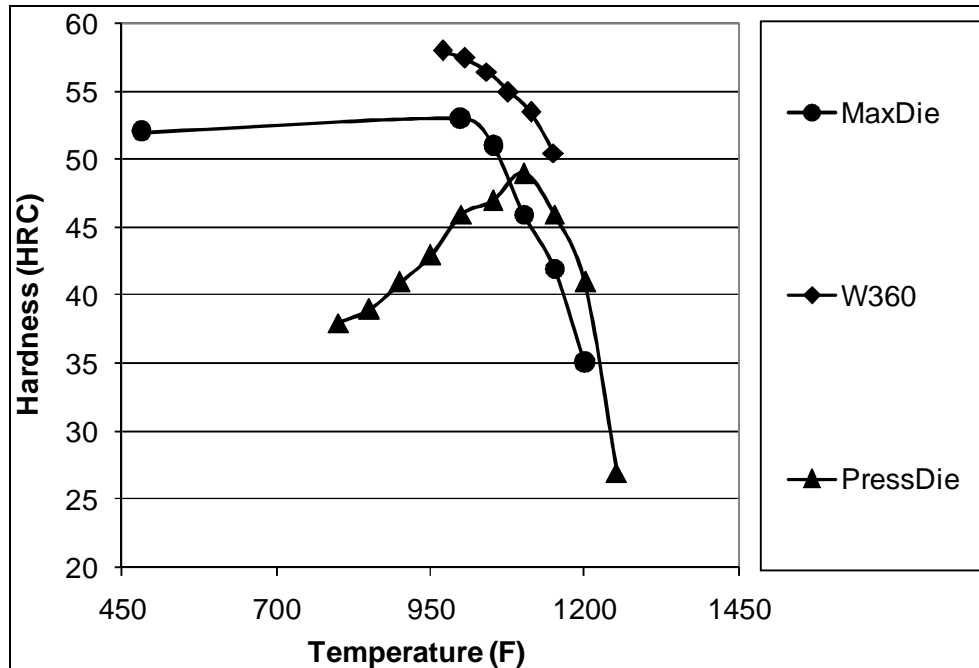
Figure 5.27: Tempering curves for the selected tool steels (thermal softening resistance) (Courtesy: Böhler-Uddeholm, Walter Metals and A. Finkl & Sons).

Vickers micro-hardness measurements were taken through the cross-section to a depth of 1500 μm (0.059 in.), starting in steps of 30 μm (0.001 in.) from the edge and increasing to 200 μm (0.008 in.) increments. The heat-treated hardness for the sample plates was found to be in the range of 51-53 HRC for the W360™ material based on the HT coupon and the die substrate layers (Figure 5.28) (Note: Sample plates were not available for PressDie™). Nitriding was found to result in up to 33% increase over the heat-treated hardness with hardness in the range of 55-70 HRC in the upper 200 μm (0.008 in.) of the surface. A consistent difference of ≈ 2 HRC was observed between the HT and HT/ST sample plates (Figure 5.28). This difference was attributed to either a) microstructural variation due to the two plates being from different production lots or b) diffusion of nitrogen, during nitriding, to a depth greater than 1500μm (0.059 in.).

110
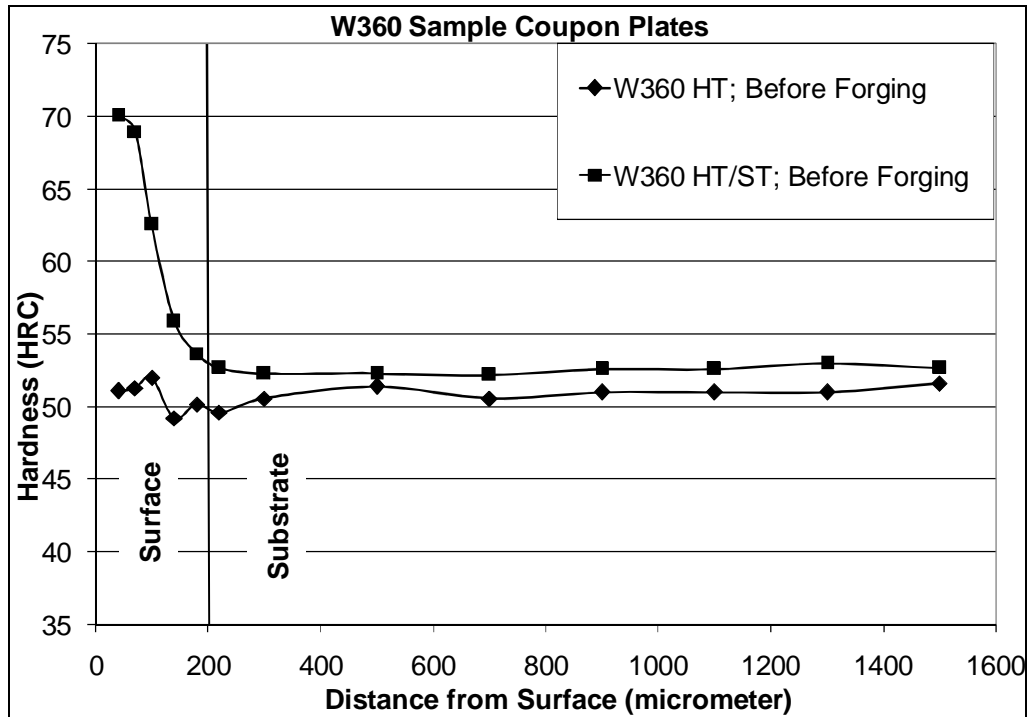
Figure 5.28: Effect of nitriding on the die surface hardness before forging (sample plates).
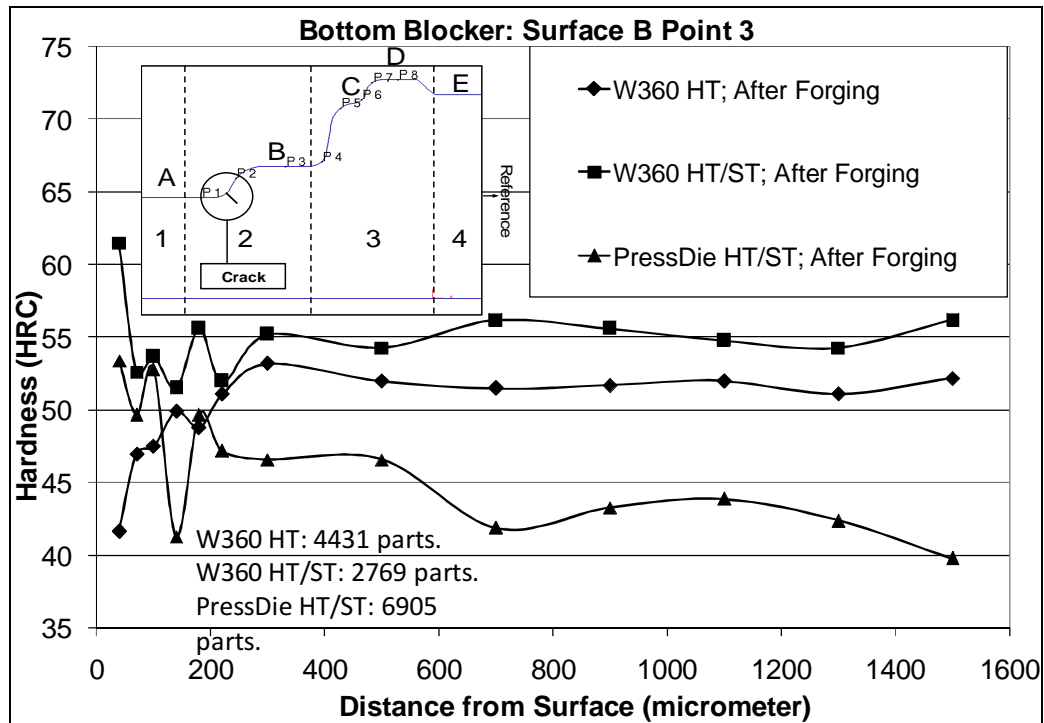
Figure 5.29: Thermal softening of production dies after forging: Surface B, Point 3.

111
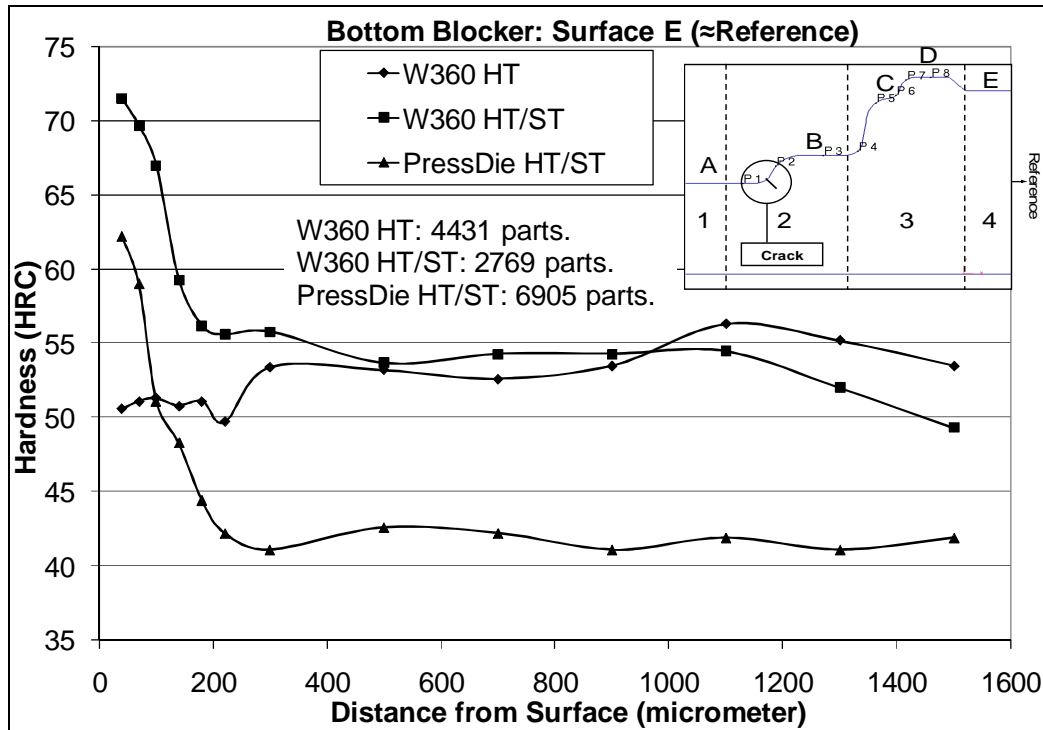
Figure 5.30: Hardness on surface E (reference) of production dies after forging.

Figure 5.29 shows the micro-hardness analysis done on the coupons obtained from the used dies. Results are presented for the most critical region of the die surface i.e. surface B. The substrate hardness of the W360™ dies was found to be in the range of 55 HRC for the HT/ST condition and 52 HRC for the HT condition. As in the case of the sample coupon plates (Figure 5.28), a consistent difference of ≈ 2-3 HRC was observed between the two surface conditions of W360™ (Figure 5.29). The reference surface E, which is not exposed to the workpiece, retains the nitrided layer and local surface hardness. This data was used to analyze the increase in local hardness of PressDie™, since sample plates were not available for this material. Based upon the substrate hardness measured after forging (≈ 42 HRC), the nitrided layer was found to be ≈ 45-55% harder (accounting for the fact that the substrate might have been affected by the precipitation process).

Thermal softening results in ≈ 20% loss of hardness on the surface of the nitrided layer (HT/ST condition) (Figure 5.31). The nitrided layer, however, is still ≈ 12% harder than the substrate (base). The HT coupon shows a drop in the surface hardness below that of the substrate (≈ 20% lower). PressDie™, being a precipitation hardening material has a substrate hardness of ≈ 40-44 HRC, which increases by ≈ 24% towards the surface (≈ 52 HRC). The PressDie™ data is only presented for qualitative comparison with W360™. It should be noted that, compared to

112

PressDie™, the W360™ HT/ST coupon, after forging, has ≈ 12% higher hardness in the upper layer and ≈ 25% higher in the substrate.
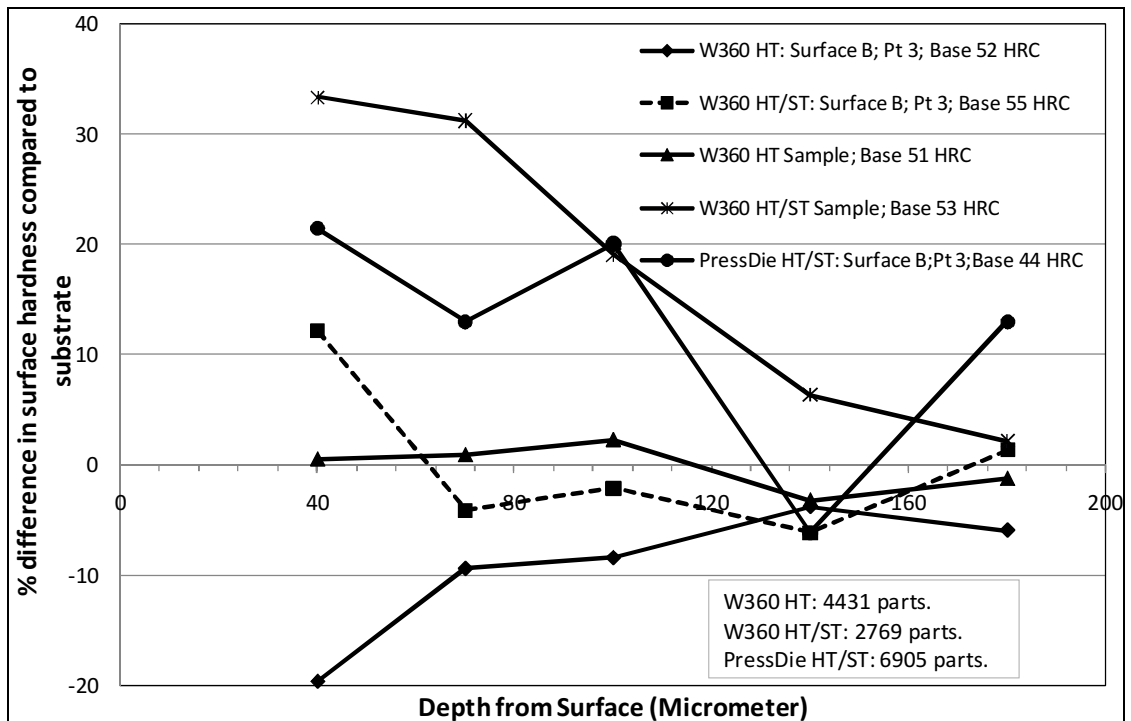
Figure 5.31: Change in surface hardness (upper 200µm; surface B, Point 3 for production die coupons from the bottom blocker) compared to that of the substrate.

5.8.2. *Metallographic Analysis of Surface Layers*

Micrographic analysis was conducted in order determine the nitrided depth and to analyze the effect of the forging process on die surface in terms of thermal fatigue. The polished die samples were etched using Nital in order to distinguish the nitrided surface from the die substrate. Figure 5.32 compares the W360™ die surface after forging to the sample coupons. The nitrided layer was etched dark and consisted of two distinct zones viz. a hard white layer of ≈ 30-40 μm on top of a nitrogen diffusion zone measuring ≈ 130-140 μm (total nitrided layer depth of ≈ 170-180 μm. The W360™ HT/ST sample appeared to retain a two-zone nitrided layer on the surface after forging (2,769 parts). No thermal fatigue cracking was observed on the die surface of either the HT/ST (≈19% of produced lot size) or HT (≈ 32% of produced lot size) coupons after forging (Figures 5.32b and c, respectively). The PressDie™ coupon shows significant heat-checking, with crack depths up to 700 μm (Figure 5.32d) after 6,905 parts (49% of produced lot size). The region of the nitrided layer is etched dark on the surface of the coupon.

113
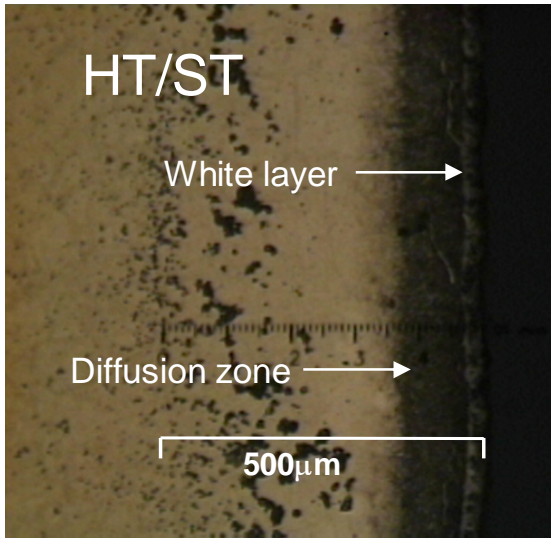
a) W360™ HT/ST Sample (before).
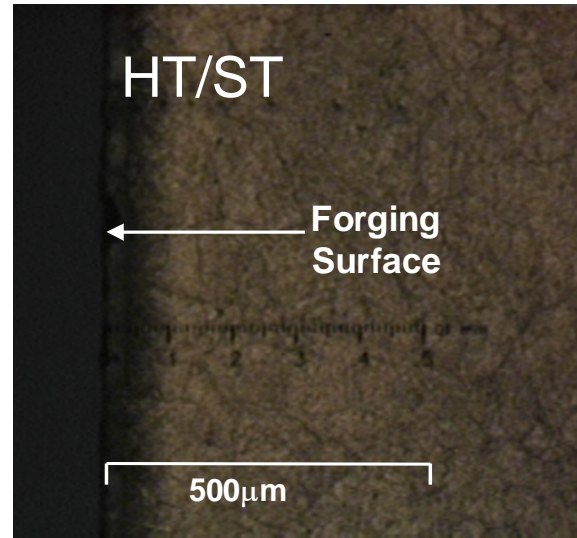
b) W360™ HT/ST Die
(after 2,769 parts; 19% of produced lot size).
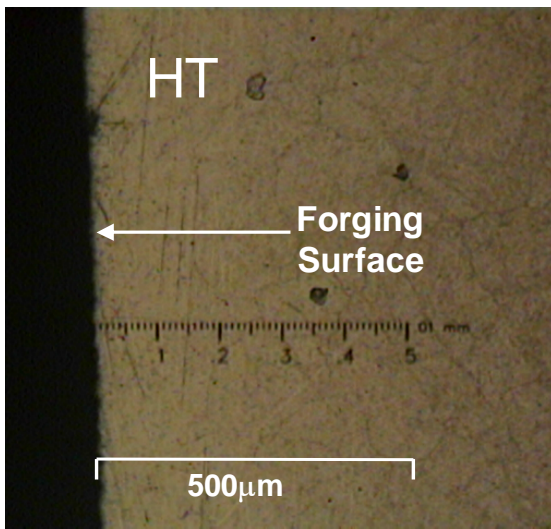
c) W360™ HT Die
(after 4,431 parts; 32% of produced lot size).
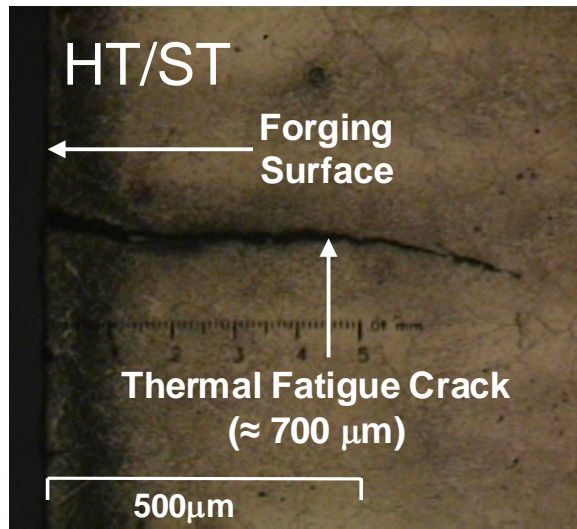
d) PressDie™ HT/ST
(after 6,905 parts; 49% of produced lot size).

Figure 5.32: Micrographs comparing the die surface before and after forging (sample coupons compared to surface B of bottom blocker).

114

5.8.3. Characterization of the Nitrided Layer

The micro-hardness analysis indicated that the nitrided layer on the die surface was depleted during the forging process. This was observed in the drop in hardness of the die surface layers Figures 5.29 and 5.31. The micrographs indicated that the nitrided depth corresponded to the micro-hardness measurements of the die samples and used die coupons. The nitrided layer was etched dark in both, the sample plate coupons and the used die coupons. In order to determine the effect of the forging process on the nitrided layer, energy-dispersive X-ray spectroscopy (EDS) was used with a scanning electron microscope (SEM). This was done under the assumption that the amount of nitrogen in the surface layer could be quantified and used as an indicator of the conditions of the nitrided surface before and after forging.

The EDS micro-analysis technique involves bombardment of the atoms comprising the sample surface with an electron beam. This beam ejects electrons from the inner shells of the target atom. The resulting vacancy is filled by an electron from the outer shell along with the emission of energy in the form of an X-ray. This X-ray is a unique characteristic of the targeted element from which it was emitted. A qualitative and quantitative analysis of the elemental/chemical composition of the sample can be conducted by comparing the emitted energy spectrum to the relative counts of the detected X-rays. Figure 5.33 shows the results of the EDS analysis conducted on the W360™ HT/ST sample plate coupon. The manufacturer-specified nominal chemical composition for W360™ is also provided for comparison with the EDS output and the two other tool steels. Carbon, nitrogen and oxygen, which are low atomic-weight elements and occur consecutively on the periodic table, could not be detected easily by EDS because of the resolution of the available instrument. However, the nitrogen in the surface layer was detected as a peak as shown in Figure 5.33, with a 6% weight content. EDS analysis of the surface B coupon from the W360™ HT/ST used production die shows a significant (≈ 76%) drop in the nitrogen content of the die surface after forging (2,769 parts; 19% of production lot size) (Figure 5.34). This is reflected in the absence of a nitrogen peak in the measured spectrum. The maximum die surface temperature during forging (Figure 5-11) was predicted to be in the range of 700-800ºF (370-425ºC). The nitriding temperature, on the other hand, is usually in the range of 800-1110°F (420-650°C). Based on the hardness profiles and EDS analysis it appears that the nitrided layer was lost during the forging process. However, the current analysis cannot specify at what point in production this depletion occurred.

115

Manufacturer specified composition

	Tradename	C	Si	Mn	Cr	Mo	V	Ni
Bohler	W360™	0.5	0.2	0.25	4.5	3	0.55	-
Finkl	PressDie™	0.2	0.25	0.7	-	3.35	-	3.25
Walter Metals	MaxDie™	0.38	0.25	0.35	5.1	1.9	0.65	-

SEM Output

W360 HT/ST	
Element	**Wt %**
N	6.00
Mo	3.19
V	0.70
Cr	5.31
Mn	0.53
Fe	82.28

EDS: Energy dispersive x-ray spectroscopy.
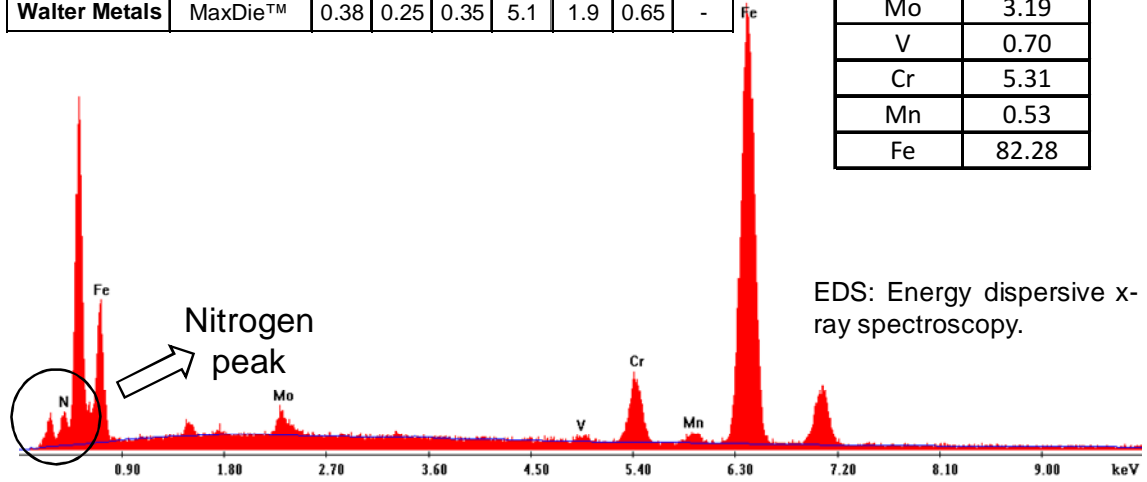
Figure 5.33: EDS results for the W360™ HT/ST sample coupon plate i.e. before forging.

W360 HT/ST	
Element	**Wt %**
N	1.44
Mo	3.08
V	0.71
Cr	4.75
Mn	0.48
Fe	89.53

EDS: Energy dispersive x-ray spectroscopy.
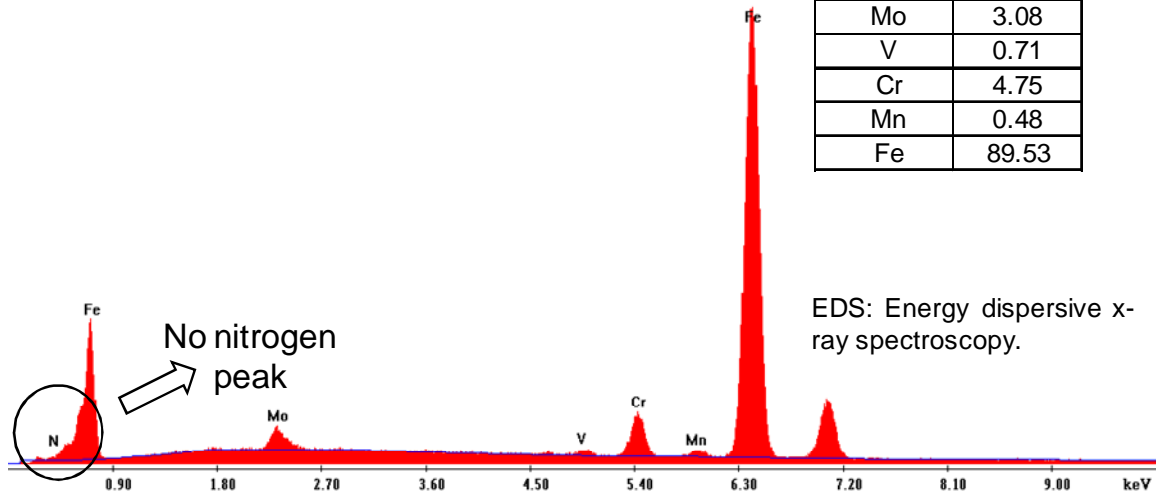
Figure 5.34: EDS results for the W360™ HT/ST die coupon (Surface B; Figure 5.25) i.e. after forging.

116

Except for manganese (Mn), the % content of the other alloying elements compares well with the nominal composition provided by Böhler-Uddeholm for W360™. The sample coupon and the one from the production die, both, showed an error of 90-110% in the detected amount (Figures 5.33 and 5.34). Since vanadium (V), chromium (Cr) and manganese (Mn) occur consecutively on the periodic table, this error might be related to the limited resolution of the available instrument as was the case for the lighter elements mentioned earlier. This is one of the limitations of EDS analysis, which is susceptible to overlap in the energy emitted by elements similar in atomic weight.
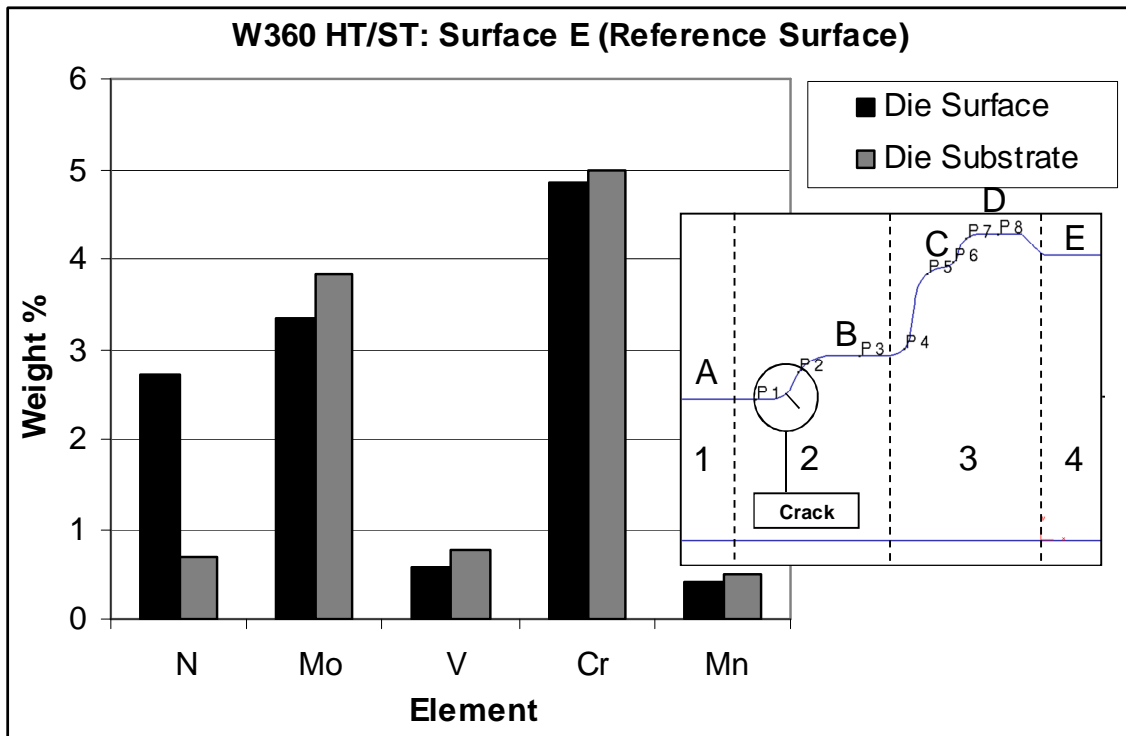
Figure 5.35: EDS results for the W360™ HT/ST die coupon; comparison of surface layer (upper 200 μm) to substrate.

Figure 5.35 compares the nitrided (reference) surface E of the W360™ die with the substrate i.e. EDS spot at the surface compared to one at ≈ 200μm from the surface. The nitrogen content is concentrated at the die surface and depletes farther into the surface away from the white layer and the diffusion zone. The nitrogen concentration was found to be 75-80% lower near the substrate region compared to the reference surface, as evidenced in the micro-hardness measurements (Figure 5.30).

117

5.9.   Summary and Recommendations

A conventional hot forging process for a disc-shaped component was selected in order to develop and apply FEA-based techniques for improvement of die life through analysis of die-workpiece interface conditions. This study was conducted in cooperation with Impact Forge of Columbus, IN under the FIERF-sponsored die wear research project. The primary die failure mechanism in this forging process was thermal fatigue, resulting in high downtime and scrap rates. The following research objectives and results were achieved through a combination of FE analysis and shop floor validation:

- Production cycle-time data was used in order to model the entire forging cycle including die hill, deformation, dwell and lubrication spray. This allowed for a more accurate analysis of the thermal cycle experienced by the die surface as opposed to only analyzing the deformation stage, as is common practice in the forging industry and academia.

- An FE simulation technique was developed for prediction of interface conditions at start-up and at steady-state through analysis of multiple forging cycles (30 cycles in this case), each consisting of the distinct stages mentioned above.

- A preform design improvement was suggested in addition to alternative die materials. The new process design reduced contact times in critical die regions by 65% resulting in 16-25% reduction in the maximum die surface temperature.

- Alternative die materials (W360™ and MaxDie™) were compared to the existing material (PressDie™) on the basis of their thermal and mechanical properties using FE analysis. The thermal fatigue performance of the selected materials was predicted on the basis of surface stress and strain amplitudes. Based on the FEA results, W360™ was predicted to have the best thermal fatigue performance, in conjunction with the new preform design.

- Production trials were conducted with the suggested preform design using the existing PressDie™ material and the new W360™ material in heat-treated and nitrided condition. A 50% reduction in scrap rates was observed with the new design and tool materials; however, the dies (bottom blocker) failed by mechanical fatigue.

- Analysis of production die coupons revealed a mechanical fatigue crack in both the die materials due to insufficient containment. A split die design (similar to finisher) was recommended for the blocker die to reduce the stress concentration and deflections at

118

the radius where the crack occurred. Nitriding delays the thermal softening occurring on the die surface, however, the nitrided layer depletes over the course of the production run, as confirmed by EDS analysis.

On the basis of these results, the following recommendations were made for improvement of thermal fatigue life of hot forging dies being used in mechanical presses:

- Die material selection: Alternative die materials should possess higher thermal conductivity and hot yield strength for improved thermal fatigue resistance through reduction of surface stress and strain amplitudes.

- Die pre-heating method: Pre-heating in an oven was recommended to ensure a relatively uniform temperature distribution throughout the bulk of the die. This, in addition to in-press heating (prior to the start of production and during stoppages), will help to minimize the surface stress and strain amplitudes during start-up.

- Preform and buster die design: Die design modifications, such as the one in the current case, were recommended for reduction of the contact time in the critical regions of the die. Reduction in the contact time can also be obtained by holding the workpiece above the die surface prior to the start of the stroke. This can be done either through a) appropriate operator training or b) programming of the transfer or knockout mechanism.

- Lubrication spray: It is recommended to program the lubricant spray in an air-water-lube sequence in order to a) reduce thermal shock, b) effectively cool the die and c) ensure lubricant adhesion. Lubricant concentration should be monitored during production unless a CNC-based mixing and delivery system is being used.

FEA was, thus, successfully used to improve die service (thermal fatigue) life in a high-volume hot forging process by optimizing the preforming and finisher die design in conjunction with selection of alternative die materials.

CHAPTER 6

CASE STUDY 2 – IMPROVEMENT OF THERMAL FATIGUE LIFE

IN WARM FORGING ON A HYDRAULIC PRESS

6.1.   Problem Statement and Process Description

Chapter 5 focused on the improvement of thermal fatigue life in a conventional hot forging process. The die design used for the reverse piston consisted of components that had slip-fit interface conditions between them. Chapter 6 considers a warm forging process, which utilizes a shrink-fit tool design requiring a much more detailed analysis approach in order to a) model the pre-stressed assembly, and b) account for loss of pre-stress from thermal expansion during pre-heating and forging. Currently, shrink-fit die designs in the forging industry are developed using room temperature die dimensions. However, thermal expansion of the die components from pre-heating and forging results in loss of the shrink-fit, possibly resulting in die failure. Thus, a correction in the dimensional interferences is necessary by determining steady-state temperature distributions as well as the effect of pre-heating, especially when ceramic or carbide die inserts are being used.

This study was conducted in cooperation with American Axle and Mfg. (Colfor Division). Proprietary details have been sanitized to maintain confidentiality. The process in question is used for forging of a mass-produced automotive transmission shaft. The schematic of the forging process is provided in Figure 6.1, which outlines the die assembly and preform geometry. The die insert is made of H-21 tungsten-based hot-work tool steel with the containment system (sleeve, backup and container) made from H-13 chromium-molybdenum hot-work tool steel. The forging process involves local upsetting of the cylindrical end of a steel preform to form a flange as shown with the dotted outline (Figure 6.1). The overall forging process consists of:

1. Die assembly: The insert is assembled into the sleeve with a negligible shrink-fit between them. This sub-assembly is then press-fitted into the container, which has interference on the inner diameter (I.D.) with the outer diameter (O.D.) of the sleeve. Thus, the insert is placed under compressive pre-stress.

120

2. Die heating: The die assembly is then heated with a gas flame on the container to reduce thermal shock on the insert upon start-up of the production run.

3. Preform heating: The preforms are locally induction-heated at one end to a temperature range of 1350-1600ºF (730-870ºC).

4. Forging: The forging process is carried out on a hydraulic press with manual part transfer and automatic lubrication spray.
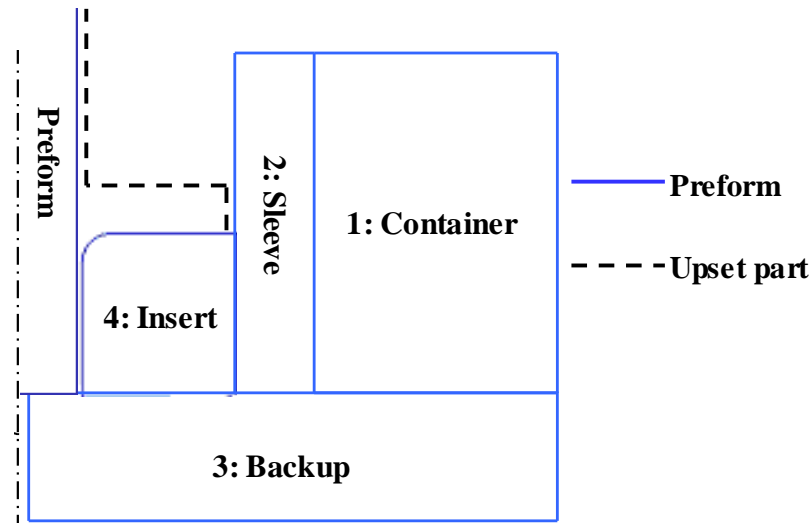
Figure 6.1: Schematic representation of the warm forging (upsetting) die assembly.

The primary die failure mechanism is through thermal fatigue occurring on the upsetting surface and the die corner radius. There is a need for evaluation of the die-workpiece interface conditions in order to select and, subsequently, compare alternative die materials and/or process designs for improved die life.

6.2. Objectives

The overall objective of this study was to improve thermal fatigue life of warm forging dies through selection as well as comparison of alternative die materials and die designs using FE simulations in conjunction with production trials. The following specific research objectives (mentioned in Chapter 2) were addressed through this study:

- Selection of die materials on the basis of observed failure mechanism and desired properties (cause and effects analysis of die failure modes).

121

- Determination of interface conditions at start-up and during steady-state using FEA of the forging process.

- Prediction of the thermal fatigue performance of selected die materials using FEA.

- Determination of the effect of die material properties (mechanical and thermal), and their relative importance, on interface conditions; specifically, those related to thermal fatigue performance.

- Design of shrink-fit dies, specifically for ceramic and carbide inserts, taking into account the thermal expansion from die heating (from pre-heating and steady-state forging).

- Investigate the possibility of applying welded overlays in warm forging tooling and develop an FE analysis methodology for the same.

This chapter addresses the objectives related to selection and comparison of hot-work tool steels. The FEA analysis approach for ceramic and carbides is touched upon briefly, with more detailed approach and results outlined in Chapter 7.

6.3. Determination of Interface Conditions in the Existing Process

The selected warm forging process is conducted on a hydraulic press, which has significantly longer contact times and thus, a longer cycle time, compared to a mechanical press as seen in Chapter 5. Figure 6.2 outlines the process sequence for the selected component.

122
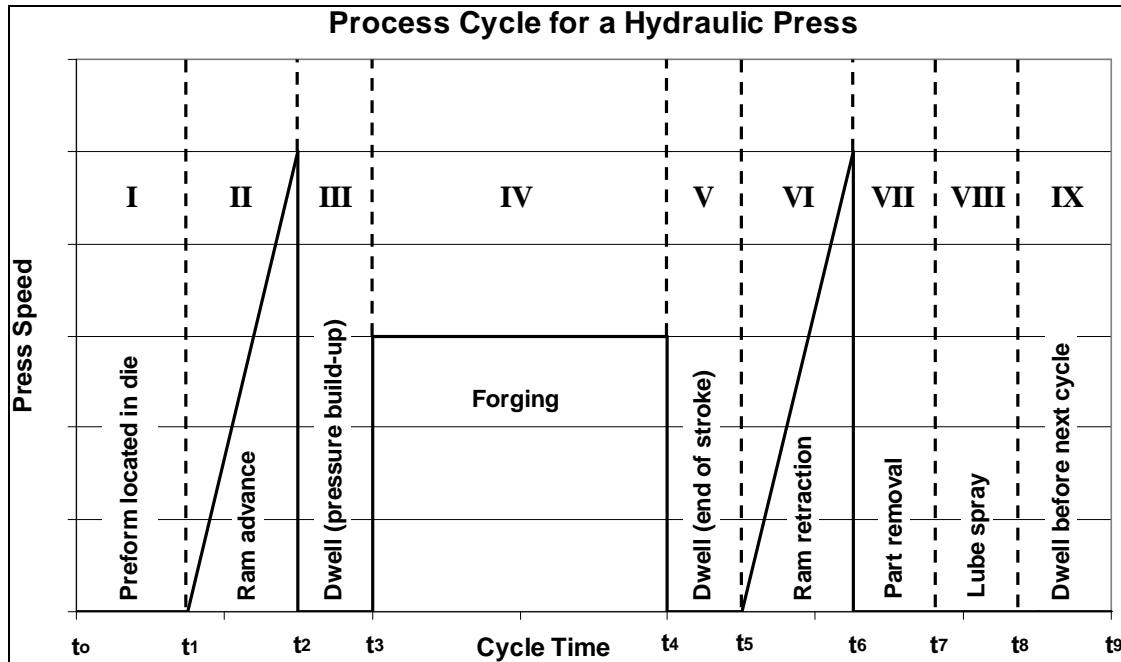
Figure 6.2: Generic process sequence for warm and hot forging on a hydraulic press.

Cycle time and die temperature data was gathered from production through the questionnaire developed for this study (Appendix-A):

- Stage (I + II): 3 seconds.

- Stage III: Currently neglected.

- Stage IV: Ram speed (1 in/sec).

- Stage V: Currently neglected.

- Stage (VI + VII): 2 seconds. Production die surface temperature after Stage VII was ≈ 600-700°F (310-370°C).

- Stage VIII: Lubricant spray time (1 sec). Die surface temperature after Stage VIII: ≈ 450°F (230°C).

- Stage IX: Dwell time before next stroke (3 sec).

- Total forging cycle: ≈ 12 seconds.

123

Data was also available on the die assembly sequence and die pre-heating. Die and workpiece geometries were obtained from production drawings. Additionally, the temperature distribution in the locally heated workpiece was also provided for use in FE analysis (Figure 6.3).

Temperature (⁰F)

A =	800
B =	904
C =	1010
D =	1110
E =	1220
F =	1320
G =	1420
H =	1530
I =	1630
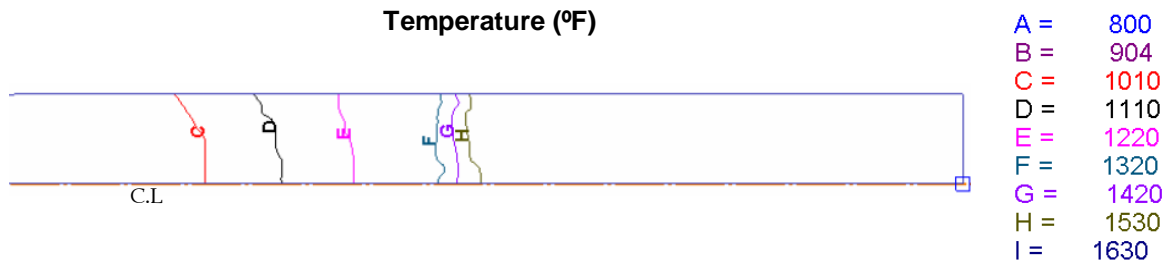
Figure 6.3: Temperature distribution in the round (cross-section) billet prior to forging; obtained from production measurements.

6.3.1. Analysis of the Die Assembly Process

The purpose of designing a shrink-fit die assembly is to put the insert into a compressive state of (hoop and radial) stress in order to counter the tensile stresses generated while deforming the workpiece (Figure 6.4). This concept is identical to that used in pre-stressed pressure vessels, since the die acts as a cylindrical shell with internal pressure during deformation. In general, there are two methods for assembling shrink-fitted dies. These are illustrated using the schematic in Figure 6.4:

1. Thermal shrink-fitting: The container is heated until thermal expansion eliminates the interference at the interface with the sleeve. Thus, the dies are assembled under slip-fit conditions at elevated temperature. The insert is placed under the designed compressive pre-stress when the container cools down to ambient temperature.

2. Press-fitting: This process is conducted on a hydraulic assembly press utilizing draft angles on the shrink-fit interfaces. Thus, the container is "pressed" onto the insert-sleeve sub-assembly or vice-versa in order to obtain the desired pre-stress.

In general, higher interference fits and accuracy can be achieved through press-fitting because of limitations on the thermal expansion and heating temperature of the heat-treated die components. A combination of the two approaches can also be used to reduce press-fitting loads. The die assembly process at AAM is achieved purely by press-fitting, with draft angles at the sleeve-container interface i.e. container I.D at the top is less than container I.D at the bottom, with the same being true for the sleeve O.D.

124
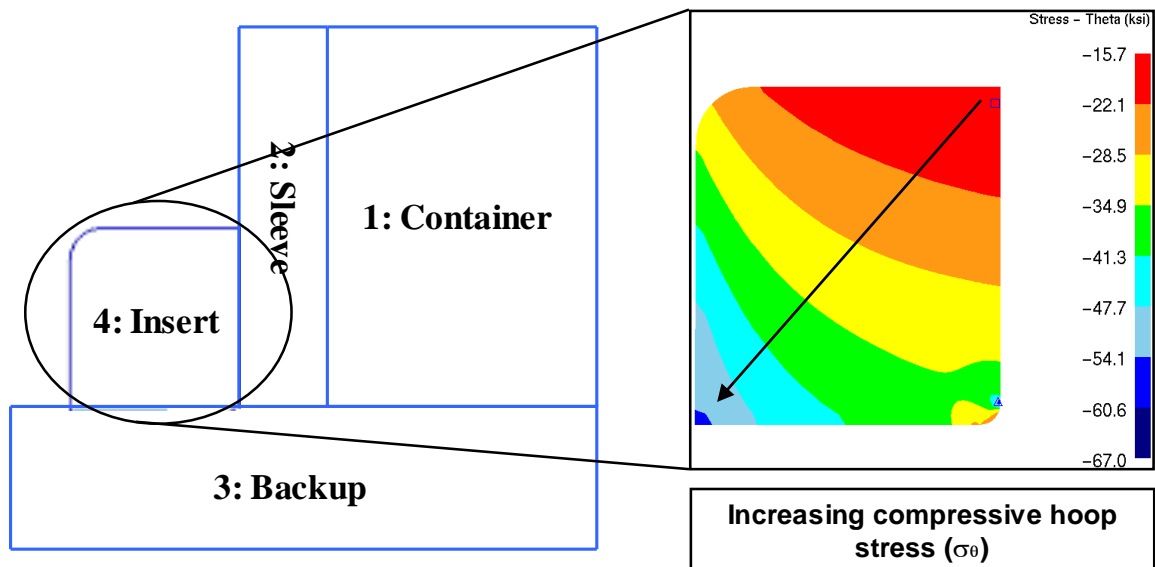
Figure 6.4: Stress distribution (hoop/circumferential direction) in the insert after die assembly (H-21 tool insert).

Current practice in the forging industry and most academic research is to simulate the die assembly process by applying displacement boundary conditions (equal to interference) on one of the two surfaces that form the shrink-fit interface. This process is conducted in a single step FE simulation, which results in the entire interface contact being generated instantaneously. This simulation approach saves a significant amount of computational time, but is suited for analysis of die assembly by thermal shrink-fitting, where component interfaces are generally straight. The error from this approximate simulation process is greater when the shrink-fit interface has a draft angle on either surface. The simulation assumes instantaneous contact with uniform pressure distribution, whereas in reality, contact is generated incrementally and is non-uniform in terms of pressure distribution. This hypothesis was tested in the current case by conducting die assembly simulations with both techniques (Figure 6.5). All die components were modeled as elastic objects. Both cases indicated that the circumferential/hoop stress increases radially inwards, which is in line with mechanical engineering principles. However, the diagonal trend in the hoop stress was opposite in the two cases. The single-step approach predicted a diagonal increase upwards from the O.D with maximum compressive stress magnitudes ≈ 140% greater than those with the incremental approach (Figure 6.5a). The resulting stress distribution, thus, assumes perfect contact and influences the directionality of the stress gradient.

125
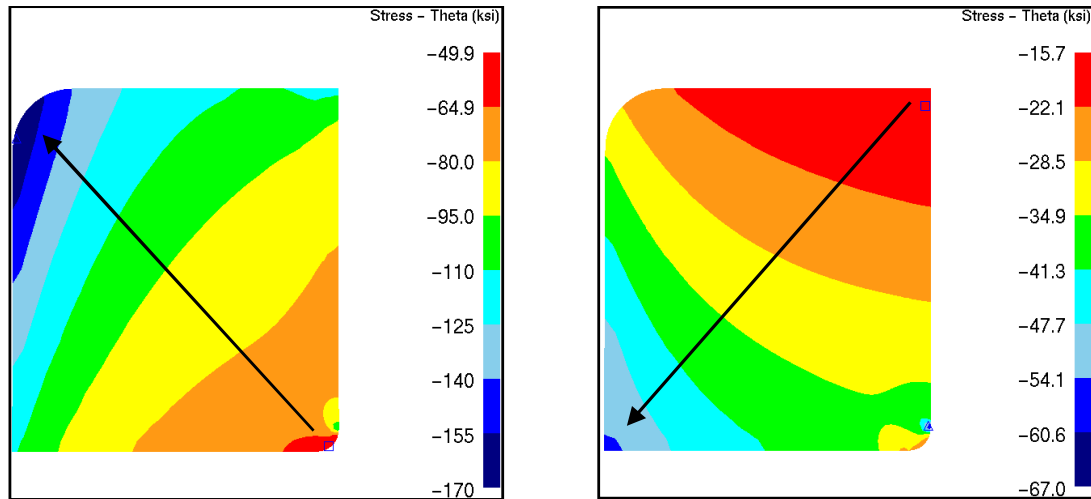
a) Single step approach.   **b) Incremental approach.**

Figure 6.5: Error introduced by conducting a single-step die assembly simulation with displacement boundary conditions (H-21 tool insert).

The incremental approach was conducted in two steps viz. a) incremental assembly of the sleeve and insert, and b) incremental assembly of the container over the sleeve-insert sub-assembly. This process used unmodified component geometries and was simulated using actual die component movement in the sequence used on the shop-floor. Thus, the directionality of the stress gradient corresponds to that of the mechanical loads applied by the draft angles during assembly.

126

Original geometry

Note: Insert, backup and container not shown.

C.L

Deflected geometry
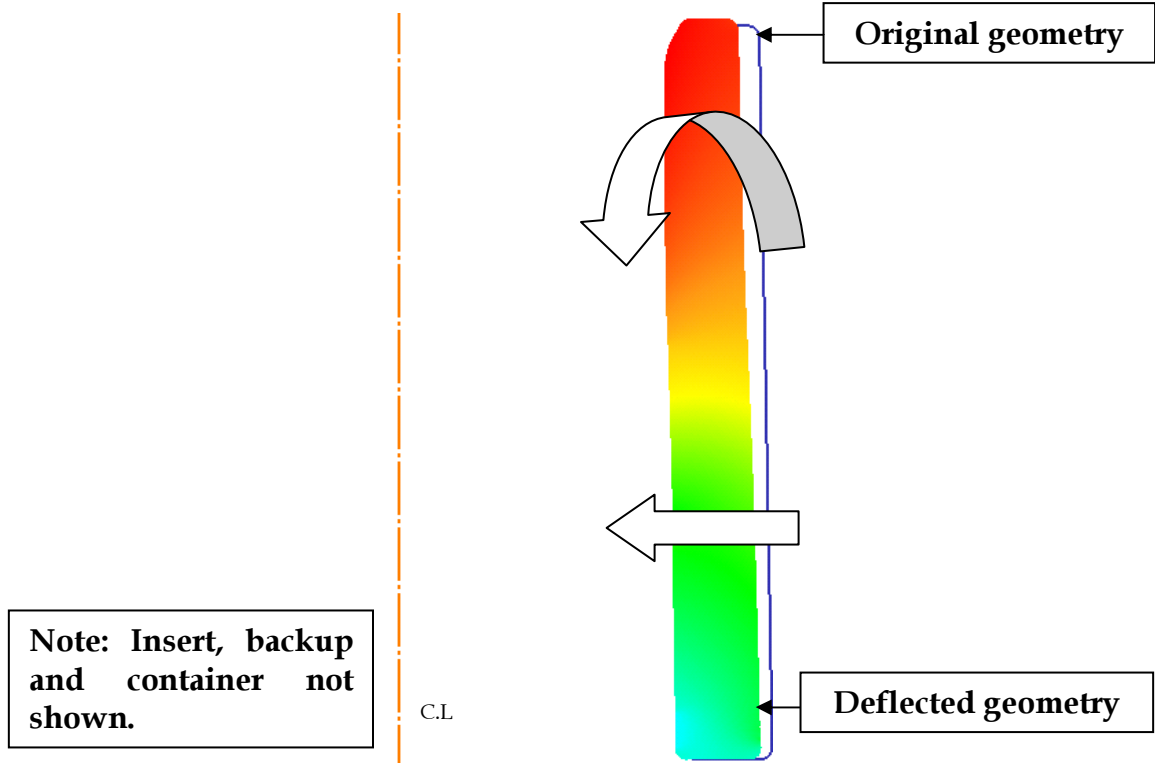
Figure 6.6: Deflection in the sleeve after assembly (magnified 20x).

The stress gradient is a consequence of the deflection of the sleeve during assembly (Figure 6.6). The stress pattern in the insert can be explained by examining the deflections in the sleeve during assembly. As the container is assembled onto the sleeve, the latter deflects initially in the radial direction. The lower part of the sleeve contacts the backup die and insert, putting them into a state of compressive pre-stress. The upper part of the insert, however, is not supported on the inner diameter and deflects inwards as shown in Figure 6.6. This deflection is responsible for the diagonal stress gradient observed in Figure 6.5b. This deflection is influenced by variations in the draft angle and interference at the sleeve-container interface. Chapter 7 summarizes the results of a basic sensitivity analysis (for a carbide insert) using dimensional variations measured on the shop floor.

6.3.2. Analysis of the Die Heating Process

Pre-heating causes thermal expansion of the die components, resulting in a change in the elastic deflections and shrink-fit conditions in the assembly. This is one of the critical reasons for failure of ceramic and/or carbide inserts. The difference in the coefficients of thermal expansion of the carbide/ceramic insert and tool steel containment results in the container and sleeve expanding

127

more than the insert. Additionally, the temperature gradient from pre-heating affects the interface conditions, which are used for prediction of thermal fatigue performance of the selected tool materials. Thus, it was decided to include the simulation of die heating in order to a) estimate the potential loss of shrink-fit during heating, b) to compare different heating methods, and c) to include a thermal gradient in the simulation of the forging process instead of assuming a uniform preheat temperature.

Two types of die heating methods were investigated in this study using production observations viz. a) gas flame on the outside of the assembly and b) gas flame on the inside, directly on the insert. The die insert was assumed to be made of carbide in order to increase the sensitivity of the shrink-fit conditions to thermal expansion. It was decided to use 2-D FEA initially, with the option of using a 3-D analysis later, to account for asymmetric heating from the use of a single flame on the container O.D (observed on the shop floor).

6.3.2.1. *Die Heating with a Gas Ring on the Container O.D*

Figure 6.7 shows the boundary conditions used for analysis of heating on the outside of the container. A non-isothermal 2-D axisymmetric (radially symmetric about the center line) model was used with the stress, deflection and contact history from the incremental assembly process. Thus, the model assumed the use of a gas ring on the container O.D instead of a single gas flame. The heating process was simulated in two steps:

- Simulation of the actual heating process (Step 1): A temperature boundary condition was assumed on the container surface using a temperature (800ºF/425ºC) below the standard tempering temperature of tool steel. The remaining surfaces of the tooling were given an interface heat transfer coefficient corresponding to natural convection with ambient conditions. A heating time of 2-3 minutes was assumed based on production input. No die surface temperature data during heating was available from AAM. The backup die, sleeve and container were restricted from moving in the Z-direction (Z = 0 in Figure 6.7) using velocity boundary conditions. Additionally, a force boundary condition was necessary on the top surface of the insert to prevent loss of contact with the backup die during thermal expansion. This strategy was used to prevent convergence problems in the FE simulation. The final stress state was then obtained by removing the force boundary condition in the last simulation step. This approach was found to be the most accurate after evaluating two other alternatives viz. a) sticking conditions at the insert-backup interface, and b) rigid die assembly for heating, with a single step elastic analysis to reach equilibrium conditions with the temperature gradient.

128

Figure 6.7: Schematic representation of boundary conditions used for simulation of die heating (gas ring on the outside of the container).

- Simulation of the dwell time from the end of heating to the start of the forging process i.e. until the first forging stroke (Step 2): This was simulated by applying ambient conditions on all the heated die assembly surfaces for an assumed dwell time of 10 minutes. Similar to Step 1, a force boundary condition was required in this step to prevent convergence problems in the FE analysis.

The radiation heat transfer between the die components and the environment was not taken into account during these simulations, since it was not computationally feasible. This decision was based on discussions with Scientific Forming Technologies Corporation (SFTC), the developers of DEFORM™.

Figure 6.8a shows the temperature distribution in the assembly at the end of heating, whereas Figure 6.8b shows the temperatures after the dwell time i.e. prior to the first forging stroke. With a heating time of 2 minutes, the insert was still approximately at room temperature. After the assumed 10 minute dwell time, however, the average temperature of the die assembly was predicted to be in the range of 250-300ºF (120-150ºC), with that in the insert being around 270ºF (130ºC). The 2 minute heating time was sufficient for thermal expansion of the container. Since the shrink-fit on the insert is influenced primarily by the sleeve-container interference, this expansion resulted in loss of contact at the insert-sleeve interface. Thus, the compressive hoop stress in the insert dropped as seen in Figure 6.9c (compared to Figure 6.9a). The tensile

129

stresses observed were due to the thermal expansion of the insert. Figures 6.9b and c show the stresses in the insert at the end of heating (removal of gas ring) and after dwell (prior to the first forging stroke), respectively.
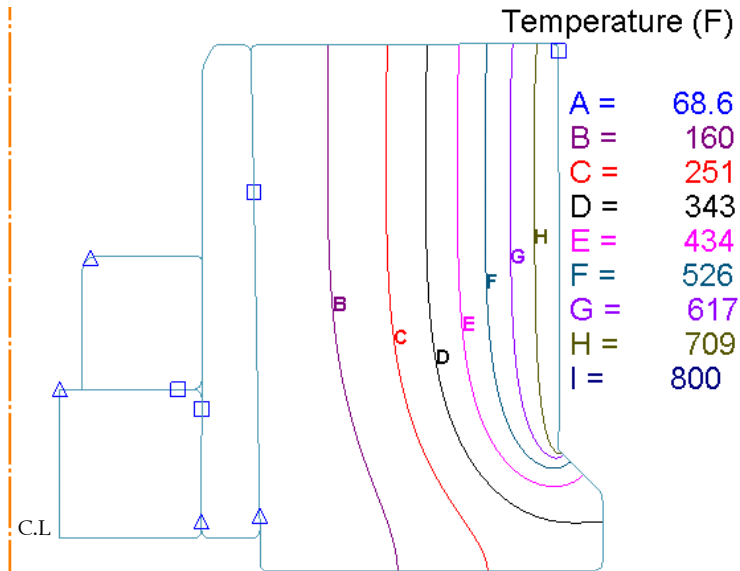
a) Temperature distribution at the end of heating.
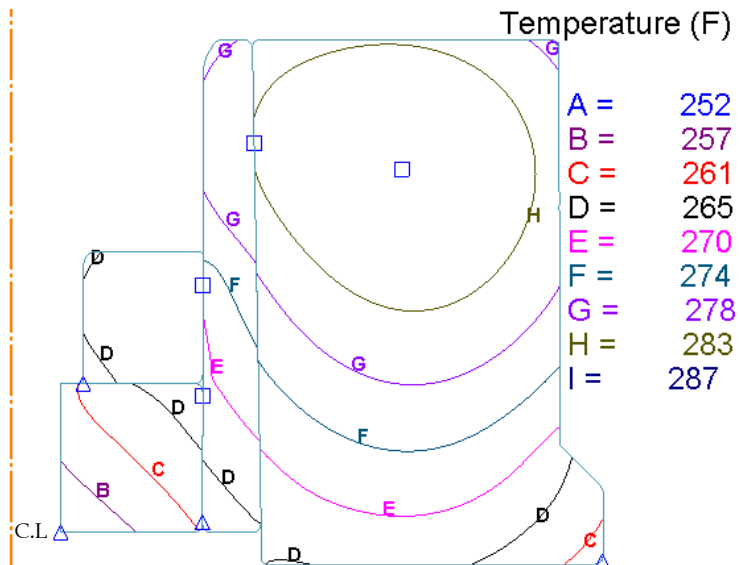
b) Temperature distribution prior to the first forging stroke.

Figure 6.8: Temperature distribution in the assembly after heating and dwell (gas ring on the outside; carbide insert).

130

The stresses in the insert are governed by the deflection in the container and sleeve during pre-heating (Figure 6.10). The bottom (back) of the container has a thinner cross-section due to the draft angle on the inner diameter and expands outwards placing an inward bending moment on the sleeve during the simultaneous radial expansion (Figure 6.10a). Thus, during heating, the bottom (back) of the sleeve expands outwards, whereas the top (front) deflects inwards. During the dwell period, however, heat dissipates throughout the assembly, and the deflection in the sleeve is reversed as the container starts to contract to its original shape (Figure 6.10b).

Stress - Theta (ksi)

A =	-127
B =	-114
C =	-101
D =	-88.2
E =	-75.1
F =	-62.1
G =	-49.1
H =	-36.0
I =	-23.0
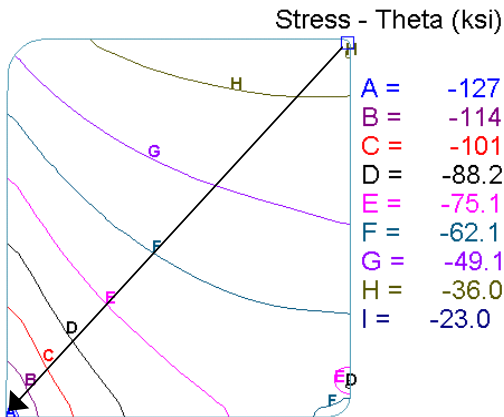
Increasing compressive hoop stress (σ_θ)

a) After assembly.

Stress - Theta (ksi)

A =	-27.1
B =	-21.1
C =	-15.1
D =	-9.09
E =	-3.09
F =	2.90
G =	8.90
H =	14.9
I =	20.9

Stress - Theta (ksi)

A =	-77.9
B =	-65.1
C =	-52.2
D =	-39.3
E =	-26.5
F =	-13.6
G =	-0.777
H =	12.1
I =	24.9
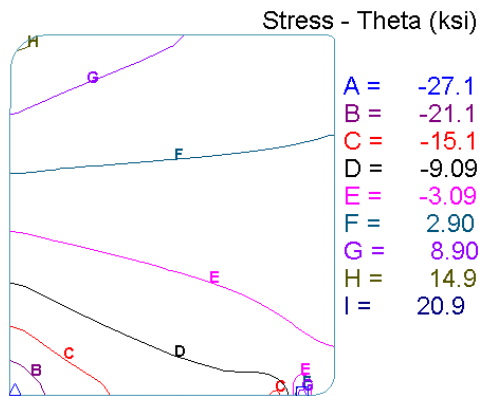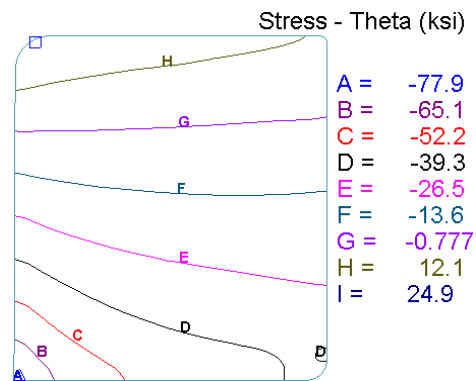
b) At the end of heating.   **c) After dwell i.e. prior to first stroke.**

Figure 6.9: Loss of shrink-fit in the insert due to pre-heating (gas ring on the outside; carbide insert).

131
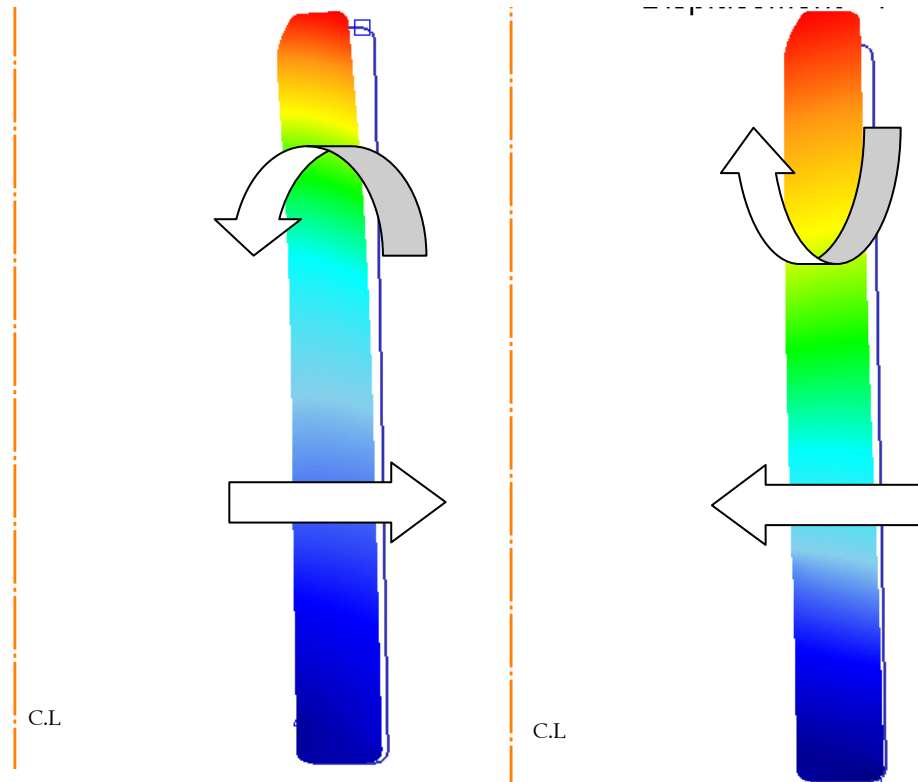
c)   At the end of heating.   d)   Prior to the first forging stroke.

Figure 6.10: Deflection in the sleeve during pre-heating (gas ring on the outside; magnified 20x; carbide insert).

6.3.2.2.   *Die Heating with a Gas Flame on the Insert and Sleeve*

An alternative heating technique was investigated in order to minimize the loss of shrink-fit, while accomplishing the functional goal of pre-heating i.e. to reduce thermal shock. This approach involved using a gas flame directly on the insert and sleeve, i.e. in the die cavity as opposed to the outer diameter of the container. A temperature boundary condition (T = 800ºF/425ºC) was, thus, applied on the entire inner diameter surface of the assembly. Apart from a change in the thermal boundary conditions, the FE modeling process was the same as that discussed in Figure 6.7. Prior to the first forging stroke, the insert temperature is predicted to be in the range of 160-170ºF (70-80ºC) (Figure 6.11b).
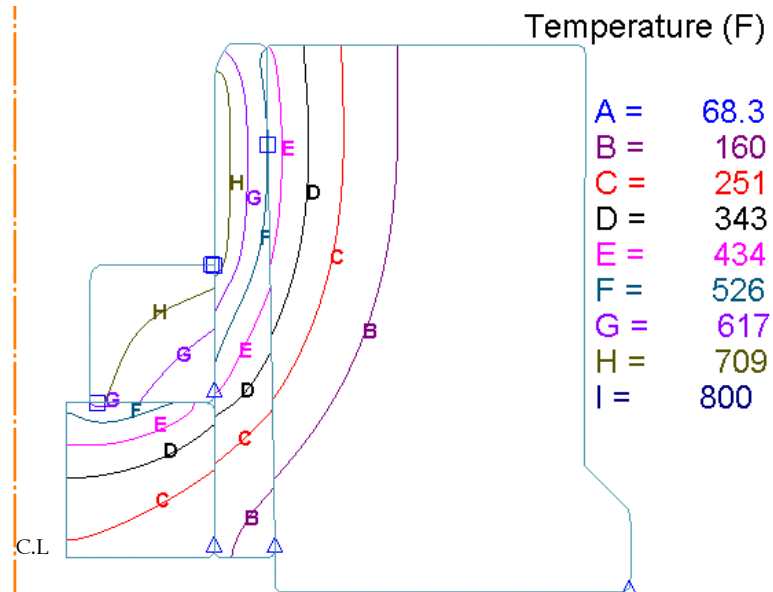
132

a)   Temperature distribution at the end of heating.
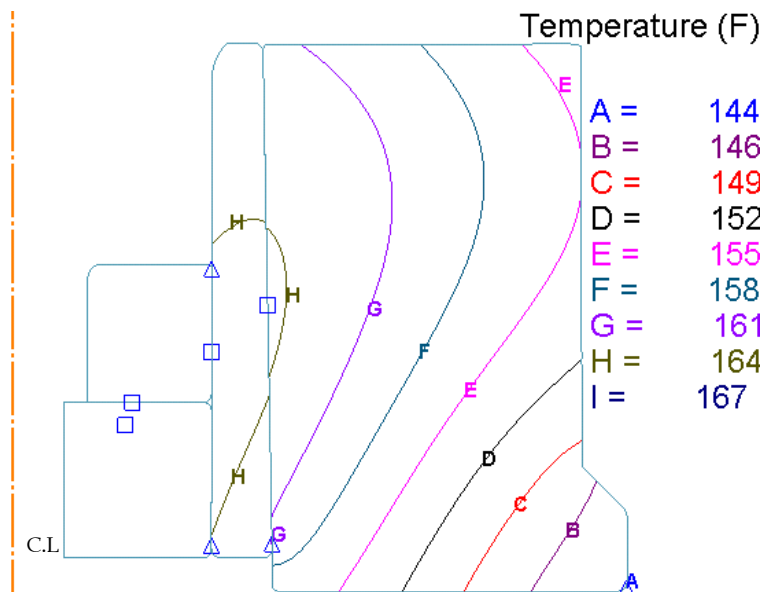
b)   Temperature distribution prior to the first forging stroke.

Figure 6.11: Temperature distribution in the assembly after heating and dwell (gas flame on the die insert and sleeve; carbide insert).

133

Stress - Theta (ksi)

A =	-224
B =	-205
C =	-186
D =	-167
E =	-147
F =	-128
G =	-109
H =	-90.0
I =	-70.9

Stress - Theta (ksi)

A =	-113
B =	-99.6
C =	-85.8
D =	-72.0
E =	-58.1
F =	-44.3
G =	-30.5
H =	-16.6
I =	-2.80

a) At the end of heating.   b) Prior to first forging stroke.
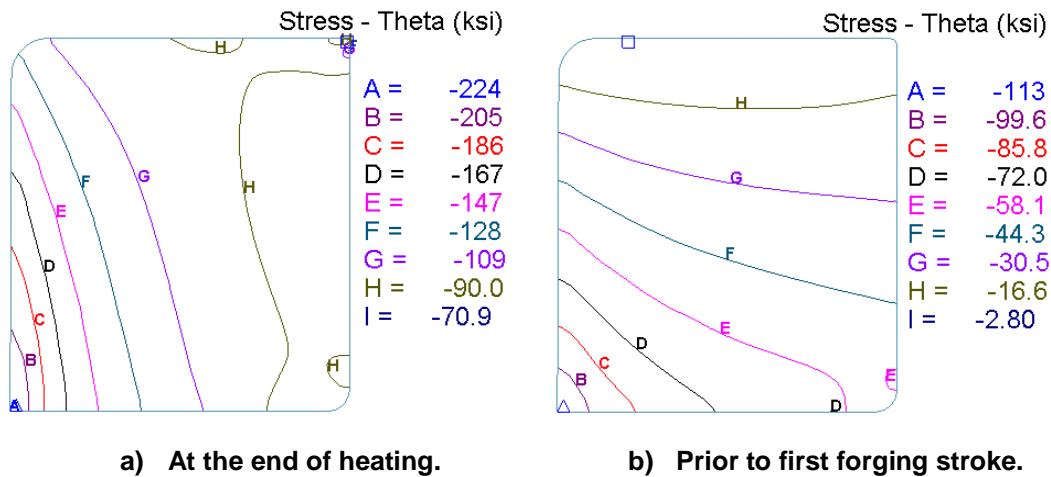
Figure 6.12: Loss of shrink-fit in the insert due to pre-heating (gas flame on the die insert and sleeve; carbide insert).

Compared to the previous technique of using a gas ring on the outside, the insert in this case (inside heating) was primarily under compressive stress during heating. This is because the thermal expansion of the insert initially results in an increase in shrink-fit (radial pressure) at the insert-sleeve interface during heating. At the end of the assumed dwell time of 10 minutes, the insert retains its compressive stress state. Similarly, compared to the outside gas ring, the deflection in the sleeve is reversed in the top (front) portion of the sleeve (Figure 6.13). The deflection in the bottom (back) of the sleeve maintains the same trend due to expansion and contraction of the insert (and backup) during heating and dwelling, respectively. The pre-heated die assembly from this analysis (heated from the inside) was, thus, recommended on the shop floor and is used for analysis of the forging process in the remaining sections of this study.

134
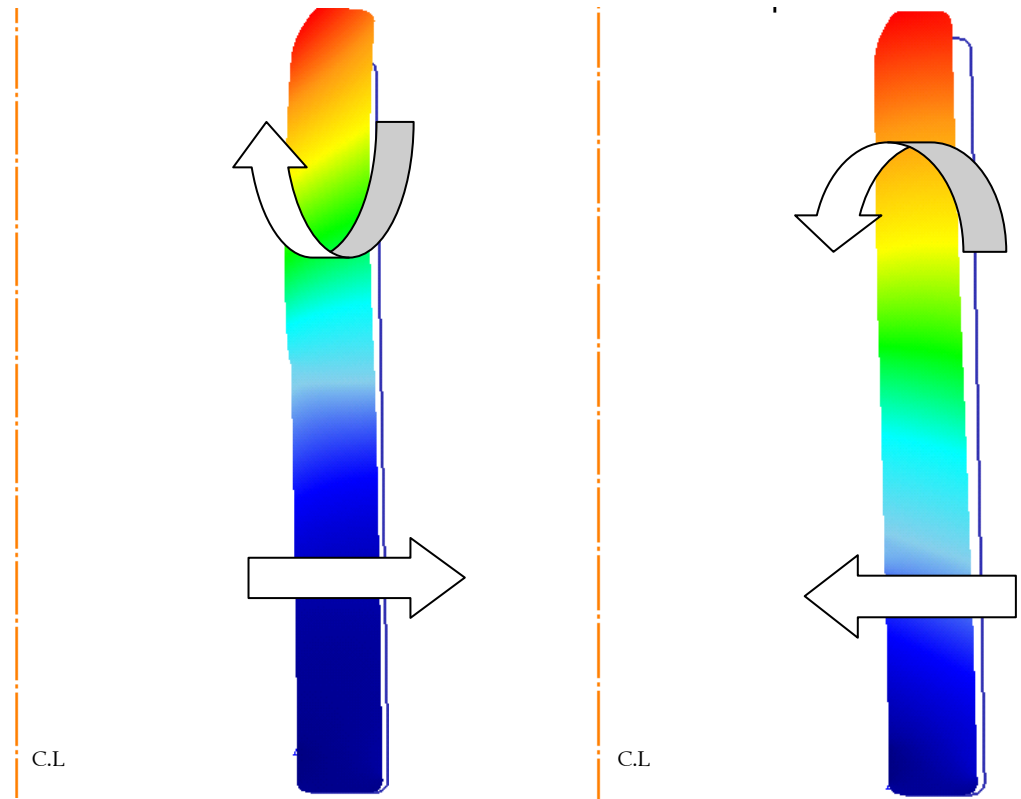
a) At the end of heating.   **b) Prior to the first forging stroke.**

Figure 6.13: Deflection in the sleeve during pre-heating (gas flame on the die insert and sleeve; magnified 20x; carbide insert).

As mentioned earlier, a 3D analysis approach was explored for die heating, using the results from 2D FEA. Figure 6.14 shows a model for the insert with the state-variable history from pre-heating. Similar models were developed for the remaining assembly components as well. This approach, however, was abandoned due to problems with inter-object contact and extremely long simulation times. The benefits of this approach did not justify the computational effort required.

135
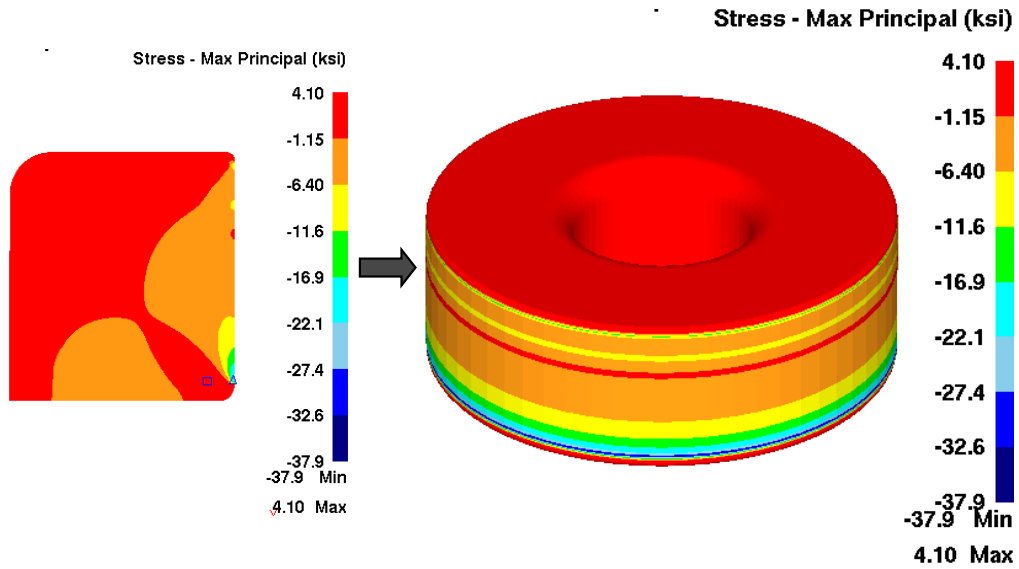
Figure 6.14: 3-D model with stress history from assembly and pre-heating generated using the 2-D analysis results.

6.3.2.3.   Effect of Die Heating on Shrink-fit

Due to differences in thermal expansion, different die materials react differently to die heating. Figure 6.15 compares four die insert materials in terms of the loss of shrink-fit after pre-heating using a gas flame on the inside. These results were obtained taking an average of the radial and hoop stresses at points 5 and 6 on the insert O.D. prior to the first forging stroke. The ceramic and carbide inserts lost 25-35% of the shrink-fit due to greater thermal expansion of the tool steel containment system (sleeve and container). The tool steel inserts, on the other hand, exhibited an increase in the shrink-fit, due to thermal expansion along with the containment system. Since the insert is at a higher temperature than the containment system, the former shows greater thermal expansion. Figure 6.15, thus, gives a) the shrink-fit correction necessary for ensuring compressive pre-stress in the insert prior to the first forging stroke, and b) changes in the heating technique required to minimize the loss of shrink-fit.

136
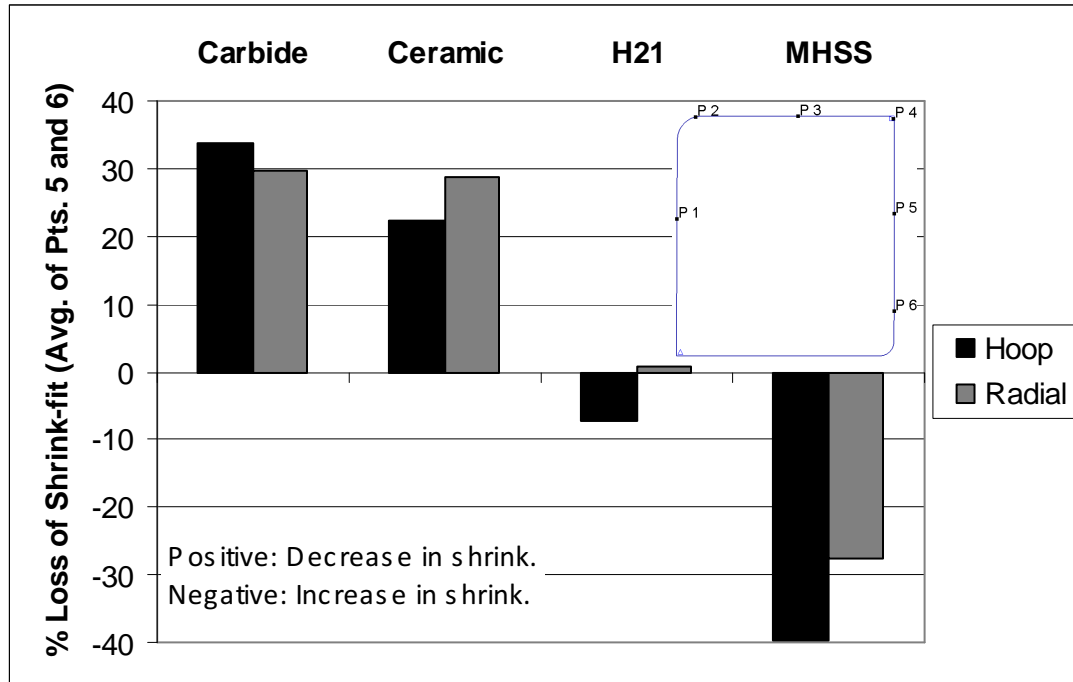
Figure 6.15: Loss of shrink-fit in different insert materials after pre-heating (gas flame on inside).

6.3.3. *Simulation of Single and Multiple Forging Cycles*

The simulation methodology developed for the reverse piston was also used for analysis of start-up and steady-state interface conditions in this process. The production cycle time data and process sequence of Figure 6.2 formed the basic input for this FEA. Thus, steady-state process conditions were determined by simulating multiple forging cycles (Figure 6.16). The die assembly models used for this analysis were obtained by a) simulation of die assembly using the incremental approach, followed by b) simulation of pre-heating assuming a gas flame on the inside. The results of these simulations are provided in subsequent sections focusing on selection and comparison of die materials.

137
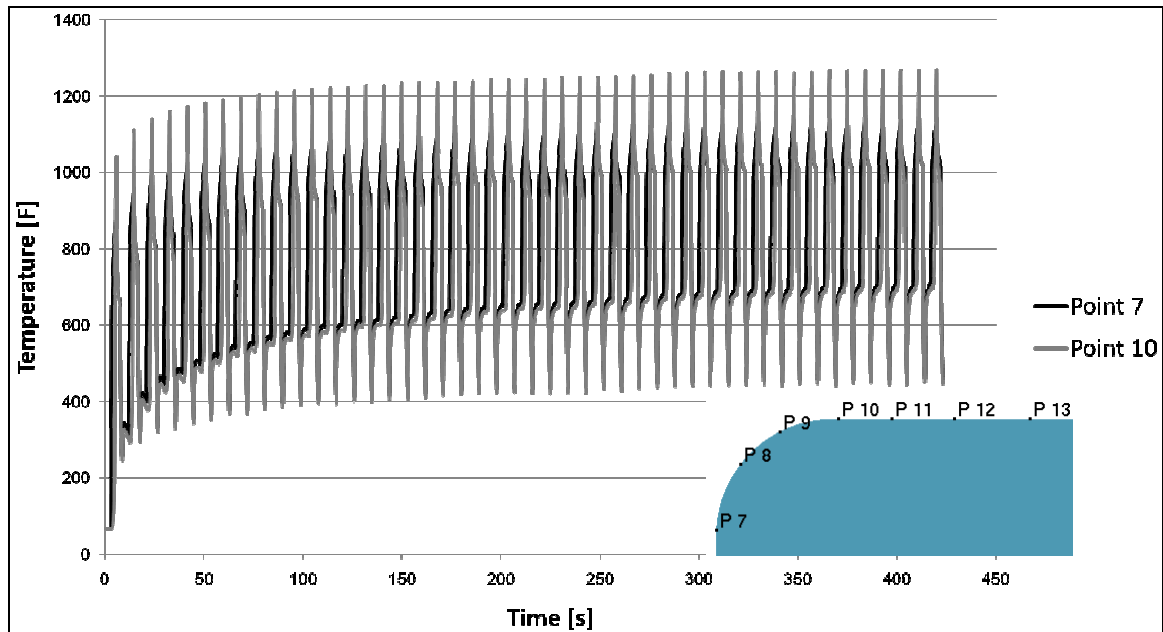
Figure 6.16: An example of temperature increase over multiple forging cycles using an H-21 insert.

6.4. Investigation of the Effect of Die Material Properties on Interface Conditions

One of the main research objectives in this study was to identify the effect of mechanical and thermal properties of the die materials on interface conditions that influence die life; in this case thermal fatigue life. This was achieved using FEA of the selected warm forging process with properties of different tool materials that were segregated into two main groups. Based upon the Ishikawa diagrams and the mechanism of thermal fatigue (Chapter 5), the focus of this study was primarily on thermal conductivity (K), coefficient of thermal expansion (α) and elastic modulus (E). A design of experiments (DOE) approach was used with simplifying assumptions in order to reduce the number of simulations and to focus on comparison of the selected material groups. The results of this study are summarized here.

6.4.1. Material Groups Selected for Analysis

The following three categories of die materials were explored for this study in order to investigate the effect of thermal and mechanical properties on interface conditions affecting thermal fatigue:

- Proprietary hot-work and/or matrix tool steels.

- Carbide and/or ceramic – based materials.

138

- Welded overlays with hot-work tool steel as the base material.

It might be recalled that, in the case of the reverse piston (Chapter 5), a 30% increase in thermal conductivity resulted in a 15-20% reduction in surface temperature. With the higher contact times of a hydraulic press, it is expected that a significantly higher increase (or decrease, as with ceramics) in thermal conductivity would be required to obtain measurable differences in interface conditions. Thus, the different values of K, α and E were selected by considering the following two material groups with significantly different material properties:

- Group 1: Hot-work tool steels and matrix high speed steels (MHSS).

- Group 2: Ceramic and carbide-based materials.

The materials properties in each group were obtained from public domain literature, such as brochures and data sheets, as well as published academic literature [Ekstroem et al, 1990; Liu et al, 1994; Yeckley, 2002; Walter Metals; Nakahama et al, 2005/Daido Steel]. In order to make the results of this study applicable to the process being analyzed, the existing tool steel (H-21), a matrix high speed steel (MHSS), a carbide grade and a ceramic grade were included. A third tool steel and a welded overlay were also added for comparison of thermal fatigue performance as explained later.

Figures 6.17 and 6.18 compare ceramic, carbide and steels on the basis of thermal conductivity, thermal expansion and modulus of elasticity. Carbide has approximately 125-250% greater thermal conductivity compared to the steels, which in turn have ≈200% greater thermal conductivity compared to ceramic. The elastic modulus of carbide is 200% greater than that of steel and 85-90% greater than that of ceramic. The thermal expansion of steel, on the other hand, is 180-200% greater than that of ceramic and carbide. Thus, the material groups selected were significantly different in properties to ensure measurable differences in interface conditions.

139
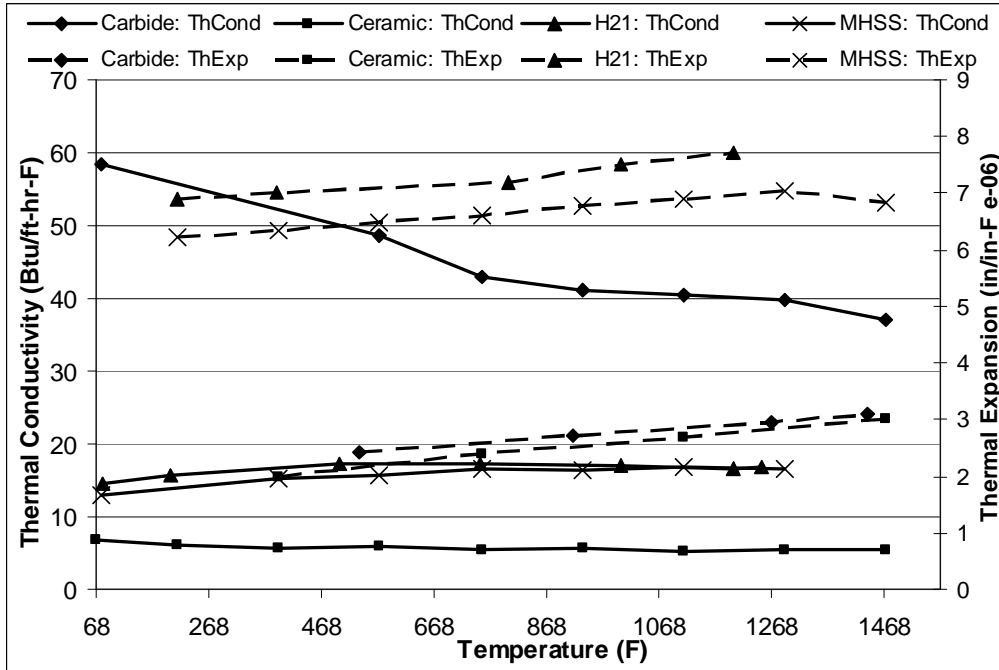
Figure 6.17: Comparison of thermal properties of carbide and ceramic to steels (ThCond: Thermal Conductivity; ThExp: Coefficient of Thermal Expansion).
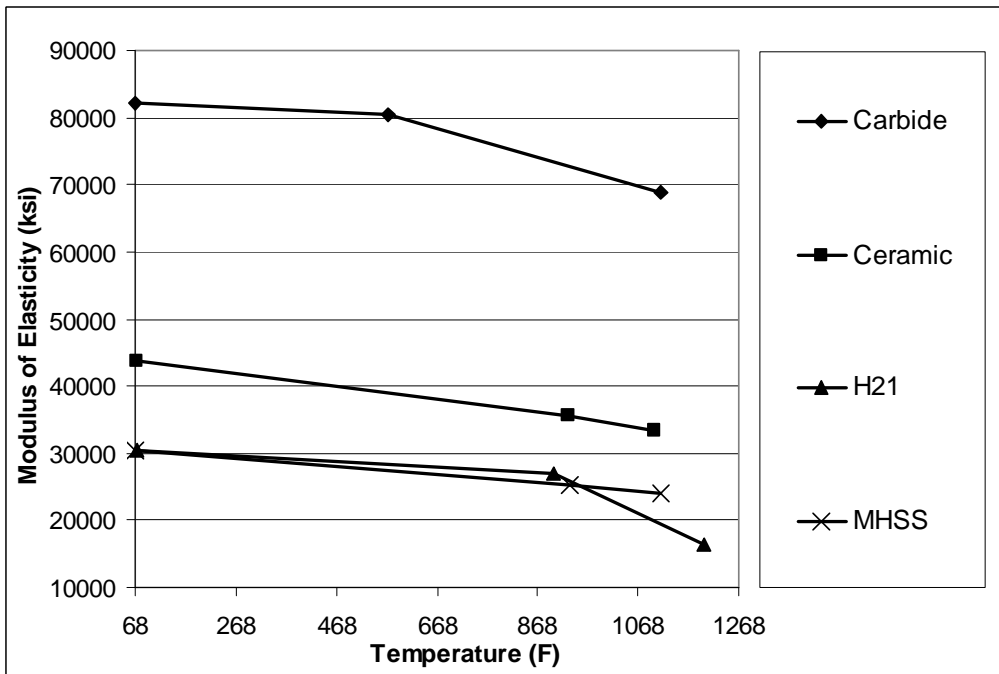
Figure 6.18: Comparison of elastic modulus of carbide and ceramic to steels.

140

6.4.2. Comparison of Selected Combinations using a Design of Experiments Approach

Based upon the material properties of the selected tool materials, three possible levels of each factor (K, α and E) were identified based upon actual properties, as shown in Table 6.1. The real or natural values were represented by coded values for simplicity in designing the combinations for the FEA study. Thus, "1" represents maximum, "0" represents the intermediate or mean value and "-1" represents the minimum value.

Property	1	0	-1	Δ (+1 w.r.t -1)	Δ (+1 w.r.t 0)	Δ (0 w.r.t -1)
K	47	17	5.5	755	176	209
(Btu/ft-hr-F)	(carbide)	(steel)	(ceramic)			
α	7	5	2.5	180	40	100
(μin/in-F)	(steel)	(N/A)	(carbide) (ceramic)			
E	75000	40000	25000	200	88	60
(ksi)	(carbide)	(ceramic)	(steel)			
Δ: % difference of one value with respect to (w.r.t) another.						

Table 6.1: Real and coded values of the selected factors.

In standard DOE set-up, the "0" value forms a mid or center-point between the two extreme values i.e. "1" and "-1". However, this approach was modified in order to include actual die materials and, ultimately, make the results applicable to the selected warm forging process. The remaining combinations were only required to statistically determine the relative importance and interactions of the selected factors. Additionally, in order to reduce the number of simulations required, the "0" value was treated as a secondary "-1" value. This approach was justified since the runs requiring this modification did not correspond to real die materials. Thus, a 2-level design with 8 runs (2^3 simulations) was used instead of one with 3-levels (3^3 simulations) (Table 6.2). It was expected that these approximations would result in certain error in predicting interaction effects. Runs 4, 7 and 8 correspond to carbide, steel and ceramic, respectively, which are the main focus groups of this analysis. In order to include a comparison of tool steels, Run 7 had four replications involving a) the existing die material (H-21), b) an alternative steel (Thyrotherm™ 2999; T2999), c) a matrix high speed steel (MHSS) and d) H-21 with a welded overlay of Hastelloy™, a nickel-based superalloy.

141

For each run, the starting point was a pre-heated die assembly with the state-variable history from assembly and heating, as explained earlier. Computational time was reduced further by using a single pre-heated simulation file for Run 7 with only a change in die insert properties for the forging process analysis. This is justified based on Figures 6.17 and 6.18, which show that the variation in thermal properties of the different steel grades is not significant. The forging process analysis focused on the start-up (first) cycle, which was proven to be the most critical for thermal fatigue since it has the highest thermal shock loading (Chapter 5). This analysis included the die chill, deformation, dwell, and lubrication stages outlined in Figure 6.2. Steady-state conditions were determined only for Runs 4, 7 (except Hastelloy™) and 8 (i.e. actual die materials) for prediction of thermal fatigue performance.

Factor Combinations for FEA				Replications			
Runs	K	α	E	1	2	3	4
1	1	1	1	Done	N/A	N/A	N/A
2	1	1	-1	Done	N/A	N/A	N/A
3	1	-1	-1	Done	N/A	N/A	N/A
4	1	-1	1	Carbide	N/A	N/A	N/A
5	-1	-1	1	Done	N/A	N/A	N/A
6	-1	1	1	Done	N/A	N/A	N/A
7	-1	1	-1	H21	MHSS	T2999	Hastelloy
8	-1	-1	-1	Ceramic	N/A	N/A	N/A

Table 6.2: Simulations conducted with selected material properties.

Some of the selected responses from the FE analysis of Table 6.2 are shown in Table 6.3. The temperature amplitude is an indication of the change in die surface temperature from BDC to lube spray. The negative sign indicates a decrease in temperature upon exposure to the lubricant. The residual stress is the instantaneous surface hoop stress (principal stress) at the end of lubricant spray. The stress reversal is the total amplitude of the surface stress at point 2 i.e. difference in stress from BDC to lube spray. The same applies to the strain reversal/amplitude. The maximum strain refers to the maximum value of the theoretical mechanical strain, which occurs at BDC when surface temperature is at a maximum as shown in Chapter 5.

142

Runs	K	α	E	Temperature Amplitude (BDC-LS)	Residual Stress (LS)	Stress Reversal (BDC-LS)	Max. Strain (BDC)	Strain Reversal (BDC-LS)
				(deg F)	(ksi)	(ksi)	(in/in)	(in/in)
1	1	1	1	-698.41	-45.09	-274.99	-0.0090	-0.0078
2	1	1	-1	-664.81	-34.27	-83.46	-0.0071	-0.0052
3	1	-1	-1	-697.15	-9.22	-13.41	-0.0012	-0.0007
4	1	-1	1	-672.05	-5.44	-128.28	-0.0036	-0.0033
5	-1	-1	1	-880.98	-39.55	-105.24	-0.0042	-0.0028
6	-1	1	1	-860.01	-22.07	-376.62	-0.0110	-0.0099
7	-1	1	-1	-858.04	-25.30	-157.68	-0.0132	-0.0114
8	-1	-1	-1	-1138.30	0.73	-124.12	-0.0058	-0.0054

Results are for point 2 on the die radius, which is the location of maximum surface temperature:
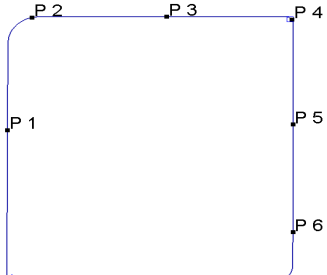
Table 6.3: Selected responses for the simulated material property combinations.

6.4.3. *Effect on Die Surface Temperature Amplitude*

The temperature magnitude and corresponding gradient reach their extreme values at BDC and the end of lube spray (LS). The difference between these two values depends upon the thermal properties of the die material and influences its thermal fatigue performance. The temperature amplitude is dominated by the thermal conductivity of the die material (Figure 6.19). This was reflected in the interaction plot of K and α as well as K and E (Figure 6.20). For a fixed value of K, FEA indicates a negative interaction between α and E, where the former is found to dominate. The thermal expansion affects heat-transfer by influencing the inter-object contact at the insert-sleeve interface. Loss of contact at this interface results in reduced heat transfer out of the insert, effectively increasing its temperature and the resulting temperature amplitude. This effect occurs due to inclusion of the pre-heating process in the analysis and would have been missed if the FE

143

analysis (first cycle) were conducted with a room temperature die assembly. Another reason for this interaction may be the approximations made while designing the simulation set-up.
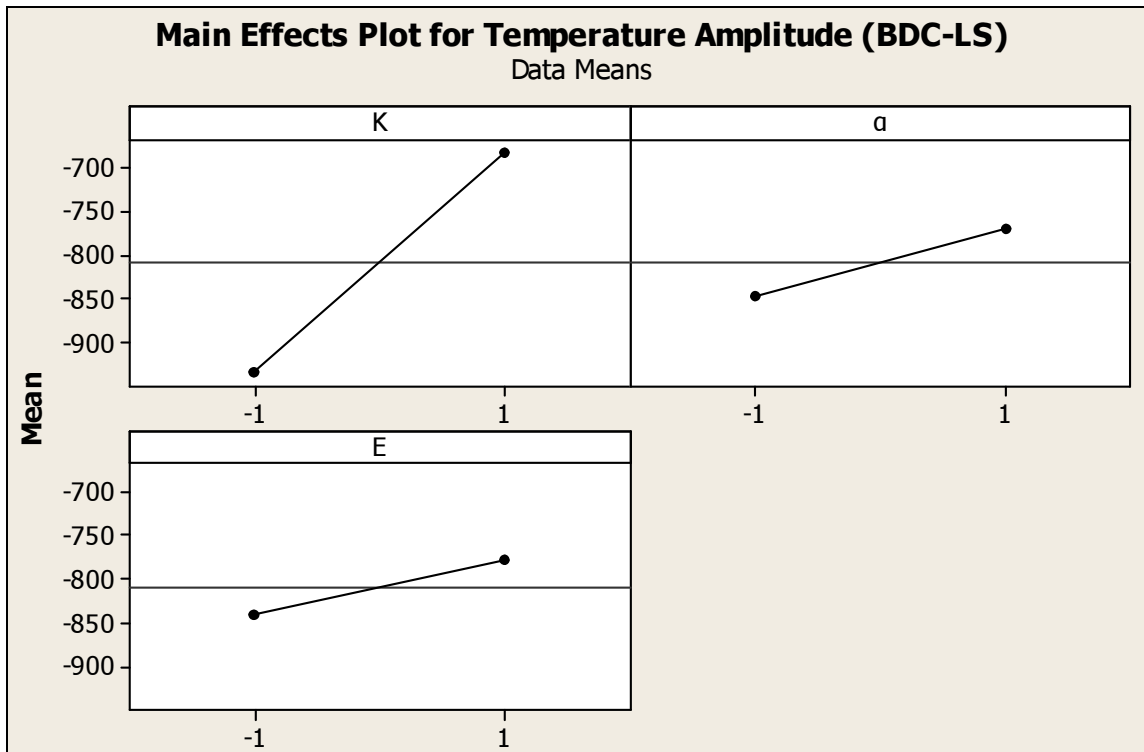
Figure 6.19: Main effects plot for temperature amplitude during forging.

144
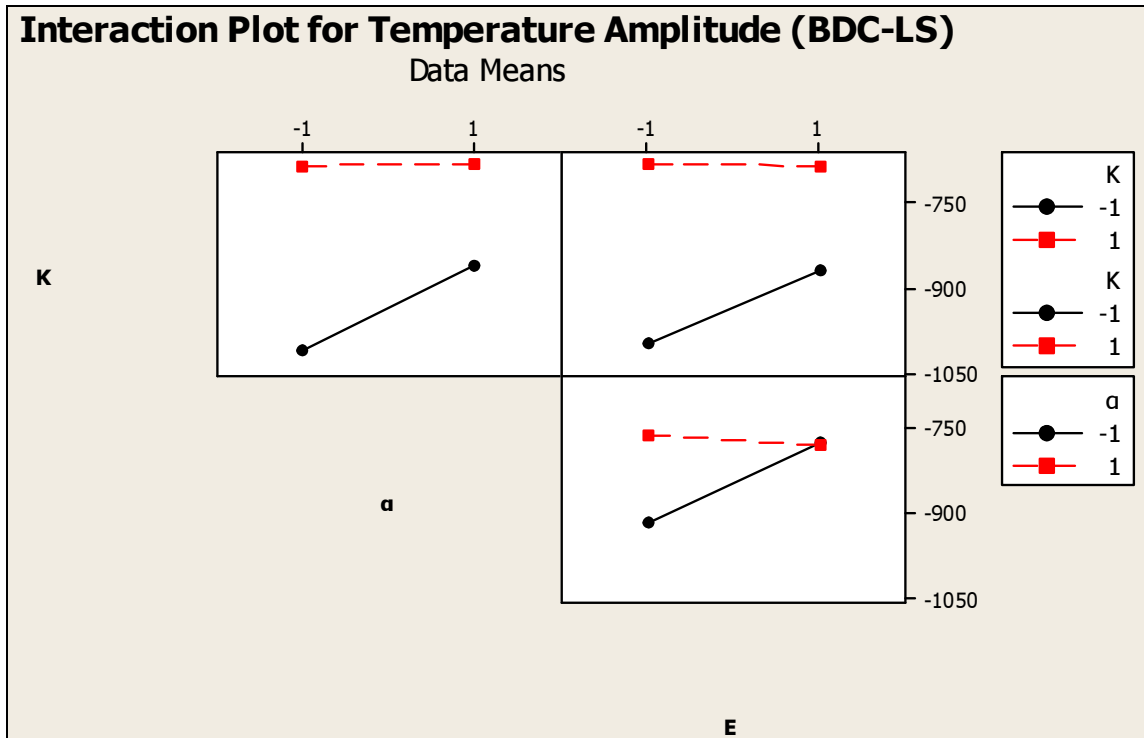
Figure 6.20: Interaction plot for temperature amplitude during forging.

6.4.4. Effect on Maximum Surface Strain and Strain Reversal

The temperature gradient in the die surface results in strain gradients as explained in Chapter 5. At BDC when the die surface temperature reaches a maximum value, the corresponding theoretical mechanical strain (compressive) is also at a maximum. During lubricant spray, the reverse situation is observed with the theoretical mechanical strain undergoing a reversal from compressive to tensile. These values of strain, as well as the total amplitude, are directly influenced by the coefficient of thermal expansion (dominant factor) and indirectly by thermal conductivity as seen in Figure 6.21. The modulus of elasticity does not affect the surface strains (Figures 6.21 and 6.22).

145
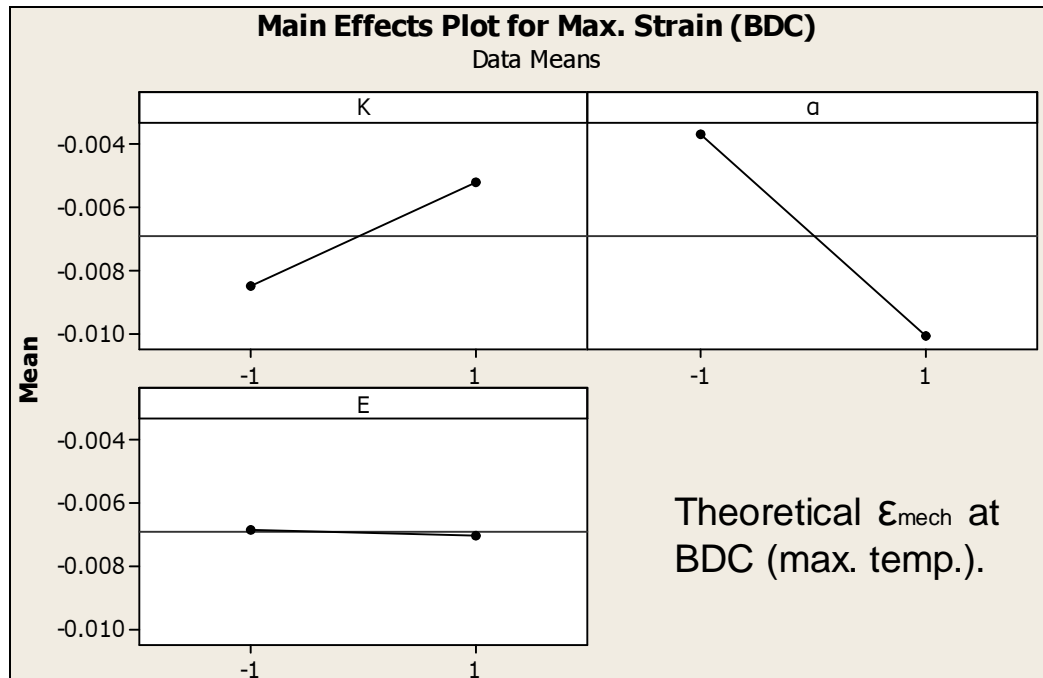
Figure 6.21: Main effects plot for maximum surface strain during forging.
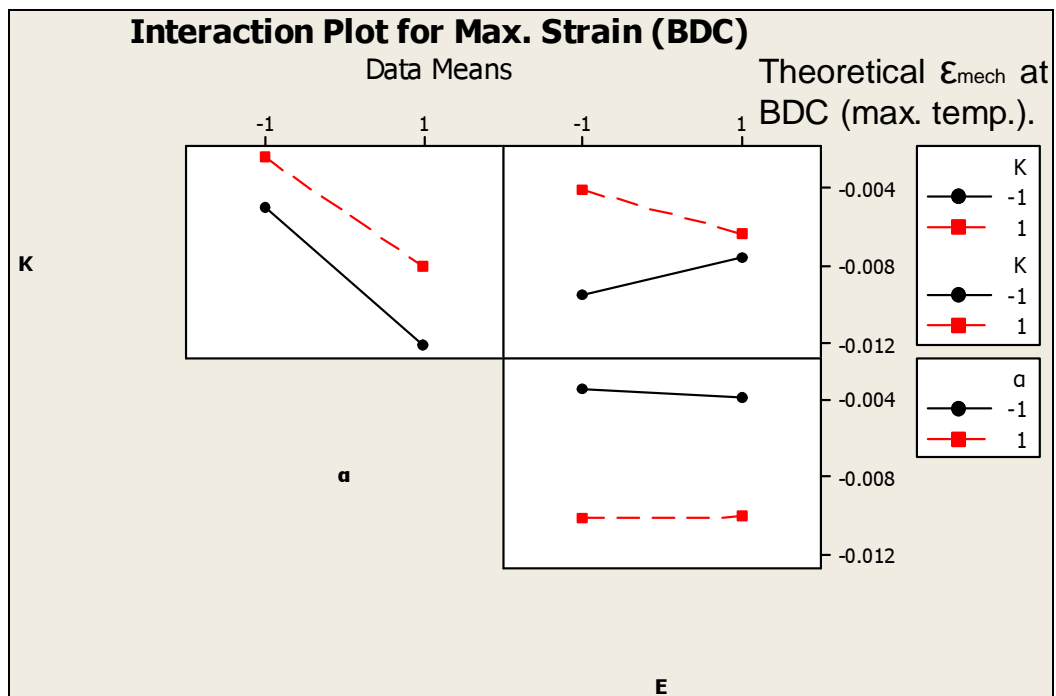
Figure 6.22: Interaction plot for maximum surface strain during forging.

146

6.4.5. Effect on Surface Stress Reversal

The surface stresses corresponding to the surface strain also reach their maximum and minimum values at BDC and end of lubrication. Thermal expansion and elastic modulus were found to have an equal effect on the stress amplitude during the first cycle (Figure 6.23). Thus, a die material with high thermal conductivity, low thermal expansion and low elastic modulus is expected to have superior thermal fatigue performance. It should be noted that low-cycle fatigue depends upon the hot yield strength of the die material, which influences the plastic strain induced in the surface layers.
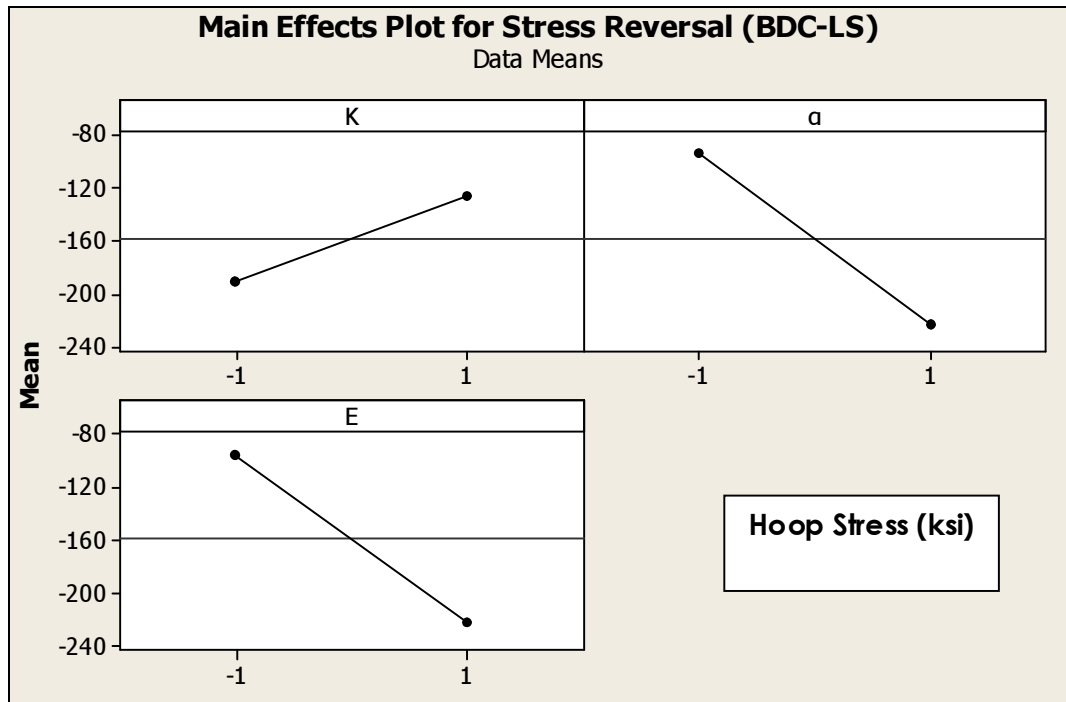
Figure 6.23: Main effects plot for surface stress amplitude during forging.

147
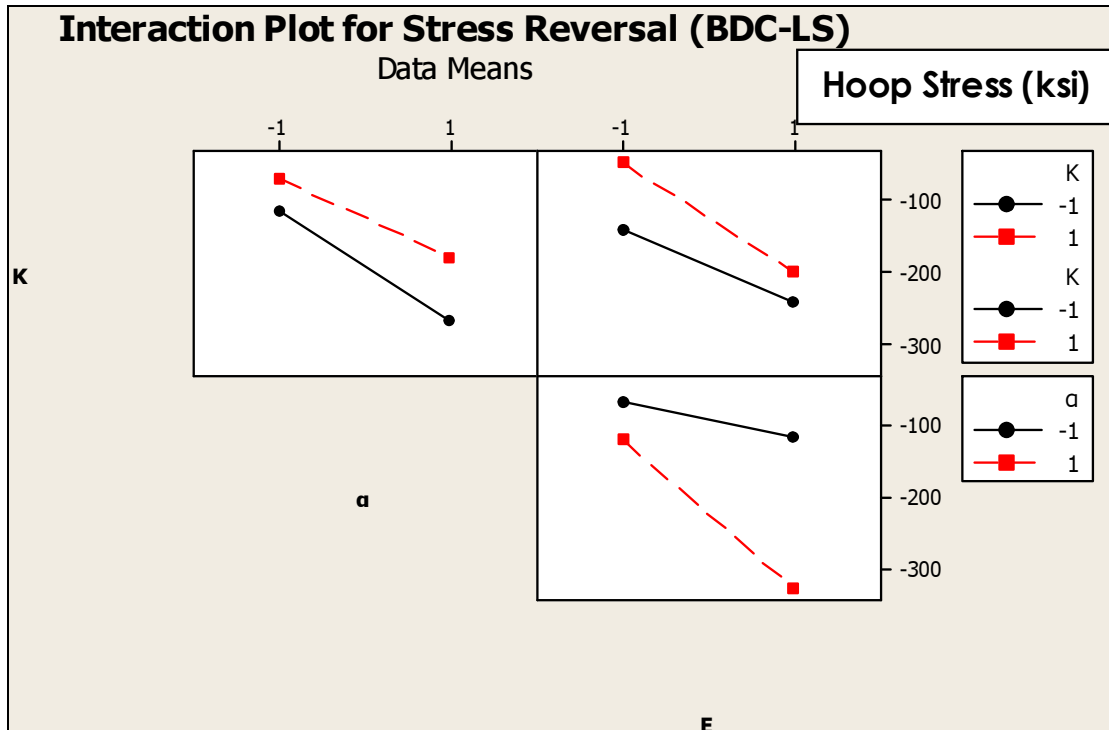
Figure 6.24: Interaction plot for surface stress amplitude during forging.

6.4.6. *Thermal Fatigue Performance of the Selected Material Groups*

As mentioned earlier, the main focus of the DOE-based analysis was to compare actual material groups for application in forging processes viz. tool steels (group 1; run 7) compared to generic carbides and ceramics (group 2; runs 4 and 8, respectively in Table 6.2). These groups were developed based upon actual material properties obtained from tooling companies and public domain literature.

6.4.6.1. *Surface Temperature at Start-up and at Steady-State*

As thermal conductivity increases, the die surface temperature decreases drastically. A ceramic insert resulted in ≈ 45% higher surface temperature during forging than carbide and ≈ 20% higher compared to steel (Figure 6.25; start-up cycle with a pre-heat surface temperature of ≈ 168ºF/75ºC). The comparative differences in thermal conductivity are given in Table 6.1, which outlines the real and coded values.

148
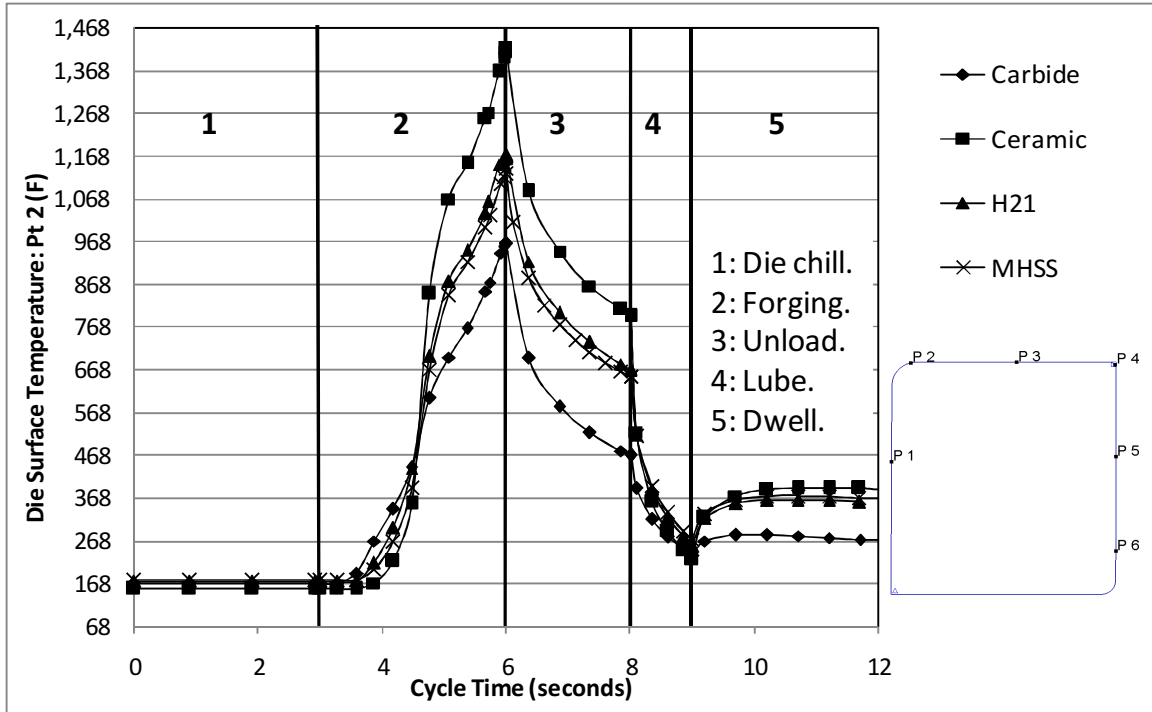
Figure 6.25: Die surface temperature during start-up for the selected material groups.
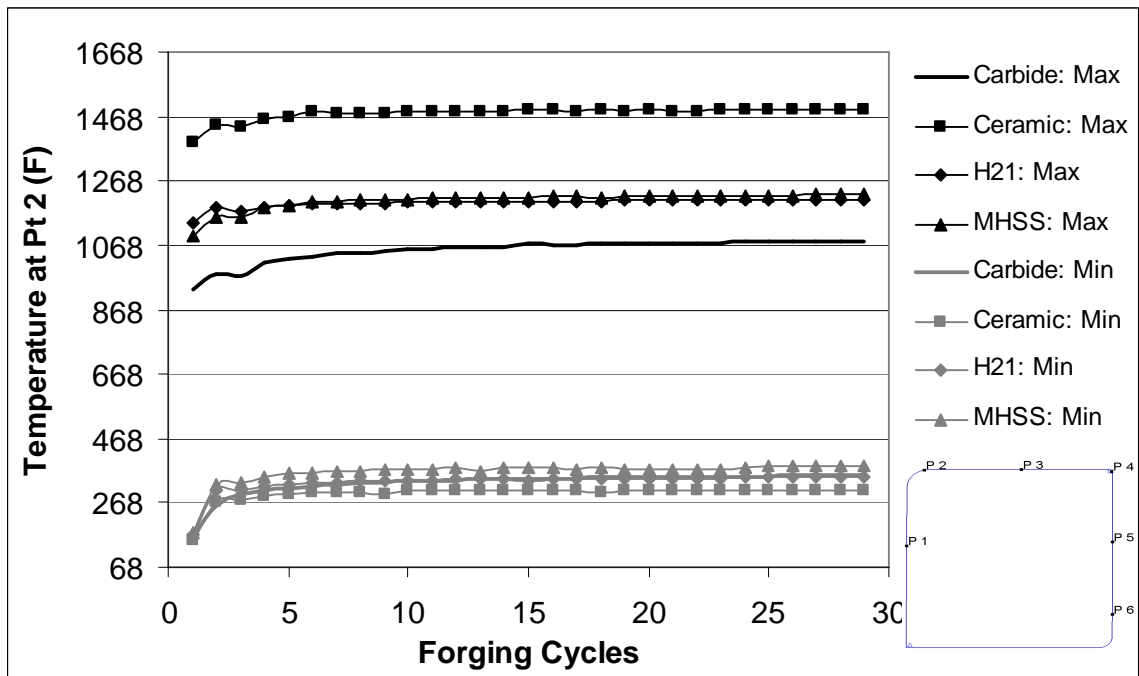
Figure 6.26: Steady-state temperature range for the selected material groups.

149

Analysis of multiple forging cycles for these four materials yields the differences in steady-state thermal cycles given in Figure 6.26. Under steady-state conditions, the 125-250% greater thermal conductivity of carbide resulted in 13-14 % lower surface temperatures in spite of the high contact times on the hydraulic press used in the current process. The ceramic insert showed ≈ 40% higher temperatures than the carbide and ≈ 22% greater than steel at steady-state conditions. The maximum increase in surface temperature was observed in the first forging cycle, which was thus, the worst case scenario for thermal fatigue and thermal shock. Thus, interface conditions at start-up form the basis for comparing die materials in terms of their thermal fatigue performance. The steady-state thermal conditions in the surface layer were achieved in the first 5-10 forging cycles (with a pre-heated die assembly) (Figure 6.27). As expected, the maximum temperature increase was observed for ceramic (≈ 125% over the pre-heat temperature) and minimum for carbide (≈ 60%). The tool steels did not show a significant difference, with the MHSS showing ≈ 6% lower temperature increase compared to the existing H-21 insert material.
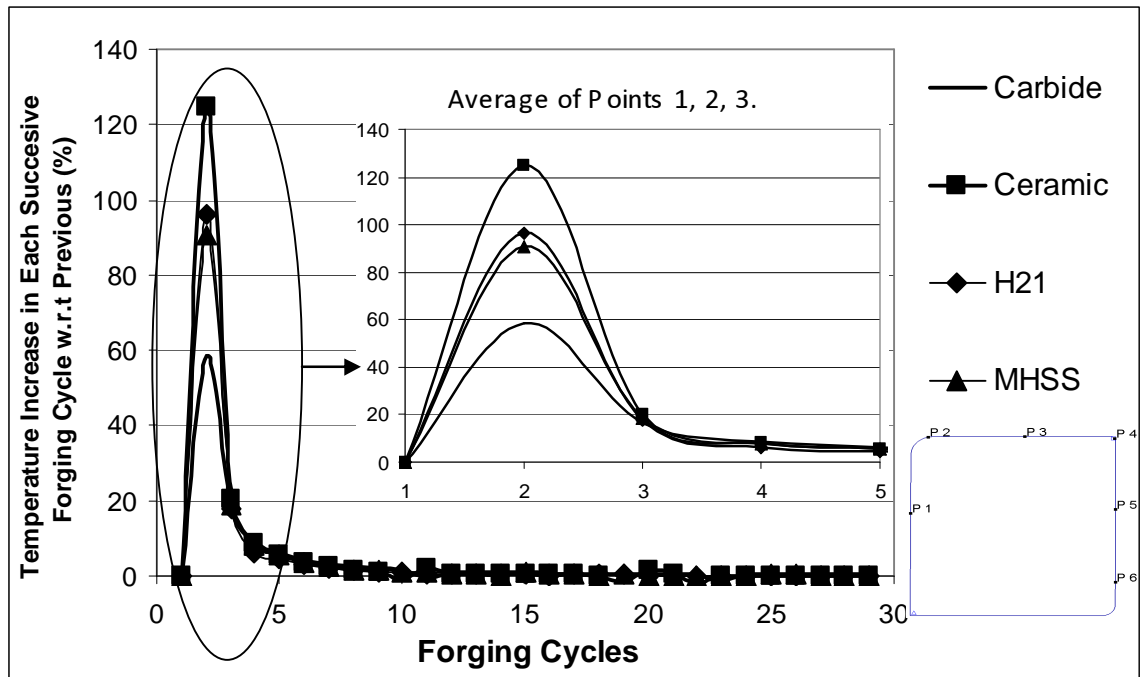
Figure 6.27: Average temperature increase on the die surface in each successive cycle.

6.4.6.2. Temperature Gradient at Start-up and at Steady-State

The temperature gradient in the die surface is influenced primarily by the thermal conductivity as shown in Figure 6.19. Thus, the ceramic and carbide inserts show the two extreme values of temperature gradient, with the tool steels giving intermediate values. The carbide insert had ≈

150

54% lower temperature gradient in the die surface at BDC (start-up cycle) compared to ceramic and ≈ 30% compared to steel (Figure 6.28). This in turn influences the stress reversal in the surface depending upon the thermal expansion and elastic modulus of the insert materials. At steady-state, the carbide insert has 22% lower temperature gradient at BDC than steel and 40% compared to ceramic (Figure 6.29).
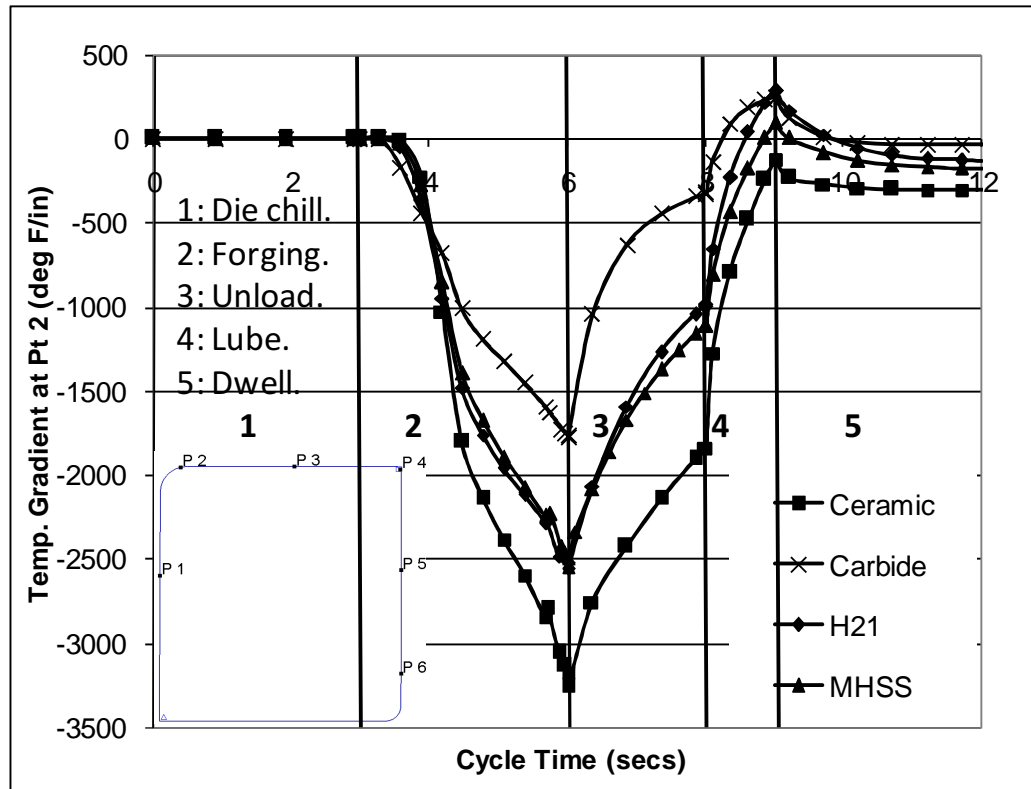
Figure 6.28: Temperature gradients for selected material groups in the start-up cycle.

151
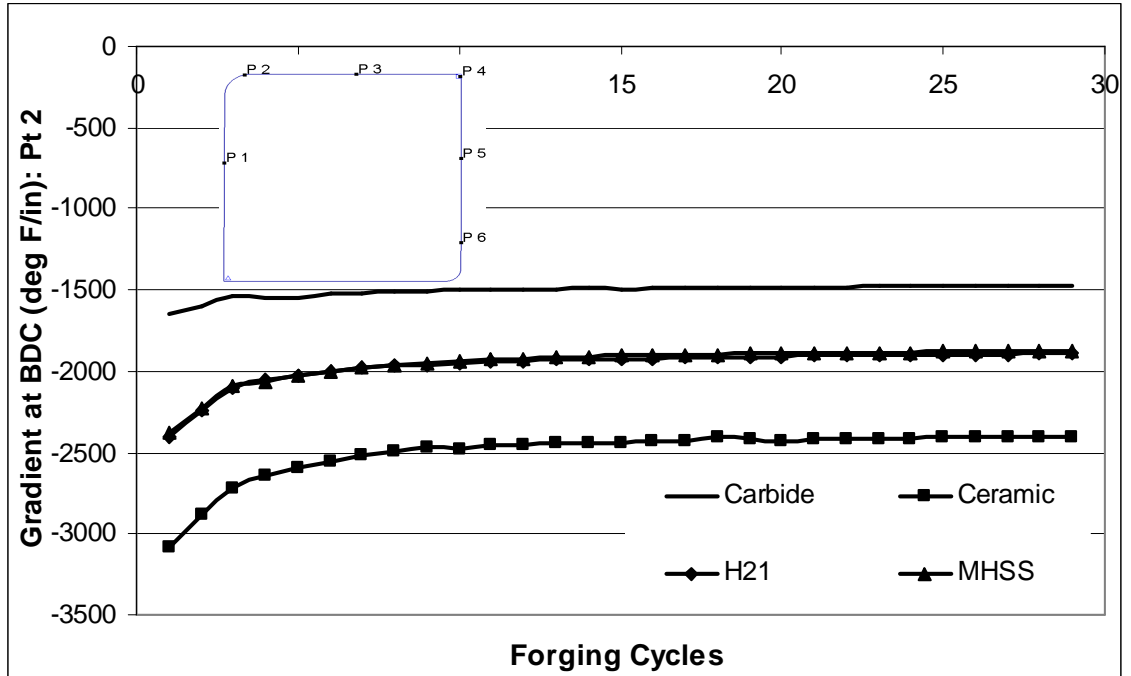
Figure 6.29: Temperature gradients for selected material groups at steady-state.

6.4.6.3.   Surface Stress Amplitude at Start-up

The thermal expansion from contact with the workpiece during deformation is resisted by the cooler die substrate resulting in the corresponding strain amplitude (Figure 6.30). Steel has 180% greater thermal expansion than ceramic and carbide, which was reflected in the H-21 and MHSS materials having high compressive strain at BDC (240-270% greater compared to carbide). The high thermal conductivity of carbide further reduced the compressive surface strain by 36-40% compared to ceramic due to a lower temperature gradient.

The stress amplitude as a result of the thermal expansion is influenced by the elastic modulus of the die material and the strain amplitude. The carbide grade has the highest elastic modulus of the selected materials (200% greater than steel; 88% greater than ceramic). However, the stress magnitude at BDC was only 10% greater in the carbide than that in ceramic; 20% less than in H21 tool steel. Also, the ceramic die insert was found to experience tensile stress upon lubricant spray. Ceramics and carbides exhibit brittle failure, and are susceptible to cracking from tensile stresses and impact loading. The current analysis focused on one local region of the die surface, which is acceptable for analysis of steels. Design of a die assembly with ceramic or carbide inserts requires stress analysis of the entire insert and its containment system. This is covered in detail in Chapter 7 for a carbide insert. Due to its higher thermal conductivity and yield strength at

152

elevated temperatures, the carbide die material was considered a viable alternative to tool steel, provided the higher die costs are amortized by superior die life.
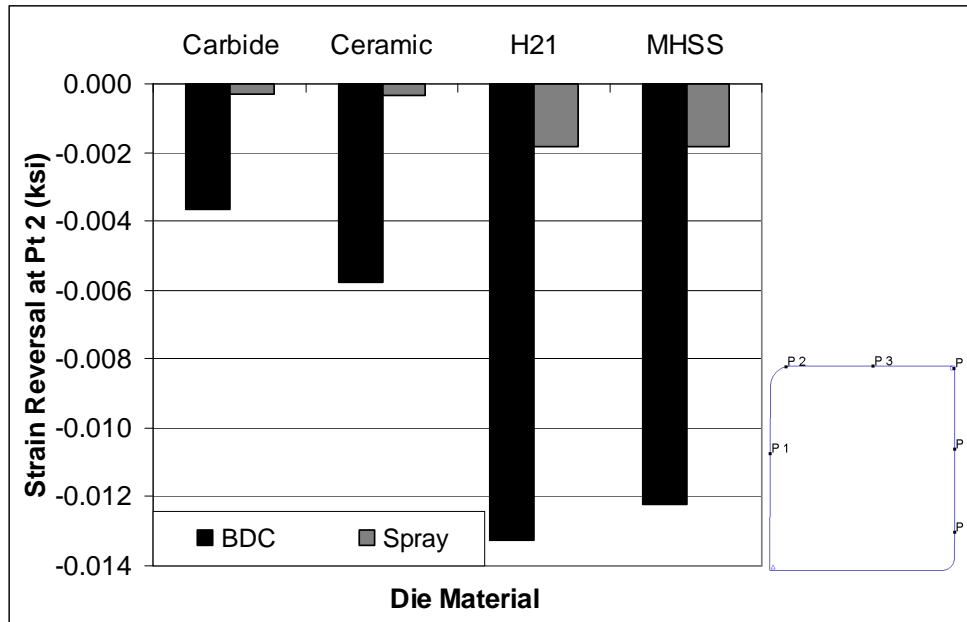
Figure 6.30: Strain (ε $_{mech}$) amplitude at start-up for the selected material groups.
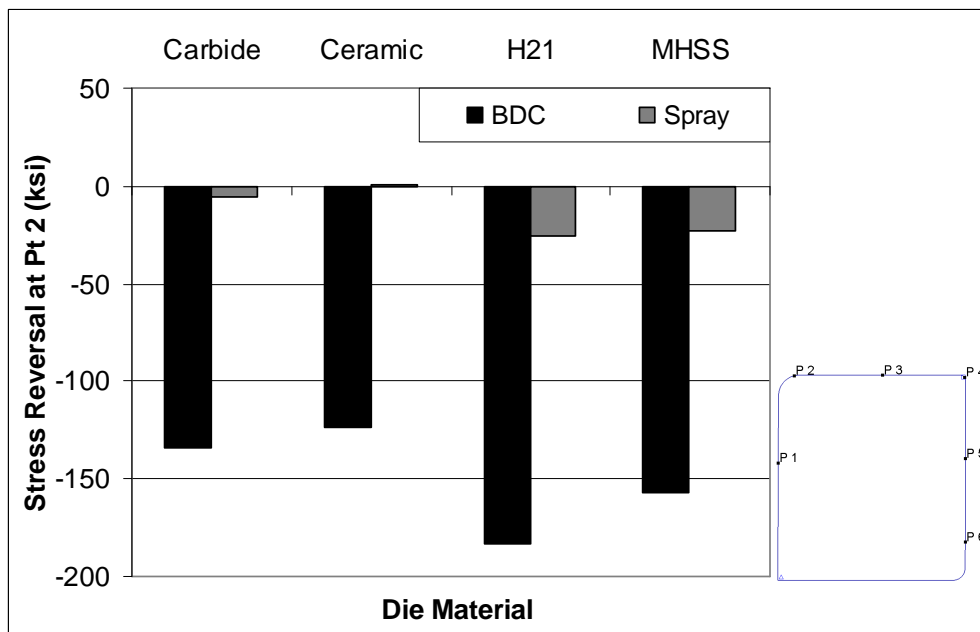
Figure 6.31: Stress amplitude at start-up for the selected material groups.

153

6.5. Selection of Candidate Hot-work Tool Steels for Improved Thermal Fatigue Life

The main drawback of ceramic and/or carbide tooling, besides their susceptibility to brittle fracture, is their high cost, both direct and indirect. The direct costs are related to the manufacturing process (powder compaction and sintering), which has higher lead time compared to the machining processes used with steel. The indirect costs are related to process design changes, which might be required in order to ensure consistent die assembly, die heating, part loading and lubrication spray. This is a daunting task in general hot forging processes with manual part transfer, where a certain amount of variability exists due to human involvement. Steels are relatively forgiving under such conditions, whereas ceramics or carbides are better suited for an automated forging cell. These materials are commonly used in cold forging, which by nature requires higher precision in die manufacturing and process operation due to the net-shape or near net-shape product being forged. The high tool costs are amortized by higher profit margins on the finished part. Additionally, thermal shock is not a factor in cold forging. Thus, it was decided to select alternative hot-work tool steels on the basis of the DOE analysis in order to provide a cost-effective means of improving die life in the current process.

Figures 6.32 through 6.34 compare some steels recommended by tooling companies for use in warm forging processes (Thyrotherm™ 2999 EFS Supra from Schmolz-Bickenbach; W400™ and 403™ from Böhler-Uddeholm, and DRM1™ and DRM2™ from Daido Steel). The existing H-21 die material and a nickel-based superalloy, Hastelloy™ (Haynes International), were also included. Hastelloy™ was included in this study only to demonstrate the possibility of applying welded overlays in warm and hot forging. All the selected tool steels are manufactured using secondary refining processes, such as electro-slag re-melting (ESR), in order to improve micro-cleanliness through removal of inclusions. These inclusions can act as stress risers for crack initiation under low-cycle thermal fatigue loading.
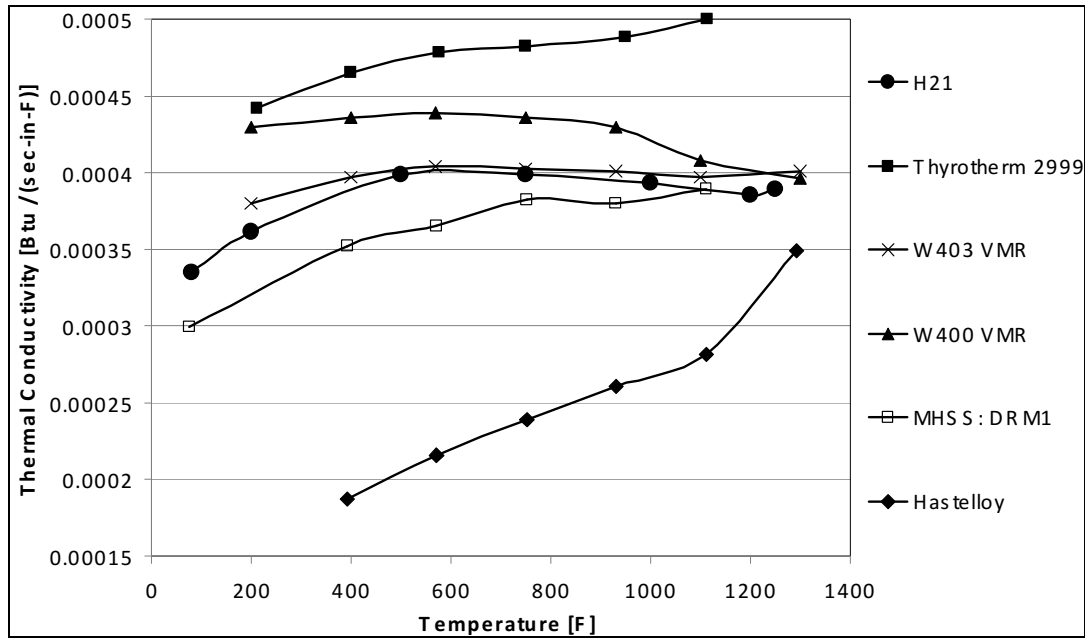
Figure 6.32: Selection of hot-work tool steels on the basis of thermal conductivity.

For superior thermal fatigue performance it is required to have high thermal conductivity and low thermal expansion in addition to high hot yield strength. On the basis of this criterion, it was decided to select Thyrotherm™ 2999 as an alternative die material for analysis. Additionally, a MHSS (DRM1™) was also included due to its high hot hardness and hot yield strength (Figure 6.33). These materials, along with H-21, were evaluated at start-up and under steady-state conditions.

155
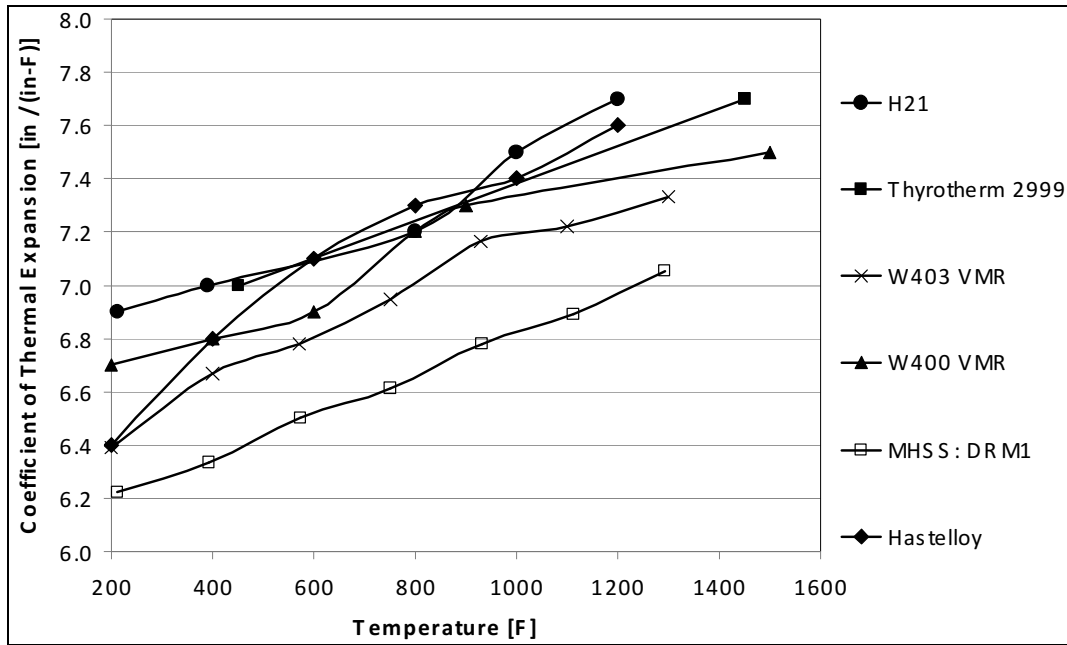
Figure 6.33: Selection of hot-work tool steels on the basis of thermal expansion.
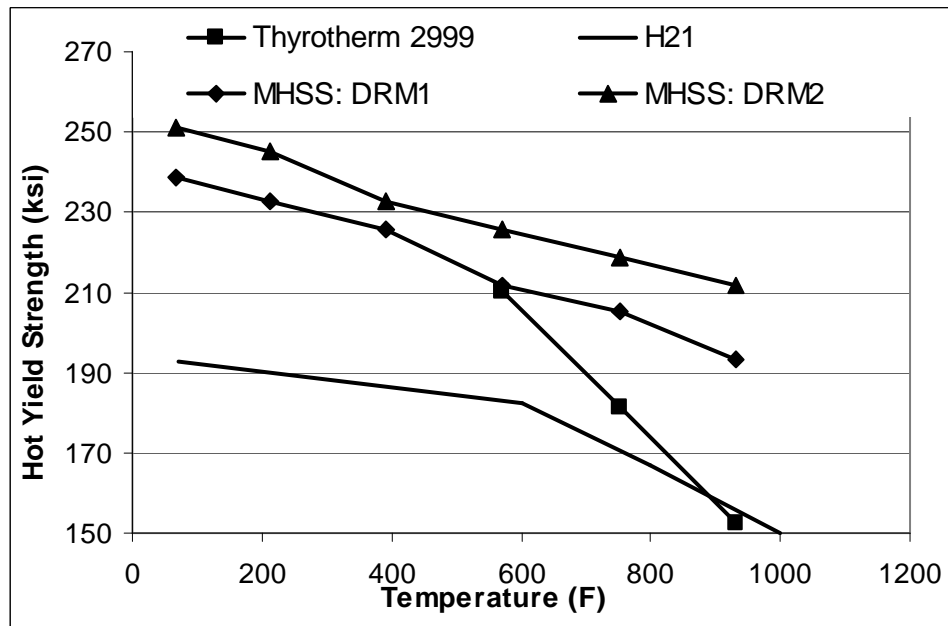
Figure 6.34: Comparison of hot yield strength of selected tool steels.

In order to consider welded overlays, it was necessary to model the insert as a single entity with different material properties in the welded zone. Figure 6.35 shows the method used in the

156

current case. It was assumed that the welded zone formed the top layer of the die surface ending at the die corner radius. All the elements above this cut-off line were given the mechanical and thermal properties of Hastelloy™. It is desired to minimize the difference in thermal expansion between the welded overlay and its substrate in order to reduce the residual stresses induced upon cooling from the welding temperature. The substrate material was, thus, chosen as the existing H-21 tool steel. After welding, a stress gradient will exist in the insert unless it is subjected to stress-relief annealing. This scenario was not modeled in the current case. Only simulations of the start-up cycle were modeled for demonstration purposes.
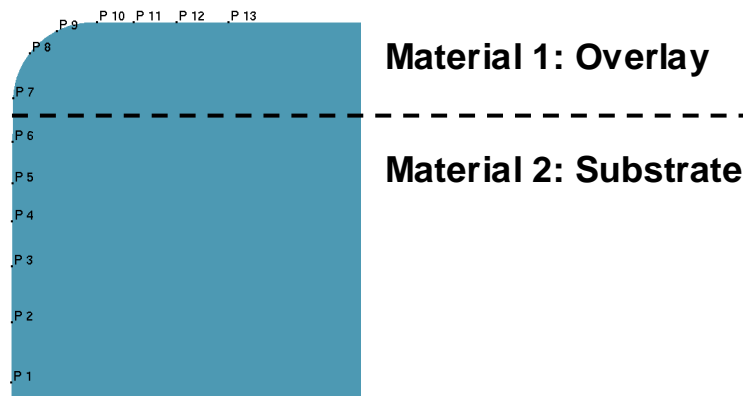
Figure 6.35: Modeling approach for considering welded overlays.

The effect of thermal conductivity was reflected in the die surface temperatures observed at start-up (Figure 6.36). Compared to H-21, the 18-20% higher thermal conductivity of Thyrotherm™ 2999 results in only 7% lower die surface temperature at BDC. The higher contact times in the hydraulic press, thus, offset the increase in thermal conductivity. The difference between the maximum die surface temperature (Hastelloy™) and Thyrotherm™ was only 11%. Similarly, the difference in the corresponding temperature gradients of these two materials was found to be within 15% at start-up and during steady-state (results not included here). Thus, due to very high contact times in the current process, reliable tool steel selection was not possible solely on the basis of thermal conductivity.

Similarly, the differences in thermal expansion were also overshadowed by the high contact times. This is seen in the strain amplitude shown in Figure 6.38. The theoretical mechanical strain was calculated by subtracting the calculated thermal strains from the predicted total elastic strain from FEA. The variation of these strain components over one forging cycle is shown in Figure 6.37. As mentioned earlier, the thermal expansion of the surface layer (thermal strain) during deformation is resisted by the cooler substrate, thus inducing a compressive strain (theoretical

157

mechanical strain). This situation is reversed during lubricant spray. Depending upon die material properties and process conditions, the surface layer can have either a) no residual strain, or b) a residual tensile strain, or c) a residual compressive strain (as in Figure 6.37).
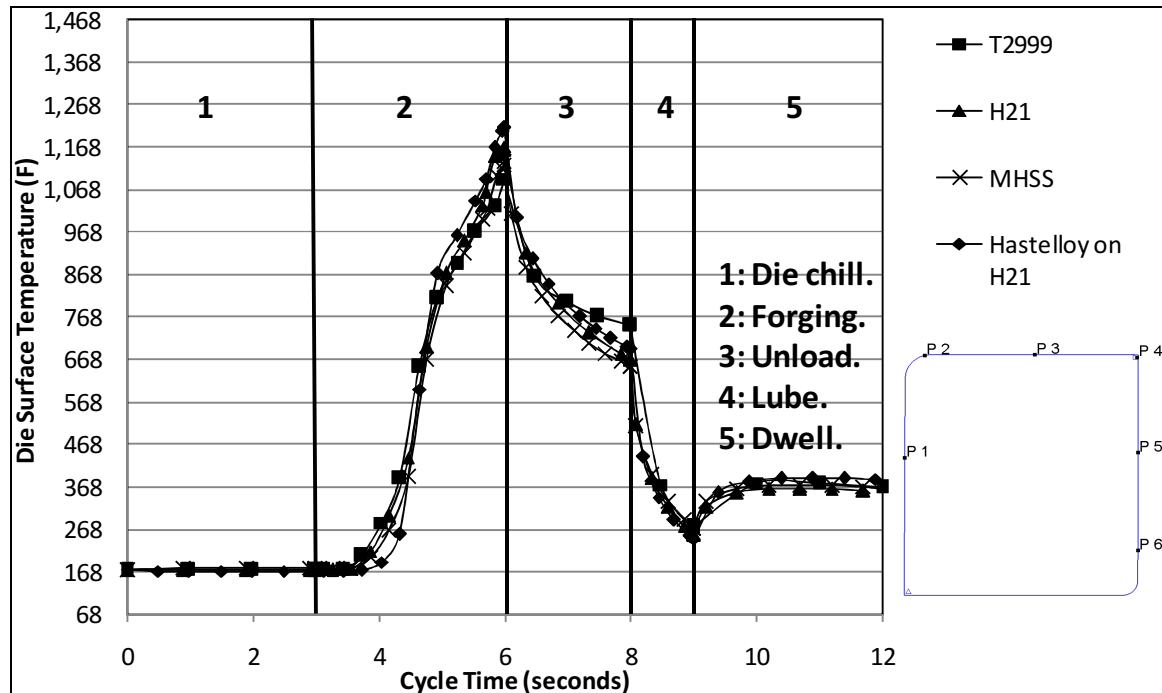
Figure 6.36: Surface temperature cycle for selected tool steels at start-up.
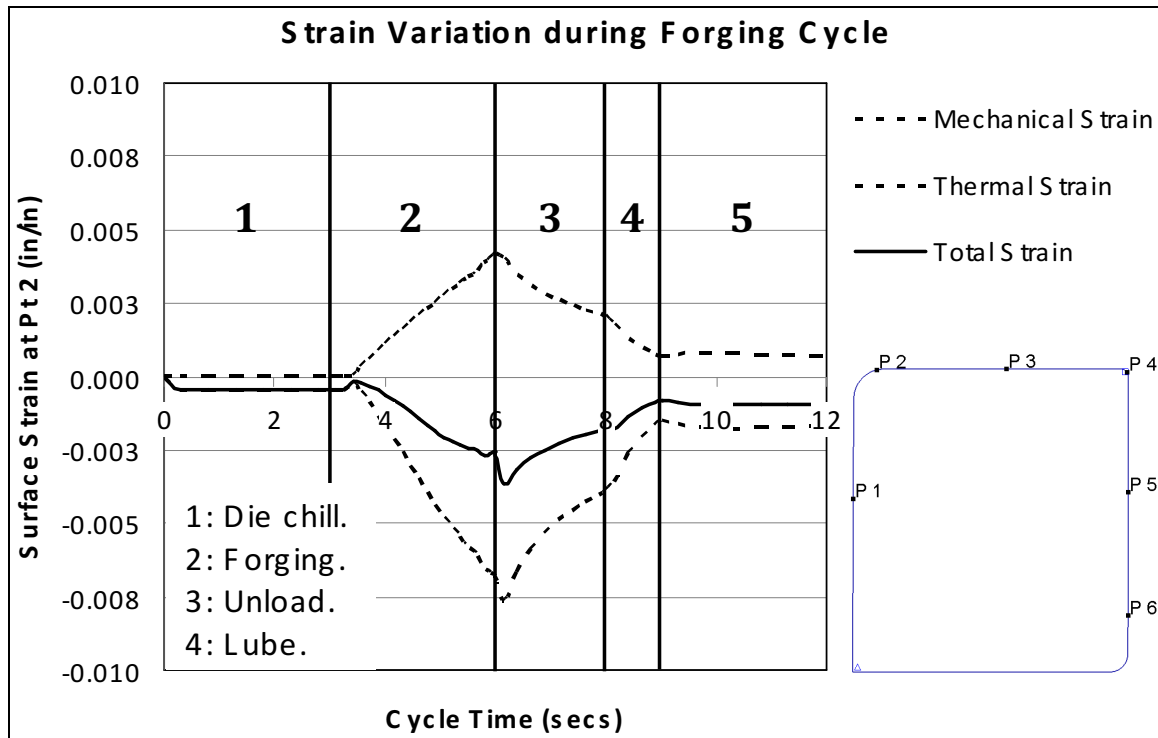
Figure 6.37: An example of strain reversal from BDC to lube spray (start-up).

The surface stress amplitude as a result of the strain amplitude is shown in Figure 6.39. This stress cycle is influenced by the elastic modulus of the die material. The matrix steel was found to have the smallest amplitude. Since the materials being considered have similar elastic properties, the differences in stress amplitude had to be analyzed by considering the ratio of the induced elastic stress to the yield strength of the die material at each discrete point during deformation i.e. with changing temperature (Figures 6.40 and 6.41). A ratio greater than 1 implies plastic strain accumulation in the surface during start-up i.e. start of low-cycle fatigue. Thus, die materials were compared at points 1, 2 and 3 in terms of thermal fatigue performance on the basis of hot yield strength (Figure 6.34), using the interface conditions influenced by thermal properties as the input data. Hastelloy™ is not included in the analysis since yield strength in the heat-treated condition was not available. Accurate yield strength data over the forging temperature range is required for reliable screening and selection of candidate materials for production trials.

159
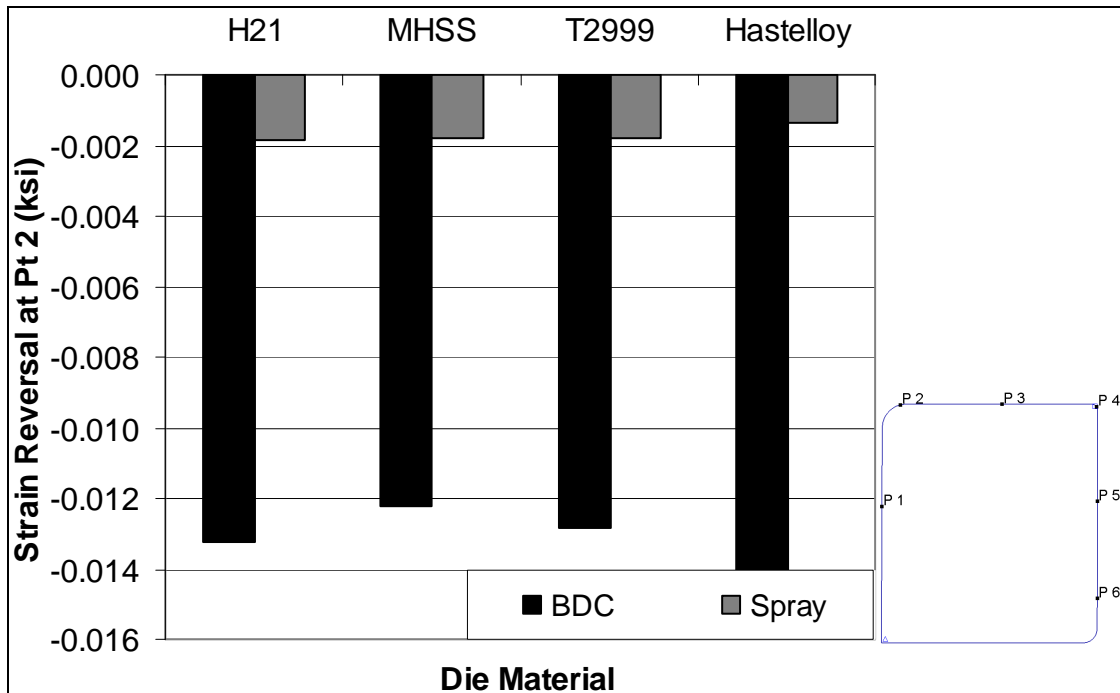
Figure 6.38: Strain (ε $_{mech}$) amplitude at start-up in hot-work tool steels.

The best thermal fatigue performance was predicted for the MHSS over the die surface considered i.e. point 1, 2 and 3. Thyrotherm™ was predicted to have intermediate thermal fatigue performance at point 1 and 3. At point 2, H-21 showed better thermal fatigue performance. It should be noted that this analysis is based on general yield strength data available from product brochures for a specific heat-treatment schedule and may not apply specifically to the heat-treatment selected for production trials.

160
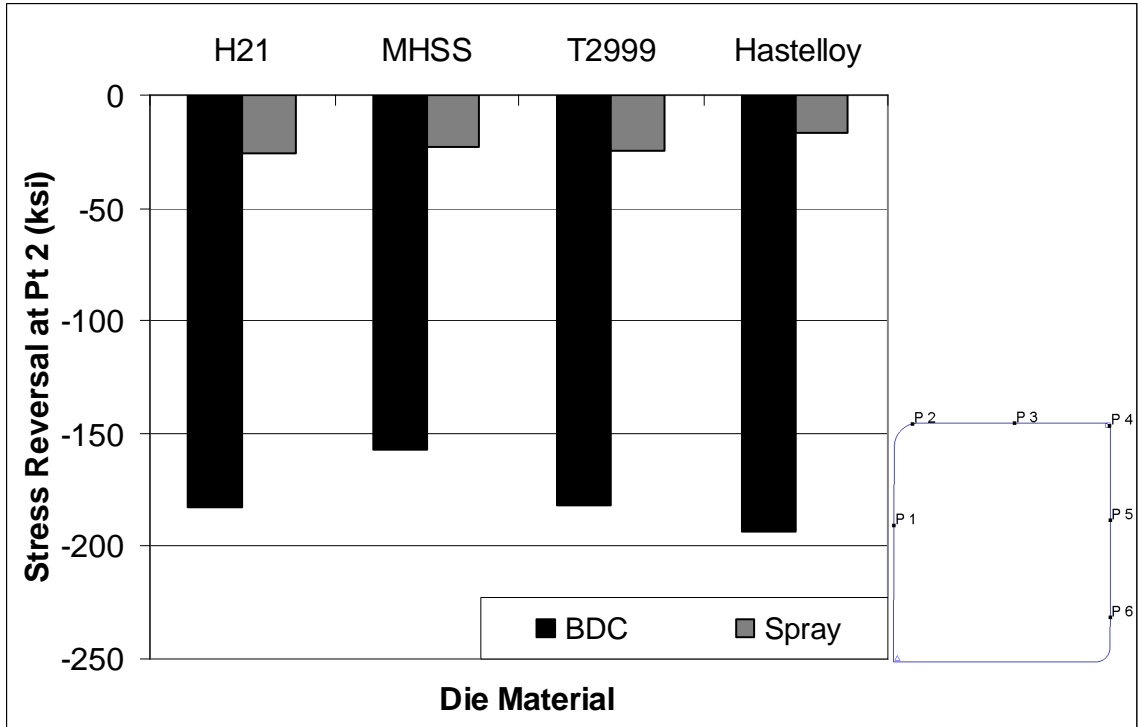
Figure 6.39: Stress amplitude at start-up in hot-work tool steels.
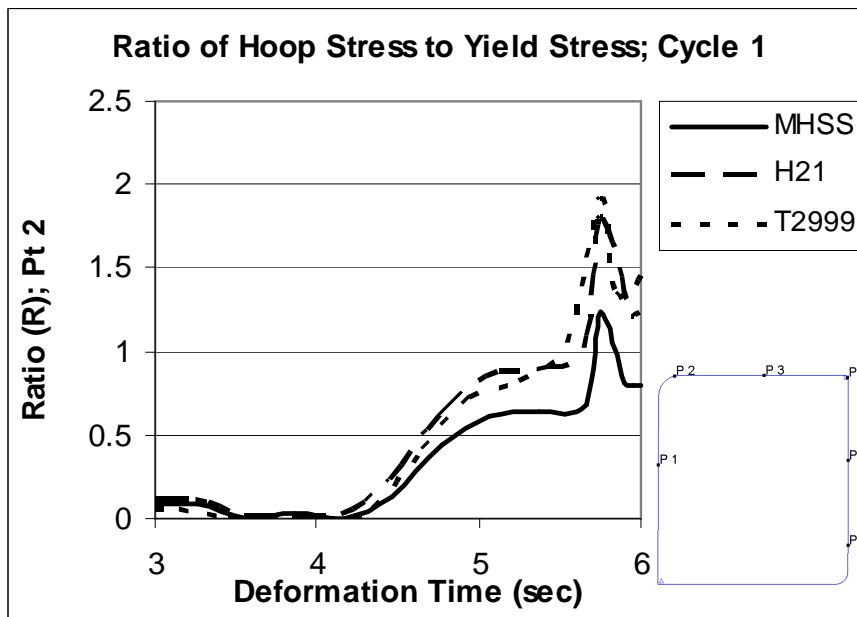
Figure 6.40: Ratio of hoop to yield stress for selected steels at start-up.

161
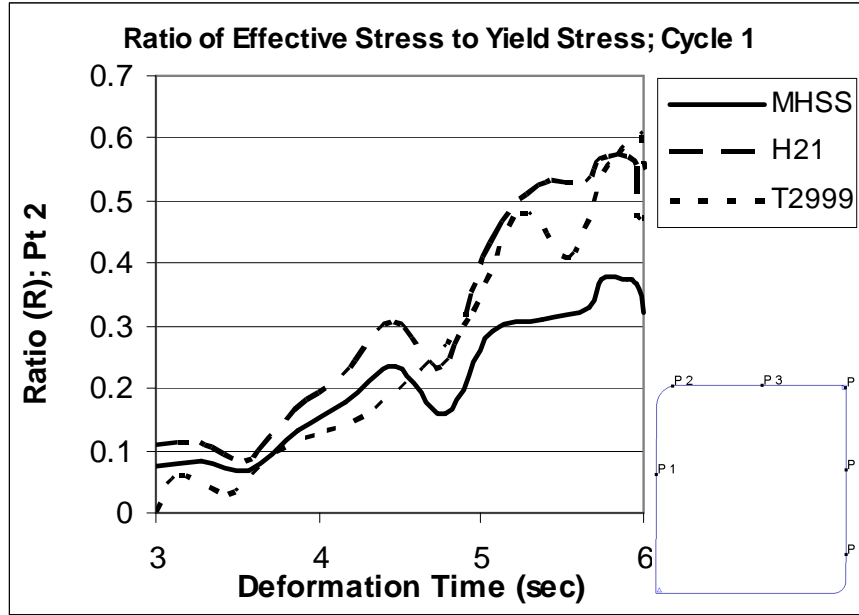
Figure 6.41: Ratio of effective to yield stress for selected steels at start-up (point 2).

6.6. Die Materials and Process Designs for Production Trials

On the basis of the FEA conducted in this study, a matrix high speed steel (MHSS) insert was recommended for production trials. The potential materials for application are a) DRM1™ (58-60 HRC) or DRM2™ (60-62 HRC) from Daido Steel, both double electro-slag re-melted (ESR), and b) DURO-F1™ from Nachi-Fujikoshi. Additionally, Thyrotherm™ 2999 was also recommended due to its higher thermal conductivity and comparable thermal fatigue performance. A nitriding surface treatment was recommended for all dies.

The current process has a large dwell time between the end of pre-heating and the start of production since operators wait for the billets to reach the target temperature. It was suggested that pre-heating be done in an oven, with in-press heating using a gas flame on the inside of the assembly prior to the start of production. Oven heating results in uniform temperature gradients as long as an appropriate time-temperature combination is selected. In-press heating is the most energy efficient option since it reduces overall set-up and dwell time.

6.7. Summary and Recommendations

A warm forging (upsetting) process for an automotive transmission shaft was selected in order to develop and apply FEA-based techniques for improvement of die life in a shrink-fitted die assembly. This study was conducted in cooperation with American Axle and Mfg. (Colfor Division)

162

under the FIERF-sponsored die wear research project. The primary die failure mechanism in this forging process was thermal fatigue, resulting in high downtime and scrap rates. The following research objectives and results were achieved:

- A die assembly simulation using incremental contact generation was used to determine accurate shrink-fit interface conditions (contact pressure and deflections). This method was compared to the standard procedure of using displacement boundary conditions and proven to be more accurate.

- A simulation technique was developed for modeling die pre-heating in order to determine the loss of compressive pre-stress prior to the first forging stroke. Two heating methods were compared viz. a) gas ring on the container O.D and b) gas flame on the inside of the assembly. The loss of shrink-fit was found to be 40-50% less in the latter case for carbide inserts, and hence is the recommended heating method. Differences in thermal expansion resulted in 30% loss of shrink-fit with ceramic and carbide inserts, whereas tool steels experiences an increase in compressive pre-stress.

- The stress amplitudes in carbide were predicted to have 20% lower than those in steel in spite of a 200% higher elastic modulus. Carbides were, therefore, found to have superior thermal fatigue resistance compared to tool steels but require special die design and analysis procedures in addition to the added cost.

- Comparison of tool steels predicted that a matrix steel would be best-suited for improvement of die life due to its higher hot yield strength and hot hardness. Thyrotherm™ 2999, with highest thermal conductivity, resulted in intermediate thermal fatigue performance.

Based on the results presented above, the following recommendations were made for improvement of thermal fatigue life of shrink-fit dies used for warm and hot forging on hydraulic presses:

- Die material selection: Among tool steels, a material with higher hot yield strength and tempering resistance was recommended to prevent heat checking and local yielding. A nitriding surface treatment should be explored for local increase in surface hardness.

- Die design: Selection of shrink-fits should take into account the thermal expansion during pre-heating and forging through the FEA described in this chapter or analytical

163

approximations based on production temperature measurements. Shrink-fits should be applied at both interfaces i.e. insert-sleeve and sleeve-container.

- Die assembly and pre-heating: (same tools, inside heat, knockout) Shrink-fit tools are sensitive to dimensional variations of the containment system. A single sleeve-container combination should be consistently used for each production job so as to subject it to the same loads and deflections (mechanical fatigue) in operation. This will help to eliminate a crucial noise variable that can affect the compressive stresses on the insert during assembly and pre-heating. In-press heating with a gas flame on the inside is recommended to minimize the loss of pre-stress.

- Billet temperature: Hydraulic presses have their maximum press load available throughout the forging stroke. This provides the possibility of reducing the billet temperature in order to reduce thermal fatigue (within the limits of maximum allowable press load, shrink-fits and die stresses).

- Forging: The knockout mechanism should be used to hold the workpiece off the die surface prior to contact with the top die. If an accumulator drive is available on the press, the approach and retraction velocity of the ram can be increased to reduce the total forging cycle and contact time.

- Lubrication spray: As mentioned in Chapter 6 an air-water-lube spray sequence is recommended for efficient die cooling and lubricant adhesion, considering the high contact times with hydraulic presses. Lubricant concentration should be monitored in production unless a PLC-based mixing and delivery system is being used.

164

CHAPTER 7

CASE STUDY 3 – APPLICATION OF CERAMIC AND CARBIDE INSERTS IN WARM AND HOT FORGING

7.1.   Problem Statement

Chapter 6 summarized the results of an FEA study to identify the effect of die material properties on interface conditions and thermal fatigue life. Two material groups were compared viz. ceramic and carbide materials versus tool steels. Due to their high thermal conductivity and low thermal expansion, carbides were identified as a possible alternative to hot-work tool steels. However, die design and analysis, along with selection of process conditions, is extremely critical to ensure that the insert is maintained under compressive pre-stress during production to prevent brittle fracture. Also critical is the sensitivity of the die stresses to dimensional variation in the die components. This study primarily investigates the application of carbide die inserts in the upsetting operation described in Chapter 6. Results for a ceramic insert were also briefly touched upon in Chapter 6. The stresses and interface conditions in the die insert were tracked from assembly all the way through heating and forging using different process scenarios based upon shop-floor observations.

7.2.   Objectives

The overall objective of this study was to develop an FE simulation-based failure prediction criterion for warm and hot forging dies with carbide and/or ceramic inserts on the basis of detailed analysis of the forging process. This criterion is necessary in order to a) understand observed failure mechanisms and, b) recommend die design changes to avoid catastrophic and/or mechanical fatigue failure in production. This study focuses on dies with carbide inserts, with the following specific objectives:

- Analysis of the failure modes on the basis of interface conditions and die stresses observed in the forging process simulation and,

165

- Design of pre-stressed hot forging dies taking into account the loss of shrink-fit due to thermal expansion from preheating and forging.

7.3. Analysis of Die Stresses Prior to Forging

The analysis techniques developed for die assembly and heating were already described in detail in Chapter 6 and will not be repeated here. These methods were developed specifically for analysis of shrink-fit tool designs assuming carbide as the insert material. The results presented here apply to specific goals with respect to die design for ceramic and carbide inserts viz. prediction of die life and elimination of possible failure mechanisms.

7.3.1. Sensitivity of the Die Assembly to Dimensional Tolerances

FEA of die assembly was conducted as mentioned in Chapter 6 using fully elastic models with inter-object contact being generated incrementally in a pre-determined assembly sequence. The dimensional variation in the die components from the manufacturing process results in variation in the compressive stress states of the insert after assembly. This variation can also carry forth into the pre-heating and forging stages depending upon the sensitivity of the die assembly to these dimensional changes. This chapter covers a basic sensitivity analysis of the die assembly based upon dimensional variation recorded on the shop floor. Actual dimensional data is provided here in the interest of confidentiality. Figure 7.1 shows the dimensional parameters of the containment ring, which is assembled on top of the sleeve-insert sub-assembly. As discussed earlier (Chapter 6), the interference at the sleeve-insert interface is negligible. Thus, any variation in the compressive pre-stress in the insert is expected to be pre-dominantly influenced by dimensional variation at the sleeve-container interface. It was found that the only significant variation was on the front side/top inner diameter of the container (ϕB in Figure 7.1). A comparison of the measured and specified values (Table 7.1) showed that other than ϕB, the remaining values were identical to the average dimensions used in the FE analysis discussed in Chapter 6. The container I.D on the rear (ϕC) and height H are reference dimensions and were, thus, maintained constant. This assumption was validated by shop floor measurements (Table 7.1).

166
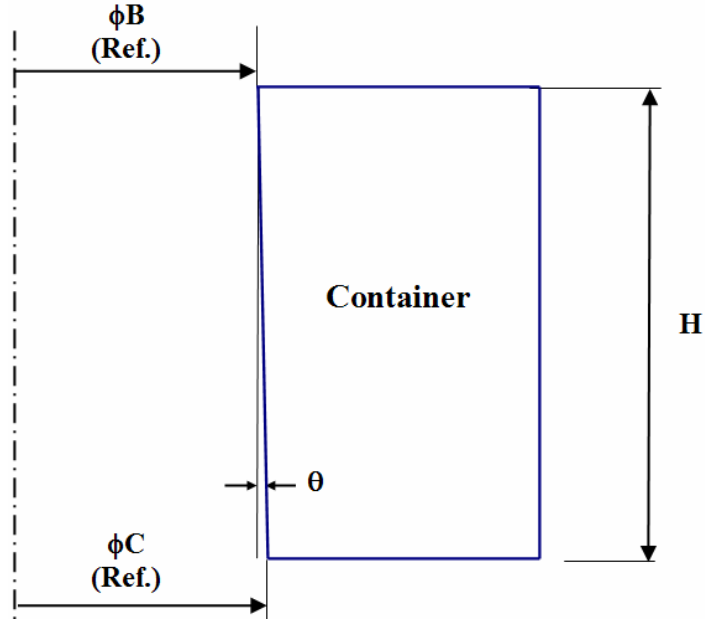
Figure 7.1: Geometrical parameters of the containment ring.

The measured value of ϕB in Table 7.1 corresponded to a draft angle, which was 0.0323º from the target value, with the container height (H) being equal to the specified nominal value. Based upon this information, the basic sensitivity analysis discussed here varied only the draft angle and thus, the inner diameter ϕB at 4 levels, 2 on either side of the reference value with average dimensions used for the remaining components i.e. two container designs each with higher and lower values of the draft angle (Table 7.2). The designs were selected with draft angle varying in intervals of 0.025º to give the 4 designs shown in Table 7.2. It was decided to base the sensitivity analysis on the shop floor data rather than the tolerances on the production drawings (± 0.5º). Additionally, sleeve and insert dimensions were also fixed in order to reduce the number of simulations required. This appears to be a valid assumption on the basis of measured dimensional data (Table 7.1). The selected designs were then analyzed in terms of the die stresses and deflections during assembly and heating. The forging process was not included in this sensitivity analysis.

www.manaraa.com

Component	Deviation from Nominal Value (inches)	% Deviation from Nominal Value
Container:		
O.D.	0.001	0.0080
Height (H)	0	0
Front/Top Side I.D. (B)	-0.0068	-0.1237
Back/Bottom Side I.D. (C)	0.0007	0.0123
Tapered Sleeve:		
Front/Top Side I.D.	-0.001	-0.0181
Back/Bottom Side I.D.	0	0
Height	0	0
I.D.	0	0
Die Insert:		
Front/Top Side I.D.	0.001	0.0602
Back/Bottom Side I.D.	0	0
Height	0.0015	0.0994
O.D.	0.0005	0.0114
Backup Die:		
O.D.	0.001	0.0228
Height	-0.001	-0.0588
I.D.	N/A	N/A

Table 7.1: Measured deviation of geometrical parameters from nominal values.

7.3.1.1.   Die Stresses in the Selected Designs after Assembly

The four designs vary in the value of the front side inner diameter. Thus, the compression fit introduced into the assembly when the container moves over the sleeve will be different in each case. Figure 7.2 shows the hoop stress in the insert at the end of assembly. Design/Assembly M2 has the highest value of ϕB (Table 7.2) and shows near tensile stresses in the region of the upsetting surface after assembly (Figure 7.2a). As in previous simulations of die assembly (Chapter 6), there is still a diagonal stress gradient in the insert with the hoop stress becoming compressive at the bottom region of the inner diameter. With a decrease in the inner diameter (ϕB) the magnitude of the compressive stresses increases, resulting in P2 having the maximum shrink-fit on the insert (Figure 7.2).

168

Parameter	Container Geometries in terms of Deviation from Nominal Design			
	M2	**M1**	**P1**	**P2**
ϕC	0	0	0	0
H	0	0	0	0
θ	-0.05º	-0.025º	0.025º	0.05º
ϕB	0.0105 in.	0.0052 in.	-0.0052 in.	-0.0105 in.
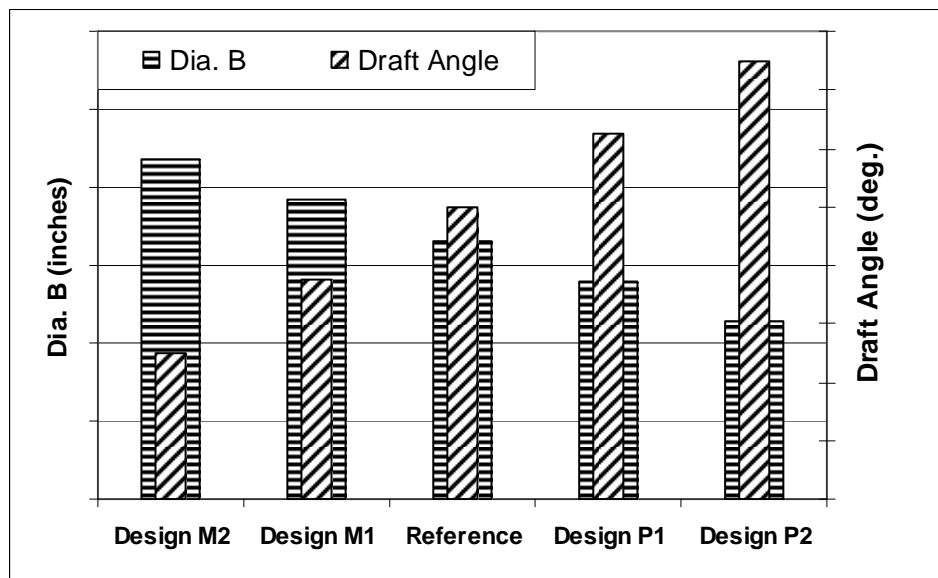
Note: The container design measured in production was an intermediate step between M1 and M2. Values of ϕB and θ are not specified to maintain confidentiality.

Table 7.2: Geometries selected for sensitivity analysis.

Figure 7.3 shows the deflection in the sleeve for the four selected geometries, at the end of die assembly. The maximum deflection for the M2 design is found to be in the area where the insert contacts the sleeve. Due to the larger value of ϕB, the top/front of the sleeve does not bend inwards significantly as seen in Chapter 6 and as observed with the other designs in Figure 7.3.

169

Stress - Theta (ksi)

A =	-99.1
B =	-84.8
C =	-70.4
D =	-56.1
E =	-41.8
F =	-27.5
G =	-13.2
H =	1.17
I =	15.5

a) Design M2.

Stress - Theta (ksi)

A =	-112
B =	-98.7
C =	-85.3
D =	-71.8
E =	-58.4
F =	-45.0
G =	-31.5
H =	-18.1
I =	-4.67

b) Design M1.

Stress - Theta (ksi)

A =	-144
B =	-131
C =	-118
D =	-104
E =	-91.1
F =	-77.9
G =	-64.7
H =	-51.5
I =	-38.3

c) Design P1.

Stress - Theta (ksi)

A =	-159
B =	-146
C =	-133
D =	-120
E =	-107
F =	-93.5
G =	-80.3
H =	-67.1
I =	-54.0
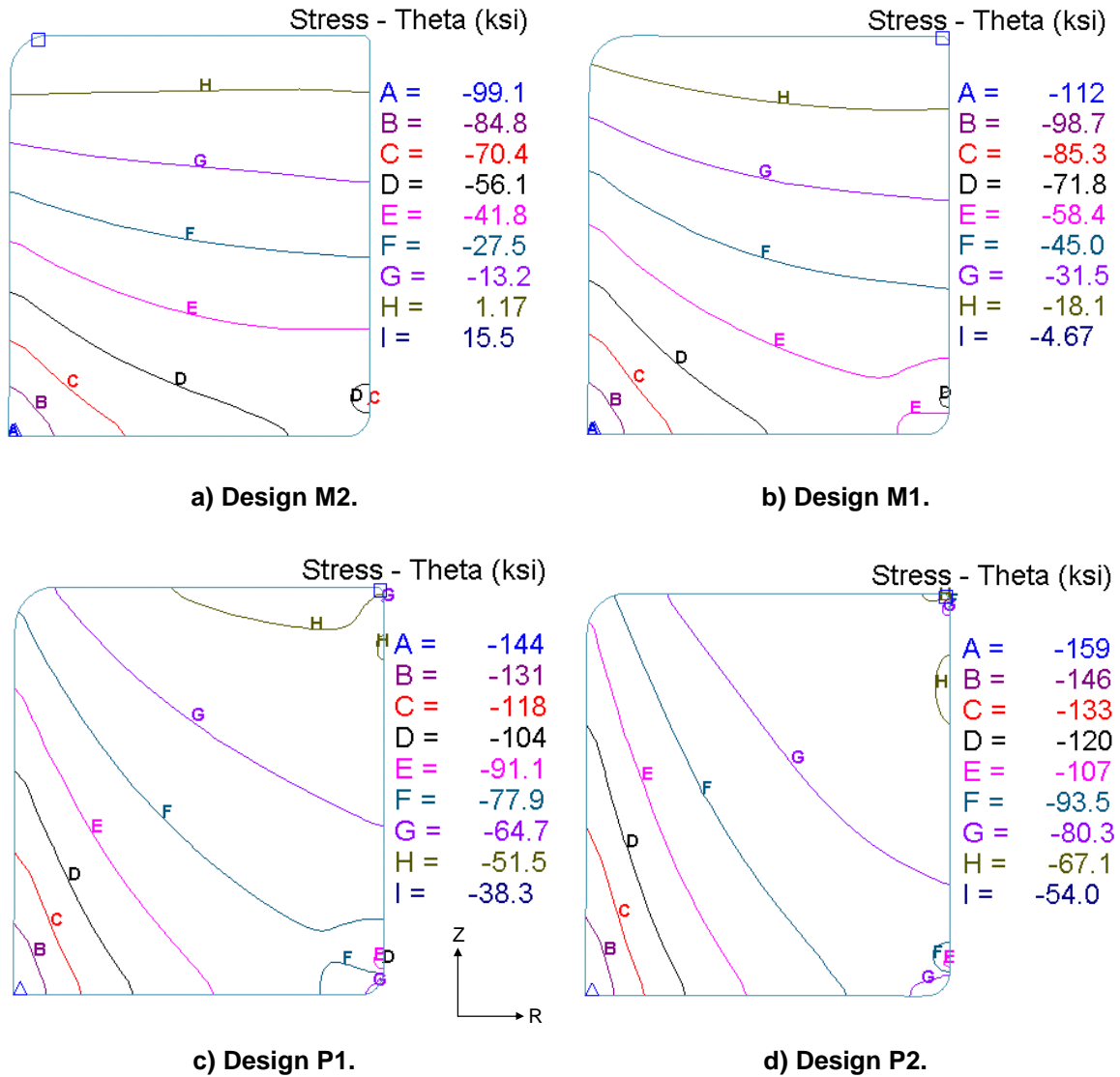
d) Design P2.

Figure 7.2: Hoop stress distribution in the selected designs after assembly.

As the diameter ϕB reduces, the front of the sleeve experiences an increasing inward bending moment. Figure 7.4 shows the change in the profile of the I.D of the sleeve at the end of assembly along with the initial profile. Point 5 near diameter ϕC was used as a reference value for all deviations. A comparison of the deviations showed that the four designs varied significantly in the deflections at the front end of the die assembly. For the region of the sleeve in contact with the insert, designs P1 and P2 showed higher deflection, and therefore, higher compressive stresses than designs M1 and M2. Based upon dimensional data (Table 7.1), the die assembly measured in production was an intermediate step between the M1 and M2 designs.

170
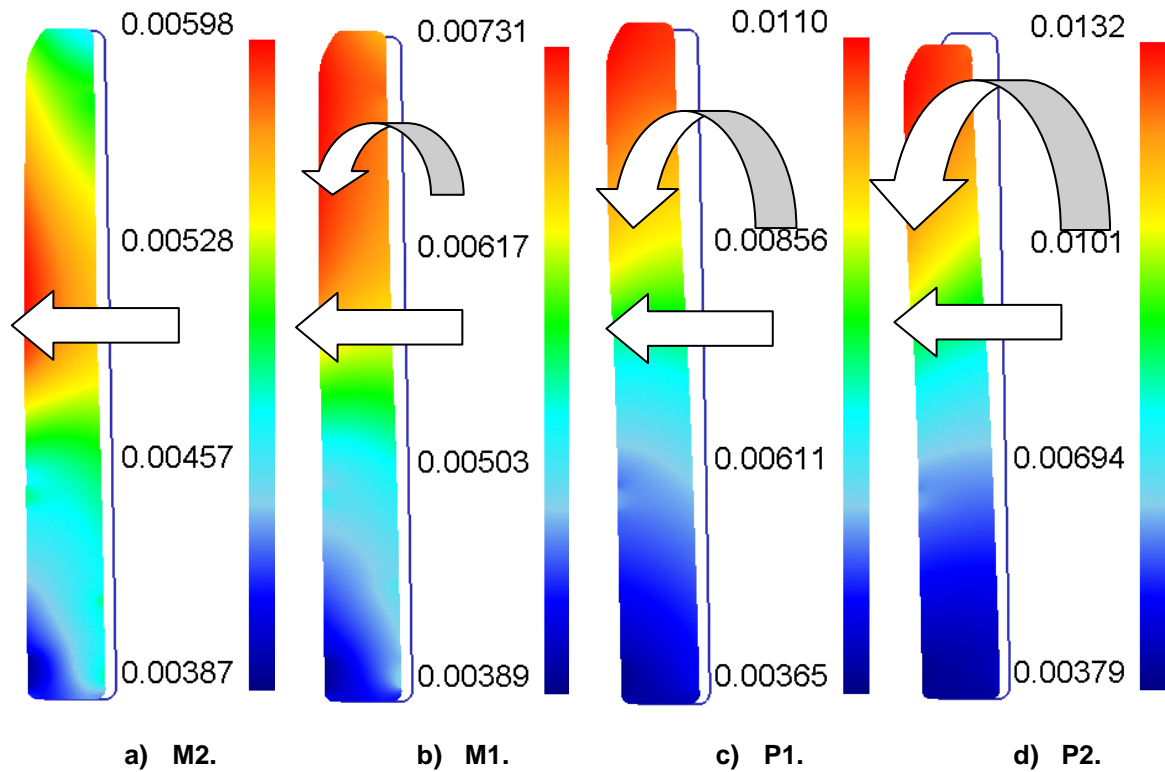
Figure 7.3: Sleeve deflection after assembly for the four designs selected (deflection in inches).

7.3.1.2. *Die Stresses in the Selected Designs after Pre-heating*

Die heating simulations were conducted in order to compare the four selected designs under a conditions of thermal expansion with a temperature gradient. The method of heating with a gas flame on the inside was assumed with a heating time of 3 minutes. No dwell time was simulated. The trends in the stresses observed during assembly carry forward into heating since the insert expands before the sleeve and container. The designs with the smaller value of ϕB have similar stress magnitudes, which are ≈ 20% greater on the maximum and ≈ 75% greater on the minimum compressive stress (Figure 7.5).

171
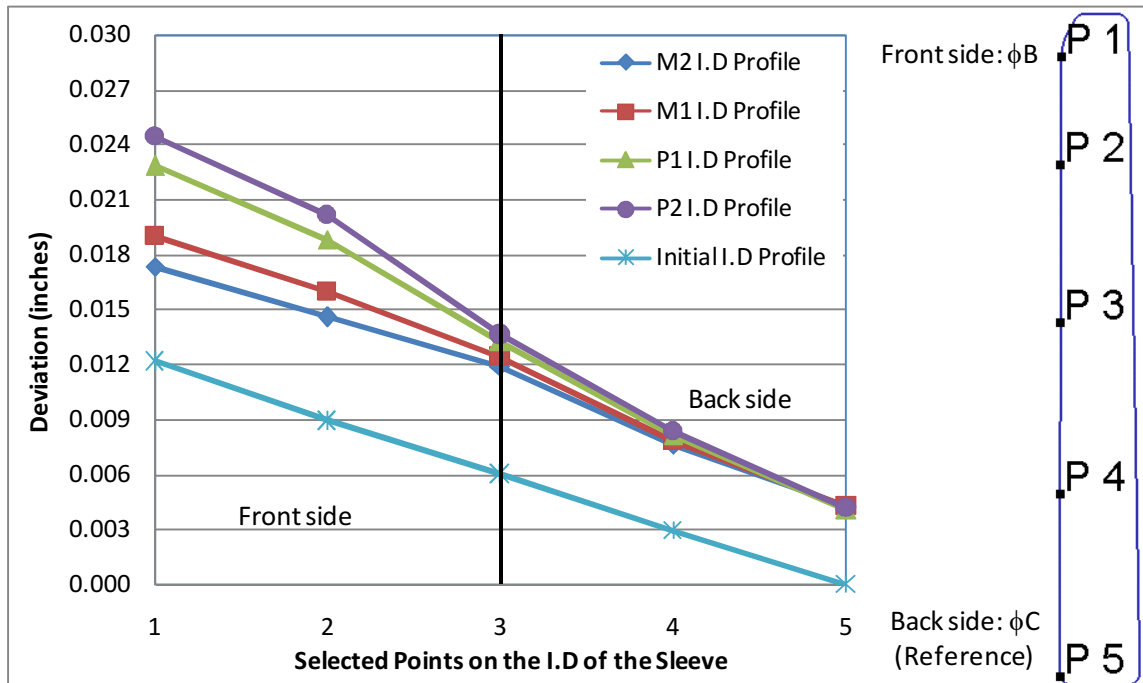
Figure 7.4: Deviation of the sleeve I.D profile with respect to ϕC after assembly.

Figures 7.6 and 7.7 give a summary of the change of hoop and radial stress on the insert O.D. through assembly and heating for the selected designs. The radial stress is equivalent to external pressure on the insert and is, thus, a measure of the shrink-fit in the die assembly. The selected designs are compared to the design with average dimensions discussed is the preceding sections of this report and (Table 7.2).

172

a) Design M2.

b) Design M1.

c) Design P1.
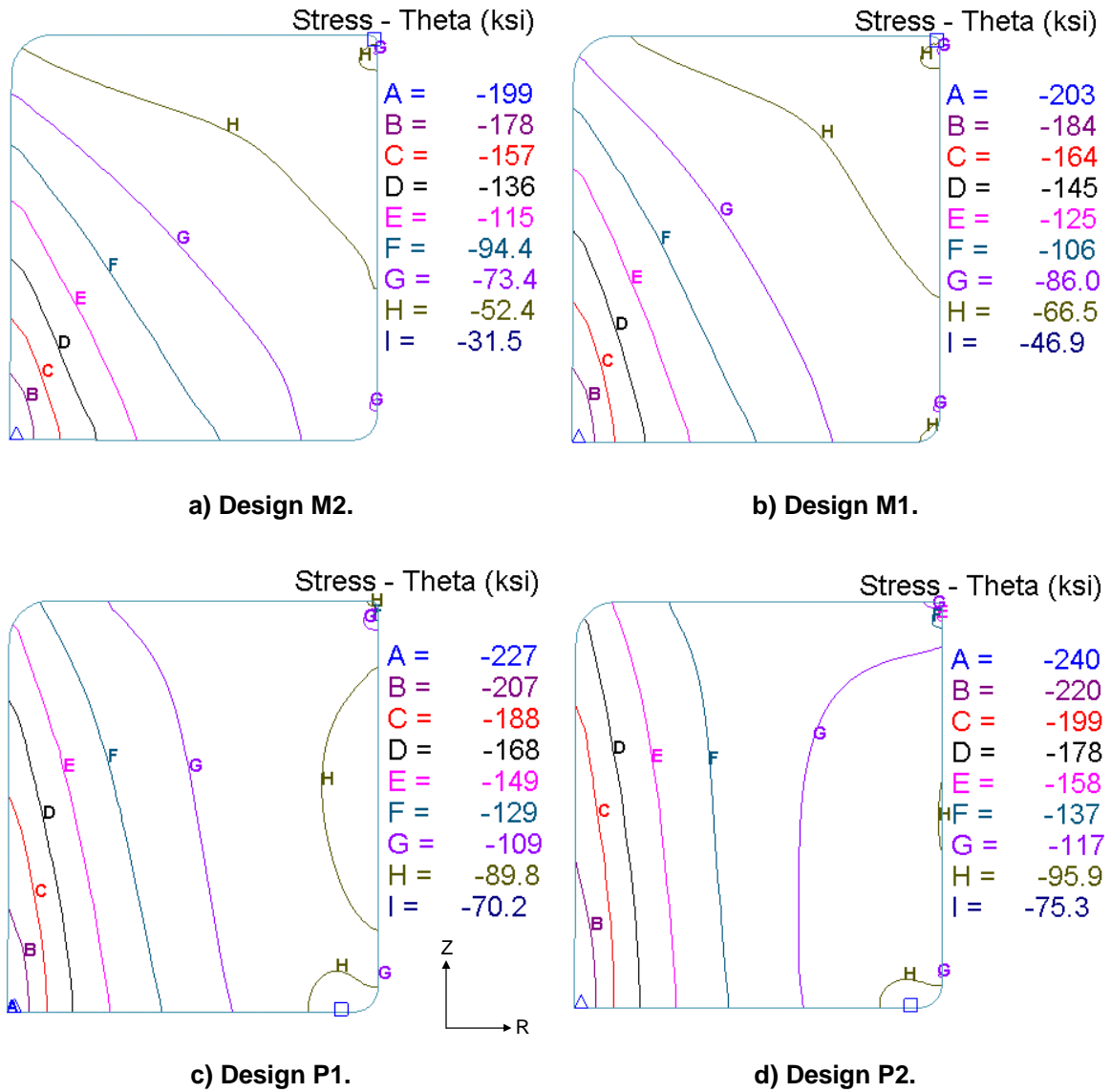
d) Design P2.

Figure 7.5: Hoop stress distribution in the selected designs after pre-heating (gas flame on the inside; no dwell simulated).
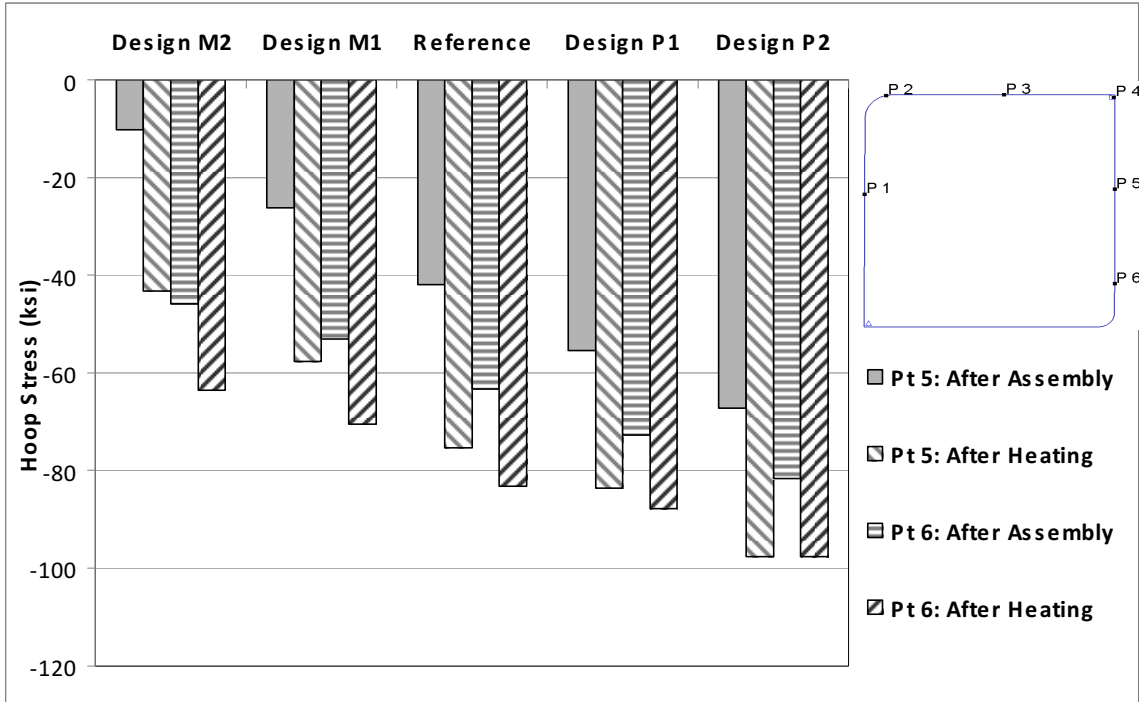
Figure 7.6: Hoop stress on the O.D of the insert for the selected designs.
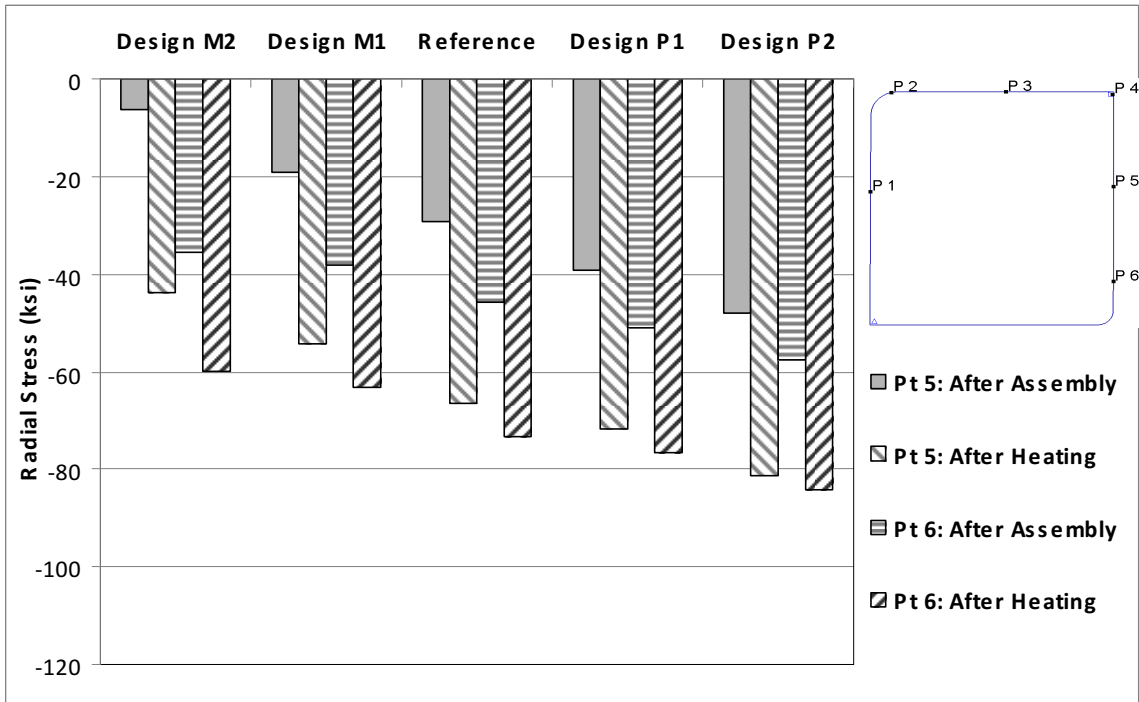
Figure 7.7: Radial stress on the O.D of the insert for the selected designs.

174

Within the range of values considered for the draft angle (θ) and diameter ϕB, an approximately linear relationship was observed between the selected parameters and the resulting shrink-fit on the insert. The trends observed in the hoop and radial stresses are consistent throughout the range of values selected for the front side inner diameter for the container (ϕB). The selected die pre-heating condition (gas flame on the inside) results in a 20-75% increase in stresses as shown in Figure 5.5. A gas flame on the outside is expected to show a reverse trend since heat is applied directly to the container resulting in thermal expansion of the sleeve and container before that of the insert (Refer Chapter 6). The dwelling after heating and the subsequent forging process were not included in the current sensitivity analysis.

7.3.1.3. *Results of the Sensitivity Analysis*

Dimensional variation from the tool/die manufacturing process influences the shrink-fit and stress distribution in the insert prior to forging. For the current tool design the dimensions at the sleeve-container interface were expected to have a significant influence on the pre-stress in the insert due to negligible interference at the insert-sleeve interface. Based upon dimensional measurements recorded on the shop-floor, four variations of the container geometry were compared using FE analysis. This single-factor sensitivity analysis varied the front-side inner diameter of the container (ϕB in Figure 7.1 and Table 7.1) on either side of the average values used in the preceding chapters. The different designs were compared on the basis of the hoop and radial stresses on the insert O.D.

Figure 7.8 compares the reference design using average dimensions with those considered in the sensitivity analysis. The measured production die assembly was intermediate to design M1 and M2 based upon the data provided in Table 7.2. The percentage change in the hoop and radial stress follows a near linear pattern with ϕB and, thus, with the draft angle. Smaller values of ϕB (larger draft angles), therefore, result in greater compression on the insert during assembly. Depending upon location, the measured production design was predicted to have 25-50% less shrink-fit on the insert O.D. than the target design (Figure 7.8).

175
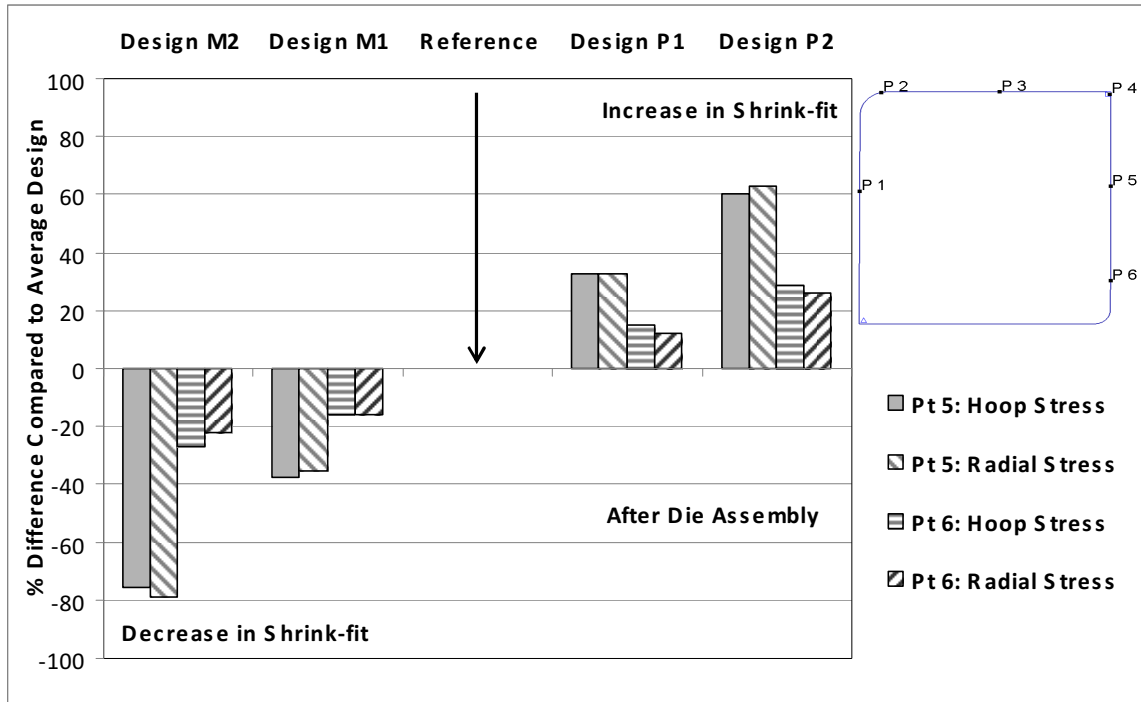
Figure 7.8: Percentage difference in the hoop and radial stresses after assembly for the selected designs with respect to the average (reference) design.

7.3.2. Analysis of Die Heating: Boundary Conditions and Effect of Heating Technique

The die insert can be considered to be a thick cylindrical shell with external pressure applied on it during assembly, from the sleeve-container interference. The compressive pre-stress from this external pressure is lost during pre-heating. The stress states on the inner and outer diameter of the insert were tracked during assembly and heating. The FEA technique used for simulation of die heating was described in detail in Chapter 6 along with the boundary conditions and underlying assumptions. Two heating methods were analyzed viz. gas ring on the container O.D., and gas flame on the inside.

Figure 7.9 compares the hoop stress on the outer diameter of the insert after pre-heating using gas flames on the inside and outside (2 minute heating followed by 10 minute dwell). Similarly, the change in external pressure (radial stress) on the insert O.D. is shown in Figure 7.10. The change in stresses during pre-heating is compared with the room temperature assembly (reference) values at the selected locations.

176

- Pre-heating with a gas flame on the outside of the container results in thermal expansion of the container and sleeve resulting in loss of contact at the sleeve-insert interface. This is reflected in the complete loss of shrink-fit (hoop and radial stresses) on the insert during heating (Figures 7.9 and 7.10; section 1).

- In the case of a gas ring on the outside, the heat dissipation and subsequent contraction of the sleeve and container during dwelling result in the insert regaining some of the compressive stress at the end of dwelling. The loss in compressive hoop stress on the insert O.D. compared to the room temperature die assembly (reference) is between 55-80%, prior to the first stroke (Figure 7.9; section 2). The loss in radial stress prior to the first stroke is between 60-75% (Figure 7.10; section 2).

- With the gas flame on the inside, the thermal expansion in the sleeve and container is delayed resulting in an increase in the compressive stress on the insert during heating (Figures 7.9 and 7.10; section 1). There is, however, a loss of compression during post-heat dwelling as heat flows from the insert into the sleeve and container resulting in thermal expansion of the latter (Figures 7.9 and 7.10; section 2). The loss in compressive hoop stress on the insert O.D. compared to the room temperature die assembly (reference) is between 30-40%, prior to the first stroke (Figure 7.9; section 2). The loss in radial stress prior to the first stroke is ≈ 30% (Figure 7.10; section 2).

The above results are summarized in Table 7.3 for a comparison of the two heating techniques compared to a room temperature assembly. Using a gas flame on the inside results in lower loss of compressive stress prior to the first forging stroke and is thus, the preferred heating method for this process. In-press pre-heating will further help to improve the compressive stress on the insert and reduce the thermal shock upon contact with the heated preform in the early stages of production.

177
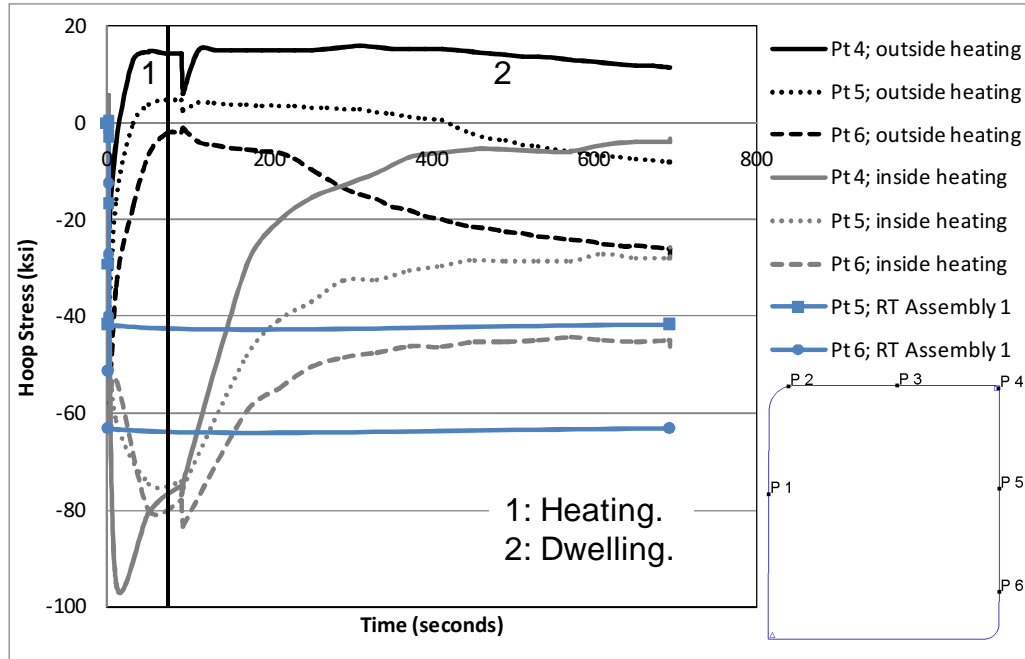
Figure 7.9: Comparison of hoop stress variation on the insert O.D with the two selected heating techniques and the room temperature (RT) assembly.
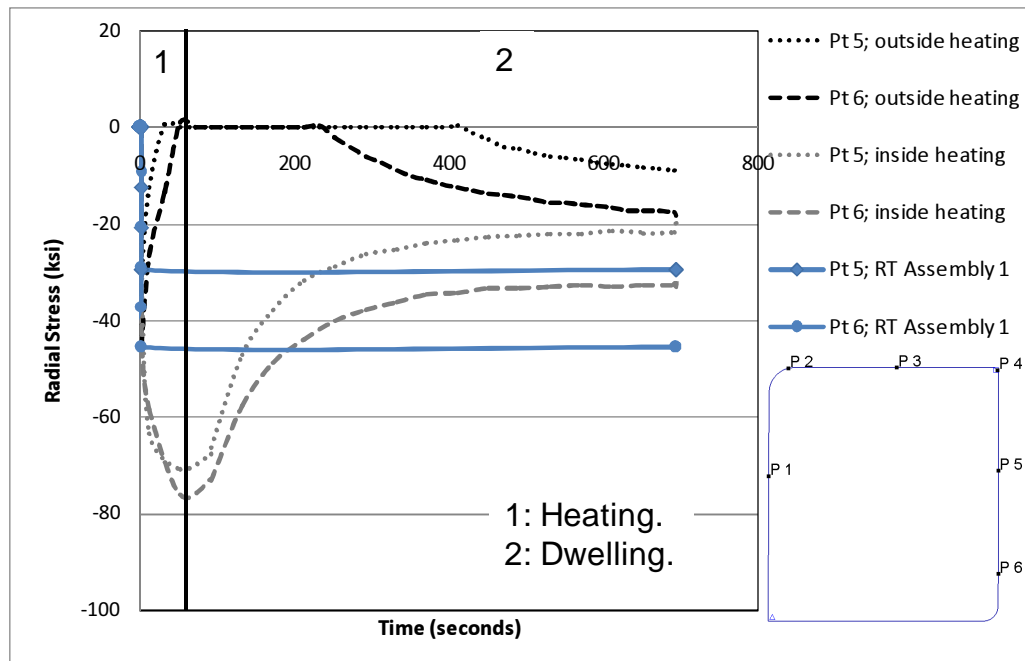
Figure 7.10: Comparison of external pressure (radial stress) variation on the insert O.D with the two heating techniques and the room temperature (RT) assembly.

178

Selected Points on Insert O.D.	Loss in compressive hoop stress	
	Gas ring on outside	Gas flame on inside
5	≈80%	≈40%
6	≈55%	≈30%
	Loss in compressive radial stress	
	Gas ring on outside	Gas flame on inside
5	≈75%	≈30%
6	≈60%	≈30%

Table 7.3: Loss in compressive stress on the insert O.D. prior to the first forging stroke compared to a room temperature assembly.

7.4.   Analysis of Thermo-Mechanical Loading during Start-up: First Cycle

Since die heating results in a loss of pre-stress prior to the first stroke, there was a need to investigate the effect of pre-heating by including a room temperature die assembly in the forging analysis. Thus, this section uses room temperature (designated Assembly 1; $T_o = 68°F/20°C$) as well as preheated (designated Assembly 2; $T_o = ≈ 170°F/80°C$) die assembly models as starting points for analysis of the thermal and mechanical loading conditions during the forging process. As discussed in Chapter 6, the forging process was discretized into 5 individual steps to account for deformation, lubrication and resting times. The analysis included single and multiple forging cycles using the simulation strategies discussed earlier.

The analysis summarized here represents the first forging cycle at the start of production. The forging process was analyzed for die assemblies under two thermal conditions. The same two die assemblies were also used for simulation of multiple forging cycles.

- Assembly 1 ($T_o = 68°F/20°C$): Room temperature assembly, assuming that the dwell time after the end of heating is large enough to make the effect of pre-heating negligible prior to the first forging stroke. The rationale behind this approach was the production observation that billet heating was sometimes started after die heating had stopped.

179

Thus, the dwell time might have been high enough to return the die temperature close to ambient conditions.

- Assembly 2 ($T_o \approx 170^oF/80^oC$): Preheated die assembly (gas flame on the inside) with a 10 minute dwell time assumed prior to the first forging stroke. Results were also obtained for the die assembly heated with a gas ring on the container O.D., but are not included, since this heating method was analyzed in Chapter 6 and is not recommended.

Figure 7.11 shows the thermal cycle experienced by the die surface during start-up; in this case, the first forging stroke with room temperature (Assembly 1) and pre-heated (Assembly 2) die assemblies. Point 2 is the location of maximum die surface temperature during the forging stroke. Figure 7.12 shows the temperature gradient at this location. Pre-heating results in Assembly 2 having ≈40% higher temperature at the deepest location (point 6) due to reduced heat dissipation from the die surface in contact with the workpiece. The temperature differential at the surface was within 5% for the two assemblies (Figures 7.11 and 7.12).
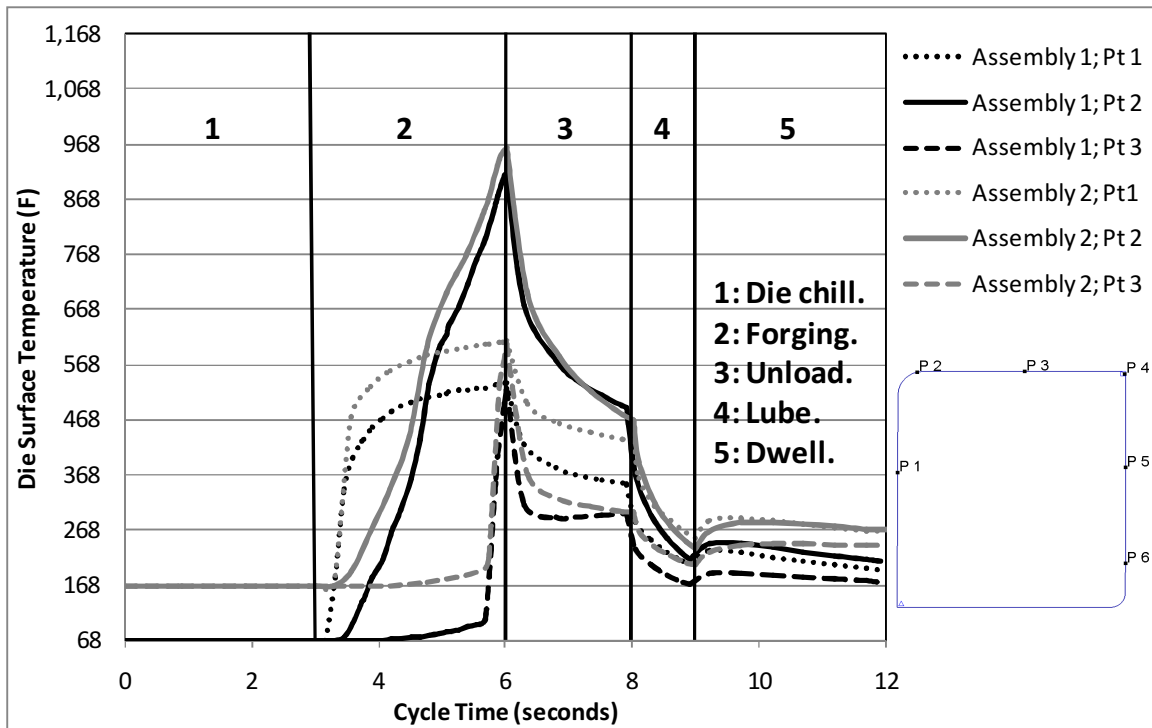
Figure 7.11: Die surface temperatures during a single forging cycle (first stroke of production).

180

Figure 7.13 shows the variation of the internal pressure (radial stress at the inner diameter) on the die insert during the forging cycle (tracked at Point 1). The internal pressure shows the same trend in Step 2 as that observed for the forging load, reaching a maximum value at BDC when complete filling is obtained. Upon unloading (ram retraction) in Step 3, the internal pressure drops resulting in "springback" or elastic recovery of the die assembly. The die assembly is returned to no-load (mechanical) condition upon part removal and lubrication spray (Figure 7.13; Steps 4 and 5). It should be noted that the mechanical loading conditions on both the die assemblies (forging load and internal pressure) are identical. However, the difference in the initial thermal condition of the die assembly result in significantly different responses to the applied loads during the forging cycle until a steady-state is reached.
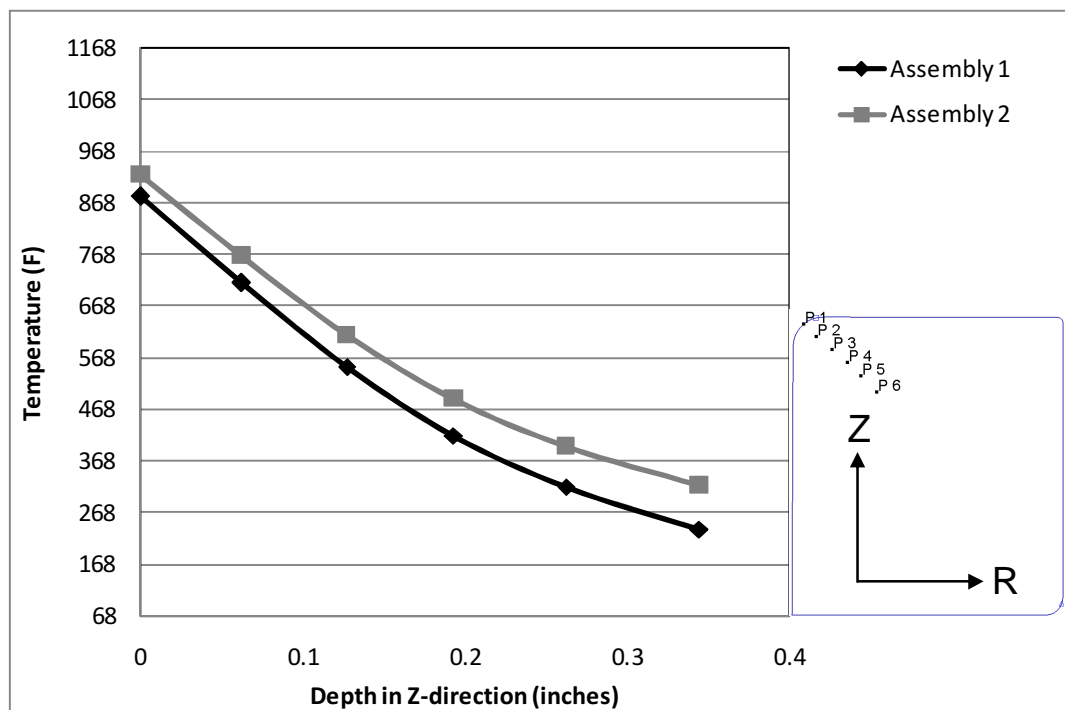
Figure 7.12: Thermal gradient at the point of maximum surface temperature i.e. Point 1 at the end of deformation (BDC); Assembly 1 – Room temperature; Assembly 2 – Pre-heated.

181
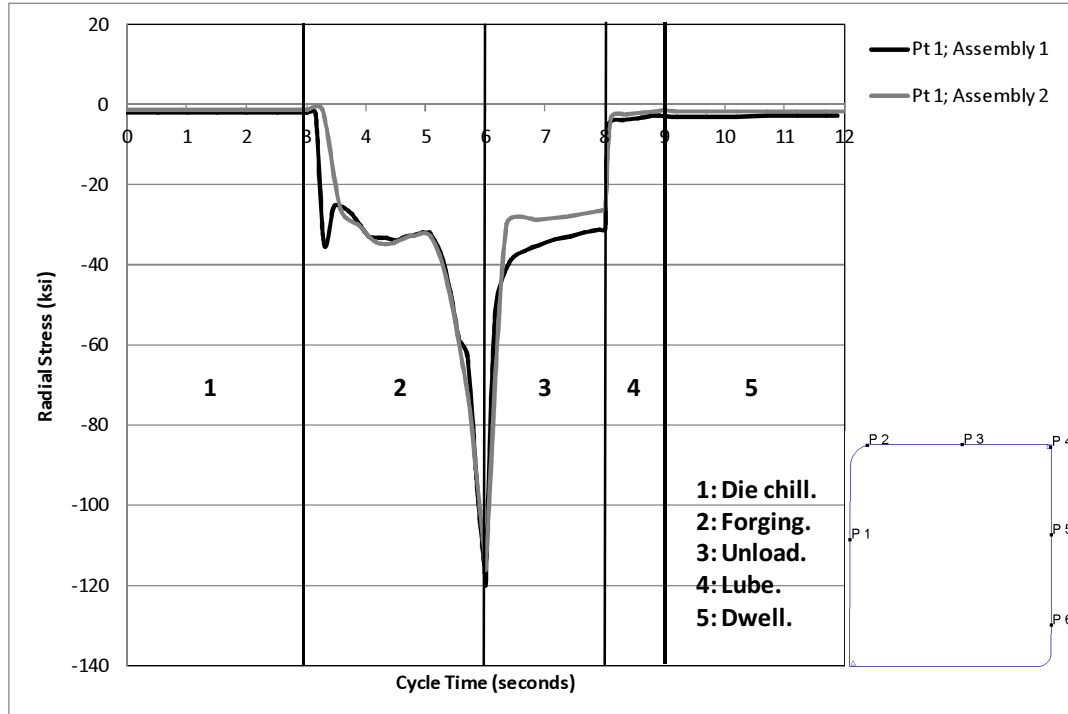
Figure 7.13: Variation of the internal pressure on the pre-stressed insert for the selected die assemblies; Assembly 1 – Room temperature; Assembly 2 – Pre-heated.

7.4.1. Die Deflections and Surface Stresses under Maximum Load

During the initial die chill phase of the forging cycle, heat transfer occurs only between the free-resting preform and the backup die. Thus, the results from this stage are not summarized. During deformation, when the heated preform contacts the upset die insert under forming pressure, the surface of the insert tends to expand from heat conduction. This expansion is resisted by the cooler die substrate, resulting in compressive stresses on the die surface layers. Due to the higher temperature gradient and thermal shock with Assembly 1 (room temperature; Figure 7.14b), the compressive hoop stresses are significantly (≈ 22%) higher than with Assembly 2 (pre-heated; Figure 7.14b). In the case of Assembly 1, the maximum thermal load occurs at ≈ 1.05 inches (≈ 27 mm) before BDC. However, with the pre-heated die (Assembly 2), the thermal shock is delayed to ≈ 0.93 inches (≈ 24 mm) before BDC (Figure 7.15).

182

a) Temperature distribution.   b) Hoop stress.

c) Shear stress.   d) Maximum principal stress.
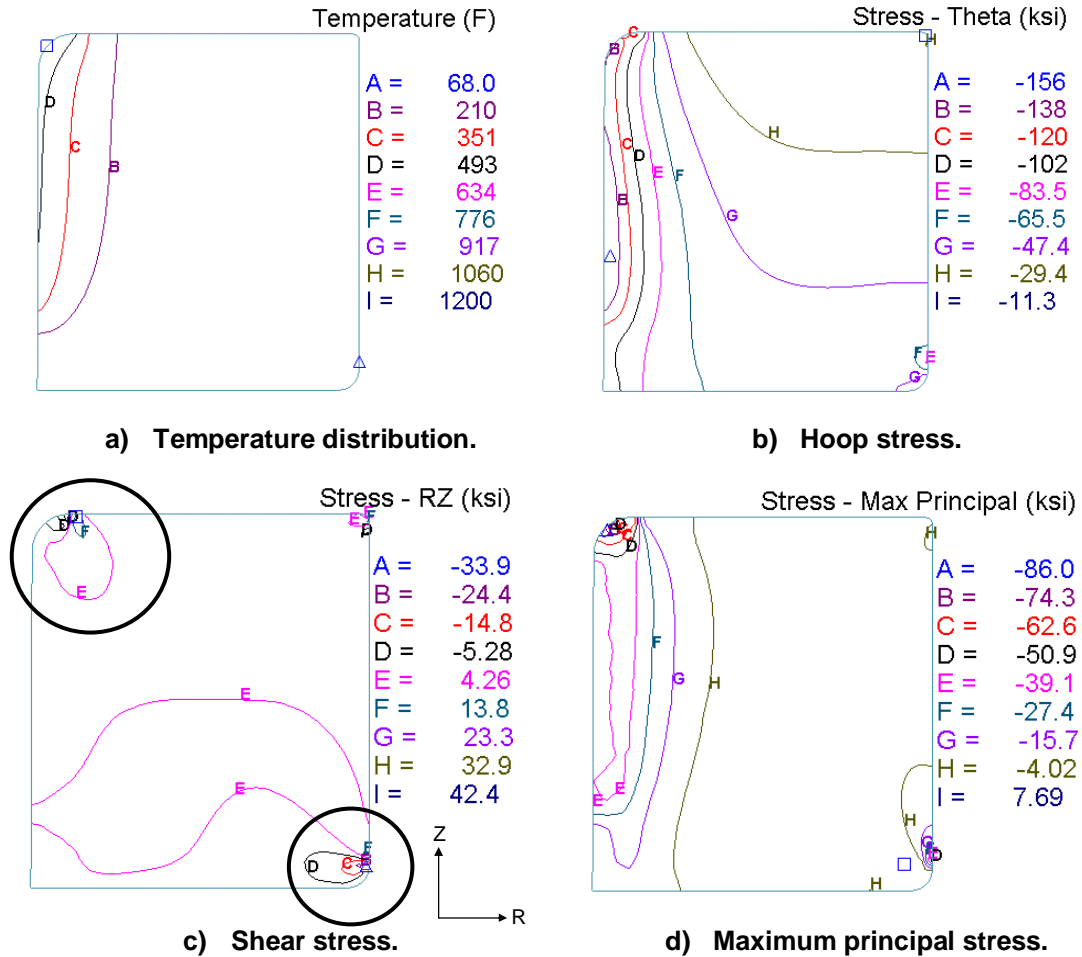
Figure 7.14: Stresses in the insert under maximum thermal load/gradient (≈ 1.05 inches from BDC) during deformation (Assembly 1).

The shear stress in the RZ plane and the maximum principal stress are also summarized in Figure 7.14 and 7.15 (c and d, respectively). The thermal shock and mechanical loading on the inner diameter of the insert result in a concentration of shear stress near the radius on the inner diameter. This can be explained by the nodal velocities (elastic deflection) of the die insert during deformation. Under maximum thermal load, the velocity vectors at the inner radius point in opposite directions resulting in a tensile shear stress (Figure 7.16a). This stress concentration was found to move radially outwards during deformation, finally occurring at the upper fillet radius on the outer diameter. As deformation progresses, the vectors align themselves along the same direction due to the forming load now being in the negative Z-direction (Figure 7.16b). Thus, under maximum mechanical load at BDC, the shear stress is concentrated at the upper fillet radius on the outer diameter of the insert (Figures 7.14c and 7.15c). The nodal velocities for the

183

pre-heated Assembly 2 are identical in trend to those for Assembly 1 (room temperature) and are, thus, not shown here.

Temperature (F)

A = 68.0
B = 210
C = 351
D = 493
E = 634
F = 776
G = 917
H = 1060
I = 1200

a) Temperature distribution.

Stress - Theta (ksi)

A = -132
B = -115
C = -97.2
D = -79.7
E = -62.2
F = -44.8
G = -27.3
H = -9.78
I = 7.71

b) Hoop stress.

Stress - RZ (ksi)

A = -20.7
B = -15.2
C = -9.75
D = -4.26
E = 1.24
F = 6.73
G = 12.2
H = 17.7
I = 23.2

c) Shear stress.

Stress - Max Principal (ksi)

A = -75.1
B = -64.7
C = -54.4
D = -44.0
E = -33.7
F = -23.3
G = -13.0
H = -2.64
I = 7.71

d) Maximum principal stress.
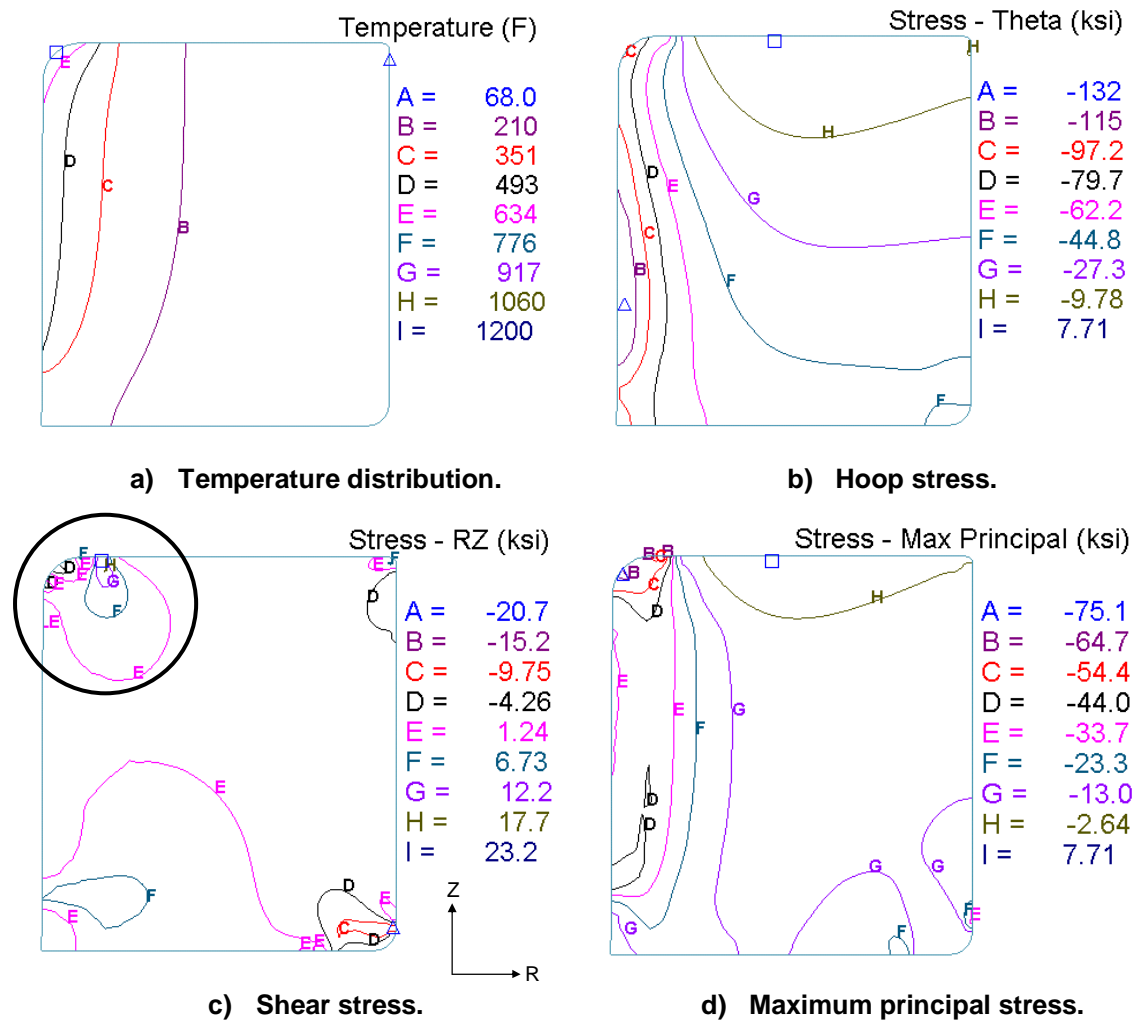
Figure 7.15: Stresses in the insert under maximum thermal load/gradient (≈ 0.93 inches from BDC) during deformation (Assembly 2; gas flame on the inside).

184

a) 1.05 inches from BDC.   b) At BDC.
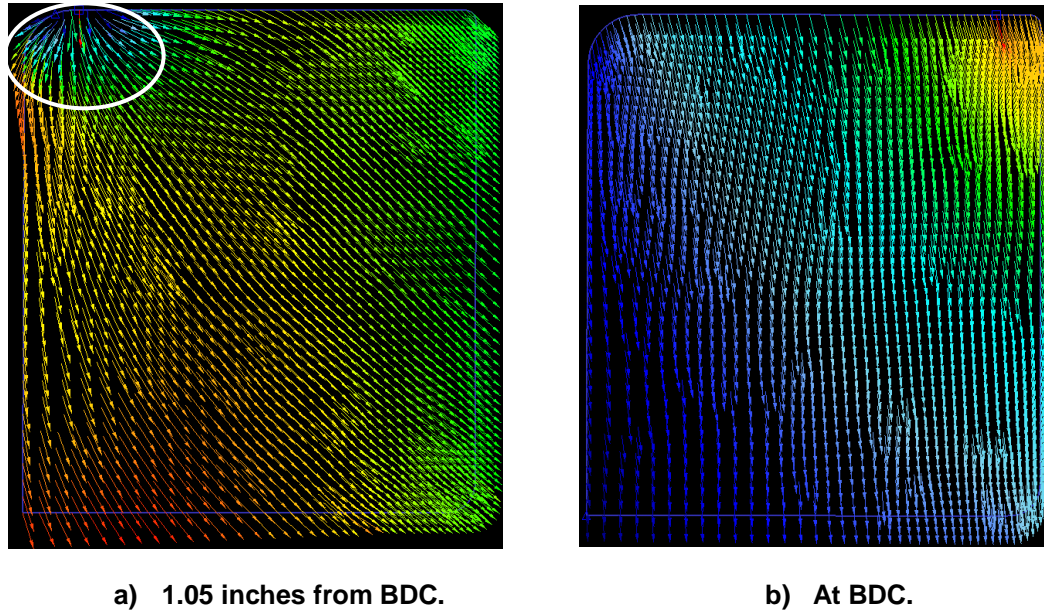
Figure 7.16: Nodal velocities (elastic deflection) of the die insert under different loading conditions during deformation (Assembly 1).

The maximum die surface temperature occurs at the end of deformation (at BDC) due to heat generation from forging and subsequent heat transfer to the die due to prolonged contact times (Figure 7.11; Figure 7.17a). Due to heat conduction, the maximum compressive stress on the die surface drops by 35-40% (Figures 7.17b and 7.18b) compared to those observed during the initial thermal shock (Figures 7.14b and 7.15b). In the case of the pre-heated assembly, these compressive stresses are ≈ 30-35% lower than those with a room temperature assembly. As explained with Figure 7.16, the maximum shear stresses around the inner diameter are observed during the initial contact and deformation of the workpiece. At the end of deformation the maximum shear stress is concentrated at the upper fillet radius on the outer diameter of the insert.

The insert in Assembly 1 is under higher compressive stress than that in the pre-heated Assembly 2. Thus, the former experiences lower elastic deflection, which is evidenced in the higher compressive stress values at BDC compared to Assembly 2 (line contours F,G and H in Figures 7.17b and 7.18b). It should be noted that the maximum compressive stress values in these results occur at the die surface and are primarily governed by the thermal loading conditions. The stresses due to mechanical loading are in the substrate/core of the insert and are influenced to a certain extent by the thermal surface stresses i.e. compressive stresses on the surface results in tensile stresses in the die core. This is one possible reason for the sub-surface

185

tensile hoop stress in the insert (Figure 7.17b and 7.18b; line contour H; ≈55% greater for Assembly 2).

a) Temperature distribution.   b) Hoop stress.
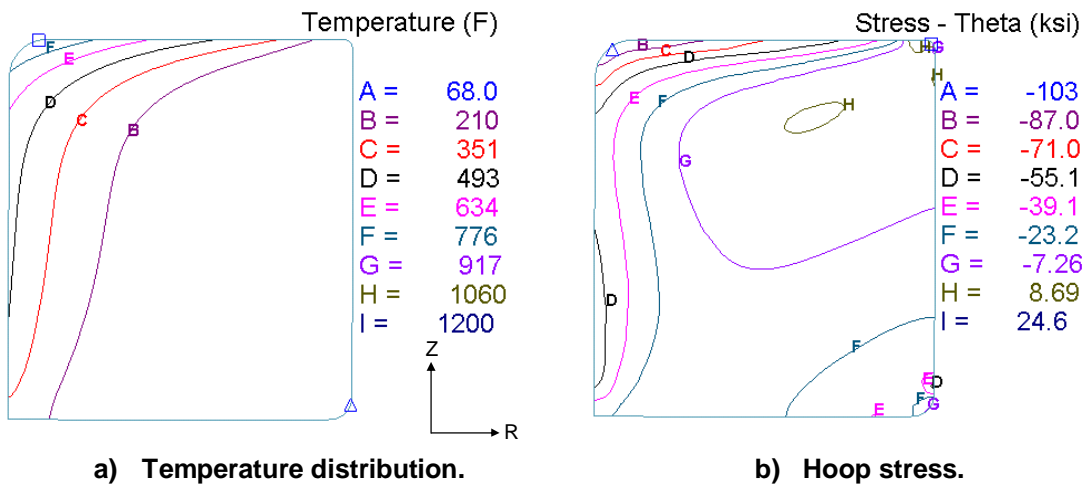
Figure 7.17: Stresses in the insert under maximum temperature and mechanical load (at BDC) during deformation (Assembly 1).

a) Temperature distribution.   b) Hoop stress.
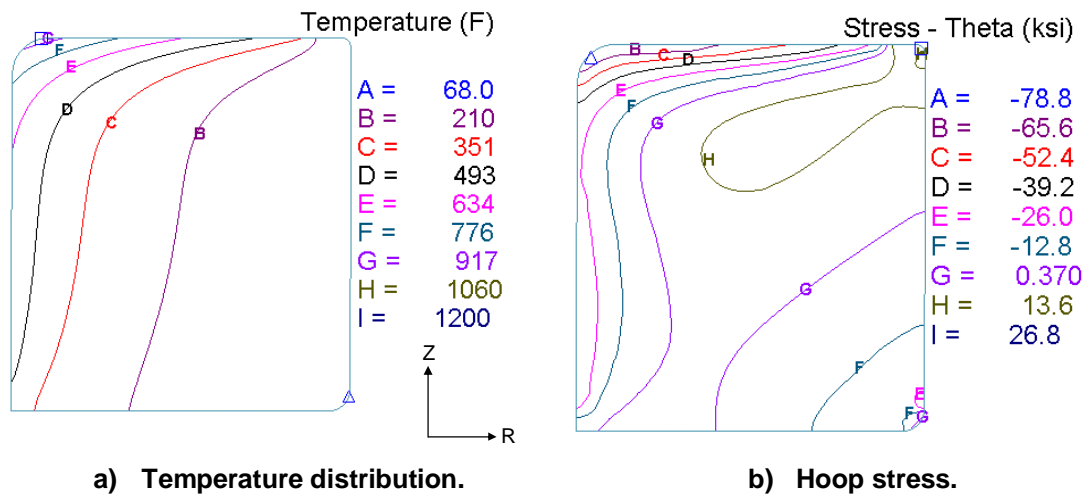
Figure 7.18: Stresses in the insert under maximum temperature and mechanical load (at BDC) during deformation (Assembly 2; gas flame on the inside).

7.4.2. *Die Deflections and Surface Stresses during Unloading and Lubrication*

The unloading simulation was conducted by reversing the movement of the top die as would normally occur in a hydraulic press. The slight dwell time expected prior to the retraction of the ram (for reversal of the hydraulic fluid flow in the ram) was not considered. However, the

186

unloading simulation accounts for the time spent by the finished part on the bottom die prior to removal (2 seconds based upon production observations by AAM).

As mentioned in the previous section, the insert in Assembly 1 deflects less than that in Assembly 2, which has been pre-heated. Thus, the "springback" from unloading is expected to be greater for Assembly 2. This is observed in the changes in the hoop stress contours of Figures 7.19 and 7.20 when the press ram retracts. The insert in Assembly 2, which showed some tensile stresses under maximum load at BDC, goes entirely into compression upon "springback". The maximum compressive stresses in both the inserts are also found to increase due to this phenomenon (≈35% for Assembly 1; ≈60% for Assembly 2). The maximum compressive stresses, as mentioned previously, are governed predominantly by thermal conditions. Thus, Assembly 1, which started off at room temperature, shows higher surface compressive stresses due to continued contact and heat transfer with the workpiece.

| a) Temperature distribution. | b) Hoop stress. |
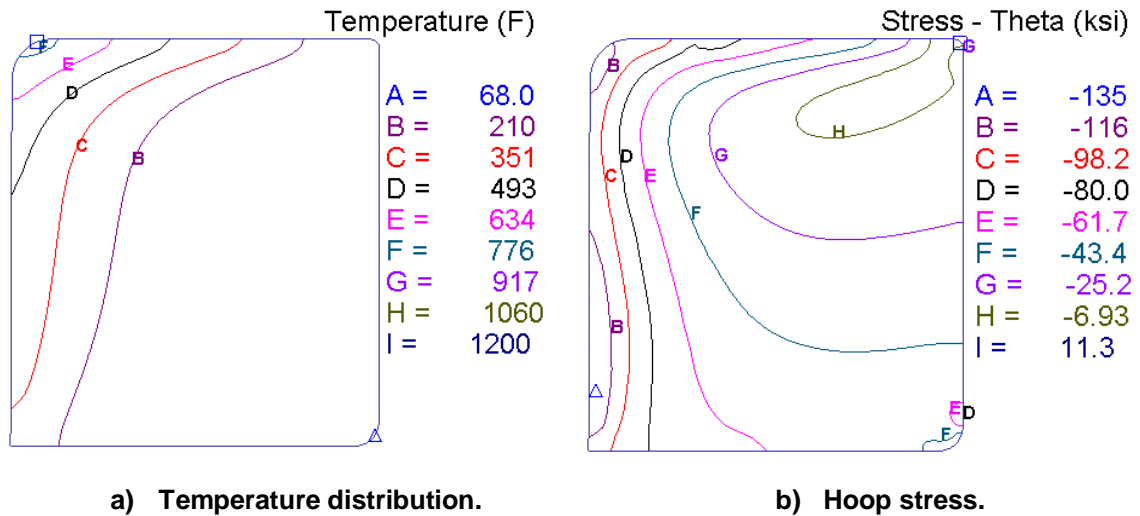
Figure 7.19: Stresses in the insert during unloading (Assembly 1).

The average stress reversal was in the range of ≈18 ksi for Assembly 1 and ≈26 ksi for Assembly 2. Thus, the latter shows 44% greater springback on unloading due to higher deflections under mechanical load. As thermal expansion increases during production, this stress reversal is expected to increase in magnitude due to loss of shrink-fit on the insert. This process results in mechanical fatigue loading of the insert and could be a possible cause of die failure.

187

a) **Temperature distribution.**   b) **Hoop stress.**
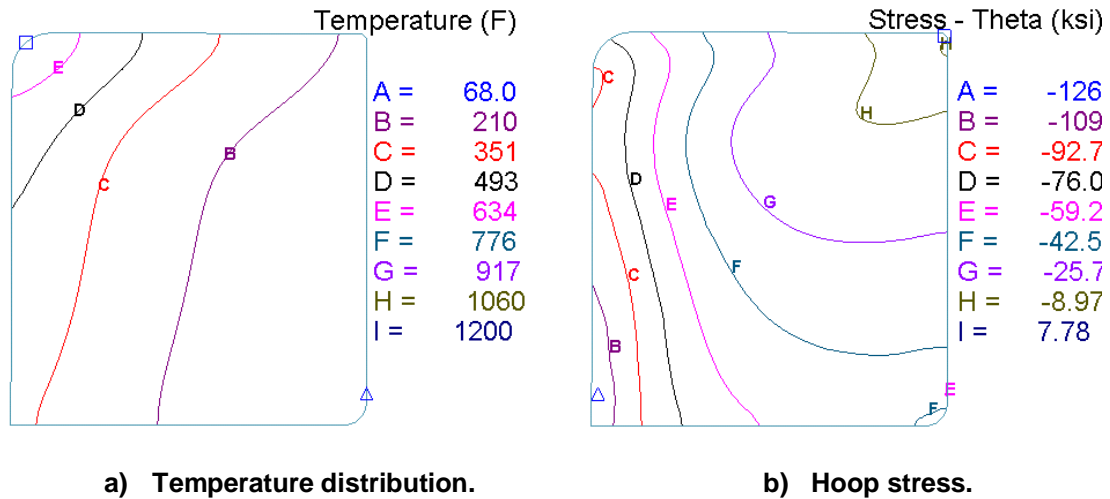
Figure 7.20: Stresses in the insert during unloading (Assembly 2; gas flame on the inside).

In the first forging stroke, the temperature gradient in the die insert in both assemblies (room temperature and pre-heated), after removal of the formed part, was not high enough to resist surface contraction when exposed to the lubricant spray. This is evident in the presence of compressive stresses on the die surface layers (Figures 7.21b and 7.22b). The increase in compressive stresses is greater (≈50-90% in the interior) for Assembly 1 due to the lower temperature and thus, less resistance to contraction of the insert surface. Assembly 2, however, shows only 10-30% increase in compressive stresses. This is because the higher insert bulk temperature resists contraction of the surface layers upon exposure to the lubricant spray. The upsetting surface in Figure 7.22b shows a tendency for going into tension with a small tensile stress at the fillet radius on the insert O.D.

It should be noted that the precise interface heat transfer coefficient is difficult to quantify due to lack of real-time die surface temperatures during the lubricant spray. The current boundary conditions are based upon calibration simulations conducted with a rough production temperature measurement used as a baseline.

188

| | |
| a) Temperature distribution. | b) Hoop stress. |
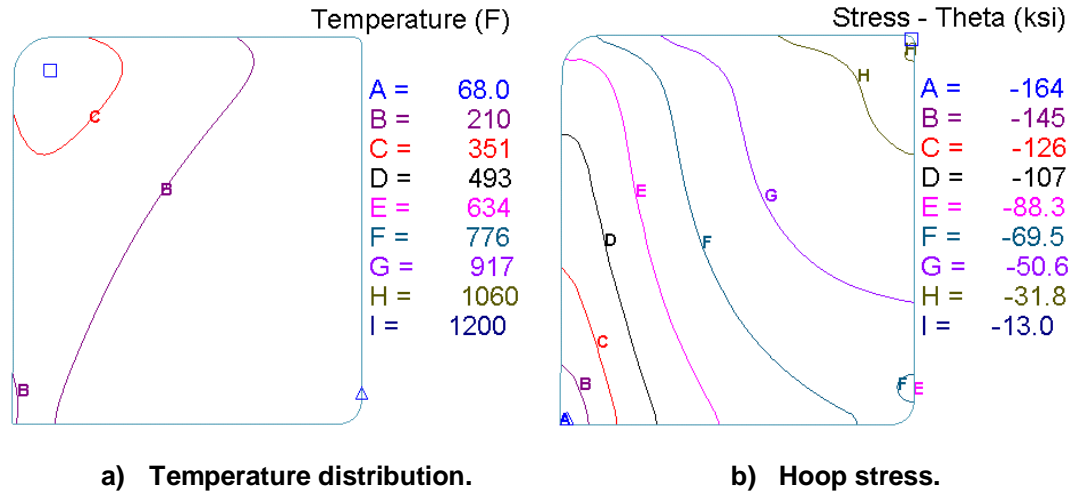
Figure 7.21: Stresses in the insert during lubrication spray (Assembly 1).

| | |
| a) Temperature distribution. | b) Hoop stress. |
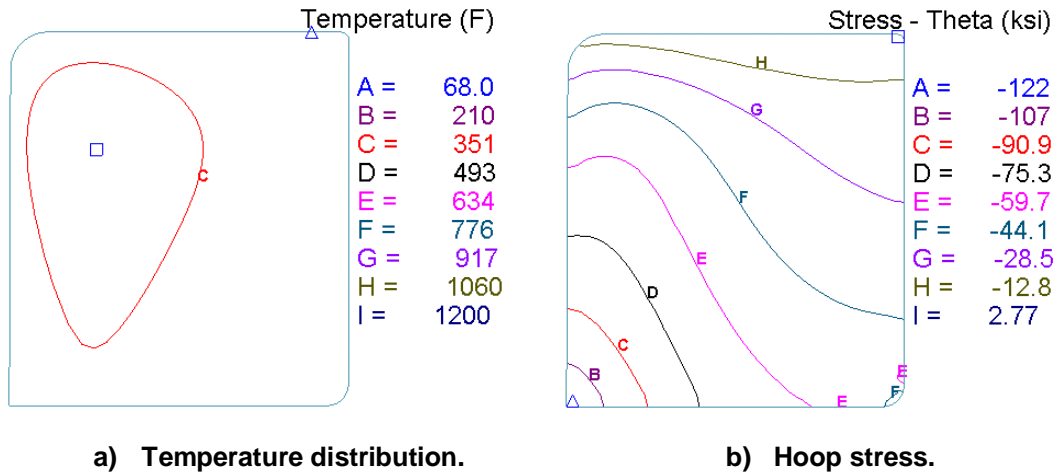
Figure 7.22: Stresses in the insert during lubrication spray (Assembly 2; gas flame on the inside).

Prior to the next forging stroke (2nd cycle), the die inserts in both the assemblies are found to be under a state of compressive pre-stress. This stress state represents the condition of the die assembly at the end of the first forging stroke. Compared to the pre-heated Assembly 2 insert, the compressive stresses are higher in the case of Assembly 1 ($\approx$ 45% in the interior; $\approx$ 80% on the surface) (Figures 7.23 and 7.24).

Assembly 2 is already at an elevated temperature due to pre-heating and is expected to reach a steady thermal cycle earlier than Assembly 1. The average insert temperature for Assembly 1 (initially room temperature; T_o = 68°F/20°C) after the first forging stroke is $\approx$ 120-200°F ($\approx$ 50-

189

90°C), whereas that for Assembly 2 is between 200-270°F (≈ 90-130°C) with a starting pre-heat temperature (T_o) in the range of 160-170°F.

Temperature (F)		Stress - Theta (ksi)	
A =	68.0	A =	-151
B =	210	B =	-135
C =	351	C =	-118
D =	493	D =	-102
E =	634	E =	-85.2
F =	776	F =	-68.8
G =	917	G =	-52.3
H =	1060	H =	-35.9
I =	1200	I =	-19.4

a) **Temperature distribution.** b) **Hoop stress.**
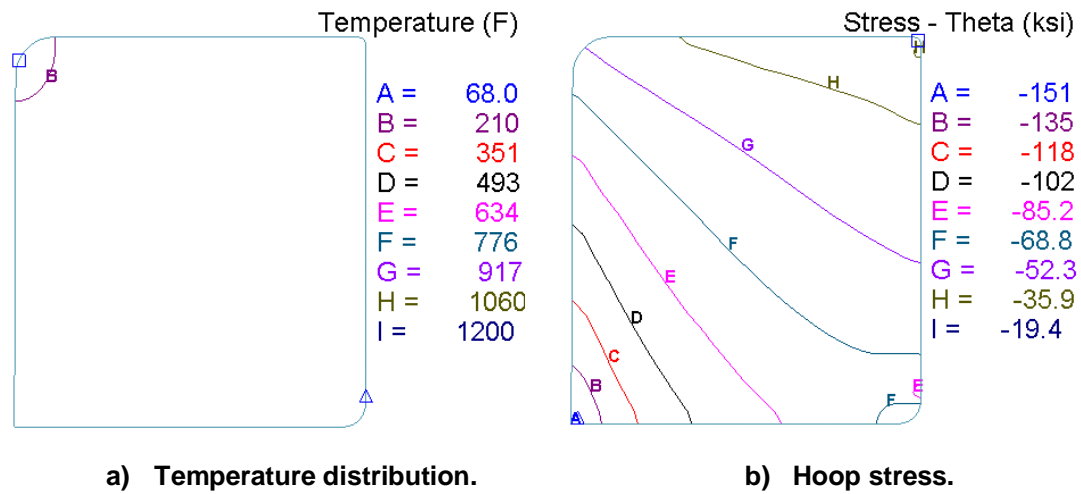
Figure 7.23: Stresses in the insert after the first forging stroke (Assembly 1).

Temperature (F)		Stress - Theta (ksi)	
A =	68.0	A =	-122
B =	210	B =	-107
C =	351	C =	-92.3
D =	493	D =	-77.7
E =	634	E =	-63.1
F =	776	F =	-48.5
G =	917	G =	-33.9
H =	1060	H =	-19.3
I =	1200	I =	-4.73

a) **Temperature distribution.** b) **Hoop stress.**
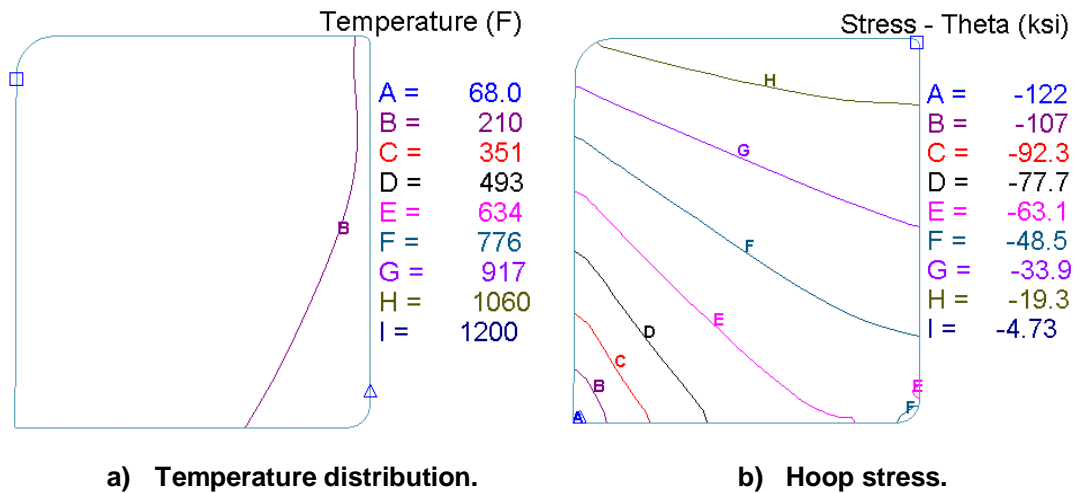
Figure 7.24: Stresses in the insert after the first forging stroke (Assembly 2; gas flame on the inside).

The stress states discussed in the previous sections are a combination of thermal and mechanical stresses as a result of the loading conditions. In order to separate the mechanical stresses, the hoop and radial stresses on the outer diameter of the insert were tracked during the entire forging cycle. These parameters are a real-time measure of the compressive pre-stress and external pressure on the insert, respectively, during deformation.

190
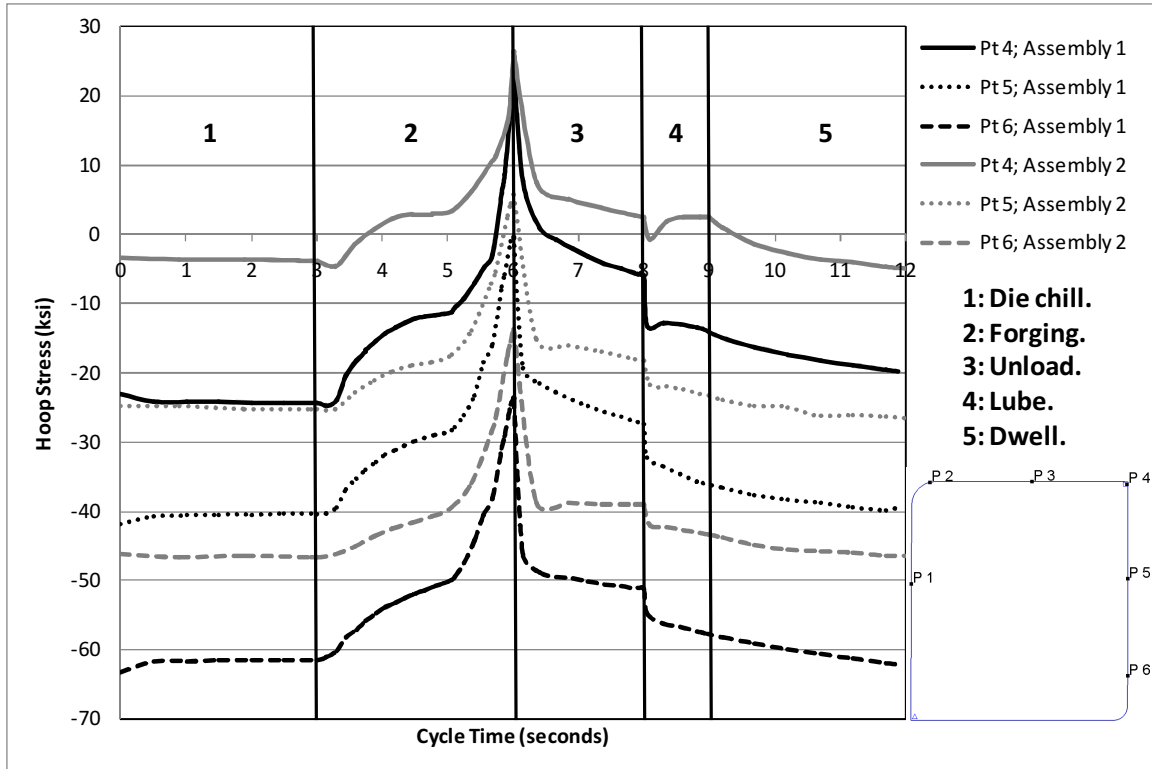
Figure 7.25: Variation of the hoop stress on the outer diameter of the insert during the forging cycle.

The variation in the hoop stress follows a pattern similar to that of the thermal cycle on the die surface (Figure 7.11) with 5 distinct regions corresponding to the 5 stage forging cycle simulated:

- Stage 1: During the die-chill stage there is no change in the compressive pre-stress from the assembly and heating process. Assembly 2 has a low value of compressive pre-stress due to thermal expansion from pre-heating (Figure 7.24).

- Stage 2: As the lead die contacts the preform and deformation begins, the insert is subjected to internal pressure resulting in tensile hoop stresses, which are expected to be counteracted by the shrink-fit in the die assembly. As seen in Figure 7.24, the compressive stresses in the pre-heated die (Assembly 2) are lower (i.e. tending towards tensile) than those in the room temperature one (Assembly 1). The region around point 4 (fillet radius on O.D.) on both assemblies experiences tensile hoop stresses.

191

- Stage 3: Upon unloading, the insert in Assembly 2 springs back more than that in Assembly 1. This is seen in the drastic drop in the maximum hoop stress at BDC (Figure 7.24). This process could be a possible cause of die failure due to mechanical fatigue.

- Stage 4: Due to cooling during the lubrication spray, as well as conduction to neighboring die components, the compressive stresses in the insert start to increase again. This increase is greater in the room temperature die (Assembly 1) due to greater temperature differential between the heated insert and room temperature components (Figure 7.24).

- Stage 5: During the dwell time prior to the next forging stroke, a further increase in compressive stresses is observed. As seen in Figure 7.24, the insert returns to its original stress state on the outer diameter after the first forging stroke.

Along with the variation in hoop stress, the change in radial pressure on the insert O.D. directly characterizes the shrink-fit during the forging cycle (Figure 7.25). The significant observations were as follows:

- Stage 2: Due to a lack of thermal expansion, the room temperature insert (Assembly 1) is subjected to 15-20% greater radial pressure on the O.D during deformation.

- Stage 3: The pre-heated assembly experiences greater springback than the room temperature assembly as seen in the drop in external pressure.

192
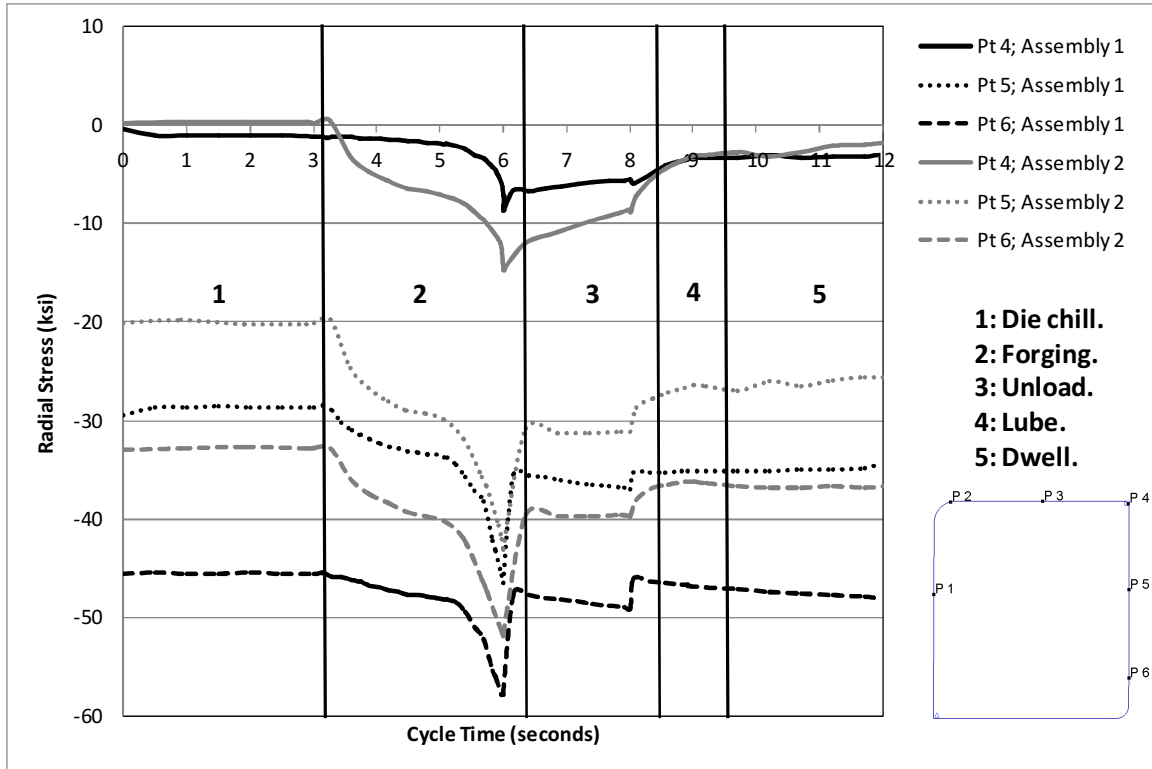
Figure 7.26: Variation of the radial stress (external pressure) on the outer diameter of the insert during the first forging cycle.

7.5. Analysis of Thermo-Mechanical Loading during Steady-state

As explained in Figure 5-6 (Chapter 5; schematic of temperature evolution in multiple cycles), the die temperature increases at the start of each consecutive forging cycle, starting with an initial temperature (T_o; either ambient or pre-heat). This temperature increase continues until a steady temperature differential is reached between the maximum and minimum recorded temperatures in successive forging cycles (Figure 7.27). In the case of a pre-heated assembly, this steady-state is reached earlier than with a room temperature assembly (Figure 7.27).

193
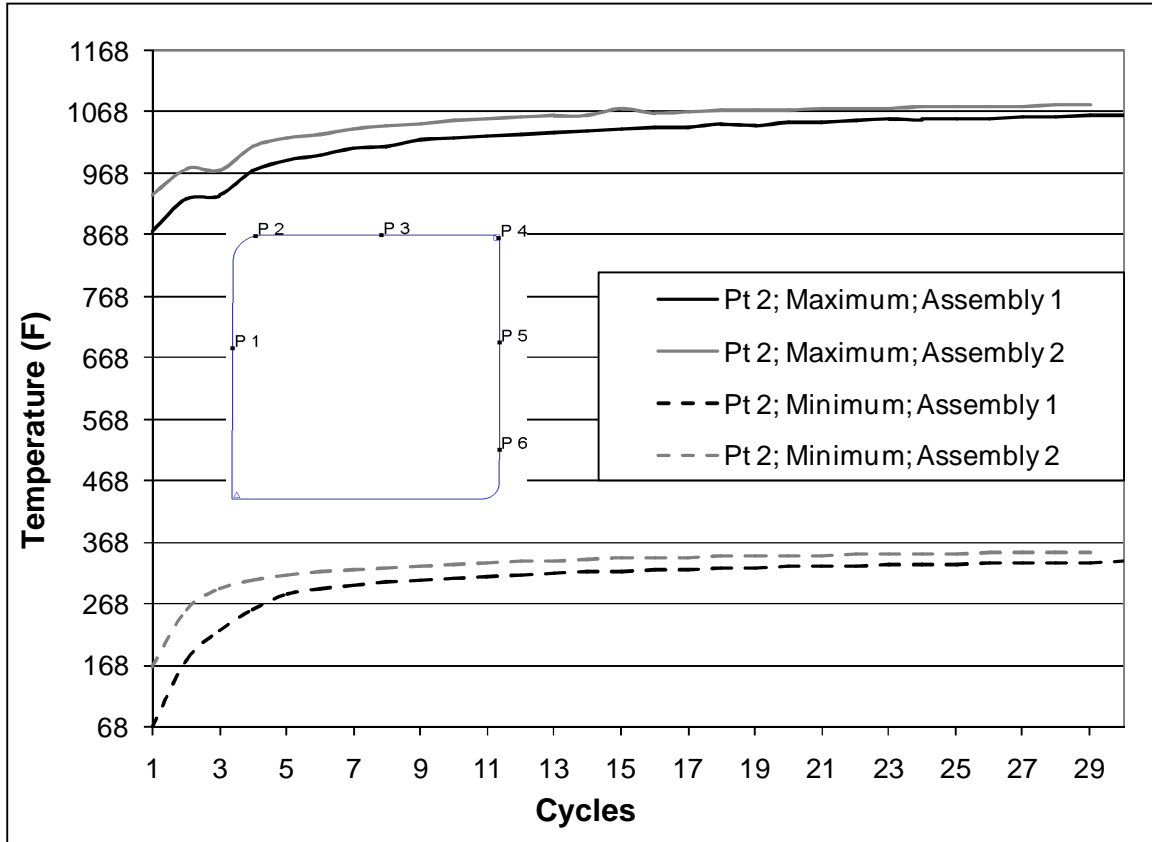
Figure 7.27: Evolution of the temperature range at the location of maximum surface temperature (point 2) over multiple forging cycles.

The biggest difference in the two die assemblies occurs in the first few forging cycles, where the room temperature assembly (Assembly 1; $T_o = 68°F/20°C$) experiences higher heat-transfer (and thermal shock) upon contact with the heated preform. Figure 7.28 compares the temperature increase between each successive forging cycle as well as that compared to the initial starting temperature (T_o). An average of the surface temperatures (before each forging cycle) at points 1, 2 and 3 on the insert was used for calculations. Assembly 1 shows a 180% increase in the surface temperature at the start of the second forging cycle due to the significant heat-exchange in the first cycle. The corresponding increase for the pre-heated assembly (Assembly 2; $T_o \approx$ 170°F/80°C) is around 55-60%. In subsequent forging cycles this temperature increase drops off for both assemblies, with Assembly 2 reaching a steady-state temperature range earlier in the production cycle. The steady-state die assembly temperatures at the start of each forging cycle are shown in Figure 7.29.

194
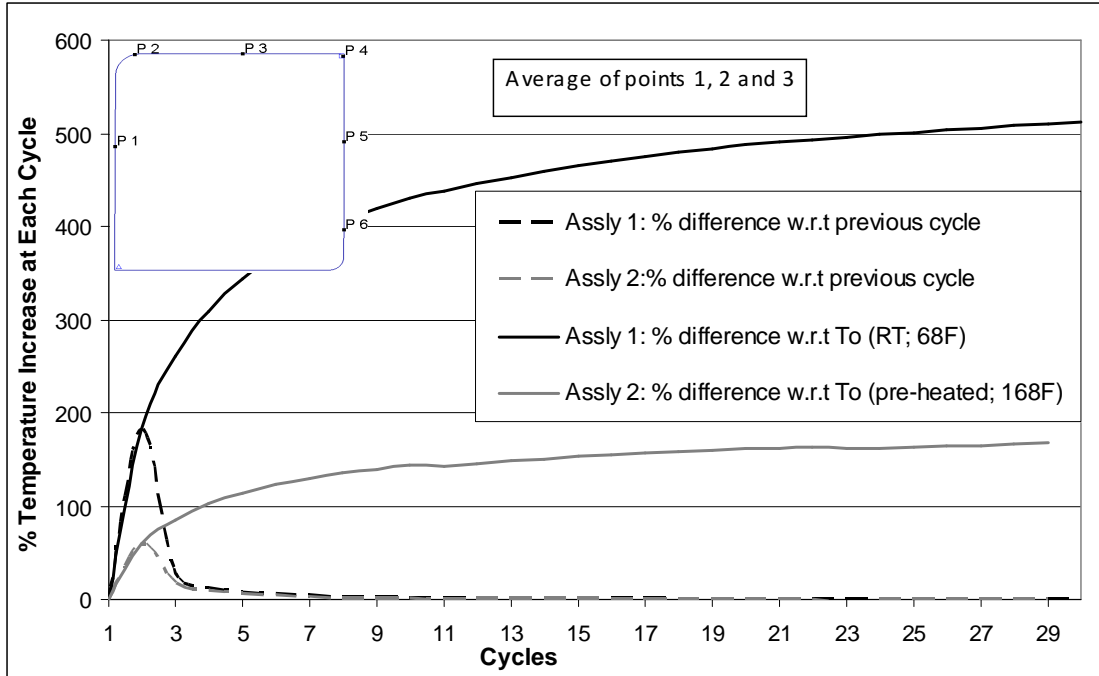
Figure 7.28: Evolution of the die insert temperature before each forging cycle (average of points 1, 2 and 3; T_o – initial die temperature, ambient or pre-heat).

a) Assembly 1 ($T_o = 68°F/20°C$).   **b) Assembly 2 ($T_o ≈ 170°F/80°C$).**
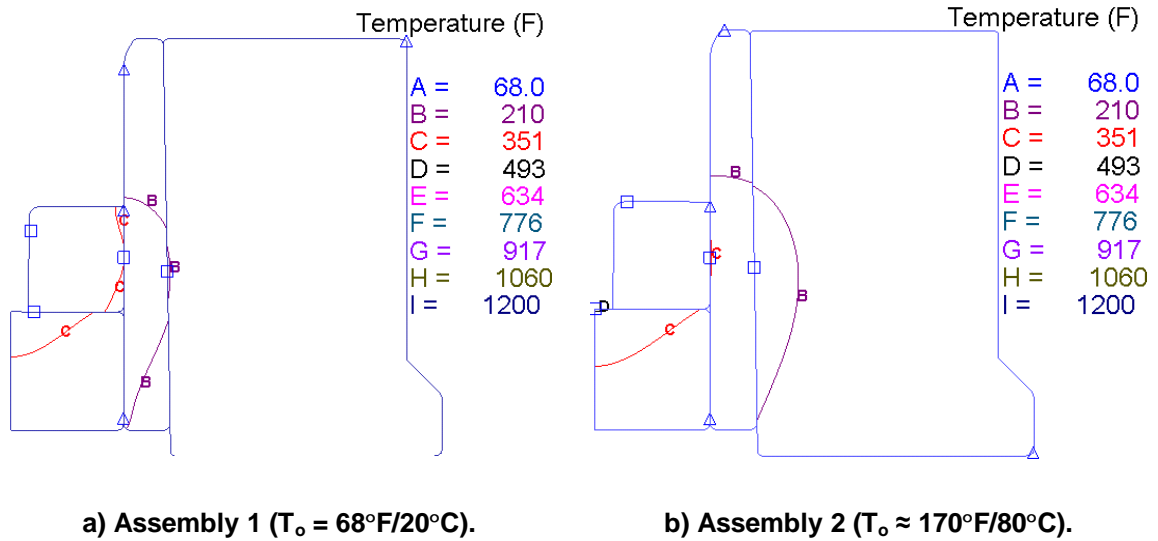
Figure 7.29: Temperature of the die assembly during steady-state production.

The multiple cycle analysis was conducted in order to determine the temperature distribution and corresponding die stresses under a steady-state of production. This process was conducted for

195

both the selected die assembly conditions i.e. room temperature (Assembly 1) and pre-heated (Assembly 2). The following observations were made:

- Both die assemblies can be assumed to have reached a steady-state of temperature variation after ≈ 15-20 forging cycles. The longer contact times in hydraulic presses result in the die assembly reaching steady-state earlier than in a mechanical press. Assembly 2, which was pre-heated, reached a steady-state earlier than the room temperature assembly. The maximum temperature increase occurred in the first 5-6 cycles, with the room temperature assembly showing a larger increase due to greater heat transfer.

- Under steady-state conditions, the surface compressive stresses, which are governed by the thermal gradients, are 50 % lower for both assemblies compared to the first forging cycle. Due to thermal expansion of the tooling, the inserts in both assemblies are primarily under a tensile stress state during the deformation stage (Figure 7.30). Assembly 2 (pre-heated) shows 50-60% greater tensile stresses under maximum forging load than Assembly 1 (initially room temperature).

	Stress - Theta (ksi)		Stress - Theta (ksi)
A =	-66.3	A =	-59.5
B =	-51.4	B =	-41.7
C =	-36.6	C =	-23.9
D =	-21.7	D =	-6.09
E =	-6.82	E =	11.7
F =	8.05	F =	29.5
G =	22.9	G =	47.3
H =	37.8	H =	65.1
I =	52.7	I =	82.9

a) Assembly 1 (BDC).   **b) Assembly 2 (BDC).**
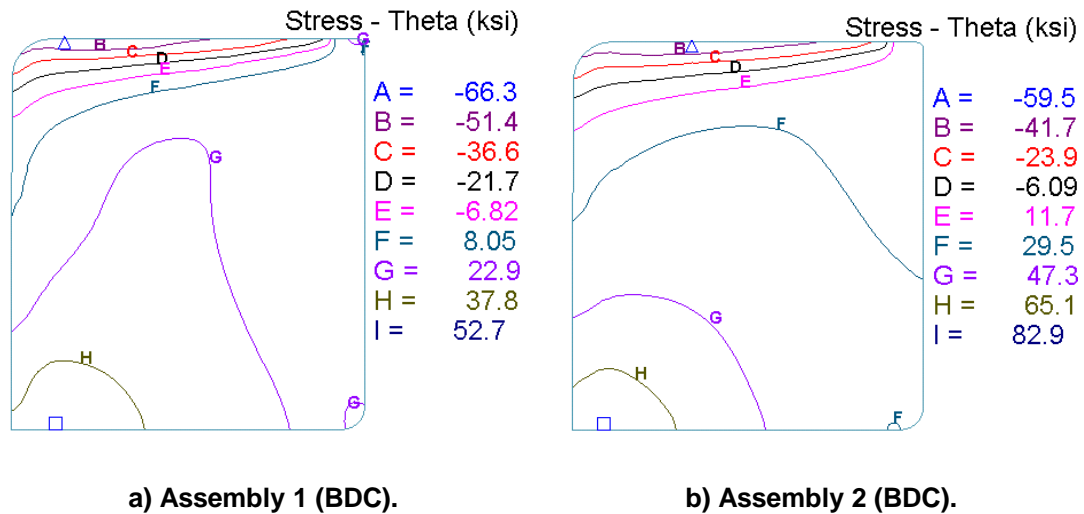
Figure 7.30: Hoop stress in the two selected cases under maximum mechanical load at BDC.

- Due to greater thermal expansion in Assembly 2, the die insert deflects more under mechanical load during deformation. Thus, ≈ 33% greater springback is observed in Assembly 2 upon unloading. The stress reversal in both assemblies under steady state is 110-120% greater than the respective values in the first forging cycle and could contribute to die failure due to mechanical fatigue.

- No significant tensile stresses were observed on the die surface during the lubrication spray. This is due to the high thermal conductivity and low thermal expansion of the carbide grade. The upsetting surface was, however, subjected to tensile stresses unlike the first forging cycle where the insert was completely under compression due to contraction.

- Under steady-state conditions the average die temperature was in the range of 350-450°F, with the initially pre-heated insert (Assembly 2) having a ≈12% higher value than Assembly 1.

7.6.   Summary and Recommendations

Carbide inserts were found to be suited for the warm upsetting operation. A detailed analysis was conducted to determine the effect of dimensional tolerances, pre-heating techniques, and temperature distribution during forging, on the compressive pre-stress and surface stress amplitudes experienced by the carbide insert. The following research objectives and results were accomplished using this analysis:

- A sensitivity analysis showed that the compressive pre-stress on the insert is directly proportional, with a linear relationship, to the draft angle on the container I.D.

- Thermal expansion during forging resulted in complete loss of shrink-fit on the insert under maximum forging load at BDC. The resulting tensile stresses (hoop and shear), however, were not in the vicinity of the failure limits of carbide.

- Due to thermal expansion, pre-heating increases the springback in the carbide insert during unloading compared to one put into operation at room temperature (44% greater at start-up and 33% greater at steady-state). The magnitude of springback increases by 100-120% from start-up to steady-state.

- The stress-analysis procedures outlined in this chapter predict mechanical fatigue as a possible cause of failure due to the loss of compressive pre-stress on the insert. The loss of external pressure and hoop stress forms the lower bound for the correction required on the shrink-fit values.

The following recommendations were made on the basis of the above observations:

- Die design: A dimensional interference needs to be incorporated at the insert-sleeve interface in order to reduce the dominant effect of dimensional variation at the sleeve-

197

container interface during assembly and pre-heating. The shrink-fit values should include a correction for thermal expansion predicted by FEA.

- Die assembly and pre-heating: The use of a single sleeve-container combination is crucial to ensure consistent application of the compressive pre-stress on the carbide or ceramic insert. Pre-heating should be done in the press using a gas flame or electric heater on the inside.

- Forging: The recommendations made in Chapter 6 for reduction of contact time apply here as well.

- Lubrication: Reduction of the thermal shock is crucial when using carbide or ceramic inserts. The cooling rate can be reduced by programming the lubrication system to spray air on the die surface prior to spraying the lubricant.

198

CHAPTER 8

CASE STUDY 4 – APPLICATION OF MATRIX HIGH-SPEED STEELS (MHSS) IN WARM EXTRUSION ON A MECHANICAL PRESS

8.1. Problem Statement

Forward extrusion is characterized by high sliding velocities and temperature generation, which depend upon the area reduction designed into the die. The lower forging temperature of warm extrusion also results in high normal pressure on the die corner radius where the reduction is being carried out. Thus, the primary failure mode in this process is commonly abrasive wear at the radius where maximum reduction is carried out. As a result, the parts are out of dimensional specifications.

An example warm extrusion process for an automotive pinion was selected for improvement of die life through application of the computational techniques developed in this study. The dies consist of hot-work tool steel inserts press-fitted into steel containment rings. The forging process is carried out in an automated forging cell consisting of a pre-coating bath, induction heater, and a mechanical forging press (4 stations) with an automated part transfer and lubrication system (Figure 8.1).
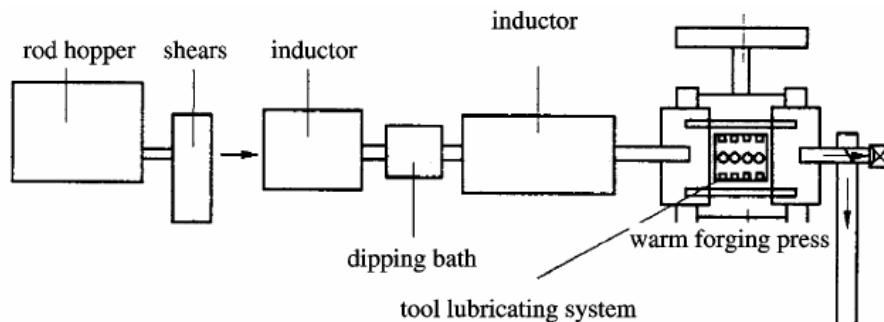
Figure 8.1: Schematic of the forging cell set-up [Sheljaskov et al, 2001].

The part is forged in three steps starting from the 2nd press station. The 1st press station acts as a staging area for the billet and was designed into the press as a buster location. For the current process, the billet simply rests on the 1st press station until it is transferred to the 2nd press station for the start of the deformation sequence. The forging sequence is as follows:

1. Billet pre-heating: The steel billets are pre-heated to 100-150ºC (300ºF) for pre-coating.

2. Billet pre-coating: As is commonly done in warm forging, the billets are pre-coated with graphite to prevent de-carburization and scale formation. This coating also acts as an additional lubricant in the first extrusion stage.

3. Induction heating: The billets are induction heated to the warm forging temperature of 960-980ºC (1760-1800ºF).

4. Station 1: Billets exiting the heater are transferred by a robotic arm to the 1st press station where no deformation is carried out. The billet simply rests for one forging stroke before being transferred to the 2nd press station.

5. Station 2: The 2nd press station is the 1st extrusion/forging station where a majority of the deformation is carried out to form the pinion stem. This die consists of three reductions as shown in the schematic of Figure 8.2. The maximum die wear occurs at the first reduction, which has the highest extrusion ratio of the three. Production stoppages and die changes are dictated by this station and specifically by Insert 2, which contains the different reductions.

6. Station 3: The extruded preform is transferred to the 3rd press station (2nd forging station) where the head of the pinion is formed.

7. Station 4: This station is used only for final calibration and for forging the center. The forged part is then cooled at a controlled rate.

The total cycle time for each part is 6.5 seconds, with all process cycle-times and forging loads being available from the press data acquisition (DAQ) system. This study was conducted in cooperation with Hirschvogel, Columbus, OH. Previous production trials with some of the other newly developed hot-work tool steels did not result in significant improvements in die life. Thus, there is a need to develop a modeling technique for analysis of the interface conditions in order to select and compare alternative die materials and process designs.

200
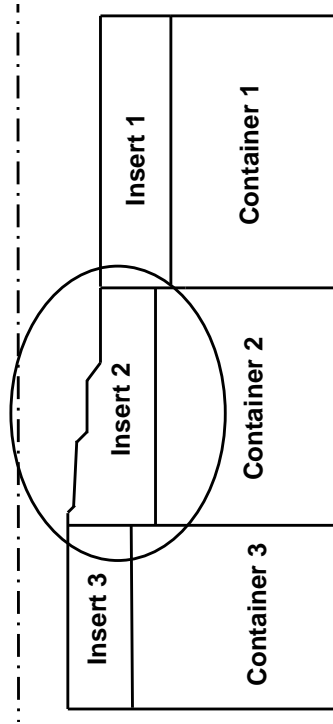
Figure 8.2: Schematic representation of the 2nd press station (1st extrusion station).

8.2. Objectives

The overall objective of this study was to reduce die wear in the warm forward extrusion process of an automotive pinion. The specific research objectives addressed through this study were:

- Determination of interface conditions in the extrusion process at start-up and under steady-state production.

- Determination of lubrication boundary conditions through an FEA-based calibration process.

- Design of shrink-fit dies for warm forging taking into account the loss of shrink-fit from thermal expansion of the die assembly under steady-state production conditions.

- Selection and comparison of alternative die materials and process designs for improved wear resistance over the existing process.

201

8.3. Determination of Interface Conditions in the Existing Process

In order to analyze the existing process, data related to cycle-times, billet temperatures and forging loads, was gathered during a production run. As in previous case studies (Chapters 5 through 7), each forging cycle was split into its discrete process steps to account for die chill, deformation, dwell and lubrication times as well as corresponding heat-transfer conditions. Following is a summary of the data collected (refer mechanical press process cycle in Figure 5.2):

- Billet temperature: Recorded as 960-980°C (≈1800⁰F) at the heater exit.

- Part location time ($t_o - t_a$): Time from billet exit to location in the 1st extrusion die; ≈ 13 second exposure to air.

- Die chill time ($t_a - t_1$): Time from press activation until top die contacts the billet ≈ 1.15 seconds.

- Deformation time ($t_1 - t_c$): Determined from press kinematics to be 0.952 seconds for ram movement starting from TDC through deformation and back to TDC (one revolution).

- Knockout and part removal time ($t_c - t_e$): Estimated to be ≈ 1.88 seconds.

- Lube spray time ($t_e - t_f$): A 1 second spray time followed by 1.5 second dwell till the start of the next cycle.

- Total cycle time for one part ($t_a - t_f$): 6.5 seconds.

- Forging load for 2nd die station (1st extrusion station): Recorded from press DAQ as 250 tons.

- Die surface temperature at steady-state: Recorded on the die surface at the first diameter reduction (1st extrusion station) as 80-90°C (170-196°F). Temperatures were recorded with a contact thermocouple after stopping the press.

In the current process, dies enter service at room temperature. Thus, the FE analysis covers only the die assembly and forging processes, with the die heating occurring only through heat-transfer during deformation.

202

8.3.1. Analysis of Die Assembly

The die assembly in the current process consists of multiple components, with the critical ones being shown in Figure 8.2. The insert container assemblies are held in a die case. Additionally, the punch, knockout pin and other auxiliary components are not shown. As mentioned earlier, the inserts are assembled into the containers using a press-fit method on a hydraulic press (explained in Chapter 6). The insert-container interface utilizes draft angles for self-centering and locking. Thus, the die insert is in a compressive state of (hoop) stress (container in tension) when the die is put into service at room temperature. The die assembly process was modeled for Inserts 1 and 2 using an incremental simulation process as described in Chapter 6. The Insert 3 sub-assembly was considered as a monolithic design since this insert is not critical for analysis of interface conditions. All objects were modeled as elastic, with nominal geometries from engineering drawings, using dimensions specified prior to press-fitting. Since Insert 2 is the tool component of interest, results of this study are presented for this sub-assembly. Figure 8.3 shows the points on the insert surface, which were selected for tracking various state-variables. Points 1 through 6 on the surface were selected to track interface temperature, contact time, sliding velocity, etc. whereas points 7 through 9 were meant for tracking the pressure at the insert-container interface as a measure of the compressive pre-stress. Points 1 through 7 (shown in the inset) through the depth of the die surface in the region of point 2, were for analysis of the temperature gradient and other state variables in this location. This was based on the production observation that point 2 is the region of maximum die wear, since the greatest reduction (≈ 47%) occurs at this point (remaining two being ≈ 40% and ≈ 18%).
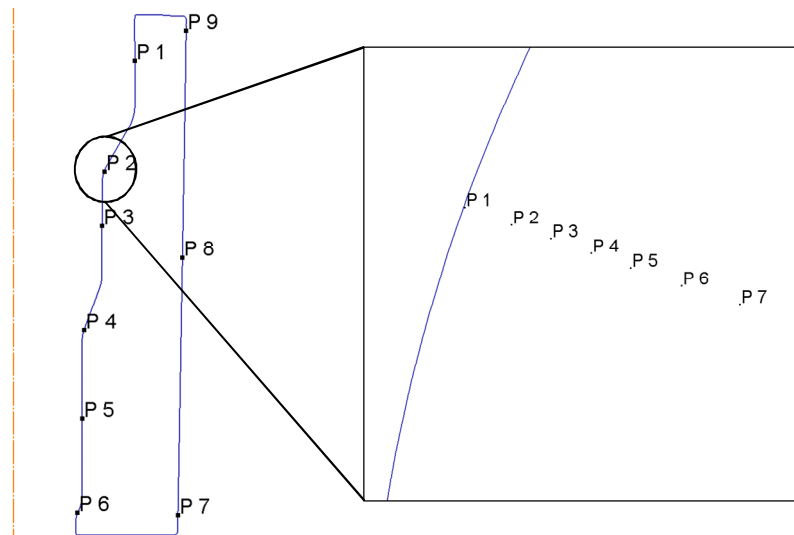
Figure 8.3: Locations selected for tracking state-variables during FE analysis.

203

The insert can be considered as a cylindrical shell with external (radial) pressure acting on it as a result of press-fitting. The assembly process, therefore, puts the insert into compressive pre-stress and the container into tension (Figure 8.4). The room temperature yield strength of the existing (H13 variant; approximated by W303™ from Böhler-Uddeholm) tool steel, heat-treated to 58 HRC, is estimated to be in the region of 1400 MPa (200 ksi). It should be noted that the maximum compressive stress values occur at isolated nodal locations and are, thus, numerical errors caused by element distortion and contact problems. The maximum compressive stress in the insert was found to be in range of 900-1000 MPa (130-145 ksi). The changes in this compressive stress were estimated by tracking the changes in the external (radial) pressure acting on the insert during forging. The models from the die assembly simulation were put together as a full tool assembly and used in the forging process simulations. Thus, all the state variable history from assembly is carried forward into the next stage.

| a) Insert 2: Sub-assembly. | b) Insert 2: Stress Distribution |
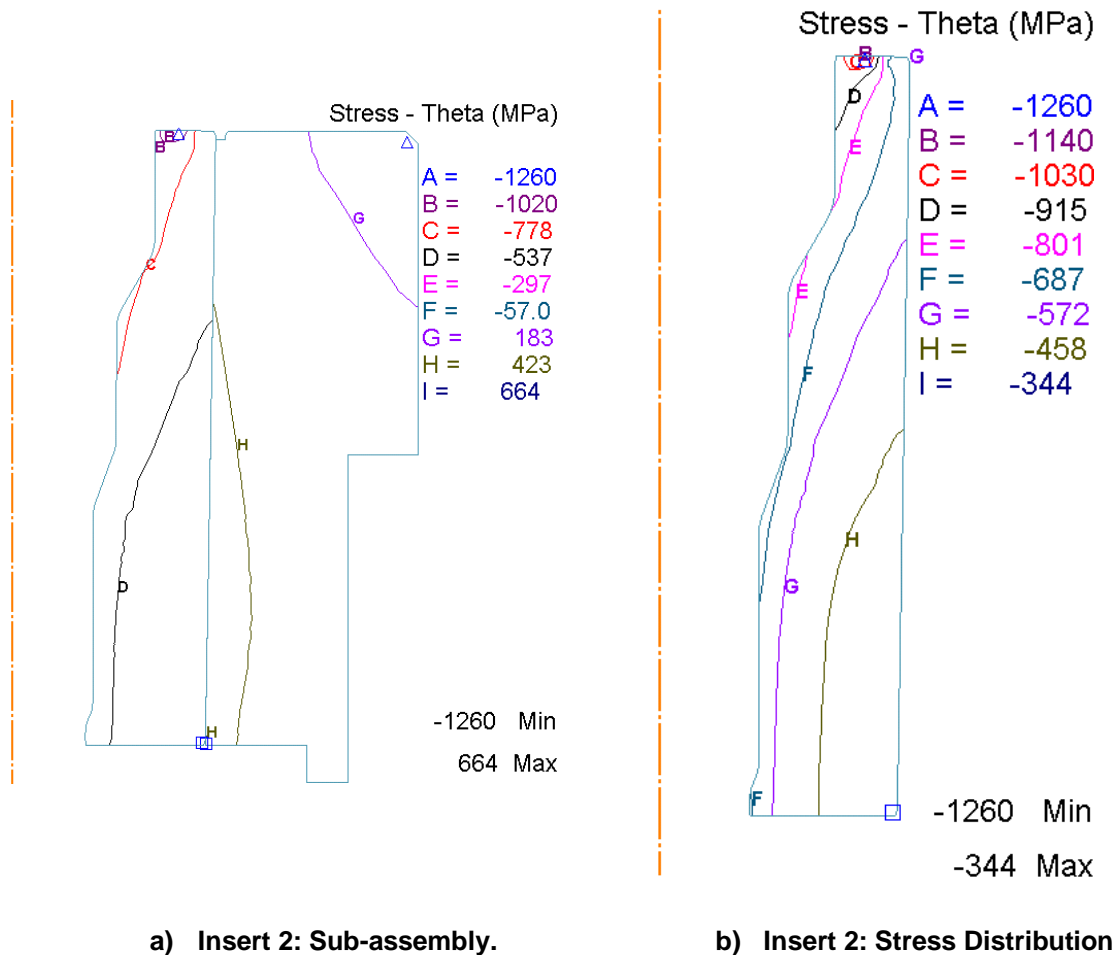
Figure 8.4: Compressive pre-stress in Insert 2 after room temperature die assembly.

204

8.3.2. Analysis of Forging: Start-up and Steady-State Conditions

The process data gathered during production was used as input for analysis of the start-up and steady-state conditions. The die assembly was modeled as rigid for FEA of the forging process. The forging simulation consisted of die chill, deformation, dwell (knockout and part removal), and lubrication stages with cycle-times provided earlier.

Temperature (C)

A = 899
B = 907
C = 916
D = 925
E = 933
F = 942
G = 950
H = 959
I = 968

899 Min
968 Max
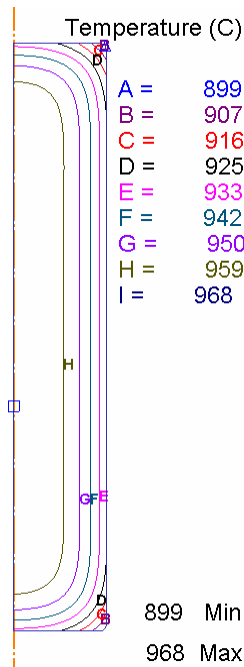
Figure 8.5: Billet temperature distribution prior to extrusion.

Material properties for the steel billet (elevated temperatures and at different strain-rates) were obtained from the DEFORM™ database. The billet is exposed to ambient conditions for 13 seconds prior to being placed in the 1st extrusion die. Due to the use of a billet pre-coat, it is expected that the temperature distribution in the billet would be maintained in this duration. However, in order to estimate the effect of this change in interface conditions and forging loads, a simulation was conducted to account for heat-transfer between the billet and the environment under conditions of natural convection. The resulting billet with a non-uniform temperature distribution (Figure 8.5) was used as the input workpiece for a forging simulation for comparison with a biller having uniform temperature. It was found that the maximum die surface temperature at point 2 increased by 5-7% accompanied by a 10% increase in forging load due to the sensitivity of the flow stress (billet material) to temperature. The forging load with a uniform billet temperature was in the range of 235-240 tons, whereas that with a temperature gradient was

205

between 245-250 tons. The press DAQ measured a load of 250 tons for the first extrusion station at start-up. Thus, it was decided to use a billet with non-uniform temperature distribution for the forging analysis.

Based on previous case studies, the default interface heat-transfer conditions (forging and free-resting) from DEFORM™ were found to give accurate results. The same was true for the interface friction conditions, which are based upon experimental data (ring compression tests). Thus, a preliminary simulation was conducted with default values for friction and interface heat-transfer, and a convection coefficient of 30 kW/m^2-K (based on literature and simulations conducted for the reverse piston; Chapter 5). The insert temperature distribution at different stages of the start-up cycle is shown in Figure 8.6. Starting at room temperature, a maximum temperature increase of 510°C (950°F) was observed, at BDC, on the die corner radius of the first reduction (point 2; Figure 8.3). A 60% drop in maximum temperature occurred during press ram retraction from BDC to TDC, during which time the workpiece rests on the die. Lubrication was predicted to result in a 70-80% reduction of the die surface temperature (knockout and part removal were simulated but results are not shown). Prior to the next forging stroke (2nd stroke), the die surface temperature was predicted to have a temperature rise of 150% over the ambient starting temperature.

However, the previous case studies were characterized by upsetting type of metal flow with relatively little relative sliding and a thermal fatigue die failure mechanism. Forward extrusion operations, such as those for pinions and engine valves are characterized by high sliding velocities and temperature generation leading to die wear i.e. parts no longer meet dimensional specifications. Thus, in the current process it was desired to investigate the effect of interface friction and extrusion velocity on the interface temperature. Additionally, the steady-state temperatures (Figure 8.7) depend upon the boundary conditions used for simulation of lubrication. Thus, an FE simulation-based calibration process was also conducted in order to determine the effect of the boundary conditions on the temperature distribution in the insert at the start of each forging cycle. The steady-state temperatures in Figure 8.7 were obtained using a convection coefficient of 30 kW/m^2-K for spray and 0.02 kW/m^2-K for dwell.

206
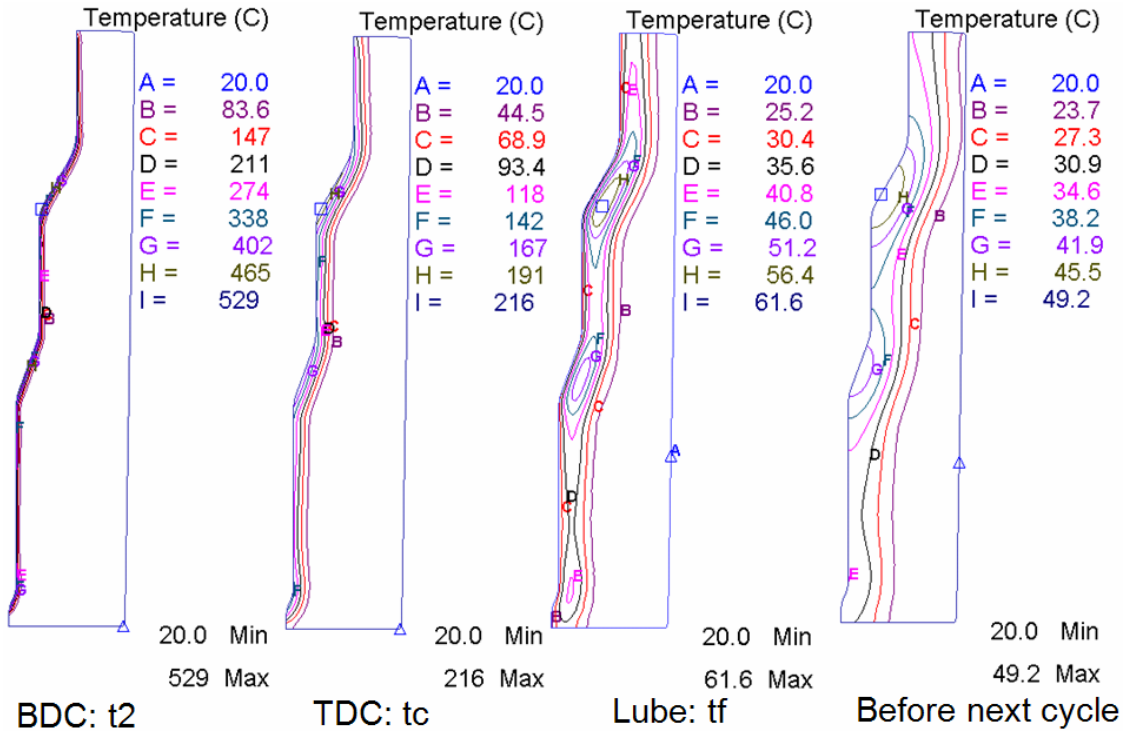
Figure 8.6: Insert temperature distribution at selected points during the start-up cycle (refer Figure 5.2 for discrete process steps).
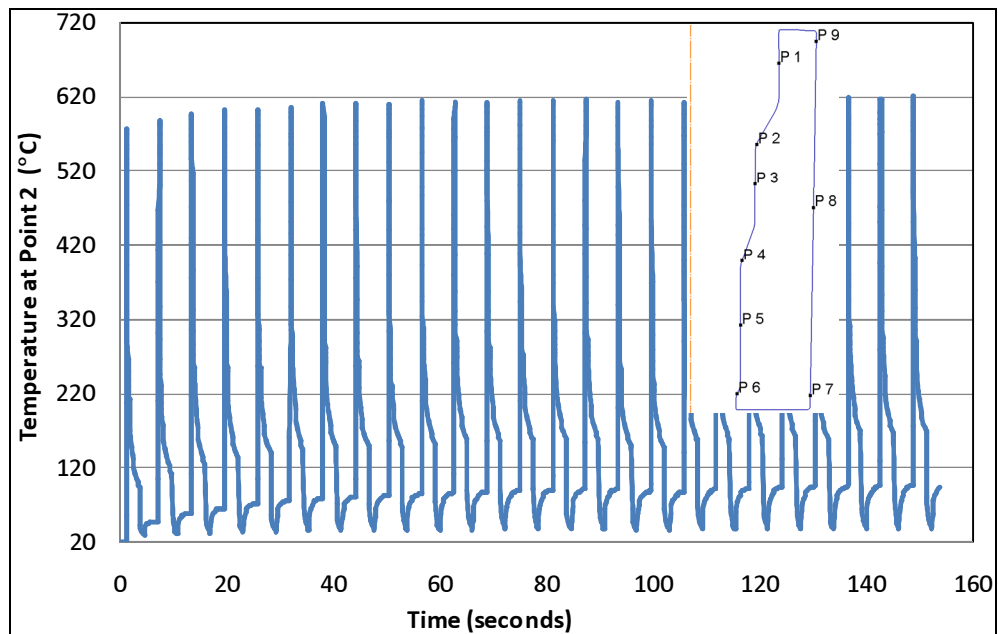
Figure 8.7: Temperature at point 2 over multiple cycles (existing process; W303™ insert).

207

8.3.2.1. Effect of Interface Friction and Extrusion Velocity

The default value recommended by DEFORM™ for the shear friction factor (m) in warm forging is 0.25 (based upon ring compression tests). The friction value affects the temperature generation at the die-workpiece interface and also the forging load. Different forging operations use varying amounts of lubrication to cool their dies and reduce forming loads. Thus, a sensitivity analysis of friction conditions is essential for analysis of interface conditions affecting die wear. To account for variability in friction conditions, depending upon the amount of lubrication spray settings, the friction value was varied by 40% to m = 0.15.

For a given die geometry, the die surface temperature during deformation also depends upon the extrusion speed (strain-rate and sliding velocity) i.e. the ram velocity vs. stroke profile. The sensitivity of the material flow stress to strain-rate and temperature accounts for the effect of extrusion speed on the normal pressure (on the die surface). The press velocity profile depends upon the kinematics of the slider-crack mechanism that most mechanical forging presses are based on (Figure 8.8). The clutch at the flywheel transmits the constant torque, M, to the eccentric (or crank) shaft. The force diagram gives the relations between the torque, M, the force on the connecting rod, P, and the tangential force, T:

$$T = P \sin (\alpha + \beta)$$
Equation 8.1

and

$$M = rT$$
Equation 8.2

Using Equation 8.1 and considering that the total press stroke is S = 2r, the machine load, L_M, acting on the ram is given by:

$$L_M = P * \cos\beta = \frac{T * \cos\beta}{\sin(\alpha + \beta)} = \frac{2M * \cos\beta}{S * \sin(\alpha + \beta)}$$
Equation 8.3

When the angles α and β approach 0, i.e., toward Bottom Dead Center (BDC), L_M may go to infinity for constant torque, M. This is illustrated in Figure 8.9a.

208
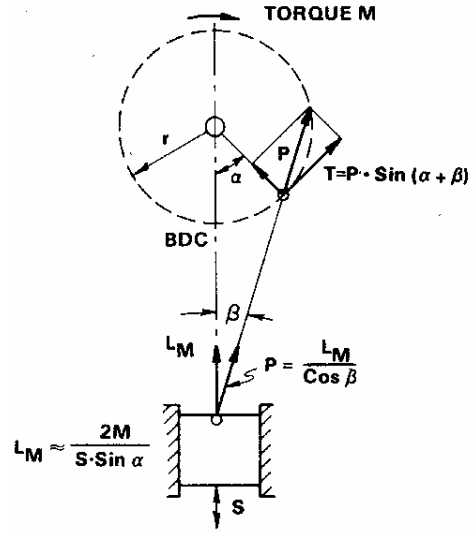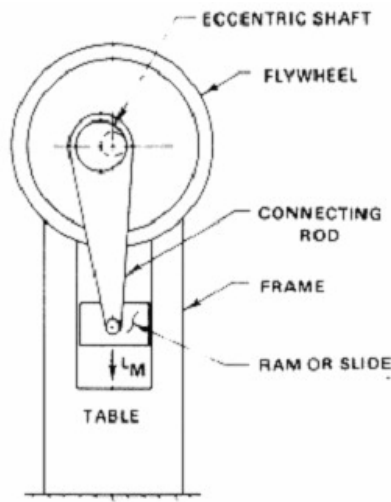
S = stroke, BDC = bottom dead center, α = crank angle before bottom dead center (BDC), L_M = machine load

Figure 8.8: Fundamentals of a mechanical forging press with eccentric drive (clutch and brake on eccentric shaft) [Altan et al, 2005].

Using the geometric relationships of Figure 8.8, the displacement and ram velocity can be expressed as:

$$h = r * (1 - \cos\alpha) + \frac{r^2}{2l} * \sin^2\alpha \qquad\qquad \text{Equation 8.4}$$

$$V = \frac{\pi n}{30} * h * \sqrt{\frac{S}{h} - 1} \qquad\qquad \text{Equation 8.5}$$

Thus, with Equations 8.4 and 8.5, the displacement (stroke position), h, and the velocity, V at each point of the ram stroke can be calculated. Figure 8.9 illustrates the variation of these values with the crank angle α before BDC. The velocity profile can be modified by using a variable speed motor to drive the flywheel. Based upon the specifications provided by the press manufacturer, the idle rate of the press can be varied from 50 to 63 strokes per minute. This determines the time for one press revolution. The ≈ 20% reduction in press idle rate results in a 26% increase in the time per stroke. The corresponding velocity and ram stroke variation over time is shown in Figure 8.10 for the two extreme values. The maximum ram velocity (90º before BDC) is reduced by ≈18% for a ≈20% reduction in idle rate.

209
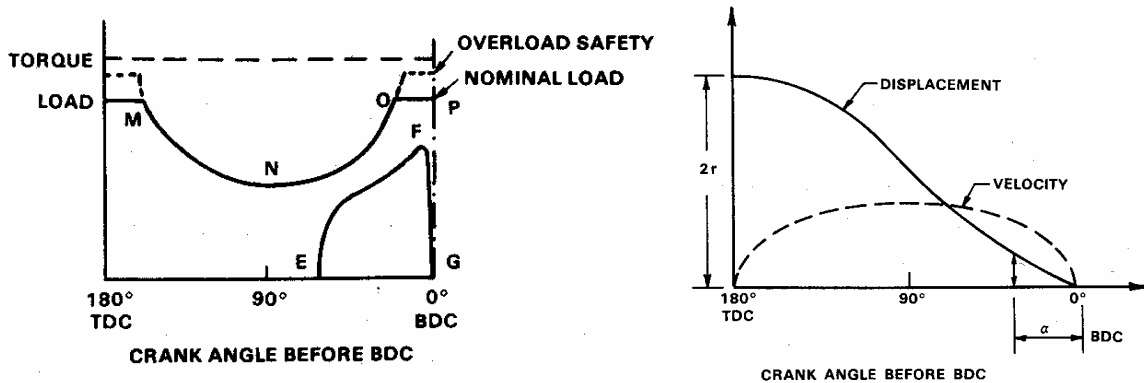
a) Variation of torque and machine load with crank angle.

b) Displacement and velocity in a simple slider-crank mechanism (stroke = 2r).

Figure 8.9: Load, velocity and displacement characteristics of a mechanical forging press with eccentric drive [Altan et al, 2005].
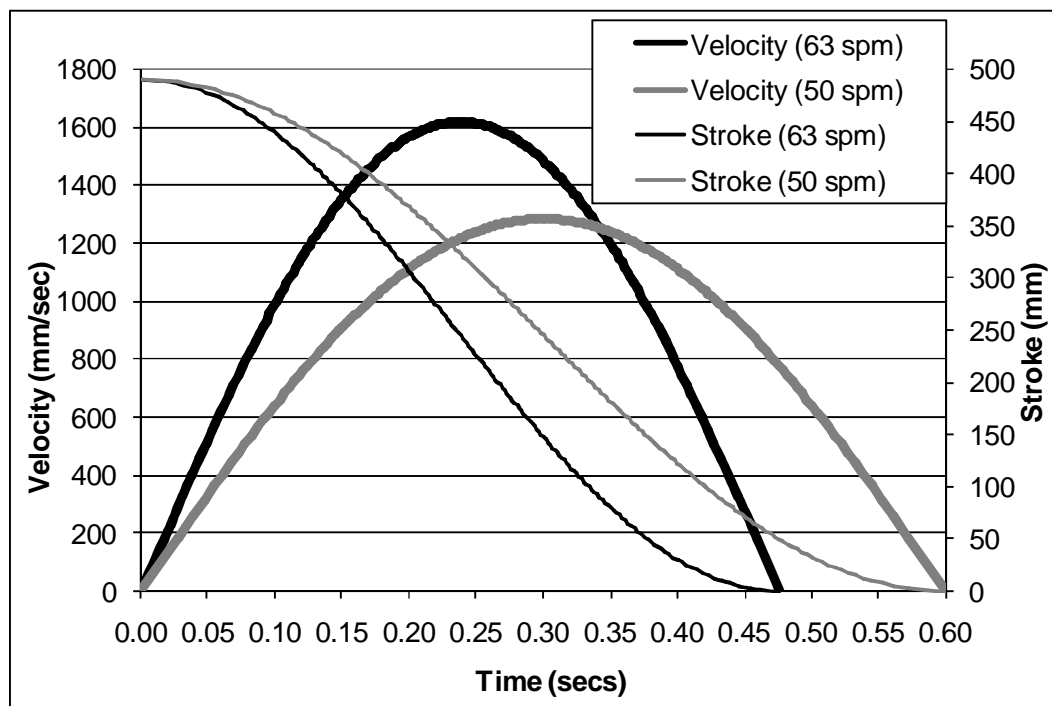
Figure 8.10: Velocity and stroke profile for the selected press operating at two different speeds.

210

Runs	Factors		Responses	
	Friction (m)	Press Velocity (strokes/minute)	Maximum Temperature at Pt 2 ($^{\circ}$C)	Load (tons)
1	0.15 (-1)	50 (-1)	443	210
2	0.15 (-1)	63 (+1)	449	210
3	0.25 (+1)	50 (-1)	517	250
4	0.25 (+1)	63 (+1)	529	250

Table 8.1: Two level sensitivity analysis for friction and press (extrusion) velocity.

Table 8.1 shows the values of friction and velocity considered for this basic sensitivity analysis along with the measured responses, primarily the maximum surface temperature predicted at point 2 (Figure 8.3), where the maximum area reduction occurs. A 40% increase in friction was found to result in a 16-18% increase in the predicted temperature and a 20% increase in forging load. Press velocity was not found to significantly affect either the surface temperature or forging load in the range of speeds considered. The reason for this observation is believed to be the higher sensitivity of the material flow stress to temperature than strain-rate. The results of the sensitivity analysis are summarized in Figures 8.11 and 8.12. The nearly parallel lines in Figure 8.12 indicate negligible interaction between friction and press velocity in the ranges considered.

The press velocity levels selected gave nearly identical load-stroke curves indicating that the energy required to forge the part did not change with velocity. Higher friction, however, will result in greater flywheel slowdown during the forging stroke due to higher energy requirements. It should be noted that operating the press at a lower flywheel angular velocity will also put limitations on the amount of permissible flywheel slowdown as well as the time required to bring the flywheel up to the pre-set speed for the next forging cycle.

The above analysis indicates that a change of settings or methodology in the parameters related to the lubrication system should be given higher priority than reduction of extrusion speed. A greater contribution of press velocity can be expected for higher reduction ratios such as those in extrusion of exhaust valves.

211
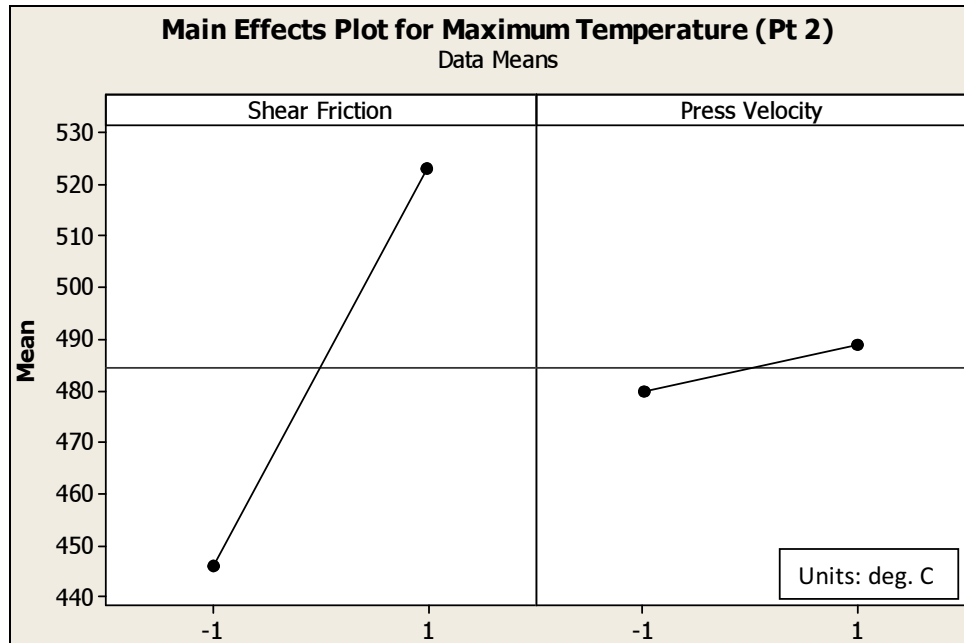
Figure 8.11: Effect of friction and press velocity on the maximum surface temperature at the first reduction radius (point 2).
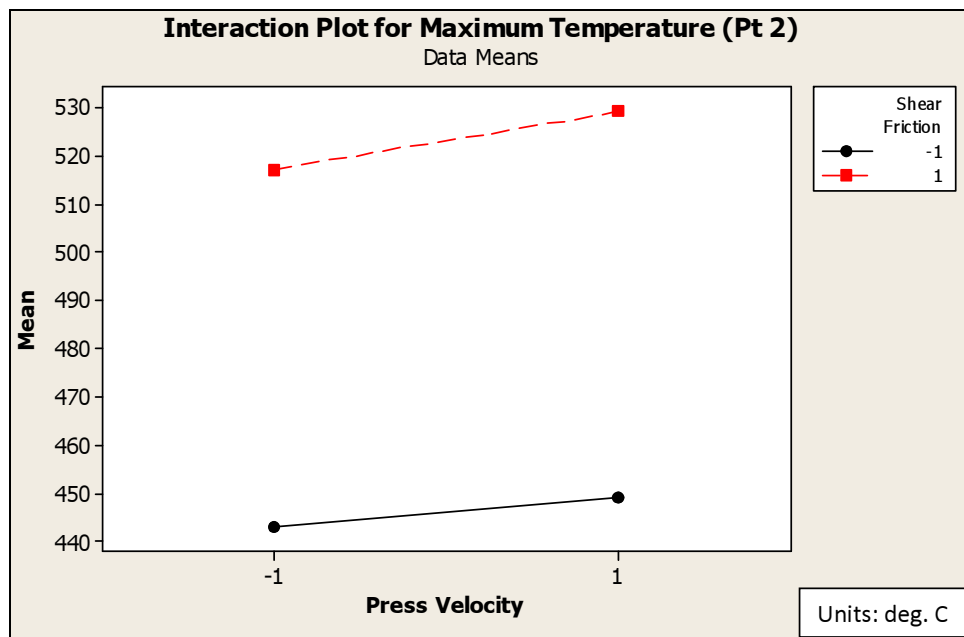
Figure 8.12: Interaction between friction and press velocity in terms of the maximum surface temperature at the first reduction radius (point 2).

212

For the lubrication stage, the automated system was pre-set for a spray time of one second. The subsequent part location time was measured as 1.5 seconds. Thus, the only variables in the lubrication process were identified as a) the convection coefficient during spray, b) the convection coefficient during the dwell time prior to the next stroke, and c) the environment temperature. The lubricant was assumed to be at ambient conditions. The default interface heat transfer and convection coefficients provided by DEFORM™ are shown in Table 8.2. For the preliminary FEA of start-up and steady-state conditions, a value of 30 kW/m^2-K (5283 BTU/hr-ft^2-F) was used for the spray stage followed by a value of 0.02 kW/m^2-K (4 BTU/hr-ft^2-F) for natural convection during dwell (Figure 8.7).

Convection and Interface Heat-Transfer (IHT) Coefficients				
		DEFORM Units		DEFORM Defaults
kW/m²-K	BTU/hr-ft²-F	BTU/sec-in²-F	N/sec/mm/C	
1	176	0.0003	1	(Free Resting)
0.02	4	0.000007	0.02	(Natural Convection)
5	881	0.0017	5	
10	1761	0.0034	10	
11	1937	0.0037	11	(Forming)
20	3522	0.0068	20	
30	5283	0.0102	30	(Reference:Initial FEA)

Table 8.2: Comparison of default DEFORM™ values with those selected for the calibration process.

For the calibration process, an initial screening analysis was done with the existing process design i.e. cycle time data from production and W303™/H13 die insert material. The following parameters and values were selected:

- Four values of convection coefficient for spray (5, 10, 20, 30 kW/m^2-K),

- Two values for convection coefficient during dwell (0.02 and 0.04 kW/m²K) and,

- Two values for environment temperature (20°C and 50°C).

This analysis was conducted for points 2, 4 and 6 on the three reductions in the first extrusion stage. However, results are presented for point 2 only. The starting FE model for all simulations was the W303™-insert die assembly prior to the lube spray with temperature distribution from the

213

start-up cycle of the forging process. Initially, simulations were conducted for spray convection coefficients of 5 and 30 kW/m²K (881-5283 BTU/hr-ft^2-F) using the different values of dwell convection coefficient and environment temperature. The latter two variables were found to have negligible effect (1-2ºC) on the die surface temperature prior to the second forging stroke. Thus, these two factors were eliminated from the study and the calibration process focused on the spray convection coefficient. Figure 8.13 shows the variation of die surface temperature at point 2 (region of maximum reduction; Figure 8.3) with the selected spray convection coefficients. The dwell convection coefficient and environment temperature were fixed at 0.02 kW/m²K (4 BTU/hr-ft^2-F) and 20°C (68°F), respectively.
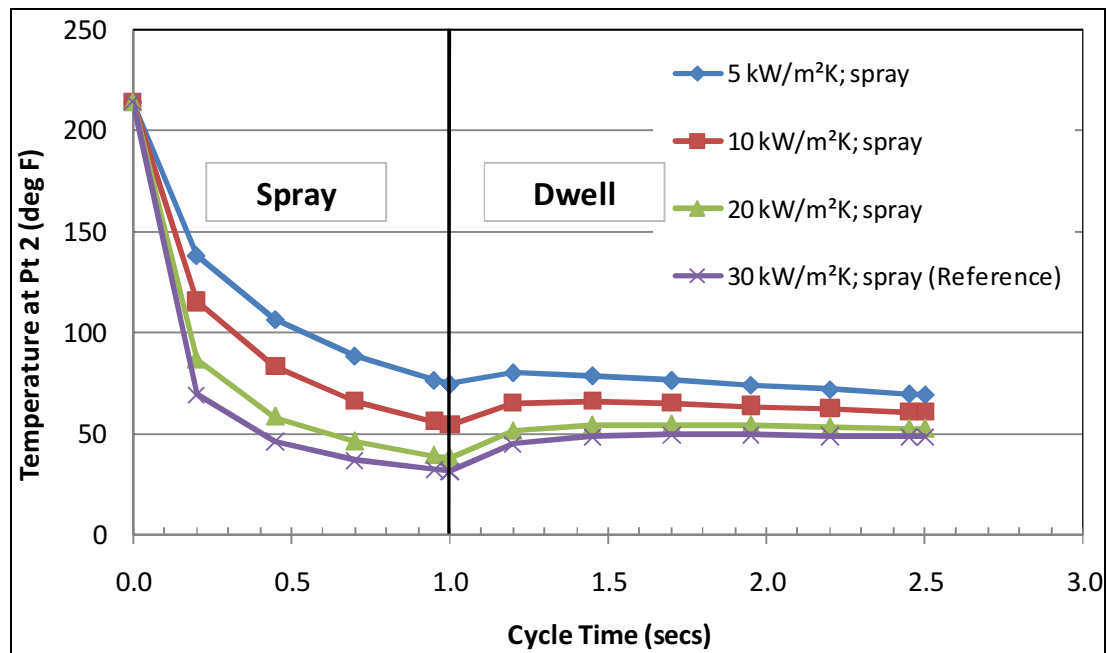
Figure 8.13: Lubrication calibration curves with the selected values of convection coefficient.

The effect of spray convection coefficient on the temperature change is summarized in Figures 8.14 and 8.15. Results are presented at two distinct points in the process cycle as seen in Figure 8-13 viz. end of lube spray and start of the next forging cycle, using the preliminary value of 30 kW/m^2-K (5283 BTU/hr-ft^2-F) as a reference (zero value on the x-axis of Figure 8.14). The change in temperature, with the corresponding change in spray convection coefficient, was found to follow an exponential pattern over the wide range of values selected (Figure 8.15). Thus, it was possible to predict the surface temperatures for points 2, 4 and 6 at the start of the second cycle for any intermediate convection coefficient. The goal of the calibration process, however, was to

214

compare the steady-state temperature measurements from production to the predictions from FEA in order to select appropriate boundary conditions without running numerous multiple-cycle forging models. Thus, it was necessary to project the results from the first cycle over multiple forging strokes. This was accomplished using two approaches based on a) the temperature trends from the reference multiple-cycle simulation (Figure 8.3; Table 8.2), and b) the correlation between convection coefficient and temperature from Figures 8.14 and 8.15.
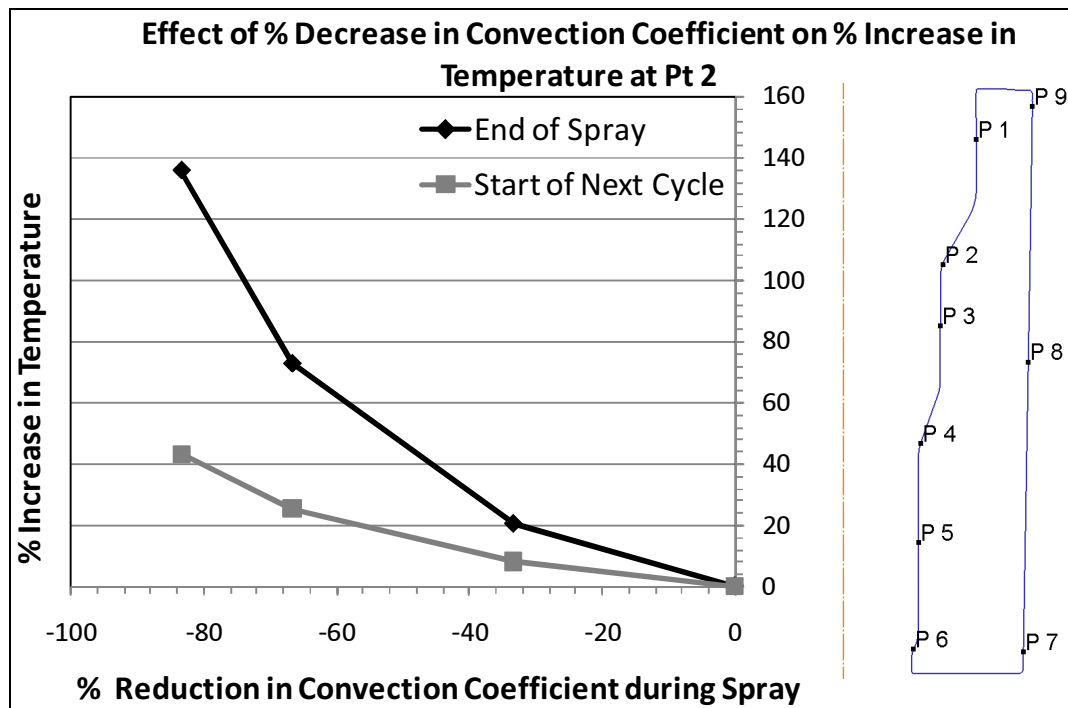
Figure 8.14: Percentage increase in temperature with reduction in spray convection coefficient during start-up cycle (point 2).

215
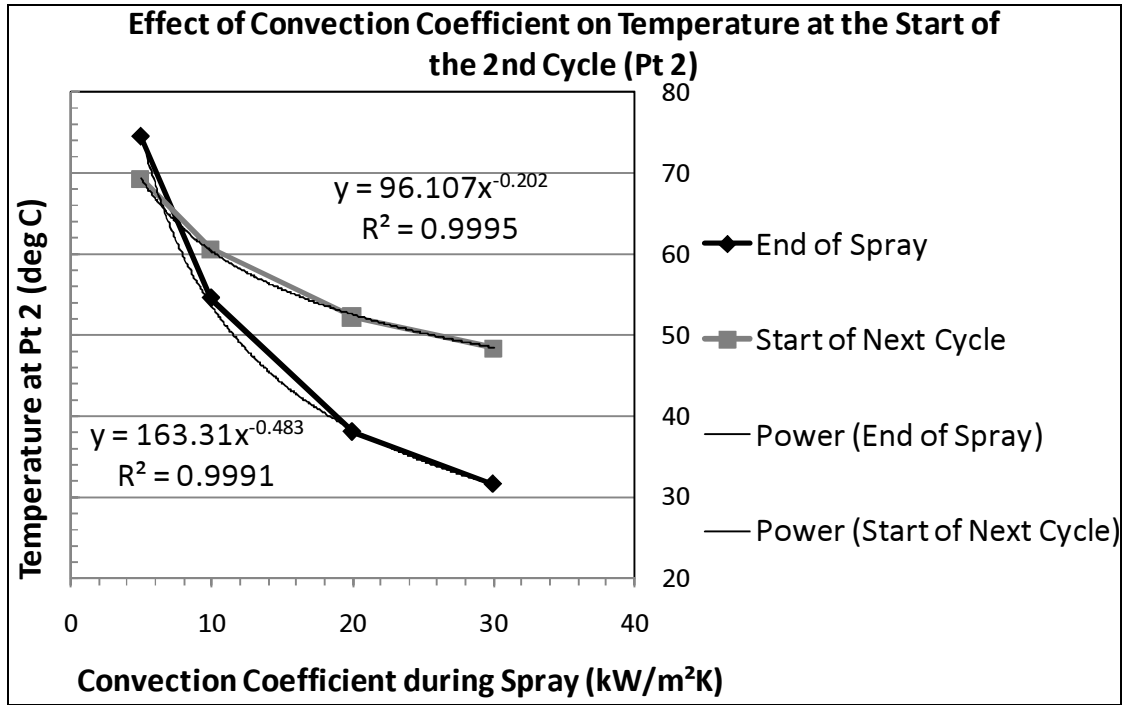
Figure 8.15: Effect of spray convection coefficient on the temperature prior to the second forging cycle (point 2).

Approach 1: This method assumed that the relationship of % increase in temperature vs. % decrease in convection coefficient (Figure 8.14) in the start-up cycle remains the same over multiple forging cycles.

- The temperature at the start of each forging cycle was plotted for the reference simulation (actual FEA with a spray convection coefficient of 30 kW/m^2-K/5283 BTU/hr-ft^2-F). The temperature was found to increase progressively from ambient temperature at start-up to a value of ≈ 90ºC (194ºF).

- For each discrete temperature value of the reference simulation the corresponding value with another convection coefficient could be predicted using the exponential relationship from Figure 8.14 and the % difference with respect to the reference value.

- Figure 8.16 shows a comparison of steady-state temperature predictions with the selected spray convection coefficients compared to the reference value (actual FEA with a value of 30 kW/m^2-K/5283 BTU/hr-ft^2-F). Temperatures were found to vary from 100ºC to 130ºC (212ºF to 266ºF) for the selected range of values.

216

Based upon the production measurements in the region of the first reduction, a convection coefficient of 30-35 kW/m^2-K (5283-6163 BTU/hr-ft^2-F) was predicted to give a steady-state temperature distribution comparable to that in production ($\approx$ 80-90°C/170-196°F). Further validation using measurements at other locations on the die surface or real-time data using a thermocouple inserted between the die sub-assemblies was explored, but found to be infeasible.
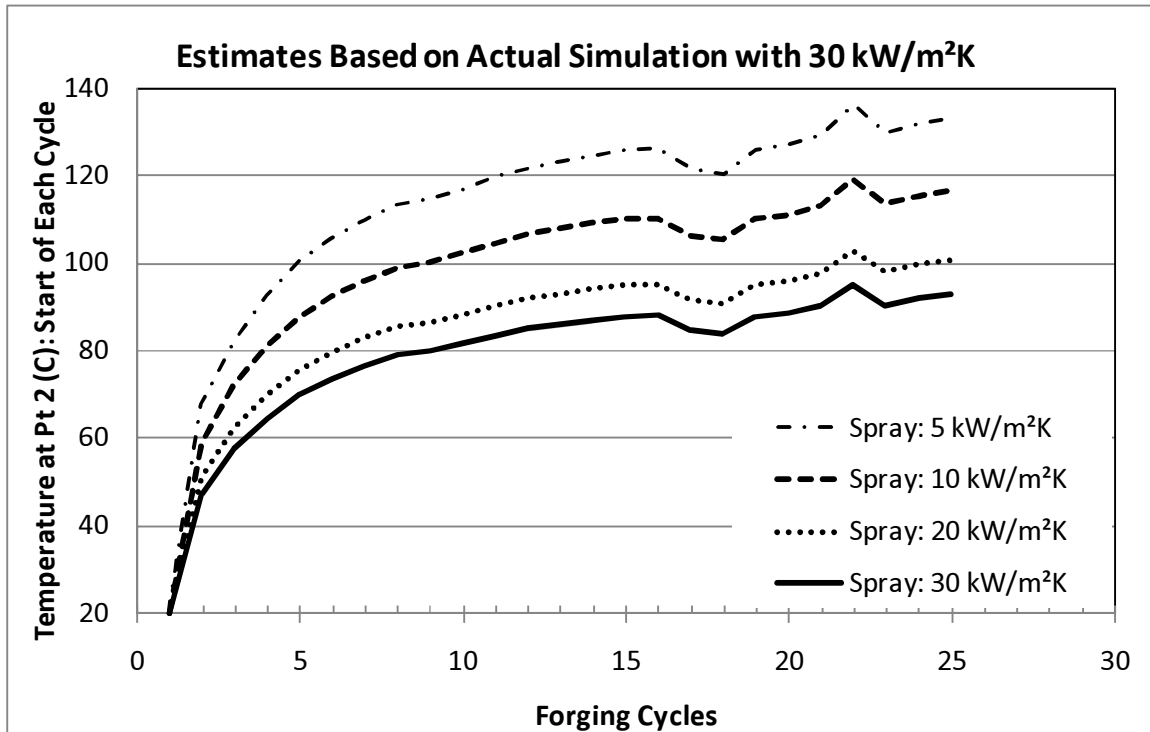
Figure 8.16: Estimation of steady-state temperatures using the start-up temperature distribution (Approach 1).

Approach 2: This method assumed that the change in die surface temperature in subsequent forging cycles followed the same trend as that for the reference simulation, with the spray convection coefficient affecting only the absolute values of temperature.

- Figure 8.17 shows the % change in temperature at the start of each forging cycle with respect to a) that of the previous cycle and b) the starting temperature (ambient conditions). The maximum temperature increase ($\approx$135%) at point 2 occurs in the first forging cycle and drops drastically in the subsequent cycles.

- In order to obtain a simplistic representation of the temperature trends, a power-law fit (T = T_o + C*t^h) was applied to this relationship, where T_o is the pre-heat or start-up

217

temperature, C is a coefficient that determines absolute temperature magnitude for the selected spray convection coefficient and h is an exponent that determines the temperature increment in successive cycles. Thus, under the assumptions of Approach 2, the exponent h remains constant, whereas the coefficient C is affected by the spray convection coefficient as shown in Figures 8.14 and 8.15.

- Using the exponential relationship from Figure 8.15, the temperature increase in the first forging cycle was predicted for a selected spray convection coefficient. The trends from Figure 8.17 were then applied to determine the % increase in surface temperature at the start of each subsequent forging cycle.

The temperature predictions for Approach 2 were 3-5% higher than those for Approach 1 (Figure 8.19). A spray convection coefficient between 30-35 kW/m^2-K (5283-6163 BTU/hr-ft^2-F) was recommended in order to match production measurements at point 2.
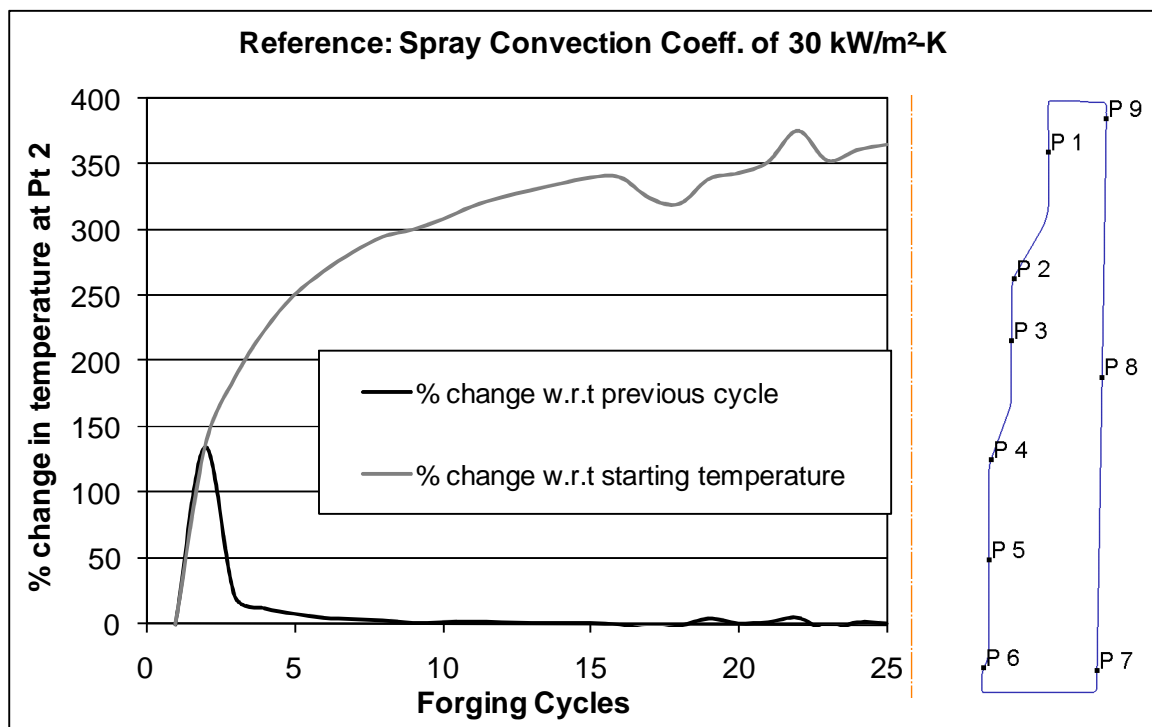
Figure 8.17: Change in die surface temperature at the start of each cycle with respect to (w.r.t) previous cycle and the start-up temperature.

218
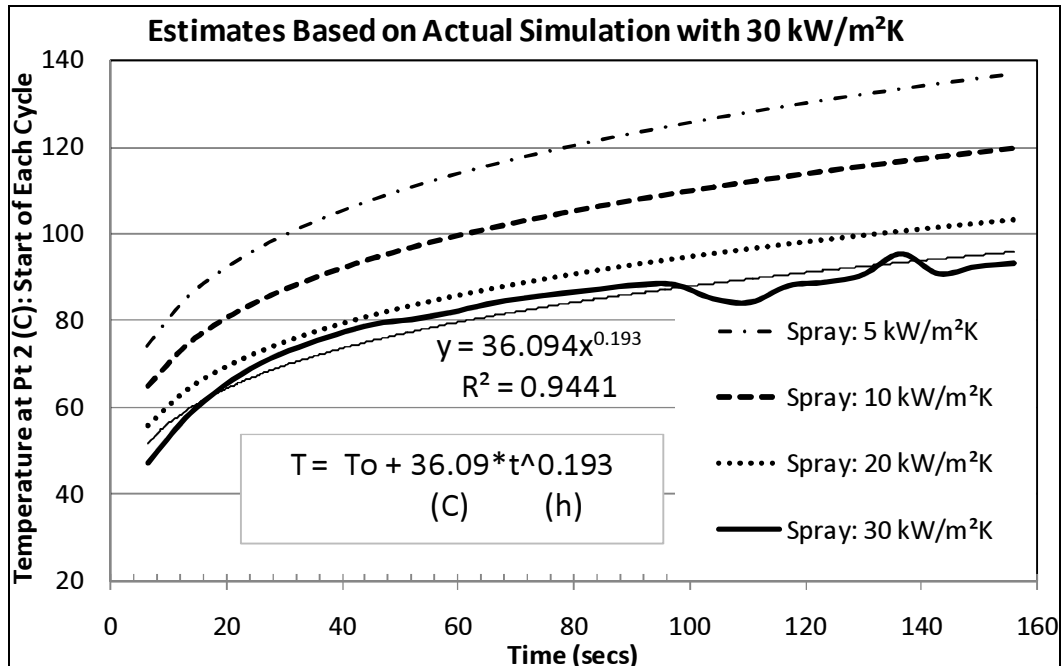
Figure 8.18: Estimation of steady-state temperatures using the start-up temperature distribution (Approach 2).
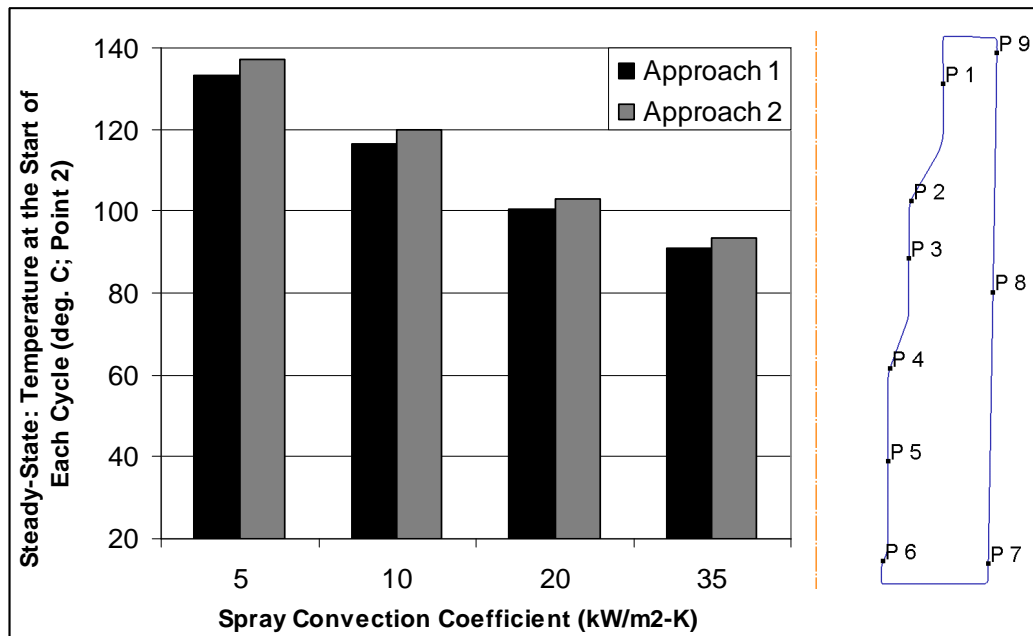
Figure 8.19: Comparison of the two approaches for selection of spray convection coefficient and estimation of steady-state temperatures.

219

8.4. Selection of Candidate Die Materials and Heat Treatments

Previous in-house production trials conducted by Hirschvogel covered a number of the tool steels considered in this research project (e.g. W360™, MaxDie™, etc.). No substantial die life improvement was achieved in these cases. Based on the failure modes analysis for die wear, alternative die materials should have higher hot hardness (and hot yield strength), higher thermal conductivity and higher tempering resistance than the existing die material. The candidate die materials selected for this study were a) matrix high speed steels (MHSS) from Nachi-Fujikoshi/Walter Metals (Duro-F1™) and Daido/International Mold Steel (DRM1™ and DRM 2™), and b) ceramic and/or carbide-based materials.

8.4.1. Matrix High-Speed Steels (MHSS): Development and Application

High speed tool steels, both tungsten (Group T) and molybdenum (Group M) based, were developed primarily for cutting tool applications. These materials are among the most highly alloyed tool steels with large amounts of tungsten or molybdenum along with chromium, vanadium and sometimes cobalt (Table 8.3). Compared to conventional tool steels these materials are capable of achieving higher cutting speeds while maintaining their hot hardness (i.e. hardness at elevated temperatures).These steels also found application in certain cold and warm forging processes, mostly in the form of punches. However, the main drawback of conventional wrought and powder metallurgy (PM) high speed steels (HSS) in these applications was found to be their low fracture toughness and susceptibility to chipping. Thus, there was scope for development of a family of tool steels with the hot hardness and temper resistance characteristics of HSS and the toughness of conventional hot-work tool steels.

Type	Chemical Composition (%)					
	C	Cr	V	W	Mo	Co
T4	0.75	4.00	1.00	18.00	-	5.00
T5	0.80	4.00	2.00	18.00	-	8.00
M2	0.80	4.00	2.00	6.00	5.00	-
M42	1.10	3.75	1.15	1.50	9.50	8.00
H11	0.35	5.00	0.40	-	1.50	-
H13	0.35	5.00	1.00	-	1.50	-

Table 8.3: Conventional tungsten and molybdenum high speed tool steels compared to their standard hot-work counterparts [Avner, 1964].

8.4.1.1.   Development of Matrix High Speed Steels (MHSS)

Matrix high speed steels (MHSS) were developed in order to fill the gap between conventional hot-work steels and HSS. The original development was done in the 1960's by Vanadium-Alloys Steel Company (VASCO), Latrobe, PA (USA) [Roberts et al, 1964; US Patent No. 3117863]. The research done as part of this development found that hardened high speed steels consisted mainly of two phases, viz. a) the extremely hard alloy carbides of (tungsten, molybdenum, vanadium) and b) an essentially martensitic "matrix" or background material. Due to their excessive carbide content, these steels possessed high strength (room and elevated temperature) but suffered from the disadvantage of being brittle. On the other hand, hot-work tool steels such as the chromium-based H-11 or H-13 possess excellent toughness but poor hot hardness and temper resistance characteristics in their standard (non-specialty) versions. Thus, the main objectives of this initial development of the MHSS family were to [Roberts et al, 1964]:

- Provide a family/class of tool steels characterized with the same approximate hardness characteristics (room and elevated temperature) of HSS and the same approximate toughness of standard hot work steels.

- Develop a method for making the new family of steels according to which the desired degrees of hardness, toughness and ductility could be conveniently and economically produced.

The steels thus developed have compositions corresponding to the matrix composition of the parent heat-treated high speed tool steel, and can be heat-treated to produce the desired high hardness and toughness. The overall procedure for development of these steels is summarized as follows:

Step 1: A heat treated high speed steel with the desired hardness characteristics was pre-selected e.g. VASCO M-2™ high speed steel shown in Table 8.4a with the matrix (base composition) in hardened state. These parent steels had mainly martensitic matrices with about 5% undissolved excess carbides.

Step 2: The matrix composition of the parent steel was determined and a new melt was prepared with this composition (Table 8.4b). This new composition was developed using refining techniques such as vacuum arc re-melting (VAR) or electro-slag re-melting (ESR), as discussed later. The chemical make-up of the new steel was such that all the excess carbides, which would normally be present in the parent steel in the annealed condition, would be dissolved when the former is re-heated for hardening. Thus, the matrix steel differed from the parent in the lack of

221

excess carbides. Subsequently, these steels gained high toughness with minimal loss of hot hardness and temper resistance.

.80% carbon	.5% carbon
6.00% tungsten	2.0% tungsten
5.00% molybdenum	3.0% molybdenum
4.00% chromium	4.6% chromium
2.00% vanadium	1.0% vanadium
and the remainder substantially iron	and the remainder substantially iron

a) Parent high speed steel (VASCO M-2™).   **b) Matrix high speed steel.**

Table 8.4: An example matrix composition based on a parent high speed steel [Roberts et al, 1964].

Step 3: The ingots cast from this new melt follow the same processing steps (bulk deformation and heat-treatment) as the parent tool steel.

This overall procedure for developing MHSS is still used today. Table 8.5 shows a comparison of the tempered hardness values for the parent and the matrix high speed steel. Table 8.6 shows a comparison of the toughness of the matrix high speed steel compared to its parent VASCO M-2™ and a standard hot-work tool steel (H-11). It was observed that the MHSS provided superior toughness (Table 8.6) for hardness values comparable to the parent M-2 steel (Table 8.5). It should be noted that standard hot-work tool steels generally cannot be hardened beyond 57-58 HRC at room temperature.

Tempering Temperature, °F.	Tempered Hardness (2 hours) Rc	
	Vasco M-2	Matrix Composition
As quenched	64.7	63.2
500	60.6	57.2
800	61.5	58.0
900	62.6	60.0
950	64.4	61.0
1,000	65.8	61.8
1,050	65.1	60.8
1,100	64.0	59.1
1,150	62.7	55.5
1,200	59.3	52.3
1,300	46.1	40.0

Table 8.5: Tempered hardness values for the matrix high speed steel compared to its parent [Roberts et al, 1964].

222

Heat Treated Hardness, Rc	Unnotched Izod Impact Strength, ft.-lbs.			V-Notch Charpy Impact Strength, ft.-lbs.	
	Standard M2 High Speed Steel	Matrix M2 Austenitized at 2225°F.	Matrix M2 Austenitized at 2050°F.	Matrix M2 Austenitized at 2050°F.	AISI H–11 Hot Work Die and Structural Steel
57.5	52	16	120+	11	12
59.0	51	17	120+	10	------------
61.0	48	19	120+	6	------------

Table 8.6: Toughness of the matrix high speed steel compared to its parent and a standard hot-work tool steel [Roberts et al, 1964].

8.4.1.2.   Recent Development of Matrix High Speed Steels (MHSS)

The MHSS steels that are currently available for cold, warm and hot forging are the result of research and development efforts primarily concentrated in Japan at companies such as Hitachi Metals (YXR™ series; www.hitachi-metals.co.jp), Nachi-Fujikoshi (MDS™ series; www.nachi-fujikoshi.co.jp), and Daido Steel (DRM™ series; www.daido.co.jp). These steels are marketed worldwide, though currently their application is restricted primarily to the Japanese forge shops. These steels are proprietary compositions and do not have any AISI or JIS designations.

These new MHSS were primarily developed for use in applications where the punches/dies were failing due to wear (hot-work tool steels) or mechanical fatigue and impact fracture (HSS). The overall goal of the development work was to reduce the excess carbide content and subsequently improve the toughness of the steel while delivering high hot hardness. Table 8.7 shows the potential applications of the DRM™ series from Daido Steel, a second generation of Daido MHSS. These steels are double electro-slag re-melted (ESR) compared to the MDS™ and YXR™ series, which are put through a single re-melting process.

DRM1™ is recommended mainly for hot and warm forging dies because of its high hot hardness and temper resistance. DRM2™ is suitable for warm and cold forging dies, especially the latter, due to its high room temperature fatigue strength. DRM3™ is a cold forging die steel, which can be applied where AISI D2 and M2 have problems in strength and toughness. As shown in Figure 8.20, DRM™ steels show higher toughness than conventional MHSS steels from Daido and are positioned between hot, cold and high speed tool steels.

223

Grade	Hardware(HRC)	Applications
DRM1™	56~58	Hot and warm working tools: High hardness (hot forging tools).
DRM2™	58~62	Warm and cold working tools: High toughness (cold forging tools).
DRM3™	62~66	Cold working tools: When AISI D2 and M2 have problems with strength and toughness.

Table 8.7: Recommended applications for the DRM™ series from Daido Steel [Nakahama et al, 2005].
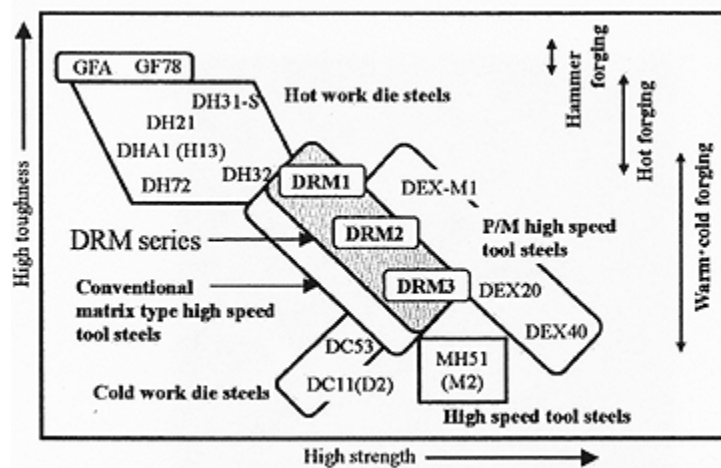
Figure 8.20: Application of DRM™ compared to other Daido steels [Nakahama et al, 2005].

8.4.1.3. Manufacturing Techniques for MHSS

As mentioned earlier, the matrix composition is prepared using vacuum arc re-melting (VAR) or electro slag re-melting (ESR) (Figure 8.21). These processes are primarily refining techniques used for producing specialty steels, their primary advantages being high micro-cleanliness (reduction of non-metallic inclusions) and improved mechanical properties.

In the VAR process (Figure 8.21a), the original steel is cast or forged into an ingot/electrode that is re-melted in vacuum. The furnace consists of a water-cooled tank above ground level that encloses the electrode, and a water-cooled copper mold in the lower section where melting and solidification takes place. ESR, like VAR, is a secondary refining process for electrode ingots of essentially the same composition as the final product. Unlike VAR, the electrode in this process does not require surface preparation. A refining slag is used in order to a) offer resistance to electric current resulting in heat generation to melt the electrode, b) protect the molten metal from oxidation and c) promote desulphurization and flotation of inclusions. Since these processes add

224

an additional step to the general tool steel manufacturing process, they are applied mostly to specialty steels, which tend to be more expensive compared to standard tool steels.
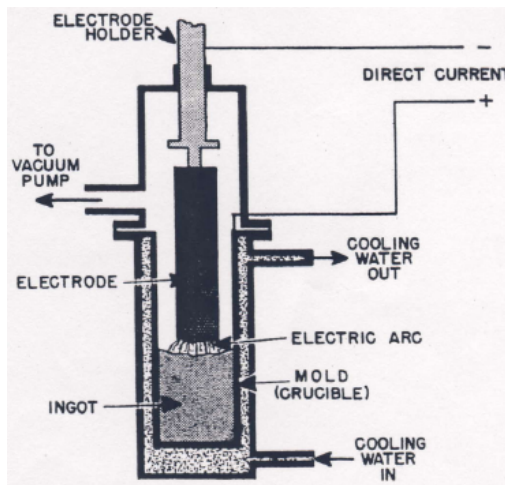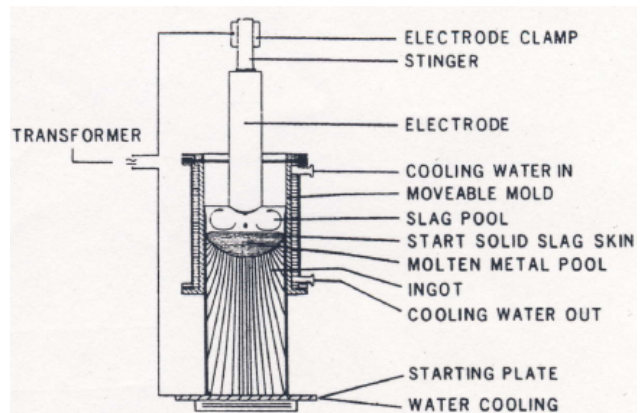
| a) Vacuum Arc Re-melting (VAR). | b) Electro Slag Re-melting (ESR). |

Figure 8.21: Manufacturing of matrix high speed steels.

8.4.1.4.   Comparison of MHSS to Existing Insert Materials

The existing forging process was simulated in DEFORM™ to determine the interface conditions during the start-up cycle and steady-state production. The current insert material (W303™/H13) was compared to a MHSS grade. The thermal conductivity of the existing die material is 7% greater than that of the MHSS grades being considered. Thus, the differences in the thermal interface conditions are negligible (Figure 8.22). However, Figure 8.23 shows that the two MHSS grades (DRM1™ and DRM2™) have 30% and 40% higher hot hardness, respectively, compared to the H13 tool steel variants and are, therefore, expected to have higher wear resistance. Similarly, MHSS grades also have higher hot yield strength compared to conventional hot-work tool steels as shown in Chapter 6.

After discussions with Hirschvogel, it was decided to conduct production trials with the existing die design, using different grades of matrix steels. The die materials chosen for these trials included:

- DRM1™ and DRM 2™ from Daido Steel at 58-60 and 60-62 HRC, respectively, along with a nitriding treatment.

- Duro-F1™ from Nachi-Fujikoshi with a nitriding treatment.

225

Trials were expected to start by the end of February 2008. Five replications will be conducted for each die material to give a total of 15 production trials.
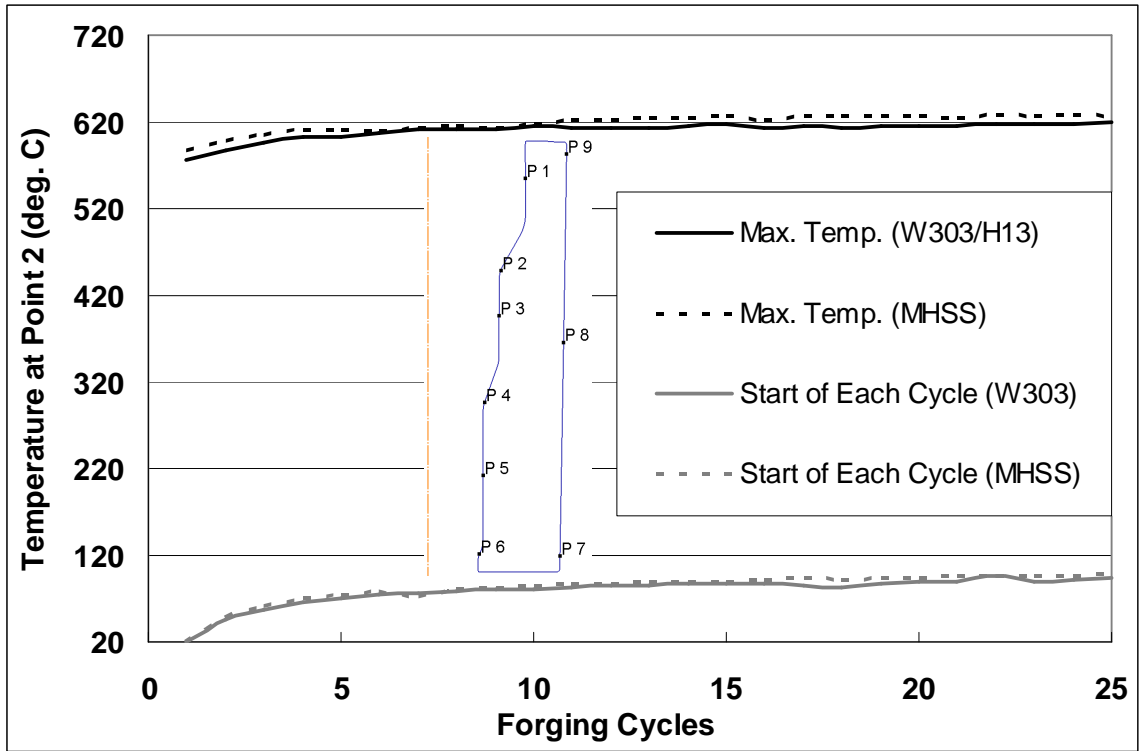
Figure 8.22: Steady-state temperature conditions for MHSS compared to the existing die material and process design.

226
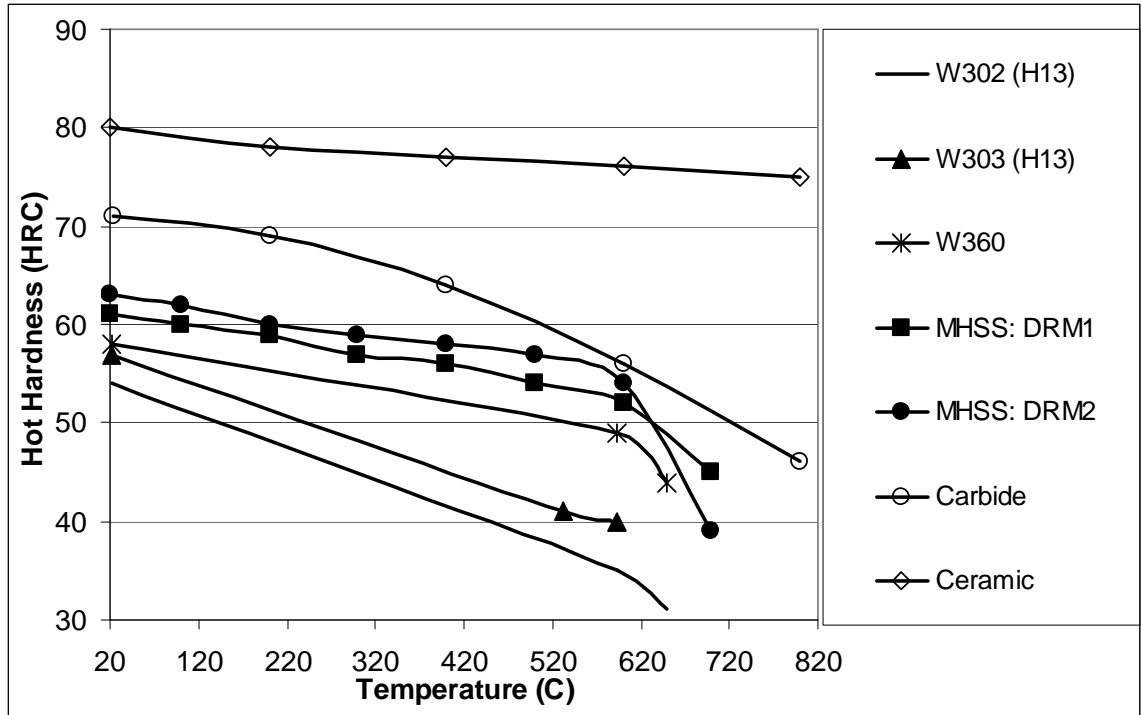
Figure 8.23: Comparison of MHSS to existing insert material on the basis of hot hardness.

8.4.2. *Application of Ceramics and Carbides*

The possible application of ceramic and carbide die inserts was also explored for the selected application. The FE analysis methods developed for the warm upsetting operation described in Chapter 7 were applied in this case study as well. Thus, the assembly process for inserts 1 and 2 with their respective containers was simulated using an incremental approach. The selected forging process does not involve die pre-heating, thus, any change in the compressive pre-stress occurs from thermal expansion during the forging process. The boundary conditions for FEA of forging were the same as those for the steel insert. Thus, it was assumed that the ceramic and carbide inserts would be subjected to the same deformation and lubrication conditions. Simulations were conducted to determine the steady-state temperature distribution and resulting thermal expansion of the die assembly. The resulting loss of compressive hoop stress is shown in Figure 8.24.

227
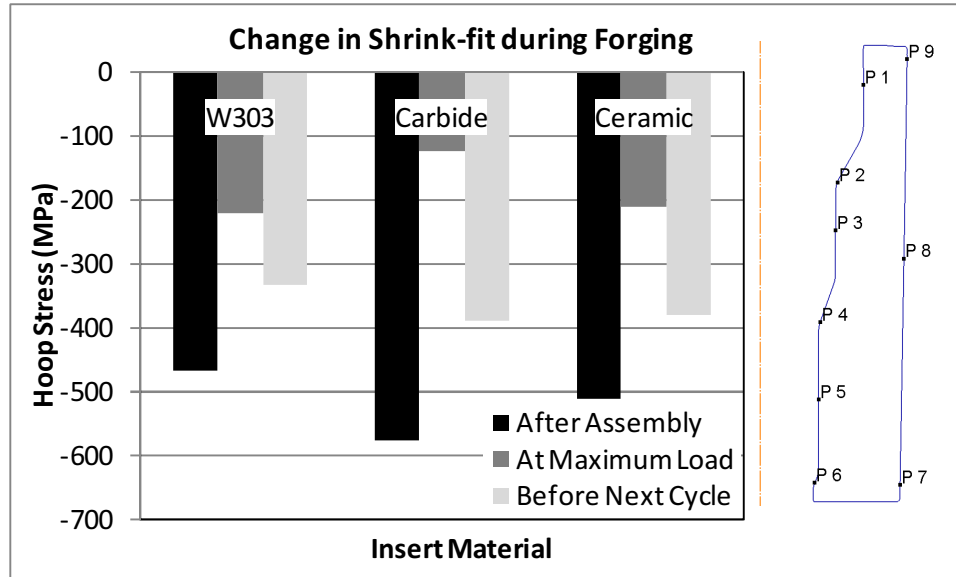
Figure 8.24: Loss of hoop stress on the insert O.D. under steady-state conditions.

For the same die design and interference fits, the carbide insert has ≈ 24% higher compressive stress than the steel insert (13% higher than that with ceramic) due to higher elastic modulus. The coefficient of thermal expansion of the carbide, however, is ≈ 65% lower than that of steel. Thus, the containment system expands more than the insert resulting in a 33% loss of compressive stress under steady-state conditions (start of each forging cycle). The ceramic insert was predicted to lose 25% of its compressive pre-stress. This loss of shrink-fit is also observed in the stresses under maximum mechanical load during extrusion. The carbide insert is predicted to lose 78% of its pre-stress versus 58% and 52% predicted for ceramic and steel, respectively. Thus, the corrections required in the interference values were established using FEA. These design changes can be implemented into the die assembly if ceramic or carbide-based materials are considered for production trials.

8.5. Summary and Recommendations

Forward extrusion processes subject dies to high temperatures and sliding velocities resulting in thermal softening and wear. The primary failure mode in this process was abrasive wear at the radius where maximum reduction is carried out. As a result, forged parts do not meet dimensional specifications. An example warm extrusion process for an automotive pinion was selected for improvement of die life through application of the computational techniques developed in this study. The following results were derived from this analysis:

228

- For the selected process conditions and forging equipment, friction was expected to have a significant impact on die wear at the region of maximum extrusion ratio. A 40% increase in friction resulted in an 18% increase in the die surface temperature. The extrusion speed was not found to affect the surface temperature with the range selected.

- An FEA-based lubrication calibration procedure was used to determine appropriate convection boundary conditions and to determine steady-state die temperatures. Two approximate methods were explored and found to match the production measurements in the region of maximum extrusion ratio.

- Production trials have been planned with three grades of matrix high speed steels (MHSS) with 5 replications of each to account for natural variation.

- Carbide and ceramic inserts were also explored for potential future use. The loss of shrink-fit from thermal expansion during forging was estimated for steady-state temperature distributions. The carbide insert was predicted to show the maximum loss of shrink-fit (78% under maximum load; 33% at the start of the forging cycle). Thus, design corrections are required to prevent failure of these die materials.

Based on the FE analysis and production data, the following recommendations were made for the warm extrusion process being carried out on a mechanical press:

- Die design: FEA predicted a loss of shrink-fit under steady-state conditions. The shrink-fit dimensional corrections mentioned above are required for application of the MHSS, ceramic or carbide grades discussed in this chapter.

- Die material selection: The existing inserts are found to fail due to excessive thermal softening. This may be due to a) inefficient cooling, and/or b) inadequate tempering resistance and hot hardness of the selected tool material. Thus, MHSS or carbide grades were proposed as possible alternatives for this application.

- Forging: Extrusion speed was not found to significantly affect die surface temperatures. However, a lower press speed was recommended as a variable in the production trials.

- Lubrication spray: The spray process was determined to be the dominant factor affecting the tool life for a fixed set of reduction ratios. Optimization of the spray settings (spray time, spray sequence and spray pressure) was recommended to complement the proposed die materials.

229

CHAPTER 9

CASE STUDY 5: IMPROVEMENT OF MATERIAL UTILIZATION IN HOT FORGING

9.1. Problem Statement

In conventional hot forging, raw material represents 40 to 60% of total forging costs, depending upon the part complexity, type of material used, and the production volume. Depending upon forging part geometry and production volume, in hot impression die forging flash losses can be in the range of 30 to 60%, while die costs are in the range of 20 to 30%. Thus, precision hot forging with minimal or no flash (flashless) is one of the requirements for improving the profitability of the forging operation.

Automotive components, such as connecting rods and control arms, are extremely high volume components that result in significant material loss through conventional hot forging practices. Thus, there is an opportunity of huge cost savings in hot forging with flash by a) identifying the optimum shape and size of the preform with the best possible material distribution to obtain complete cavity filling without defects, and b) modifying the flash design of the blocker & finisher die to minimize the loss of material into flash.

The example part selected for this study was submitted by a major tier-1 automotive supplier looking to improve the profitability of the forging process by increasing material yield and reducing lead times from quotation through product development. The forging process is conducted on an automated mechanical press forging line in the sequence shown in Figure 9.1. The workpiece material in this case was a 6xxx series aluminum alloy in the form of a billet with a polygonal cross-section. The billet is induction heated and reducer rolled in two steps to obtain the desired material volume distribution. The rolled preform is then bent at elevated temperature before being transferred to the forging cell. The forging process takes place in two steps viz. blocker and finisher, followed by trimming and heat treatment. The material yield in the existing process was estimated to be ≈70% i.e. 30% of the incoming billet volume was lost in the form of flash. In order

230

to maintain confidentiality of process and die design, proprietary information has been replaced with general schematic representations and verbal description where required.
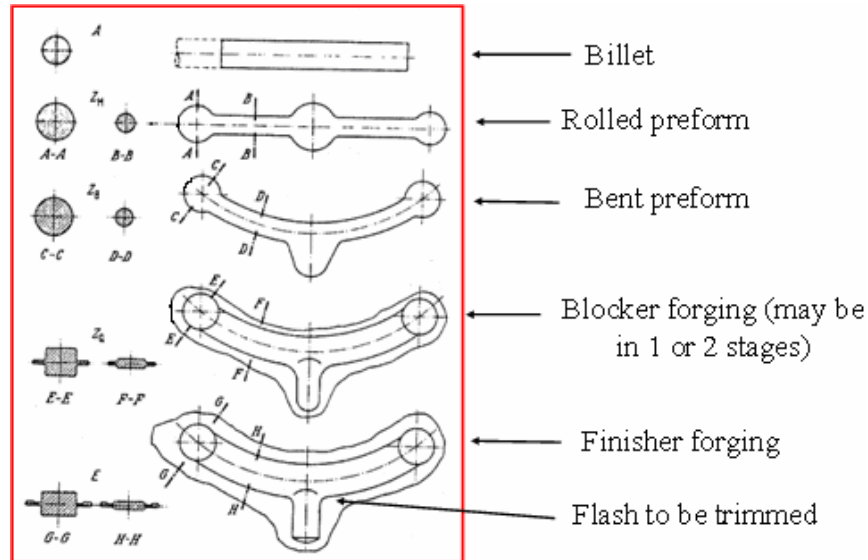
Figure 9.1: Forging sequence for a commercial automotive component [Altan et al, 2005].

9.2. Objectives

The overall objective of this study was to improve the material yield in a conventional hot forging process by optimizing the preform shape and die design. The specific research objectives addressed through this study include:

o Optimization of preform design for an existing forging die design (blocker and finisher) to reduce flash losses.

o Optimization of the blocker die design, for reduction of flash losses, by utilizing a combination of 2-D and 3-D sectional analysis.

o Implementation of a standardized design process in order to ensure rapid die and process development while maintaining quality standards.

9.3. Analysis of the Existing Forging Process

The first step towards achieving the goals of this study was to develop and validate an FE modeling method for the different deformation stages of the forging process viz. reducer rolling, blocker forging and finisher forging. Die-workpiece geometries and process data from production were used input to the FE analysis, the results of which were then compared to production

231

observations in the form of forged part dimensions, defects, etc. This step was crucial in ensuring the accuracy of the analysis and predictions made in the subsequent design stages for material yield improvement. Thus, this stage analyzed the existing reducer rolling and forging stages using the commercial FEA code DEFORM™.

9.3.1. *Preforming by Reducer Rolling*

The reducer rolling process can be considered as a pre-forming operation, which changes the volume distribution of the incoming billet of uniform cross-section. This is a crucial step in optimizing material yield when forging parts of complex geometries (connecting rods, controls arms, etc.) that have different volume requirements in different sections as seen in Figure 9.1. Since the two ends of the finished part have greater cross-sectional area than the arms, they require greater material volume in order to fill the die cavity. The reducer rolling operation required for the current process was simulated taking into account the heat-transfer between the rolls and the workpiece. The rolling process is carried out in two steps (two passes) to go from the uniform cross-section to a double dog-bone shape shown in Figure 9.2.
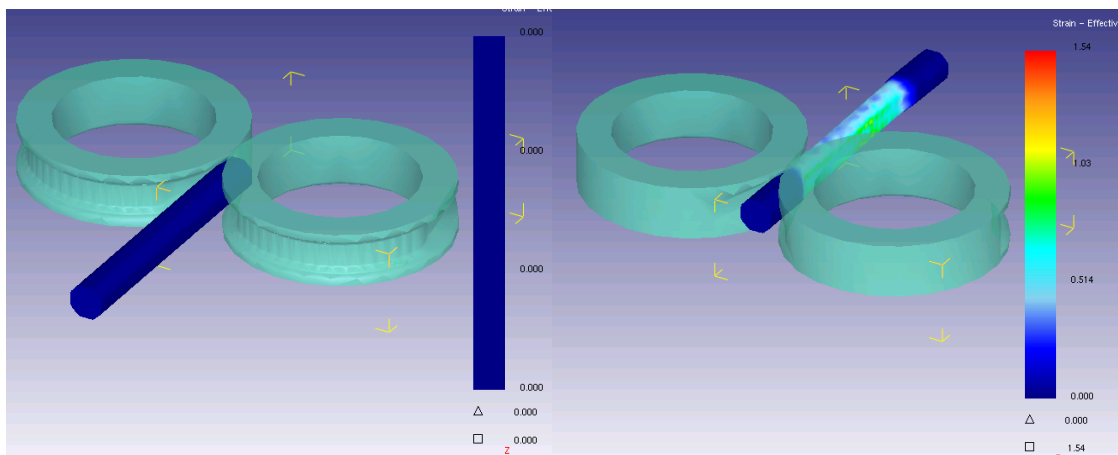
a) First stage of the reducer rolling process.
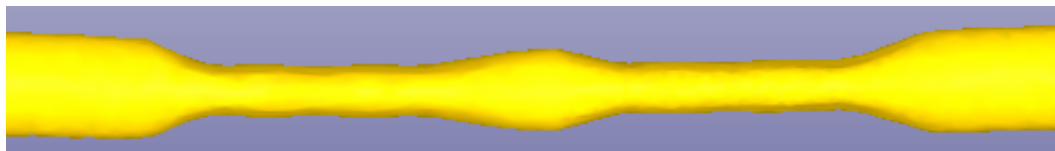
b) Reducer rolled preform prior to the bending operation.

Figure 9.2: Hot reducer rolling process for distribution of material volume.

232

This preform is then bent immediately after rolling i.e. in the same heat, to give the preliminary geometric form of the upper control arm. This geometry, shown in Figure 9.3 is used as the preform for the two-stage forging process. In the current analysis, the bending operation was not considered for simulation, since the added simulation step does not have any significant benefits for die design and metal flow analysis. Thus, a solid model of the preform, with a uniform temperature distribution, was used for FEA of the forging process.
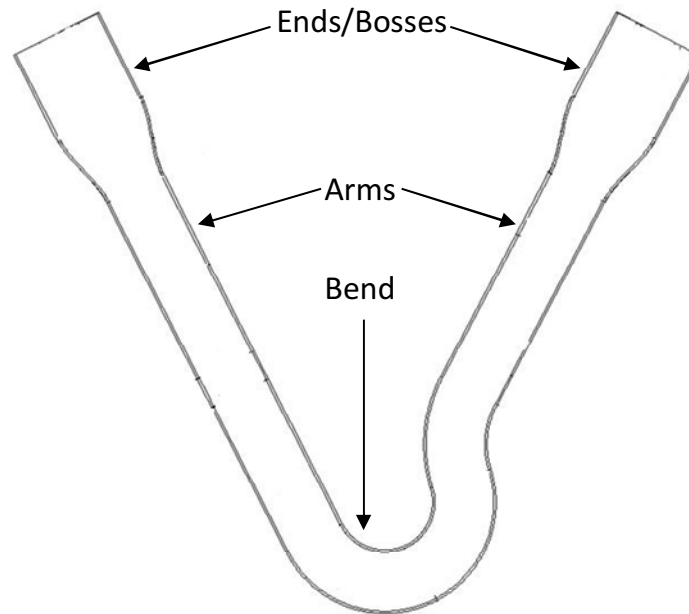
Figure 9.3: Plan view of the bent preform for the forging process.

9.3.2. *Analysis of Blocker and Finisher Forging*

The forging process simulations were conducted using non-isothermal 3-dimensional models of the die and preform geometries. The press ram velocity for deformation was selected using specifications of the mechanical forging press used for this process. The dies were assumed to have an initially uniform pre-heat temperature. This assumption was based on the use of heating/cooling channels in the die block to maintain the die temperature during production. The dies are manufactured from commonly used H13 hot-work tool steel. Thus, mechanical and thermal properties of this steel were used for the FE analysis. The workpiece was modeled with material properties, from DEFORM™, for a 6xxx series aluminum alloy. The forging process was analyzed in two steps:

233

- Simulation of blocker forging: The bent preform, with a uniform temperature distribution, was deformed using the specified press velocity profile to the flash thickness determined from production drawings.

- Simulation of finisher forging: The blocker forging was subsequently positioned in the finisher die cavity and deformed to the final dimensions. Thus, the state variable history (temperatures, strains, grain directionality, etc.) from blocker forging was carried forward into the finisher forging process.

For each forging stage, the workpiece dimensions along the curvilinear length, the part quality (die filling, folds, etc.), the forging load and the resulting die stresses were analyzed. The following predictions were made based on the FEA results:

- The part was designed to have a tab forged in the bend region to facilitate transfer from the blocker to the finisher die cavity using robotic grippers. FEA predicted that this tab had a significant amount of underfill in the blocker stage. Underfill was also observed in the region where the arms transition into the bend (Figure 9.3). These observations were confirmed by the project sponsor based upon initial production trials.

- It was observed that a significant amount of the preform material, primarily the ends (Figure 9.3), was lying in the flash region at the beginning of the forging operation. Thus, the bending process was not optimized for the forging process. In order to have a rough estimate of the amount of material lost as flash without any contribution to die filling, a simple Boolean operation was performed. The part of the preform lying outside the die cavity at the start of forging was subtracted from the blocker cavity volume. It was found that $\approx$ 22% of the preform material volume was converted into flash during blocker forging, without contributing to die filling.

- The finish forged part was found to meet all dimensional specifications i.e. complete die filling was observed for the finisher stage. Excessive material losses were observed in the region of the ends and the arms (Figure 9.3).

The flash losses during forging were quantified using a volume distribution diagram as shown in (Figure 9.8). This diagram was developed by on the basis of a cross-sectional area and volume analysis as described below:

- An imaginary axis was considered along the geometric profile of the preform and used as a reference for a curvilinear abscissa.

234

- Several planes orthogonal to this axis were used as cutting planes for all the components that are involved in the process (namely preform, blocker and finisher die cavity, blocker forging and finisher forging) (Figure 9.4).

- The cross-sectional area values obtained by analyzing the selected sections were plotted against the curvilinear abscissa i.e. the curvilinear length of the preform and part (Figure 9.5).

It is evident that the larger the number of sections taken, the more precise and reliable the information given by the diagram. On the other hand increasing the number of sections makes the procedure more complicated and time consuming. For the current study it was decided to take 15 sections along the preform (Figure 9.4). This was considered a good compromise between the need for precise design evaluation and the time constraints on process development and tryout. A uniform distance was maintained between each section. Special care was taken to locate the sections in all the critical regions of the die cavity, paying particular attention to areas where the 3-D blocker simulation had shown underfill.
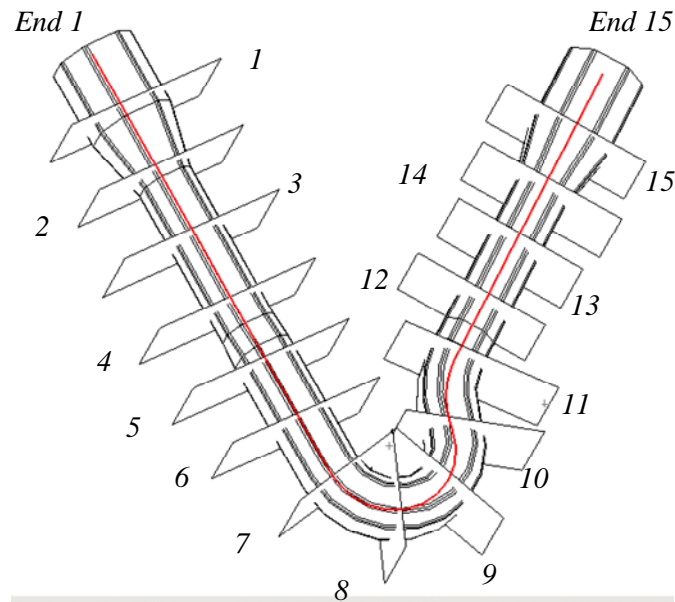
Figure 9.4: Sections selected along the length of the part for determination of flash losses.

235
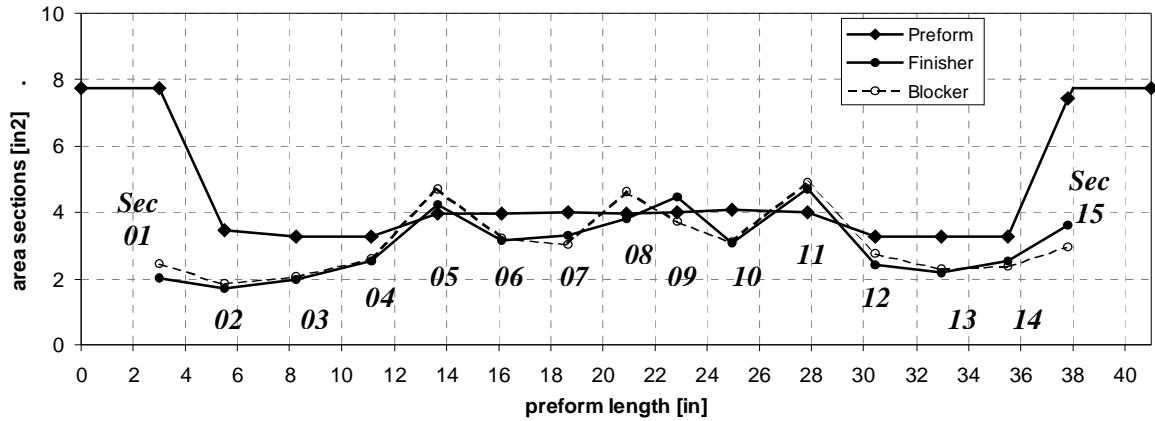
Figure 9.5: Distribution of cross-sectional areas obtained using the 15 sections.

Once the cutting locations were established the cutting operation was performed using generic 3-D CAD software. For each section, the cross-sectional area of the die cavity was compared with that of the preform cross-section forged in that location/section (Figure 9.5). In the region of the bend, from sections 5 to 11, the amount of extra material present in the preform is $\approx$ 5 %, increasing toward the arms of the part until it reaches a maximum of 50% and 60% near to the ends (Figure 9.6).

	sec 01	sec 02	sec 03	sec 04	sec 05	sec 06	sec 07	sec 08	sec 09	sec 10	sec 11	sec 12	sec 13	sec 14	sec 15
	74%	51%	40%	23%	-6%	21%	17%	4%	-12%	25%	-18%	26%	33%	23%	51%
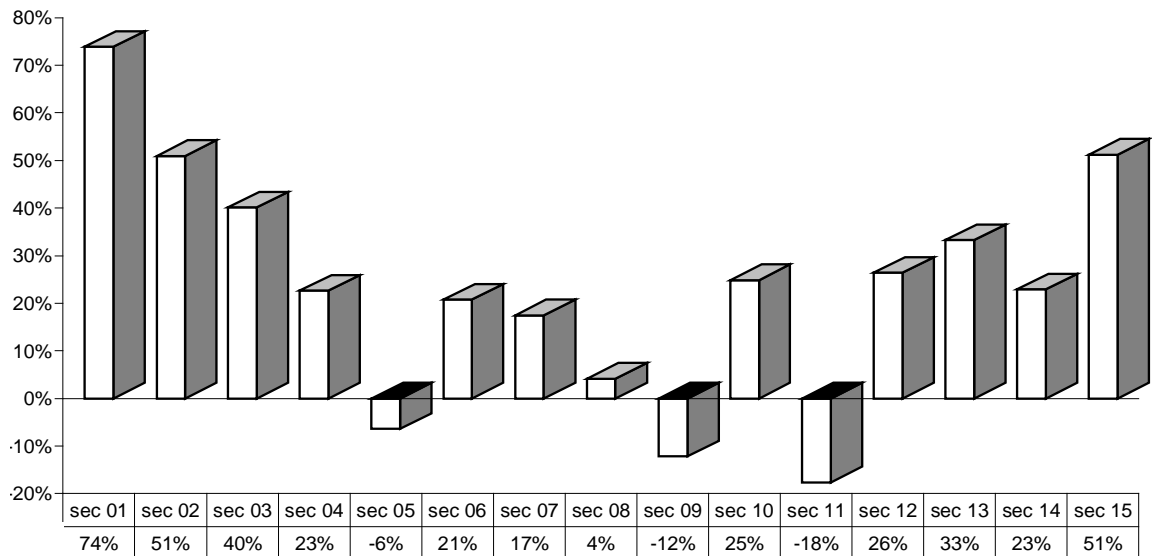
Figure 9.6: Percentage difference between cross-sectional areas of the preform and finisher.

236

An alternative method of obtaining material distribution was to cut the part, and the preform used to form it, in several 3-D sections (Figure 9.7). The 3-D models of the preform and the final product were cut in 16 portions, with the cutting planes used being the same as in 2-D analysis of Figure 9.4. By measuring the volume instead of cross-sectional area, a similar comparison was made to determine the volume of material lost as flash in different regions of the part (Figure 9.8).

For all the locations where the amount of longitudinal metal flow was not significant, the 3-D modeling problem was simplified to a 2-D analysis using either a plane strain or axisymmetric assumption. The plane strain assumption implies that metal flow occurs only in the lateral/transverse direction perpendicular to the assumed curvilinear axis of the preform. This assumption was applied to sections 2 through 6 and 10 through 14 i.e. the arms of the part (Figure 9.4). The sections in the bend region were analyzed using an axisymmetric model with the central axis assumed as the axis of the bend. The ends were analyzed using 3-D sections of those local regions.

| Name | Volume [in^3] | | Δ V |
	Product	Preform	%
END 1	13.12	20.31	35%
SEC 1-2	4.37	15.31	71%
SEC 2-3	4.98	9.19	46%
SEC 3-4	6.16	9.33	34%
SEC 4-5	8.50	9.27	8%
SEC 5-6	8.30	9.8	15%
SEC 6-7	8.19	9.98	18%
SEC 7-8	6.55	8.6	24%
SEC 8-9	7.46	8.35	11%
SEC 9-10	7.45	9.13	18%
SEC 10-11	12.40	11.8	-5%
SEC 11-12	7.02	8.22	15%
SEC 12-13	6.17	8.81	30%
SEC 13-14	5.69	8.16	30%
SEC 14-15	7.05	13.08	46%
END 15	17.29	23.89	28%
TOT	**130.7**	**183.2**	
Weight [lb]	12.81	17.96	
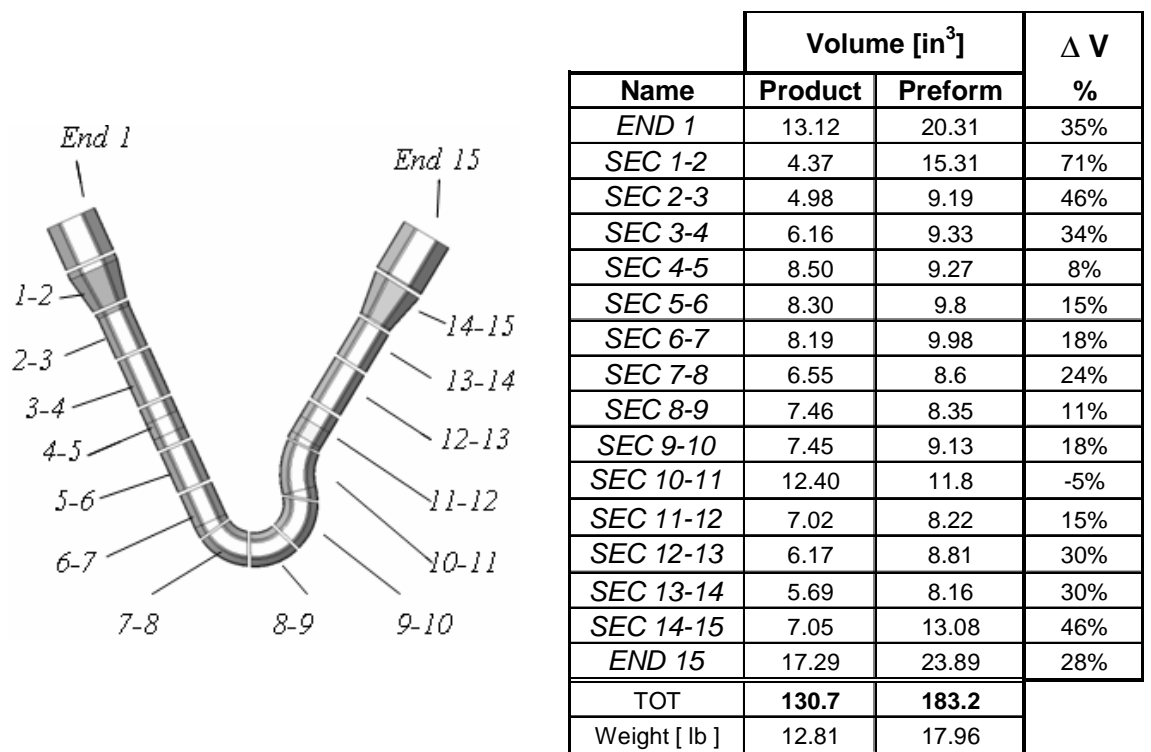
a) 3D sections selected. **b) Volume loss (ΔV) in selected sections.**

Figure 9.7: 3D volume analysis for investigation of material distribution.

237

	END 1	SEC 1-2	SEC 2-3	SEC 3-4	SEC 4-5	SEC 5-6	SEC 6-7	SEC 7-8	SEC 8-9	SEC 9-10	SEC 10-11	SEC 11-12	SEC 12-13	SEC 13-14	SEC 14-15	END 15
Product	13.12	4.37	4.98	6.16	8.50	8.30	8.19	6.55	7.46	7.45	12.40	7.02	6.17	5.69	7.05	17.29
Preform	20.31	15.31	9.19	9.33	9.27	9.8	9.98	8.6	8.35	9.13	11.8	8.22	8.81	8.16	13.08	23.89
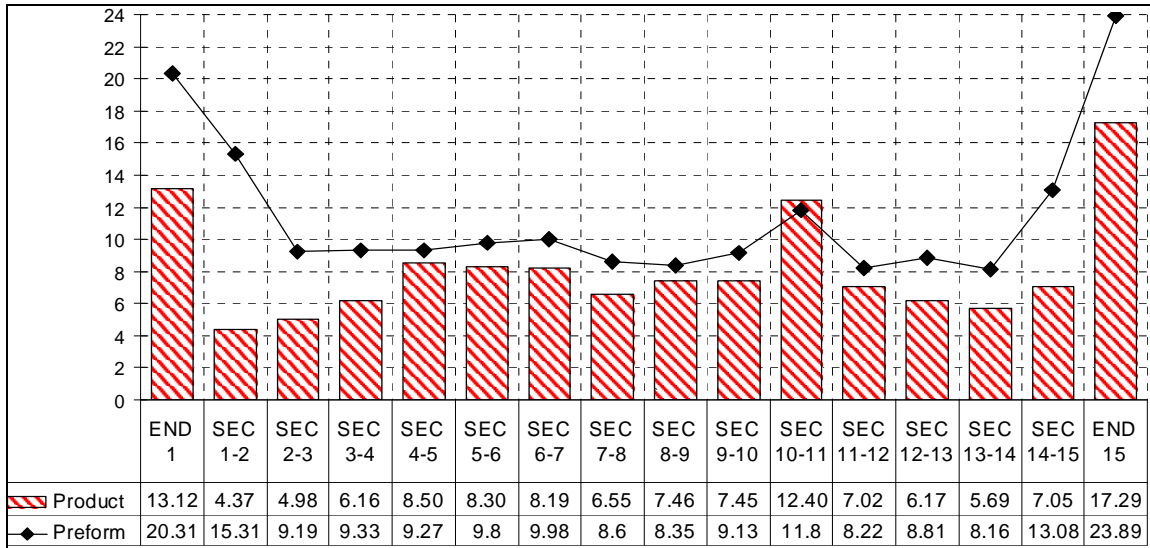
Figure 9.8: Volume distribution diagram obtained by the 3D sectional analysis.

A 3-D sectional forging analysis (blocker) was conducted to verify the validity of the plane strain assumption. One of the arms of the preform (sections 10 through 14) was forged as a 3-dimensional part without any displacement boundary conditions on the sectioned ends i.e. material was free to flow longitudinally. Figure 9.9 shows the 3-D section and the corresponding blocker forged geometry. Complete die filling was observed in this stage. Additionally, a comparison of material volumes within the coordinates of the sectioned ends before and after forging showed a 2% difference i.e. 2% of the material volume was lost as longitudinal increase in length. This analysis confirmed the plane strain metal flow assumption for analysis of the forging process.

Thus, analysis of the existing forging process outlined the need for optimization of the die and preform design based upon the material lost as flash. On the basis of detailed metal flow analysis, the complex 3-dimensional problem was simplified into separate 2-D analyses using assumptions of plane strain and axisymmetric metal flow. These 2-D sections were used for optimization of the preform geometry and the subsequently, for blocker die design. Final validation was conducted using full 3-D FEA and production validation.

238
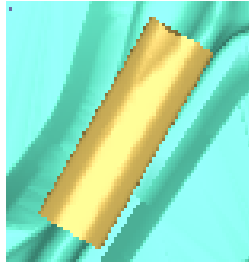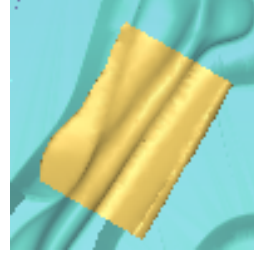
| a) Before forging. | b) After forging. |

Figure 9.9: Validation of the plane strain assumption for section 10 through 14 using 3-D sectional analysis.

9.4. Preform Optimization for the Existing Die Design

The objective of this task was to improve the material yield without altering the existing die geometry. This process established a feasible reducer-rolled preform geometry for further optimization in order to maximize the material savings.

9.4.1. Recommended Preform Design Improvements

Analysis of the metal flow in the existing blocker forging process had indicated that a significant amount of the flash losses and underfill were due to the workpiece material lying outside the die cavity at the start of forging. The blocker and finisher die cavities were both elliptical in nature along the cross-sections of the arms. The original preform cross-section, however, was circular in nature (a regular polygon) resulting in upsetting type of metal flow in the flash region. The goal of flash formation is to create backpressure during forging, thus, helping to fill the die cavity. Thus, an extrusion-type metal flow is desired. This was achieved by changing the circular preform cross-section to one that was elliptical in nature.

- A parametric study was conducted using 2-D simulations to develop elliptical preform cross-sections that would first fill a significant portion of the die cavity by upsetting before generating flash in order to ensure complete filling. Optimized cross-sections were developed for the arms and the bend region using the plane strain approximation and volume/area distribution diagrams (Figures 9.5 and 9.8). Additionally, the problem of under-fill along the straight section was eliminated by optimizing the preform cross-section.

239

- A majority of the flash was found to be generated at the ends (Figures 9.5 and 9.8). Thus, a modification of the preform ends was extremely crucial for improvement of material yield. In the new design, the ends were bent inwards with respect to the axis of the arms so as to reduce the material lying in the flash region prior to forging. Without changing the geometry of the ends, a material yield improvement of only 4 % could be realized. The modified preform (Design 1) was predicted to result in a material yield of 83%, which was an improvement of 11% over the original preform geometry.

- The geometry of the transition from the bend to the arm between sections 9 through 11 was modified to better align the preform during location for forging. Thus, the amount of material lying in the flash region was reduced.

- One end of the finish forged part (End 15; Figure 9.7) was 36% greater in volume than the other. Thus, one end of the reducer rolled preform was designed to have 36% less material in order to reduce flash losses. This rolled preform (Design 2) was, thus, asymmetrical with a material yield of 87%, an improvement of 4% over the symmetric design (Design 1).

These preform design modifications were made within the constraints of the reducer rolling equipment (maximum 50% reduction in each forging pass). This modified preform was used as a starting point for further optimization of the forging process.

9.4.2. Production Validation of Optimized Preform Design

The above mentioned design and analysis procedures were conducted while the production process was undergoing the tryout and set-up stage at the sponsor's facility. The design recommendations regarding the change in the bending process i.e. bending the ends inwards, resulted in a 10% improvement in material yield. The change in the reducer rolling process was not tried on the shop floor since this would have required new rolls to be machined.

240
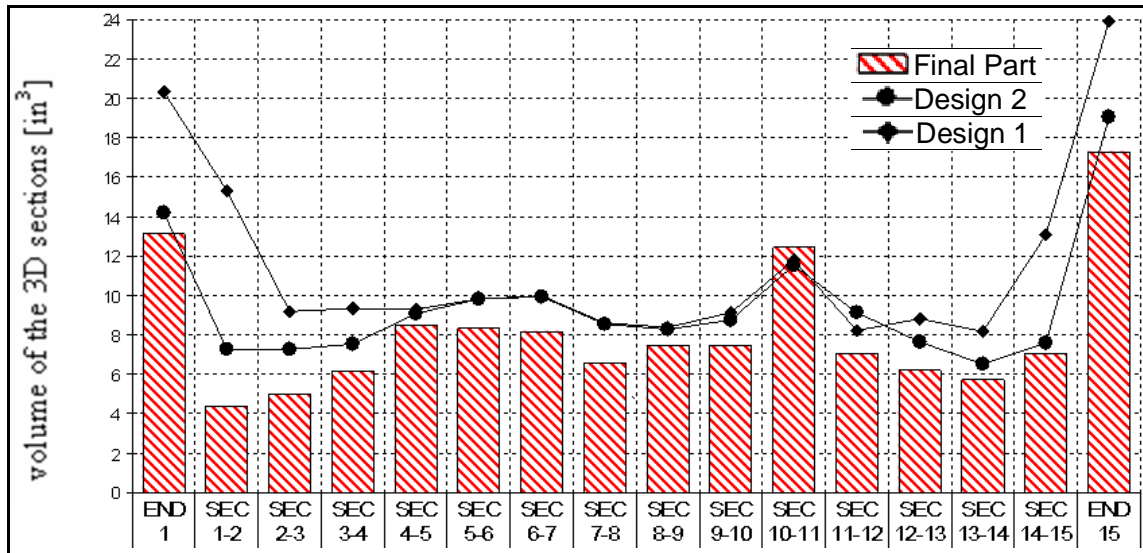
Figure 9.10: Volume distribution for the modified preforms.

9.5.   Blocker Die Design for Improvement of Material Yield

The next step in improvement of the forging process was to modify the blocker die to achieve further material savings by reducing the flash generated. Two methodologies were considered for designing the blocker die using 2D FE simulation (to be verified by 3D FEM).

9.5.1.   *Method I: Forward Design Process Sequence*

1. Consider several critical cross-sections of the final part or finisher die for 2D analysis.

2. Identify the design parameters of the critical sections of the finisher die/final part (rib height, rib width, draft angles, corner radii, etc).

3. Using empirical design rules (Table 9.1) establish a blocker design for the finisher sections being considered. This blocker design forms a starting point for the blocker optimization process.

4. Identify the significant geometrical parameters of the blocker design to be used for optimization. Select the appropriate ranges for these parameters.

5. Identify the design constraints on the selected parameters and the resulting blocker design. Constraints can be placed on the blocker area (flash allowance), resulting forging loads, die stresses, damage values, etc.

241

Dimensions of the finish forgings	Dimensions of the preforms
Web thickness (t_F)	$t_P \cong (1\text{--}1.5) * t_F$
Fillet radii (R_{FF})	$R_{PF} \cong (1.2\text{--}2) * R_{FF}$
Corner radii (R_{FC})	$R_{PC} \cong (1.2\text{--}2) * R_{FC}$
Draft angle (α_F)	$\alpha_P \cong \alpha_F + (2\text{--}5°)$
Width of the rib (w_F)	$w_P \cong w_F - 0.8$ mm (1/32 in.)

t_P, web thickness of preform; R_{PF}, fillet radii of preform; R_{PC}, corner radii of preform; α_P, draft angle of preform; w_P, width of preform rib.

Table 9.1: Empirical rules for blocker design of Aluminum forgings [Altan et al, 2005].

6. Identify an appropriate preform shape for the blocker design evaluation. This shape can be identified by trial simulations on the initial empirical blocker design or an appropriate shape can be assumed.

7. Conduct a parametric design study (using FE simulations) with the geometrical parameters considered in Step 4 subject to the constraints of Step 5.

8. Identify the candidate designs that satisfy the constraints.

9. The optimum design can be identified based upon design objectives (material utilization, die wear, equipment capabilities, etc).

9.5.2. *Method II: Backward Design Process Sequence*

1. Consider several critical cross-sections of the final part or finisher die for 2-D analysis.

2. Identify the design parameters of the critical sections of the finisher die/final part (rib height, rib width, draft angles, corner radii, etc).

3. Select the desired flash allowance for the blocker. Different sections will have different flash allowances based upon the shape complexity.

4. Select the design parameters to be analyzed. Depending upon the number of levels selected for these parameters, construct the different blocker designs all having the same flash allowance (cross-section area).

5. Evaluate the designs using FE simulation, subject to the required constraints as mentioned earlier.

6. Identify the candidate designs that satisfy the constraints.

242

7. The optimum blocker is selected based upon design objectives (material utilization, die wear, equipment capabilities, etc).

9.5.3. Optimization of Blocker Die Cross-sections

The goal of this case study was to optimize the material utilization (reduction of flash) while ensuring part quality. Hence, it was decided to implement an optimization methodology that evaluated designs with varying cross-sectional areas using the areas of the current blocker and finisher as the upper and lower control limits, respectively. Thus, the methodology adopted for the blocker design process was based on Method I (Forward Design scheme) mentioned in the preceding section. It was based on the assumption that a valid finisher die design is already available. If not, one needs to either develop an appropriate finisher die design or use the cross-sectional geometries of the final part. The process is summarized as follows for an example cross section, in this case Section 2 on the arms (Figure 9.4):

9.5.3.1. Identification of Design Objectives

The objective of the blocker design/optimization stage was to maximize the material utilization by reducing the flash generated in the blocker stage. Thus, the goal of this stage was the reduction of the flash allowance without increasing the forging loads or die stresses beyond acceptable limits. This goal was achieved by concentrating the majority of the metal flow in the blocker stage and thus, making the finisher more of a calibration operation to impart the final dimensions to the part. By reducing metal flow in the finisher, die life and part quality (dimensional tolerances) can be increased, thus ensuring the production of consistently accurate parts. Thus, at the conclusion of this design stage, the new blocker die was closer in volume to the finisher than the original blocker die.

9.5.3.2. Selection of Finisher Section for Optimization

Section 2 was selected for demonstration of the optimization process. The selected section was from a region in which the plane strain assumption was proven to be valid. The preform cross-section found to be optimum for this cross-section was used for evaluation of die design alternatives.

9.5.3.3. Identification of Design Parameters

The various geometrical parameters of the finisher are identified and dimensioned as shown in Figure 9.11. Based on a basic sensitivity analysis, the flash width in the current geometry was not found to have a significant effect on die filling and hence was not considered as an active design

243

variable. For the optimization process, the rib height (H) and rid width (w) were selected as design parameters so as to keep the number of required simulations at a necessary minimum.
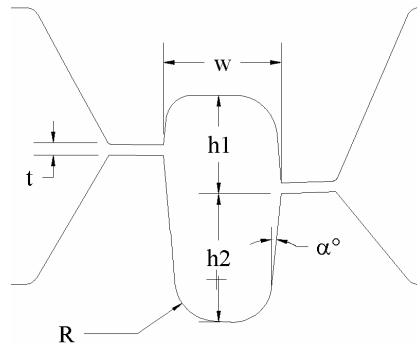
t – flash thickness

w - rib width

R – corner radius

H = h1 + h2 – rib height

α - draft angle

Figure 9.11: Design parameters for the finisher at Section 2.

9.5.3.4.   Selection of the Design Constraints

For selecting candidate blocker designs, constraints were initially placed on the blocker cross section area (A_b) using the areas of the finisher (A_f) and current blocker (A_{cb}) as the upper and lower control limits, respectively. The rib height (H) and width (w) of the blocker were selected using the corresponding values from the finisher and current blocker as lower and upper control limits, respectively (Table 9.2). Thus, the designs were subjected to the constraint that $A_f \leq A_b \leq A_{cb}$ to improve the material yield.

Case No.	Simulation	Area of Blocker
1	H_b, w_b	1.8398 in^2
2	H_a, w_b	1.7081 in^2
3	H_b, w_a	1.7019 in^2
4	H_a, w_a	1.6556 in^2
A_{cb} = 1.8478 in^2		A_f = 1.6511 in^2
H_a – high value; H_b – low value.		W_a – high value; w_b – low value.

Table 9.2: Candidate design matrix for Section 2 of the blocker die.

244

9.5.3.5. *Evaluation of Designs using FE Simulation*

The four candidate designs satisfying the area constraints were evaluated using FE simulations for the blocker and finisher. Figure 9.12 shows the FE simulation model for the four designs in the blocker stage. Instead of running individual models, the method shown in Figure 9.12 was used to reduce the number of simulations. Thus, all four die geometry variants were evaluated simultaneously. It should be noted that the preform geometry was maintained the same for the selected designs. In this case, the Design 2 variant was used with the cross-section optimized for Section 2.

H_a, w_a H_b, w_b H_b, w_a H_a, w_b
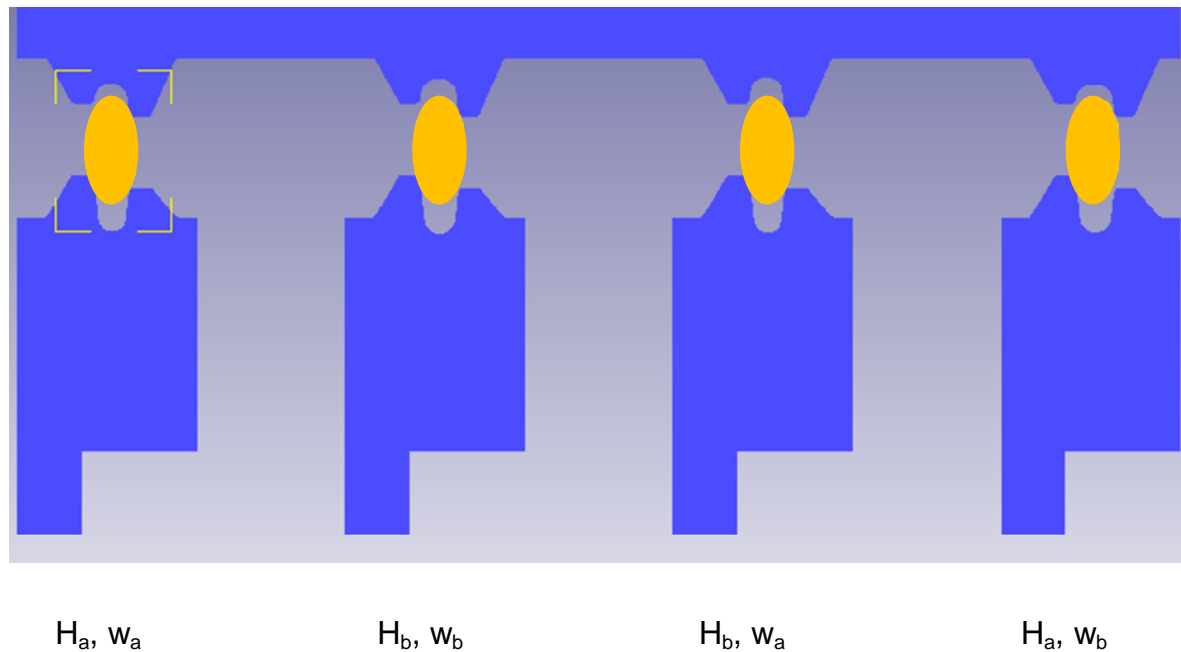
Figure 9.12: FE simulation set-up for the four candidate designs of Section 2.

9.5.3.6. *Selection of Optimum Design based on Design Objectives*

The optimum blocker die design was selected subject to the following criteria:

- Blocker die cross sectional area vs. forging load.

- Die filling in the finisher.

- Defect-free forging in blocker and finisher.

Thus, an optimum design was defined as one that gave the least increase in the forging load (compared to original blocker) with maximum improvement in material yield (reduction in cross-

245

sectional area compared to the original blocker). The values of cross-sectional area and forging load for the various designs were normalized with respect to those of the original blocker (Table 5.3). The least value of $[(A/A_o)*(L/L_o)]$ corresponds to the optimum design.

9.5.3.7.   Optimization of Preform Geometry for the New Blocker Die Design

For the initial blocker optimization stage a common preform shape (Design 2 preform cross-section at respective 2-D sections) was used in all the candidate designs as a starting point (Figure 9.12). During FE simulations it was observed that this preform shape resulted in folding in the flash region close to the die cavity (Figure 9.13). Thus, after selection of the optimum blocker design for the selected section, it was necessary to optimize the preform shape in order to:

- Maximize material utilization by reducing flash and thus further reducing forging loads.

- Determine a suitable shape that eliminates forging defects.

Thus, a new blocker design was selected for Section 2 along with an optimum preform shape for the new design in order to optimize the material savings while maintaining the part quality. In order to overcome the limitations of the reducer rolling equipment, the cross-section of the incoming forging stock (extruded billet) was modified from circular to an elliptical shape, while maintaining the same extrusion ratio.
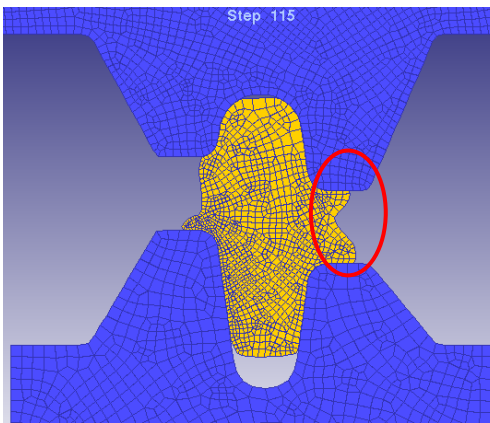
Figure 9.13: Folding observed during blocker optimization of Section 2.

The above design methodology was applied to the remaining sections along the straight legs of the upper control arm (Sections 2 to 4 and 12 to 14) where the plane strain approximation has been proven to be valid.

246

9.6.   Summary and Recommendations

A design methodology was developed for improvement of material yield in the hot forging of mass-produced automotive components (Figure 9.14). The techniques summarized in this chapter were developed using the forging process of an aluminum upper control arm as an example. The complex geometry of this component required the use of 2-D and 3-D FEA using assumptions of plane strain and axisymmetric metal flow. The following is a summary of the results and recommendations made on the basis of the FE analysis:

- FE simulation models were developed and validated for preforming with reducer rolling by comparison with production observations. Reducer rolling is used to achieve optimized volume distribution in the preform in order to reduce flash losses. Thus, successful design and simulation of this process are critical in order to achieve the desired material savings.

- FE models for the existing forging process were developed through validation with shop-floor observations in terms of part quality, forging loads, etc. These models were used as starting points for optimization of the forging process. The metal flow in blocker and finisher forging was analyzed in detail using 2-D and 3-D sectional analysis. Area and volume distribution diagrams were developed to determine the origins of the material lost as flash.

- Two alternative preform shapes (Design 1 with ends of the same size and Design 2 with asymmetric ends) were developed for the original die design in order to improve the material yield without having to remanufacture the dies. A change in the bending operation was also recommended. FEA predicted an improvement between 11-15% depending upon the choice of the preform shape. Shop-floor validation confirmed an improvement of 10% through implementation of one of the design alternatives.

- An optimum blocker die design was developed, along with a corresponding preform design, in order to further maximize material savings. Selected geometric parameters of the blocker cross-sections were optimized using the corresponding finisher cross-section as an upper bound and the existing blocker cross-section as a lower bound.

247

Step 1: 3D simulation of current billet preforming (reducer rolling) and forging operations to validate the FE simulation model of the forging process.
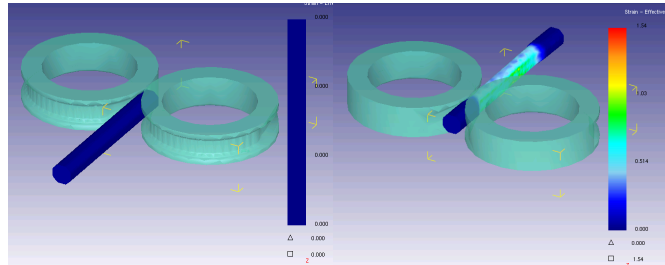
Simulation of the reducer rolling process.

Step 2: 2D simulations at various sections/locations on the preform using the assumptions of plane strain/axisymmetric flow to optimize the shape & size of the preform and the design of the blocker die.
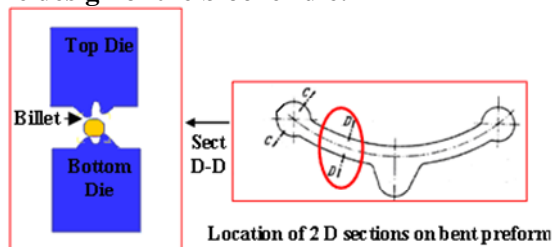
2D FE simulations using plane strain approximation.

Step 3: 3D simulation of sections which cannot be analyzed in 2D FEM using simplifying assumptions.
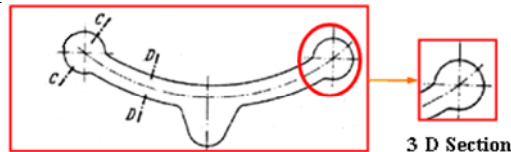
FE simulation of 3D sections.

Step 4: Final validation of the optimized preform shape and blocker design using 3 D simulation of the forging process.

Figure 9.14: Methodology for improvement of material yield in hot forging.

The final process design (optimized preform and blocker geometry) gave a material yield of ≈ 90% (subject to verification by 3-D FEM and feasibility of reducer roll design). It should be noted that the Design 2 preform gave a material yield of approximately 87% without any change to the forging dies. The blocker design study thus, gave an additional improvement of 3% over the Design 2 preform and 7% over the Design 1 preform. The final optimized preform required a change in the cross-section of the incoming extruded forging stock. The extrusion ratio, however, was maintained the same so as not to exceed the press tonnage required to extrude the shape.

248

Thus, an FE simulation-based design process was developed for preform and blocker design of a complex geometry through a combination of 2-D and 3-D analysis. Material yield was improved by $\approx$ 19% by optimizing the preform and blocker die design. A yield improvement of $\approx$ 15 % was obtained with only preform optimization i.e. the incoming forging stock and reducer rolling operation were optimized to improve the material yield with the existing die designs. Prediction of the material yield at the design stage also helped the forging company to be more competitive in the quotation process. Thus, besides improving the profitability of the forging process in terms of material utilization, this design methodology also significantly reduced the development costs and time for taking a product from the quotation stage to production.

249

CHAPTER 10

SUMMARY AND IMPACT OF THE RESEARCH

10.1. Summary and Conclusions

The main thrust of this research was on improvement of profitability in industrial warm and hot forging processes by increasing die life and material yield. In order to achieve these goals and remain competitive, forging companies in industrialized countries need to apply advanced computational tools such as FE simulation, besides practicing efficient shop-floor management. Some of the needs of the forging industry deemed relevant to the theme of this dissertation were a) determination of die-workpiece interface conditions under steady-state production, b) selection and comparison of optimum die materials (prediction of die life), c) design of shrink-fit dies with ceramic and/or carbide inserts for warm and hot forging, and d) optimization of preform and blocker die design for improved die life and material yield. The desired solutions and computational techniques were developed using actual production examples through active cooperation with the forging industry and affiliated companies.

To achieve the outlined goals it was first necessary to identify the root causes of die failure and material loss. This was done by developing "fishbone" (Ishikawa) diagrams identifying the main causes as well as interactions between them. This background work was supplemented with an in-depth technical literature review on die life research conducted by industry and academia. Using a hot forging process as an example, FE simulation techniques were developed for determination of die-workpiece interface conditions at start-up and under steady-state production. The current industry and academic practice in forging simulations is to consider only the deformation part of the forging cycle. The simulation methods developed during this research used detailed production cycle-time data to simulate the forging cycle from the time the billet is placed on the die to the time the forged part is removed. Additionally, the lubrication spray process was also analyzed using FEA. Repetitive simulations of these discrete process steps facilitated the prediction of steady-state interface conditions. This simulation approach added a significant amount of accuracy to the analysis of cyclic thermo-mechanical loading of the die surface and, subsequently, the prediction of die life. Alternative die materials were selected based

250

upon a virtual FEA comparison of their thermal fatigue performance under the predicted interface conditions. Also crucial to this analysis process was the optimization of the preform shape to reduce contact times and relative sliding. Production trials with the new preform design and an alternative die material showed 50% reduction in scrap rates with significantly reduced thermal fatigue on the critical regions of the die.

Current shrink-fit die design methods used by the forging industry make use of room temperature dimensions for the analysis of compressive pre-stress under warm forging conditions. The thermal expansion and subsequent loss of pre-stress during pre-heating and forging is not accounted for, which is critical when considering ceramic or carbide inserts. A simulation technique was developed for analysis of die assembly and pre-heating as well as the effect of different pre-heat methods. This, in combination with the multiple-cycle simulation technique developed earlier, helped to determine the loss of shrink-fit in the die inserts. Thus, the corrections and process changes necessary to maintain the inserts under compression were determined. The effect of dimensional tolerances of the die components on the compressive pre-stress was also analyzed. Carbides and matrix steels were recommended for improved thermal fatigue performance on the basis of FEA predictions.

The research goals of material yield improvement were accomplished using the forging process of an aluminum upper control arm as an example. Based on the metal flow and volume distribution analysis of the existing process, two optimized preform geometries were developed, while maintaining the die design. A material yield improvement of 10-15% was predicted and subsequently, validated on the shop floor ($\approx$ 10% improvement). The blocker die design was then optimized by varying selected geometrical parameters to achieve a total predicted yield improvement of $\approx$ 19%. The reduced lead time from quotation to production, upon application of the developed FEA methods, was expected to further maximize the total potential cost savings.

10.2.   Impact of the Research

The research objectives selected for this study were designed to be of direct relevance to warm and hot forging processes commonly encountered in the automotive industry and affiliated academic fields i.e. metal-forming research and development. The impact of the research contributions can be summarized as follows:

- Identification of factors and interactions affecting die failure and die wear, and the subsequent visualization of the same using Ishikawa diagrams.

251

- Determination of the die-workpiece interface conditions at start-up and at steady-state by considering the total forging cycle time (die chill, forging, dwell and lubrication) over single and multiple cycles.

- FEA-based methodology for the selection of die materials on the basis of material properties and predicted thermal fatigue performance under selected process conditions.

- Fundamental understanding of the effect of die material properties and surface condition on die life.

- Design and analysis of shrink-fit dies for warm and hot forging taking into account thermal expansion during pre-heating and forging.

  o Analysis of die assembly using actual component movement to incrementally assess contact generation and resulting pre-stress.

  o Selection of optimum pre-heating methods for steel, ceramic and carbide inserts by determining the changes in compressive pre-stress with different pre-heating techniques.

  o Determination of appropriate boundary conditions for simulation of the lubrication spray stage of the forging cycle.

  o Determination of the correction required in interference values to account for loss of pre-stress due to thermal expansion under steady-state production conditions.

  o Assessment of the die wear and thermal fatigue resistance of matrix high speed steels (MHSS) under warm forging conditions.

- FEA-based design methods for optimization of preform and blocker die design in order to improve die life and material yield.

  o Design and analysis of reducer rolling operation to achieve the desired material volume distribution on the optimized preform.

  o Optimization of blocker die design to reduce material flow in the finisher die and improve material utilization in the forging process.

- Collaboration between industry and academia for development and application of accurate and practical die life prediction and improvement techniques.

252

- Improvement of the global competitiveness of US forging industry through the use of predictive modeling to estimate and improve die life.

The goals outlined at the outset were, thus, achieved by forming mutually-beneficial alliances with the forging industry in order to develop the necessary computational design and analysis techniques, and validate them under actual production settings. The application of these methods in an efficiently managed production environment will enable forging companies to achieve and maintain a competitive edge in the global marketplace.

253

REFERENCES

[A. Finkl & Sons]   Hot-work Die Steel Brochures [www.finkl.com].

[Altan et al, 2005]   Altan, T., Ngaile, G. and Shen, G. "Cold and Hot Forging-Fundamentals and Applications", ASM International, 2005.

[Archard, 1953]   Archard, J., "Contact and Rubbing of Flat Surfaces", Journal of applied Physics, Vol. 24, 1953, pp. 981-988.

[Avner, 1964]   Avner, S., "Introduction to Physical Metallurgy", McGraw-Hill, Inc., 1964.

[Babu et al, 1999]   Babu, S., Ribeiro, D., and Shivpuri, R., "Material and Surface Engineering for Precision Forging Dies", prepared for the Precision Forging Consortium, Ohio Aerospace Institute and National Center for Manufacturing Sciences, 1999.

[Babu et al, 2004]   Babu, S., "A Material Based Approach to Creating Wear Resistant Surfaces for Hot Forging", PhD Dissertation, The Ohio State University, 2004.

[Behrens et al, 2005a]   Behrens, B.A., and Schaefer, F., "Prediction of Wear in Hot Forging Tools by Means of Finite Element Analysis", Journal of Materials Processing Technology, Vol. 167, 2005, pp. 309-315.

[Behrens et al, 2005b]   Behrens, B.A., Barnert, L., and Huskic, A., "Alternative Techniques to Reduce Die Wear – Hard Coating or Ceramic?", Annals of the German Academic Society for Production Engineering (WGP), 2005.

[Behrens et al, 2005c]   Behrens, B.A., Dähndel, H., and Huskic, A., "Quality Assurance for Precision Forging Processes by Process Management and Control of Die Wear", Proceedings of the 8th ICTP, October 9-13, 2005, Verona, Italy.

[Böhler-Uddeholm]   Hot-work Die Steel Brochures [www.bucorp.com].

[Bjork et al, 2001]   Bjork, T., Berger, M., Westergard, R., Hogmark, S. and Bergstrom, J., "New Physical Vapor Deposition Coatings Applied to Extrusion Dies", Surface and Coatings Technology, Volume 146-147, p 33-41, 2001.

[Brockhaus et al, 2002]   Brockhaus, H., Guderjahn, J., and Schruff, I., "Improving the Performance of Forging Tools – A Case Study", The Use of Tool Steels: Experience and Research, Proceedings of the 6th International Tooling Conference, Karlstad, Sweden, September 10-13, 2002, pp. 113-128.

[Cho et al, 2003]   Cho, H., Ngaile, G. and Altan, T. "Simultaneous Determination of Flow Stress and Interface Friction by Finite Element Based Inverse Analysis Technique, annals of CIRP, Vol.1, 2003, pp.221-224.

[Cho et al, 2005]   Cho, H. and Altan, T. "Determination of Flow Stress and Interface Friction at Elevated Temperatures by Inverse Analysis Technique" Journal of Materials Processing Technology, Vol. 170, 2005, pp.64-70.

[Chollacoop et al, 2003]   Chollacoop, N., Dao, M., and Suresh, S., "Depth-sensing Instrumented Indentation with Dual Sharp Indenters," Acta Materialia, No. 51, 2003, pp. 3713-3729.

[Cooke et al, 2004]   Cooke, K, Yang, S., Selcuk, C., Kennedy, A., Teer, D. and Beale, D., "Development of Duplex Nitrided and Closed Field Unbalanced Magnetron Sputter Ion Plated CrTiAlN-based Coatings for H-13 Aluminum Extrusion Dies", Surface and Coatings Technology, Vol. 188-189, 2004, pp. 697-702.

[Cser et al, 1993]   Cser, L., Geiger, M., Lange, K., and Hansel, M., "Tool Life and Tool Quality in Bulk Metal Forming", Proc. Instn Mech Engrs, Vol. 207, 1993.

[Dahl et al, 1998]   Dahl, C., Vasquez, V., and Altan, T., "Effect of Process Parameters on Die Life and Die Failure in Precision Forging", ERC for Net Shape Manufacturing, Report No. 98-R-15, 1998, The Ohio State University.

[Dahl et al, 1999]   Dahl, C., Vasquez, V., and Altan, T., "Analysis and Prediction of Die Wear in Precision Forging Operations", ERC for Net Shape Manufacturing, Report No. 99-R-21, 1999, The Ohio State University.

[Dalton et al, 1999]   Dalton, G.M., and Zaccone, D.C., "Oil Migration on Sheet Steels and the Effect on Performance in Metal Stamping", SAE Technical Paper No. 1999-01-0682, 1999.

[Dao et al, 2001]   Dao, M., Chollacoop, N., Van Vliet, K., Venkatesh, T., and Suresh, S. "Computational Modeling of the Forward and Reverse Problems in Instrumented Sharp Indentation," Acta Materialia, No. 49, 2001, pp. 3899-3918.

[Dobrzanski et al, 2005]   Dobrzanski, L., Polok, M. and Adamiak, M., "Structure and Properties of Wear Resistance PVD Coatings Deposited onto X37CrMoV5-1 Type Hot Work Tool Steel", Journal of Materials Processing Technology, Vol. 164-165, 2005, pp. 843-849.

255

[Doege et al, 1994]   Doege, E., Naegele, H., and Schliephake, U., "Aspects of Wear Prediction in Precision Forging", Proceedings of the Institution of Mechanical Engineers, Vol. 280, 1993, pp. 111-119.

[Doege et al, 2001a]   Doege, E., Huskic, A., Barnert, L., Gulde, M., and Hornhardt, Ch., "Reduction of Wear of Forging Dies by Use of New Technologies", New Developments in Forging Technology, University of Stuttgart, 2001, pp. 315-327.

[Doege et al, 2001b]   Doege, E., Huskic, A., Barnert, L., and Gulde, M., "Wear Reduction in Hot Die Forging by Application of New Ceramic Coatings, Inlays and Lubrication Technologies", Proceedings of the 3rd International Conference on Industrial Tools, April 22-26, 2001, Maribor, Slovenia.

[Doege et al, 2001c]   Doege, E., Barnert, L., Hallfeldt, T., Kulp S., and Neumaier, T., "Ceramic Components for Metal Forming Tools", Ceramic Materials and Components for Engines, 7th International Symposium, 19th – 21st June (2000), Wiley-VCH Heinrich, J.G. Aldiger, F. Ceramic Materials and Components for Engines ISBN: 3-527-30416-9 (2001).

[Doege et al, 2004]   Doege, E., Alasti, M., and Schmidt-Juergensen, R., "Accurate friction and Heat Transfer Laws for Enhanced Simulation Models of Precision Forging Processes", Journal of Materials Processing Technology, Volume 150, p 92-99, 2004.

[Dohda et al, 1989]   Dohda, K. and Kawai, N., "Correlation Among Tribological Indices for Metal Forming", Journal of the Society of Tribologists and Lubrication Engineers, Vol. 46, 1989, pp. 727-734.

[Ekstroem et al, 1990]   Ekstroem, T. and Persson, J., "Hot Hardness Behavior of Yttrium Sialon Ceramics", Journal of American Ceramic Society, Vol. 73, 1990, Issue 10, 1990, pp. 2834-2838.

[Fisher et al, 2002]   Fisher, K., Schweiger, H., Hasenberger, J., and Dremel, H., "New Tool Steel for Warm and Hot Forging", The Use of Tool Steels: Experience and Research, Proceedings of the 6th International Tooling Conference, Karlstad, Sweden, September 10-13, 2002, pp. 129-139.

[Gariety et al, 2003a]   Gariety, M., Ngaile, G., and Altan, T., 2003, "A Twist Compression Test for the Evaluation of Friction and Lubrication in Metal Forming Processes", ERC for Net Shape Manufacturing, Report No. THF/ERC/NSM-03-R-91, 2003, The Ohio State University.

[Gariety et al, 2003b]   Gariety, M., Altan. T., Botz, F. and Handley, M. "Viability of the Twist Compression Test for Screening Tube Hydroforming Lubricants" to be submitted to Journal of STLE Tribology Transactions, Sept. 2003.

[Haggag, 1993]   Haggag, F. "In-situ Measurements of Mechanical Properties Using Novel Automated Ball Indentation System," Small Specimen Test Techniques Applied to Nuclear Reactor Vessel Thermal Annealing and Plant Life Extension, ASTM STP 1204, 1993, pp. 27-44.

256

[Hanada et al, 2004]   Hanada, K., Zhang, Q., Umeda, K., Ishiwata, M., and Tsukita, M., "Surface Modification of Tool Steel by MoS_2 Powder Shooting", Journal of Materials Processing Technology, Vol. 153-154, 2004, pp.170-173.

[Hanada et al, 2005]   Hanada, K., Hatsukano, K., Matsuzaki, K., Umeda, K., Ishiwata, M., and Tsukita, M., "Graphite Coating of Tool Steel by Pressure Spraying", Journal of Materials Processing Technology, Vol. 164-165, 2005, pp.856-861.

[Haynes International]   Product Brochures [www.haynesinternational.com].

[Herbert, 2001]   Herbert, E., Pharr, G., Oliver, W., Lucas, B., and Hay, J., "On the Measurement of Stress–Strain Curves by Spherical Indentation", Thin Solid Films, Vol. 398-399, 2001, pp. 331-335.

[Holm, 1946]   Holm, R., "Electrical Contacts", Almquist and Wiksells, Stockholm, Section 40, 1946.

[Horie et al, 1995]   Horie, N., Sato, K., Kanda, Y., Mitamura, K., Hamazaki, K., and Kori, T., "Cermet hot forging die", Asahi Glass Company, Tokyo, Japan, US Patent # 5406825, April 1995.

[Inoue, 2004]   Inoue, Y., "Coated Tool for Warm and/or Hot Working with Superior Galling Resistance Property and Superior Wear Resistance", US Patent No. 6811899, 2004.

[Iwase et al, 1999]   Iwase, S., Yoshizaka, M., Yamada, S., and Fujimoto, H., "Hot forging of Ti alloy valve preforms", Aisan Kogyo Kabushiki Kaisha, Obu, Japan, US Patent # 5964120, October 1999.

[Kang et al, 1999a]   Kang, J., Park, I., Jae, J., and Kang, S., "A Study on a Die Wear Model Considering Thermal Softening: (I) Construction of the Wear Model", Journal of Materials Processing Technology, Vol. 96, 1999, pp. 53-58.

[Kang et al, 1999b]   Kang, J., Park, I., Jae, J., and Kang, S., "A Study on a Die Wear Model Considering Thermal Softening: (II) Application of the Suggested Wear Model", Journal of Materials Processing Technology, Vol. 94, 1999, pp. 183-188.

[Kim et al, 2005a]   Kim, D., Lee, H., Kim, B. and Kim, K., "Estimation of Die Service Life Against Plastic Deformation and Wear During Hot Forging Processes", Journal of Materials Processing Technology, Vol. 166, 2005, pp. 372-380.

[Kim et al, 2005b]   Kim, D., Kim, B., and Kang C., "Die Life Considering the Deviation of the Preheating Billet Temperature in Hot Forging Process", Finite Elements in Analysis and Design, Vol. 41, 2005, pp. 1255-1269.

[Klimek et al, 2003]   Klimek K., Ahn, H., Seebach, M., Wang, M. and Rie, K., "Duplex Process Applied to Die Casting and Forging Tools", Surface and Coatings Technology, Vol. 174-175, 2003, pp. 677-680.

257

[Klocke et al, 2002]   Klocke, F., Beck, T., Hoppe, S., Krieg, T., Mueller, N., Noethe, T., Raedt, H-W., and Sweeney, K., "Examples of FEM Application in Manufacturing Technology", Journal of Materials Processing Technology, Vol. 120, 2002, pp. 450-457.

[Koitabashi, 1995]   Koitabashi, T., "Application of Ceramics in Hot Forging Dies", Journal of the Japan Society for Technology of Plasticity, Vol. 36, No. 418, 1995, pp. 1221-22.

[Knoerr et al, 1989]   Knoerr, M., Shivpuri, R., and Altan, T., "Failure in Forging Dies", ERC for Net Shape Manufacturing, Report No. ERC/NSM-89-15-B, 1989, The Ohio State University.

[Lange et al, 1992]   Lange, K., Cser, L., Geiger, M., and Kals, J., "Tool Life and Tool Quality in Bulk Metal Forming", Annals of CIRP, Vol. 41, No. 2, 1992, pp. 667-676.

[Lee et al, 2003]   Lee, R. and Jou, J., "Application of Numerical Simulation for Wear Analysis of Warm Forging Dies", Journal of Materials Processing Technology, Vol. 140, 2003, pp. 43-48.

[Liu et al, 1994]   Liu, D-M., Chen, C-J., and Lee, R.-R., "Thermal Diffusivity/Conductivity in Sialon Ceramics", Journal of Applied Physics, Vol. 77, 1995, Issue 2, pp. 494-496.

[Mahrenholtz et al, 2005]   Mahrenholtz, O., Bontcheva, N., and Iankov, R., "Influence of Surface Roughness on Friction During Metal Forming Processes", Journal of Materials Processing Technology, Vol. 159, 2005, pp. 9-16.

[Mitamura et al, 1999]   Mitamura, K., and Fujikawa, S., "Application of Boride Cermet in Warm Forging Dies", (Nissan Mortor Co., Ltd.).

[Mitterer et al, 2000]   Mitterer, C., Holler, F., Ustel, F., and Heim, D., "Application of Hard Coatings in Aluminum Die Casting – Soldering, Erosion and Thermal Fatigue Behavior", Surface and Coatings Technology, Vol. 125, 2000, pp. 233-239.

[Mitterer et al, 2001]   Mitterer, C., Holler, F., Lugmair, C., Noebauer, R., Kullmer, R., and Teichert, C., "Optimization of Plasma-Assisted Chemical Vapor Deposition Hard Coatings for their Application in Aluminum Die Casting", Surface and Coatings Technology, Vol. 142-144, 2001, pp. 1005-1011.

[Morris et al, 2005a]   Morris, E., Cho, H., Sartkulvanich, P., Altan, T., "Determining the Flow Stress at the Surface of Materials using Indentation Testing with Conical or Spherical Indenters", ERC for Net Shape Manufacturing, Report No. HPM/ERC/NSM-05-R-25, 2005, The Ohio State University

[Morris et al, 2005b]   Morris, E., Cho, H.J., Sartkulvanich, P., and Altan, T., "Determination of Engineered Surface Layer Through an FEM Inverse Analysis of Instrumented Indentation Tests", in preparation for journal publication, 2005.

258

[Müller, 2002]   Müller, K., "Deposition of Hard Films on Hot Working Steel Dies for Aluminum", Journal of Materials Processing Technology, Vol. 130-131, 2002, pp. 432-437.

[Nachi-Fujikoshi]   "Extremely Tough Cold Work Die Steels, MDS Series", White Paper, Nachi-Fujikoshi, Japan.

[Nakahama et al, 2005]   Nakahama, S-S., Yukinori, M., Namiki, K., and Ozaki, K., "The Development of High Hard and Tough Matrix Type High Speed Tool Steels", Denki-Seiko (Electric Furnace Steel), Vol. 76, No. 4, 2005, pp. 279-286.

[Navinsek et al, 2001]   Navinsek, B., Panjan, P. and Gorenjak, F., "Improvement of Hot Forging Manufacturing with PVD and DUPLEX Coatings", Surface and Coatings Technology, Vol. 137, 2001, pp. 255-264.

[Nishimura et al, 1995]   Nishimura, T., Sato, T. and Tada, Y., "Evaluation of Frictional Conditions for Various Tool Materials and Lubricants Using the Injection Upsetting Method", Journal of Materials Processing Technology, Vol. 53, 1995, pp. 726-735.

[Nishimura et al, 1996]   Nishimura, T., Sato, T. and Tada, Y., "The Evaluation of Anti-galling Characteristics by Observation of Adhesion Morphologies Using Injection Upsetting", Journal of Materials Processing Technology, Vol. 62, 1995, pp. 235-241.

[Oliver et al, 1992]   Oliver, W., and Pharr, G., "An Improved Technique for Determining Hardness and Elastic Modulus Using Load and Displacement Sensing Indentation Experiments", Journal of Materials Research, Vol. 7, 1992, pp. 1564-1583.

[Painter et al, 1996]   Painter, B., Shivpuri, R., and Altan, T., "Prediction of Die Wear During Hot Extrusion of Engine Valves", Journal of Materials Processing Technology, Vol. 59, 1996, pp. 132-143.

[Persson et al, 2004]   Persson, A., Hogmark, S., and Bergstroem, J., "Temperature Profiles and Conditions for Thermal Fatigue Cracking in Brass Die Casting Dies", Journal of Materials Processing Technology, Vol. 152, 2004, pp. 228-236.

[Persson et al, 2005]   Persson, A., Hogmark, S., and Bergstroem, J., "Thermal Fatigue Cracking of Surface Engineered Hot Work Tool Steels", Surface and Coatings Technology, Vol. 191, 2005, pp. 216-227.

[Roberts et al, 1964]   Roberts, G. and Hamaker, J., "Alloy Steels", US Patent No. 3117863, 1964.

[Saiki et al, 1997]   Saiki, H., Ngaile, G., and Ruan, L., "Influence of Die Geometry on Workability of Conversion Coatings Combined with Soap Lubricant in Cold Forming of Steels", Journal of Materials Processing Technology, Vol. 63, 1997, pp.238-243.

259

[Saiki et al, 2003]   Saiki, H., and Marumo, Y., "Influence of the Roughness Geometry of Tool Surface and the Flow Stress of Coated Solid Lubricants on Tribo-conditions in Cold Forging", Journal of Materials Processing Technology, Vol. 140, 2003, pp.25-29.

[Salas et al, 2003]   Salas, O., Kearns, K., Carrera, S. and Moore, J., "Tribological Behavior of Candidate Coatings for Aluminum Die Casting Dies", Surface and Coatings Technology, Vol. 172, 2003, pp. 117-127.

[Sawamura et al, 2005]   Sawamura, M., Yogo, Y., Kondo, S., Tanaka, T., Nakanishi, K., Suzuki, T., and Watanabe, A., "Estimation of Spray Lubrication and Die Temperature for Die Wear Life Prediction in Hot Forging", R & D Review of Toyota CRDL, Vol. 40, No. 1, 2005.

[Schmolz-Bickenbach]   Hot-work Die Steel Brochures [www.schmolz-bickenbach.com].

[Schneider et al, 2006]   Schneider, D., and Stephens, L., "An Experimental Study on the Impact of Interface Temperature on Thermally Induced Wear Transitions in Dry Sliding", Journal of Tribology, Transactions of ASME, Vol. 128, 2006, pp. 460-468.

[Schrader et al,2007]   Schrader, T., Shirgaokar, M. and Altan, T., "A Critical Evaluation of the Double Cup Extrusion Test for Selection of Cold Forging Lubricants", Journal of Materials Processing Technology, Volume: 189, Issue: 1, July 6, 2007, pp. 36-44.

[Sheljaskow, 2001]   Sheljaskow, S., "Tool Lubricating Systems in Warm Forging", Journal of Materials Processing Technology, Vol. 113, 2001, pp. 16-21.

[Shirgaokar et al,2002]   Shirgaokar, M., Ngaile, G. and Altan, T., "Multistage Forging Simulations of Aircraft Components," Engineering Research Center for Net Shape Manufacturing, Report No. ERC/NSM-02-R-84, 2002.

[Shirgaokar et al,2003]   Shirgaokar, M., Ngaile, G. and Altan, T., "Forging of Internal Combustion Engine Pistons for Racing Applications," Engineering Research Center for Net Shape Manufacturing, Report No. ERC/NSM-03-R-84, 2003.

[Sjoestroem et al, 2004]   Sjoestroem, J., and Bergstroem, J., "Thermal Fatigue Testing of Chromium Martensitic Hot-Work Tool Steel after Different Austenitizing Treatments", Journal of Materials Processing Technology, Vol. 153-154, 2004, pp. 1089-1096.

[Sjoestroem et al, 2005]   Sjoestroem, J., and Bergstroem, J., "Thermal Fatigue in Hot-Working Tools", Scandinavian Journal of Metallurgy, Vol. 34, 2005, pp. 221-231.

[Stahlberg et al, 1999]   Stahlberg, U., and Hallstroem, J., "A Comparison Between Two Wear Models", Journal of Materials Processing Technology, Vol. 87, 1999, pp. 223-229.

260

[Starling et al, 1997]   Starling, C. and Branco, J., "Thermal Fatigue of Hot Work Tool Steel with Hard Coatings", Thin Solid Films, Volume 308-309, pp. 436-442, 1997.

[Tamura, 2006]   Tamura, Y., "Prolonging Die Life by Means of the Combination of Die Materials and Surface Treatment Presents Cost Reduction", supplemental information, JSTP 4th International Seminar on Precision Forging, 2006, Nara, Japan.

[Tanaka et al, 2005]   Tanaka, T., Nakanishi, K., Yogo, Y., Kondo, S., Tsuchiya, Y., Suzuki, T., and Watanabe, A., "Prediction of Hot Forging Die Life Using Wear and Cooling Model", R & D Review of Toyota CRDL, Vol. 40, 2005, No. 1.

[Tercelj et al, 2003]   Tercelj, M., Perus, I. and Turk R., "Suitability of CAE Neural Networks and FEM for Prediction of Wear on Die Radii in Hot Forging", Tribology International, Vol. 36, 2003, pp. 573-583.

[Tsuchiya, 1999]   Tsuchiya, Y., "Trend in Process Tribology Focusing on Die Life- Key Technology for Precise and Efficient Production", R & D Review of Toyota CRDL, Volume 34, No. 4, 1999.

[Usui, 1982]   Usui, E. and Shirakashi, T., 1982, "Mechanics of Machining from Descriptive to Predictive Theory, on the Art of Cutting Metals – 75 Years Later," ASME-PED, Vol. 7, pp. 13-15.

[Vardan et al, 1987]   Vardan, O., Bagchi, A., and Altan, T., "Investigation of Die Wear in Upsetting Using the FEM Code ALPID", Proceedings of NAMRC, 1987, pp. 386.

[Vasquez et al, 2000]   Vasquez, V. and Altan, T. "New Concepts in Die Design – Physical and Computer Modeling Applications", Journal of Materials Processing Technology, Vol. 98, 2000, p. 212-223.

[Walter Metals]   Hot-work Die Steel Brochures [www.waltermetals.com].

[Walters et al, 2000]   Walters, J, Wu, W., Arvind, A., Li, G., Lambert, D. and Tang, J., "Recent development of process simulation for industrial applications", Journal of Materials Processing Technology, Vol. 98 (2000), p - 205-211.

[Yeckley, 2002]   Yeckley, R., "Sialon Materials Development at Kennametal", Hot-Section Materials Development for Advanced Microturbines, RFP No. 3400020692, presented at the Environmental Barrier coatings Workshop, Nashville TN, November 6, 2002 (public domain presentation).

[Yen et al, 2004a]   Yen, Y.-C., Söhner, J., Lilly, B. and Altan, T., "Estimation of Tool Wear in Orthogonal Cutting using Finite Element Analysis," Journal of Materials Processing Technology, Vol. 146, 2004, pp. 82-91.

[Yen et al, 2004b]   Y.-C. Yen, A. Jain, P. Chigurupati, W.-T. Wu, and T. Altan, "Computer Simulation of Orthogonal Cutting using a Tool with Multiple Coatings," Machine Science and Technology, Vol. 8, No.2, 2004, pp. 305-326.

APPENDIX-A: PROCESS DATA QUESTIONNAIRE

1. General Summary
1.1 Company Information
Name:
Address:
Contact Person Name : _____ Phone: _____ Fax: _____ Email:_____
1.2 Example/Case Study
Part Name:_____ Brief Description (Include a drawing by email if possible; hand sketch is also acceptable):

2. Die Wear Information

Note: The following information should be provided for a single die that has frequent problems. For multiple dies, please make copies of this form and attach extra sheets.

2.1 Primary Failure Mechanism

Wear ☐   Thermal Fatigue ☐   Mechanical Fatigue ☐   Plastic Deformation ☐

Catastrophic Failure (cracking/breakage) ☐   Not sure ☐   Other ☐

Brief Description:

a) No. of parts forged before die repair/replacement _____ (applicable to wear or fatigue failure)

b) Reason for replacement:

- Part out of tolerance ☐

- Surface finish unacceptable ☐

- Other ☐

2.2 Secondary Failure Mechanism in Same Die (if applicable)

Wear ☐   Thermal Fatigue ☐   Mechanical Fatigue ☐   Plastic Deformation ☐ Catastrophic Failure (cracking/breakage) ☐   Not sure ☐   Other ☐

Brief Description:

2.3 Sketch of the die showing failure zones

Please attach a production drawing or sketch indicating the regions of die failure or wear. In case of multiple failure mechanisms, please rank as primary, secondary, etc. Please provide pictures if available.

264

2.4 Finite Element (FE) Simulation

Note: The ERC/NSM uses the commercial code DEFORM® for analysis of forging processes to predict metal flow, die stresses, temperatures, etc. As part of this project, certain selected forging processes will be simulated for prediction of wear and design modifications to improve die life.

a)   Does your company have FE simulation software for simulation of forging processes?

   Yes ☐, Code used:_____ (mention 2D, 3D or both)

   No ☐,

b)   Has the current process been simulated (in-house or sub-contracted)?

   Yes ☐, No ☐

c)   If Yes, can you at a later stage provide simulation results?

   Yes ☐, No ☐

d)   If No, would you be interested in having us simulate the process?

   Yes ☐, No ☐

3. Billet Information

3.1 Billet Material

a) Alloy designation:_____

b) Condition:

Heat treated (annealed, homogenized, etc) Yes ☐, No ☐

Please specify:_____

3.2 Billet cross-section geometry (provide drawing if possible, or provide following information *with tolerances*):

a) Cross Section:

☐ Round: _____(Dia)

☐ Round Cornered Square: _____(Dimensions)

☐ Other:_____

b) Billet Length (in) : _____

c) Billet Weight (lb) : _____

3.3 Billet Preparation:

Cold Sheared ☐   Hot Sheared ☐   Sawed ☐

Any edge preparation? Yes ☐, No ☐

3.4 Billet Sorting:

Yes ☐, No ☐

If yes,

By weight ☐, Tolerance (lb): _____

By length ☐, Tolerance (in): _____

3.5 Please specify any pre-forging treatments to the billet (i.e. sand blasting, tumbling, etc):

4. Billet Heating

4.1 Heating Type (induction/furnace): _____

4.2 Controlled Atmosphere: Yes ☐, No ☐

If Yes, specify:

4.3 Billet Temperature (°F) : _____ Heating Time (sec): _____

266

Temperature Control System: _____

4.4 Part Transfer:

Manual ☐ Automated (Robot, conveyor, etc) ☐

4.5 Is billet temperature measured (infrared) prior to forging? Yes ☐, No ☐

4.6 Is billet de-scaled before forging? Yes ☐, No ☐

If Yes, how? _____

If No, amount of scale allowed on billet: None ☐   Light ☐   Heavy ☐

5. Preform Heating

Note: The following questions are relevant only to those processes where preforms need to be re-heated prior to finish forging.

5.1 Heating Type (induction/furnace): _____

5.2 Controlled Atmosphere: Yes ☐, No ☐

If Yes, specify:

5.3 Preform Temperature (°F) : _____ Heating Time (sec): _____

Temperature Control System: _____

5.4 Part Transfer:

Manual ☐ Automated (Robot, conveyor, etc) ☐

5.5 Is preform temperature measured (infrared) prior to forging? Yes ☐, No ☐

5.6 Is preform de-scaled? Yes ☐, No ☐

If Yes, how? _____

267

If No, amount of scale allowed on billet: Light ☐ Heavy ☐

6. Forging Equipment

6.1 Press Type:

Vertical Mechanical ☐   Screw ☐   Hydraulic ☐

Upsetter or Horizontal Forging Machine ☐

Brand:_____

6.2 Press Specifications:

Load Capacity (tons):_____

Strokes/minute (idle):_____

Stroke Length (mechanical press) :_____

Production rate (parts/min):_____

Contact Time (sec):_____ (rough estimate, if possible)

6.3 Mode of Operation: Manual feed ☐ Automatic feed ☐

6.4 Load Monitoring: Yes ☐, No ☐

Are several dies loaded during one stroke? Yes ☐ (6.4.1) , No ☐ (6.4.2)

Please specify:_____

6.4.1 If Yes,

Is load monitored for every die?

If Yes ☐, please provide the approximate maximum load per station (tons):	If No ☐, for one stroke when several die stations are loaded, please provide the total maximum press load (tons): _____

6.4.2 If No, Please provide the approximate maximum load on single die (tons):_____

6.5 Knockout Mechanism None ☐   Hydraulic ☐   Mechanical ☐   Other:_____

7. Forging Dies

7.1: Die or Insert Material:_____ Attach chemical composition for non-standard designation.

7.2 Die Manufacturing: EDM ☐   Machine + Harden ☐   Machine only ☐ Comments:

7.3 Heat Treatment: Yes ☐, No ☐ Hardness:_____ (as-received or after hardening before die/insert is installed in press)

7.4 Finishing: As machined ☐   Grinding ☐   Polishing ☐   Other:_____ Surface Roughness (approximate):_____

7.5 Die Surface Treatments: (nitriding, boriding, hard facing, etc.) Yes ☐, No ☐ Please specify:

269

Any quality control on surface treatment? Yes ☐, No ☐
7.6 Die Coatings: Yes ☐, No ☐ Please specify:_____ Any quality control on coating? Yes ☐, No ☐ Is die polished before ☐ or after ☐ coating?
7.6 Die Repair Welding ☐   Re-sinking ☐   Insert change   Other:_____
8. Lubrication/Cooling System
8.1 Brand and Supplier (if possible to provide) :_____
8.2 Lubricant Type: Water-base Graphite ☐   Water-base Synthetic ☐   Oil-base Graphite ☐ Synthetic ☐ Molybdenum Disulfide ☐ Other:_____
8.3 Mode of Application: Manual ☐   Robot ☐   Fixed Spray ☐   Reciprocating Spray ☐   Swab ☐
8.4 Lubrication Frequency: After every blow ☐   After _____ blows ☐
8.5 Billet Lubrication (if any): Graphite-base Coating ☐ Molybdenum Disulfide ☐ Other:_____
8.6 In addition to lubricant spray is the die cooled?

270

Yes ☐, No ☐

9. Process Conditions

9.1 Approximate die surface temperature during production (before start of forging stroke) (°F) :

Are dies pre-heated before start of production? Yes ☐, No ☐

If Yes, to what temperature (°F):_____

Method of die pre-heating:

Oven ☐   Induction ☐   Flame ☐   Hot forging stock ☐

Other:_____

Die temperature monitoring: Yes ☐, No ☐

9.2 Number of forging operations (stations) for the selected part:

We presume that this form is completed for one station only viz. the one with maximum die wear. However, it is useful to know how many operations the part goes through i.e. bust, pre-blocker, blocker, finish, etc.

	Type of Operation	Job Description
1.		
2.		
3.		
4.		
5.		

Approximate transfer time between stations (secs):_____

271